

MICROPALAEONTOLOGÍA

REVISTA ESPAÑOLA DE

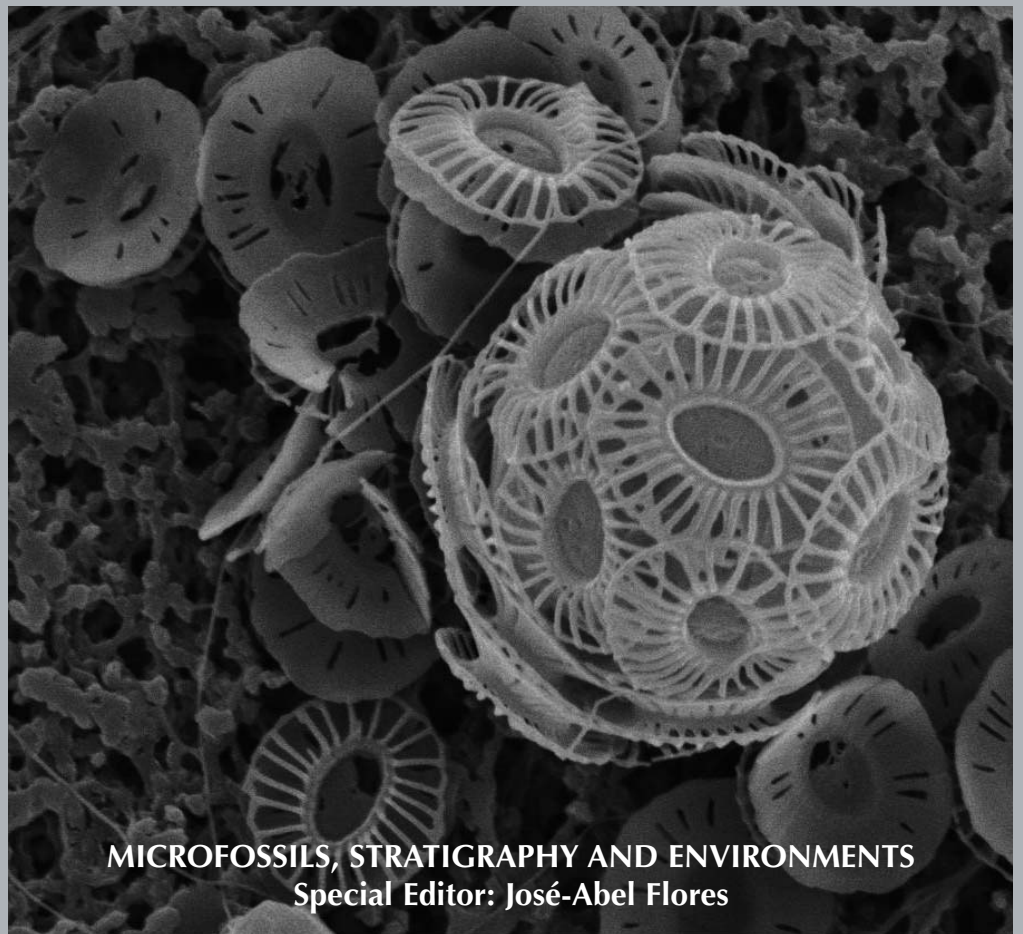
VOLUMEN 42

*

SEPTIEMBRE-DICIEMBRE 2010

*

NÚMERO 3



ISSN 0556-655X



MINISTERIO
DE CIENCIA
E INNOVACIÓN



Instituto Geológico
y Minero de España

VOLUMEN 42
NÚMERO 3

SEPTIEMBRE-DICIEMBRE 2010

REVISTA ESPAÑOLA DE MICROPALEONTOLOGÍA

REVISTA ESPAÑOLA DE MICROPALÉONTOLOGÍA
Revista cuatrimestral editada por el Instituto Geológico y Minero de España
Issued by the Geological Survey of Spain
www.igme.es

Editora/Editor: Isabel RÁBANO
Editor adjunto/Managing editor: Eduardo BARRÓN
Comité Editorial/Editorial Board

J. A. ARZ, Zaragoza, España; S. M. BERGSTRÖM, Columbus, OH, USA; M. BILOTTE, Toulouse, Francia;
J. C. BRAGA, Granada, España; J. CIVIS, Salamanca, España; T. M. CRONIN, Reston, VA, USA; S. GARCÍA
LÓPEZ, Oviedo, España; C. HERRERO MATESANZ, Madrid, España; L. HOTTINGER, Basilea, Suiza;
S. IACCARINO, Parma, Italia; E. MOLINA, Zaragoza, España; J. PAIS, Lisboa, Portugal; F. PARIS, Rennes,
Francia; D. RIO, Padua, Italia; J. RODRÍGUEZ LÁZARO, Bilbao, España; B. RUIZ ZAPATA,
Alcalá de Henares, España; L. C. SÁNCHEZ DE POSADA, Oviedo, España;
F. J. SIERRA SÁNCHEZ, Salamanca, España; M. TONGIORGI, Pisa, Italia; J. VANNIER, Lyon, Francia;
A. de VERNAL, Quebec, Canadá; R. C. WHATLEY, Aberystwyth, Gran Bretaña.

Enviar los manuscritos a/Address manuscripts to:
Isabel Rábano
Instituto Geológico y Minero de España
Ríos Rosas, 23
E-28003 Madrid (Spain)
Tel.: (34) 91 349 58 19 - Fax: (34) 91 349 58 30
i.rabano@igme.es

Suscripciones

La tarifa ordinaria de suscripción para el año 2011 es de 59 euros (España) y 72 euros (extranjero). Librerías y agencias (25% descuento), 44 euros (España) y 54 euros (extranjero). El pago se realizará mediante transferencia bancaria (IBAN: ES69-0049-3026-80-2114353997) o cheque a nombre de Instituto Geológico y Minero de España. Toda la correspondencia relativa a suscripciones y números atrasados debe dirigirse a: Servicio de Publicaciones, Instituto Geológico y Minero de España, Ríos Rosas 23, 28003 Madrid (España), fax: +34-91-3495830, e-mail: publicaciones@igme.es

Subscriptions

Regular subscription price (2011) 72 euros, in Spain 59 euros. Agencies (25% discount) 54 euros, in Spain 44 euros. Payment should be made in euros by banker's order (IBAN: ES69-0049-3026-80-2114353997) or check drawn on a Spanish bank, payable to Instituto Geológico y Minero de España. Correspondence concerned with subscription orders and back numbers should be directed to Servicio de Publicaciones, Instituto Geológico y Minero de España, Ríos Rosas 23, 28003 Madrid (Spain), fax: +34-91-3495830, e-mail: publicaciones@igme.es

Portada: Cocosfera de *Emiliana huxleyi* (Cocolitóforo) recuperada en la columna de agua durante la campaña del RV Polarstern ANT XVIII/5 (sector subantártico del Pacífico). Los cocolitos que aparecen junto a la cocosfera son vistas proximales de la misma especie. Microfotografía: José-Abel Flores.

Cover: Coccosphere of Emiliana huxleyi (Coccolithophore) recovered from water samples during RV Polarstern expedition ANT XVIII/5 (Subantarctic sector of the Pacific ocean). The coccoliths that appear next to the coccosphere are proximal views of same species. Microphotography: José-Abel Flores.

Fecha de publicación/Publication date: Diciembre 2010

© Instituto Geológico y Minero de España
Ríos Rosas, 23 - 28003 Madrid
Depósito legal: M. 2733 - 1969
ISSN: 0556-655X
NIPO: 474-10-008-X

El Instituto Geológico y Minero de España hace presente que las opiniones y hechos consignados en sus publicaciones son de la exclusiva responsabilidad de los autores de los trabajos.

Los derechos de propiedad de los trabajos publicados en esta obra fueron cedidos por los autores al Instituto Geológico y Minero de España.

MICROFOSSILS, STRATIGRAPHY AND ENVIRONMENTS

The recognition that marine microfossils are useful for the correlation between ocean basins, as well as for environmental characterization, contributed to the increasing independence of the study of microfossils from mainstream Paleontology since the first quarter of the 20th century. Their utility in the oil industry and in the ocean exploration, especially in relevant projects concerning large geoscience programs such as Deep Sea Drilling Project, Ocean Drilling Program and Integrated Ocean Drilling Program, contributed to the proliferation of microfossil laboratories and specialists around the world.

Most of the first studies concerning micropaleontology focused on the development and standardization of zonations using planktic foraminifera, calcareous nannofossils, diatoms, radiolarians or palynomorphs. More recently, microfossils have been increasingly utilized as environmental markers, thus improving environmental reference schemes. However, *classical* Biostratigraphy has been overtaken by Biochronology, once ages are assigned to zonal boundaries. Improvement of geochronological ages, especially those that are astronomically calibrated, have opened a new perspective for marine microfossils.

The development of more ecological information concerning extant microorganisms, and particularly biochemical and sedimentological markers to groundtruth the behavior of fossil elements, have added value to ocean history interpretations supported by marine microfossil records. Critical components like temperature, salinity, and the availability of nutrients can be inferred with the analysis of microfossil assemblages. Today, the value of marine microfossils goes beyond the chronological and stratigraphic, and has added significantly to a host of paleo-environmental studies.

This volume of *Revista Española de Micropaleontología* is a singular example of these trends in Micropaleontology.

Three studies in this volume are focused on the improvement of biostratigraphic patterns, including the identification of new events (or refining previous ones), and adding an environmental component that allows for reconstruction at orbital and suborbital level.

Mejía-Molina and collaborators studied the composition of *Sphenolithus* (a calcareous nannofossil taxon) in several sequences from Colombia, ranging from shallow to open ocean regions, for an Eocene-Miocene interval. Besides the recalibration of some biostratigraphic events involving this genus, they contribute to the reconstruction of sea surface dynamics, interpreting peaks of this taxon as intense water stratification.

Buitrago-Reina and collaborators recalibrated a series of events in the nannoplankton assemblages in the Caribbean Sea, for the Miocene-Pliocene interval using an astronomically-tuned curve. Additionally, they define some new micropaleontological horizons with the objective of improving the regional biostratigraphic pattern.

It is interesting to note that these two contributions were carried out under the coordination with the Colombian oil company Ecopetrol.

Lancis and collaborators described a detailed sequence of events using calcareous nannofossils and planktic foraminifers, providing a correlation tool between Mediterranean basins in a critical episode of their geological history: the Tortonian, just prior the Messinian Salinity crisis.

Narciso and coworkers performed a high resolution analysis of calcareous nannoflora identified in late Pleistocene sediments from a site drilled in the Adriatic sea. They correlate several Mediterranean sapropels with variations in the autochthonous assemblage as well as with changes in the record of reworked material.

Álvarez and collaborators show a new pattern of biogeographical distribution of Coccolithophores in the western Mediterranean Sea, improving substantially the existing data-base. The Coccolithophore assemblages defined are correlated with environmental and oceanographic features, providing an interesting framework for future work.

Finally, as an example of the utility (and necessity) of correct cataloging of microfossil for biostratigraphic purposes, Espitia and coworkers present a study explaining how the Instituto Colombiano del Petróleo manages their micropaleontological collections. This is a valuable effort to standardize the available information in a research institute.

Thus, six different contributions with a common thread: the potential of microfossils in geological and environmental reconstruction, and the extent to which different groups can help carry this out.

With these lines I would like to express my gratitude to the dozens of referees that selflessly contributed to the review of the studies, to the Editor and to the Instituto Geológico y Minero de España for the opportunity to develop this project, and especially to all the involved authors who, with dedication and patience, provided their manuscripts to be published in this volume.

José-Abel Flores
Universidad de Salamanca

Distribution of calcareous nannofossils in Upper Eocene-Upper Miocene deposits from Northern Colombia and the Caribbean sea

Alejandra Mejía-Molina^{1,2}, José-Abel Flores¹, Vladimir Torres Torres² and Francisco Javier Sierra¹

¹ Departamento de Geología, Universidad de Salamanca. Plaza de la Merced s/n, 37008 Salamanca, España. alejandra@usal.es

² Instituto Colombiano del Petróleo-ECOPETROL. Bucaramanga, Colombia.

Resumen

Se analizaron muestras provenientes del registro sedimentario de tres secuencias del Caribe colombiano. Dos de ellas corresponden a secciones tomadas en continente, en tanto que la tercera corresponde al testigo oceánico ODP 999 recuperado en el mar Caribe. El registro en todas las secuencias es generalmente continuo y la preservación de la asociación de nanofósiles es buena. Para este estudio se han empleado las propuestas bioestratigráficas de Martini (1971), Bukry (1973, 1975) y Okada & Bukry (1980) para subdividir el Oligoceno y Mioceno porque estas zonaciones se establecieron con base en secuencias muy detalladas del Caribe. El intervalo estudiado comprende desde el Eoceno superior hasta el Mioceno superior. El género *Sphenolithus* está presente en todo el registro en diferentes patrones de abundancia y grados de preservación de los especímenes. Se realizaron análisis para clarificar aspectos relacionados con los patrones de distribución, abundancia y morfología de éstos taxones. Este estudio resalta algunas dificultades taxonómicas en el reconocimiento de *Sphenolithus* spp. y hace énfasis en la ausencia de reconstrucciones paleoecológicas basadas en este género. Algunas de estas inquietudes son retomadas mediante el análisis bioestratigráfico disponible, patrones de abundancia y caracterización morfológica de las especies de *Sphenolithus* identificados. Notables abundancias en *Sphenolithus heteromorphus* fueron observadas tanto en la sección del Carmen de Bolívar, Estratigráfico 4 como en el ODP 999. Además, *Sphenolithus abies* también registra un importante incremento en su abundancia en el ODP 999. Ambas especies, *S. heteromorphus* y *S. abies* llegan a ser dominantes en la asociación de nanofósiles identificada constituyendo intervalos de abundancias destacadas (SDI, *Sphenolithus Dominance Interval*). *Sphenolithus* sería un género indicador de condiciones oligotróficas adaptado a una mayor estratificación de las masas de agua superficial y con una respuesta positiva ante el incremento de la temperatura superficial. Al menos para el Norte de Colombia y mar Caribe *Sphenolithus* habría constituido intervalos de dominio SDI (*Sphenolithus Dominance Interval*), tanto en ambientes proximales (Carmen de Bolívar, Estratigráfico 4) como en mar abierto (ODP 999).

Palabras clave: Nanofósiles calcáreos, *Sphenolithus*, Cenozoico, Bioestratigrafía, Paleoecología, Mar Caribe, Colombia.

Abstract

In this work, a detailed study based on the genus *Sphenolithus* was carried out in three sequences. Two were recovered onshore in Colombia –the Arroyo Alférez and Carmen de Bolívar, Estratigráfico 4 sequences– and one offshore, in the Caribbean Sea –ODP 999–. In all sequences the record is generally continuous and the preservation of the nannofossil assemblage is good. In this research, the standard biozonations of Martini (1971), Bukry (1973, 1975) and Okada & Bukry (1980) for the late Eocene to the late Miocene were

used. *Sphenolithus* is consistently present in the sequences. Differences among the patterns of distribution, abundance and morphological aspects of *Sphenolithus* spp. were analyzed. The results of the study highlight certain taxonomic problems and the almost complete absence of paleoecological reconstruction, reflecting the fact that there have been relatively few studies undertaken on the *Sphenolithus* group in recent decades. Here, some of these limitations are overcome by combining the biostratigraphic Caribbean–Colombian pattern and morphometric analyses of selected taxa of *Sphenolithus*. Exceptional abundances in *Sphenolithus heteromorphus* were recorded in both the ODP 999 and Carmen de Bolívar, Estratigráfico 4 sections. Also, a very high abundance in *Sphenolithus abies* was identified in ODP 999. Both *S. heteromorphus* and *S. abies* become the dominant components of the nannofossil assemblage, constituting the SDI (*Sphenolithus* Dominance Interval) episodes. During the SDI, the dominance of smaller specimens of *S. heteromorphus* and *S. abies* was observed. *Sphenolithus* is considered to be a proxy for oligotrophic conditions that is adapted to an enhancement in ocean stratification, with a positive response to increases in superficial temperatures. In Northern Colombia and the Caribbean Sea, *Sphenolithus* had its SDI in both shallow–water (Carmen de Bolívar, Estratigráfico 4) and open marine (ODP 999) paleoenvironments.

Key words: Calcareous Nannofossil, *Sphenolithus*, Cenozoic, Biostratigraphy, Paleoecology, Caribbean Sea, Northern Colombia.

1. INTRODUCTION

Very few stratigraphic and biostratigraphic studies have been proposed in land areas of NE South America based on marine microfossils, and few modern paleoceanographic and biostratigraphic calcareous nannofossil reconstructions have been performed (Mejía-Molina *et al.*, 2006, 2008; Fiorini & Jaramillo, 2006; Mejía-Molina *et al.*, 2010, in prep.). Better approximations to paleoceanographic conditions for offshore Colombia are compiled in several publications referring to the ODP 165 expedition, in particular for site 999 (Kameo & Bralower, 2000 and references therein). Calcareous nannofossils are one of the best micropaleontological groups used in paleoenvironmental reconstruction and stratigraphy. In this study, the standard biostratigraphic calcareous nannofossil-based schemes proposed by Martini (1971), Bukry (1973, 1975) and Okada & Bukry (1980) for the subdivision of the Cenozoic were used because they have been established in detailed sequences of the Caribbean Sea. Many other supplementary biohorizons, which improve the biostratigraphic resolution of the records, have been documented. In particular, the distributions of the genus *Sphenolithus* described underscore their biostratigraphic importance in the NN1 (CN1) to NN4 (CN5) zones of Martini (1971) and Okada & Bukry (1980), belonging to the early Miocene. Biozonal boundaries are traced according to the zonations of Martini (1971) and Bukry (1973, 1975), later coded by Okada & Bukry (1980).

The sphenoliths have a continuous distribution recorded from the Paleogene to the Pliocene. A schematic calcareous

nannofossil-based biostratigraphy zonation is presented for all sequences, referring exclusively to the data on *Sphenolithus* because the characterization of the records focuses on this genus. The time interval considered here corresponds to from the late Eocene to the late Miocene [NP18 (CP15a) to NN10 (CN8), Martini (1971); Okada & Bukry (1980)]. Mejía-Molina (In prep.) has reported a detailed study concerning the calcareous nannofossil assemblages in the Caribbean region for the Oligocene–Miocene interval. This study addresses the *Sphenolithus* record, a genus that is very well represented and that is useful for both stratigraphic and paleoecological purposes.

1.1 Geological setting

1.1.1 The Arroyo Alférez and Carmen de Bolívar, Estratigráfico 4 onshore sections

The San Jacinto Fold Belt is located in the Lower Magdalena Valley of Northwest Colombia, South America, between the Sinú and San Jorge–Plato basins. Sediment distribution and non-deposition or erosion are important in the sedimentary and tectonic history of the San Jacinto Fold Belt and adjacent basins. The unconformities reflect tectonic events and, although they cannot be easily identified in the seismic profiles, they are widely documented in stratigraphic studies addressing the Lower Magdalena Valley (Duque-Caro, 1984; Caro & Spratt, 2003). During the Oligocene to Miocene, either the uplifting of the San

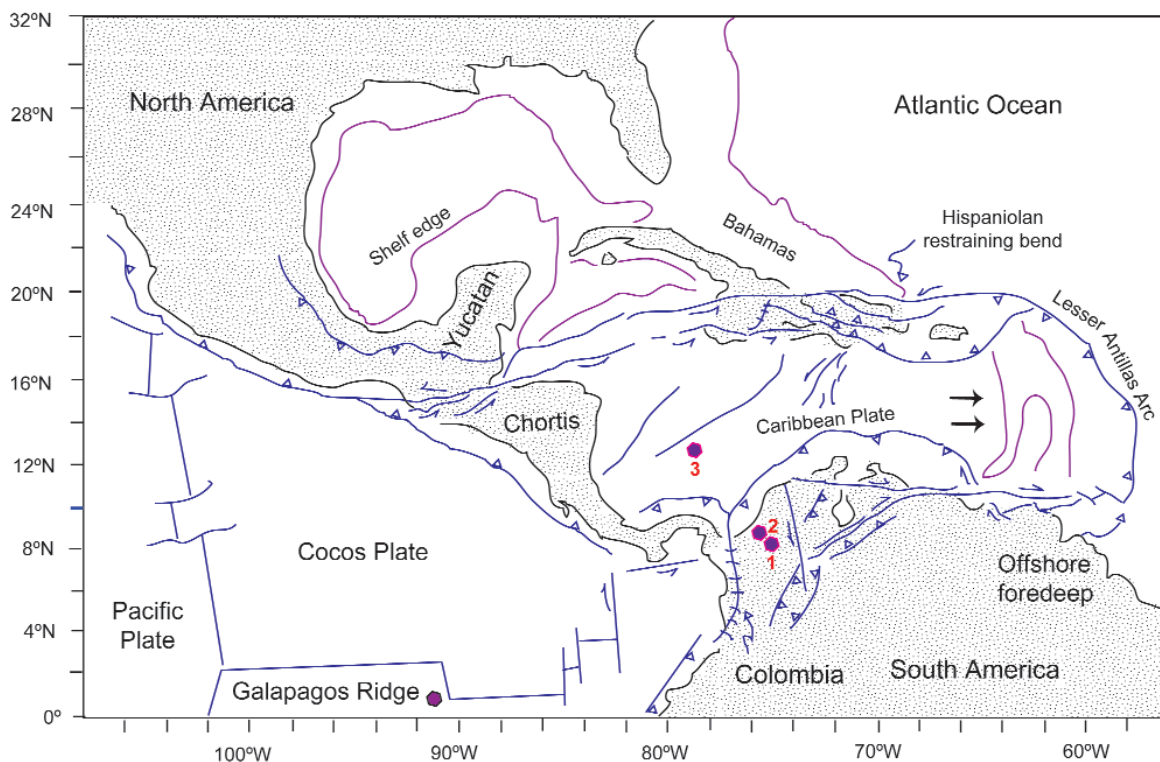


Figure 1. Geographical setting. 1. Arroyo Alférez section; 2. Carmen de Bolívar, Estratigráfico 4 section; 3. ODP Site 999. Modified of Acton *et al.* (2000).

Jacinto rift continued or the San Jacinto rift remained emergent. On the flanks of the San Jacinto rift -or graben- the upper part of the Ciénaga de Oro and El Carmen formations were deposited. These two formations are the first post-rift deposits in the area (Caro & Spratt, 2003). Sediments typical of these basins include *in situ* pelagic and hemipelagic sedimentation in a deep ocean floor environment.

The Arroyo Alférez section (Initial point: 9° 43' 10.77" N/75° 9' 9.50" E. Final point: 9° 42' 41.31" N/75° 7' 3.67" E) is situated close to Carmen de Bolívar city in Colombia (Fig. 1). The samples taken from the Arroyo Alférez sequence belong to El Carmen Formation. The sediments mostly consist of a massive succession of dark grey silty mudstones with occasional glauconitic sandstone intercalations. 104 samples were chosen for calcareous nannofossil studies. Both the base and the top are barren of calcareous nannofossils. The Carmen de Bolívar, Estratigráfico 4 (X 1566076/Y 886804) section was recovered near to Carmen de Bolívar city in Colombia (Fig. 1). This section consists almost entirely of a massive succession of dark grey silty mudstones. Occasional glauconitic sandstone levels have been reported. Discrete clay-rich layers

and sand layers are present throughout. The upper part of the section is devoid of calcareous nannofossil 183 samples were studied. Both sections were carefully sampled without a systematic interval and are stored at the Instituto Colombiano del Petróleo-Ecopetrol (Colombia).

1.1.2 Site ODP 999

The Caribbean plate currently lies between the North and South American plates at a latitude between 10°N and 18°N. The position and motion of the Caribbean plate prior to recent times have been even more poorly constrained because the plate boundary zones are complex and mainly destructive. Taken together, the recent plate motion estimates and the sparse paleomagnetic data suggest a more southerly position for the Caribbean plate since the late Cretaceous (Acton *et al.*, 2000). In this location ODP 999 was drilled, recovering material from the late Maastrichtian to recent. A comparison of logging records and sediments suggests that a nearly complete boundary sequence was retrieved (Sigurdsson *et al.*, 1997). The composition of this terrigenous sediment is closely linked to the history of the Magdalena Fan, which has grown in response to the uplifting and erosion of the

Andean Cordillera (Shagam, 1975, Benjamin *et al.*, 1987; Case *et al.*, 1990). Growth of the submarine fan has been particularly active since the late Miocene, as evidenced by a marked increase in terrigenous mass accumulation rates. The transition from the mid- to the late-Miocene is distinguished by a sharp reduction in carbonate contents and a marked increase in magnetic susceptibility and in terrigenous mass accumulation rates. This interval is correlative with the late Miocene "carbonate crash" of the central and eastern equatorial Pacific (Farrell *et al.*, 1995; Lyle *et al.*, 1995; Pias *et al.*, 1995). ODP 999 site (12°44.639' N/78°44.360' W) is located on the Mono rise in the Colombian Basin (Western Caribbean) (Fig. 1). The section mainly consists of clay-rich carbonates classified as nannofossil and foraminiferal clayey mixed sediments. Discrete ash layers are found throughout the section. 99 samples were chosen for calcareous nannofossil studies. All samples were taken from Hole 999 A, with no systematic interval. The record is generally continuous and the preservation of the calcareous nannofossils is good.

1.2 Material and techniques

Slides for LM (Light Microscopy) were prepared using the decantation method of Flores & Sierro (1997), which allows homogeneous and comparable data analyses of samples and the possibility of estimating relative coccolith/nannolith abundances to be performed. The analyses were carried out with a Leica DMRXE™ combined with the Leica QWin-Photo-Program™ at magnifications of 1000X, 1250X and 1600X at the University of Salamanca. Selected samples were prepared to estimate the nannofossil preservation state and morphological features with the combined dilution/filtration technique of Backman & Shackleton (1983) and the improved method of Andrúleit (1996) as a standard preparation for SEM (Scanning Electronic Microscopy). SEM investigation was performed with a™CamScan 44 at IFG at a magnification of 5000X. For the taxonomy of *Sphenolithus*, the criteria of Perch-Nielsen (1985), Jordan & Kleijne (1994) and Bown (1998) were adopted (Appendix A).

The abundance of *Sphenolithus* species was coded as follows: A: Abundant (more than 10 nannoliths per field of view), C: Common (6-9 nannoliths per field of view), F:

Few (1-5 nannoliths per field of view), B: Barren/Absent (no record) (Fig. 2). In order to compare the abundance of *Sphenolithus* among other significant taxa in the calcareous nannofossil assemblages (*Reticulofenestra* <5µm and *Discoaster* spp.), a quantitative analysis was carried out, affording the percentages of this group. Also, the total number of nannofossil per gram of dry sediment was calculated to gain an idea about total nannofossil abundance (Flores & Sierro, 1997).

2. SPHENOLITHUS STRATIGRAPHIC RANGE IN NORTHERN COLOMBIA AND THE CARIBBEAN SEA

2.1 Some considerations about *Sphenolithus*

Perch-Nielsen, 1985 commented: "The sphenoliths are nannoliths with a proximal shield or proximal column, one or several tiers of lateral elements and an apical or distal structure which is often elongate and sometimes bifurcating". *Sphenolithus* are a useful stratigraphic marker because of their short time distribution. The only exception is perhaps *Sphenolithus moriformis*, a generally abundant species which, however, is the most common sphenolith in the material studied. *Sphenoliths* can be identified readily with crossed nicols (LM) due to the different figures observed at 0° and 45°. Perch-Nielsen (1972, 1985) noted that *Sphenolithus* is more common in relatively shallow-water paleoenvironments, and Edwards (1971) and Pospichal *et al.* (1992) confined these species to low latitudes, which restricts their biostratigraphic value. However, although some of the datum events were not consistent or statistically reliable (Olafsson & Villa, 1992), *Sphenolithus* is a very important taxon for Oligocene and Miocene stratigraphies.

Biostratigraphic events based on *Sphenolithus* were used by Bergreen *et al.* (1995) to approximate magnetostratigraphic units. Other authors (e.g., Hilgen, 1991a, b; Langeris & Hilgen, 1991; Lourens *et al.*, 1992; Raffi *et al.*, 2006) also used events involving *Sphenolithus* for the calibration of the astrochronologic timescale in the Mediterranean and other oceanic sequences (Abels *et al.*, 2005;

Raffi *et al.*, 2006; Di Stefano *et al.*, 2008; Hüsing *et al.*, 2010; among others).

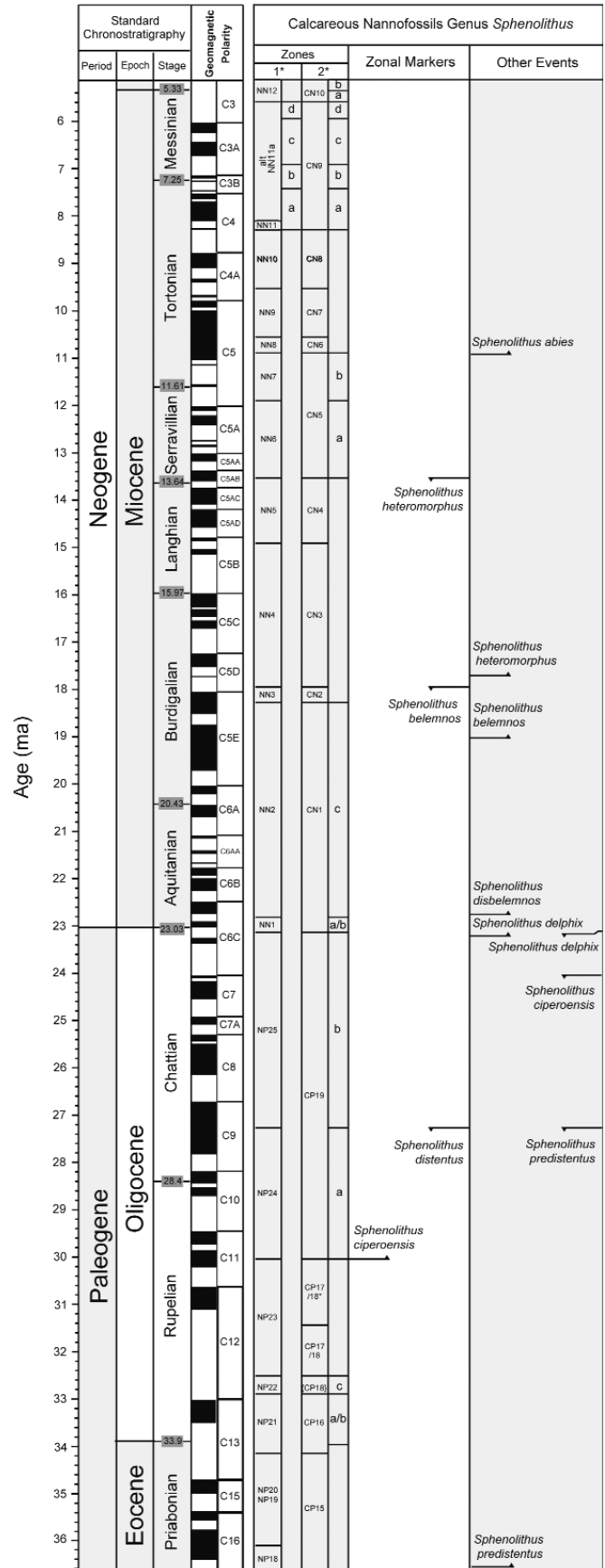
Another important contribution of *Sphenolithus* is the use of this taxon for the estimation of chronostratigraphic boundaries. In fact, the Oligocene-Miocene boundary was defined in the Lemme-Carrosio section in northern Italy by the Last Occurrence (LO) of *Sphenolithus ciproensis*; the LO of *Sphenolithus delphix*; the LO and Highest Occurrence (HO) of *Sphenolithus capricornutus* and the HO of *S. delphix*. Some authors (e.g. Maiorano & Monechi, 1998; Fornaciari & Agnini, 2009) have proposed new species of *Sphenolithus* (e.g. *Sphenolithus milanetti*, *Sphenolithus tintinnabulum*, *Sphenolithus pseudoheteromorphus*), but their stratigraphic significance is still under debate.

2.2 Biochronology

This study adopted the 'Astronomically Tuned Neogene Time Scale' (ATNTS2004) (Lourens *et al.*, 2004), improved by Lisiecki & Raymo (2005) and Hüsing *et al.* (2007, 2010). From the late Eocene to the late Oligocene there is no orbitally tuned time scale available. For this interval, the calibration of *Sphenolithus* events has been established by direct correlations with paleomagnetic scales (Berggren *et al.*, 1985). After the FO/LO of *S. delphix* at the Oligocene/Miocene boundary, the horizons are based on the new calibrations obtained in the tuned interval by Raffi *et al.* (2006). In recent years, mid-late Miocene nannofossil events have been re-calibrated in Mediterranean sequences (Hüsing *et al.*, 2007, 2010), but in general the ages calculated are younger than the data obtained at Atlantic sites. Only one datum, the LO of *S. capricornutus* (recorded in the Carmen de Bolívar, Estratigráfico 4 section), was considered here.

Table 1 shows a list of the *Sphenolithus* events that define the zonal boundaries reported in Figure 2, together with estimations of their ages. The presence of two intervals of

Figure 2. Stratigraphic distribution of *Sphenolithus*. Standard calcareous nannoplankton zonation: 1*, Martini (1971) and 2*, Bukry (1973, 1975) and Okada & Bukry (1980). In this table only standard biostratigraphical *Sphenolithus* markers have been included, as well as other significant *Sphenolithus* events. Chronostratigraphy modified of the International Commission on Stratigraphy (www.stratigraphy.com).



high abundance of *S. heteromorphus*, clearly marked in the Carmen de Bolívar, Estratigráfico 4 section and at ODP Site 999, allows the acme of *S. heteromorphus* to be defined. There are no calibrated events near this acme interval, but in both sections a high abundance is recorded before the FO of *Discoaster signus* (15.702 Ma; Raffi *et al.*, 2006) and the LO of *Helicosphaera ampliaperata* (14.914 Ma; Raffi *et al.*, 2006). This biochronology agrees with that reported in previous studies (Berggren *et al.*, 1985; Kameo & Bralower, 2000; Raffi *et al.*, 2006). It is important to note the hiatuses in the stratigraphic record in the shallow sequences (Arroyo Alférez and Carmen de Bolívar, Estratigráfico 4; Mejía-Molina, in prep.), which, however, do not affect the zonal boundaries. In contrast, the ODP Site 999 shows a continuous record.

3. SPHENOLITHUS IN NORTHERN COLOMBIA AND THE CARIBBEAN SEA

Sphenoliths are present in most of the samples analyzed and represent one of the major constituents of the Cenozoic nannofossil assemblages in the Atlantic Ocean (e.g. Edwards, 1971; Perch-Nielsen, 1985; Pospichal *et al.*, 1992; Raffi & Flores, 1995) and Caribbean sea (Kameo & Bralower, 2000, Mejía-Molina *et al.*, 2006, 2008). In the Colombian Caribbean sections, they are common in Miocene sequences and less abundant during the Eocene and Oligocene (Figs. 3, 4, 5, 6 and 7). Fifteen *Sphenolithus* species were identified in this study (Plates 1 and 2): *S. abies*, *Sphenolithus belemnus*, *Sphenolithus calyculus*, *S. capricornutus*, *S. ciproensis*, *Sphenolithus compactus*, *Sphenolithus conicus*, *S. delphix*, *Sphenolithus disbelemnus*, *Sphenolithus dissimilis*, *Sphenolithus distentus*, *S. moriformis*, *Sphenolithus neoabies*, *S. heteromorphus* and *Sphenolithus predistentus*. *S. abies* and *S. neoabies* have been grouped as *S. abies* in the range charts because of the presence of intermediate forms. The general pattern of *Sphenolithus* is characterized by slight peaks in abundance in some levels. Exceptional abun-

Arroyo Alférez <i>Sphenolithus</i> Event	Sample	Stratigraphic Position (m)	Age (Ma)
FO <i>Sphenolithus heteromorphus</i>	G05-CB-700	1640.625	17.721 (2)
LO <i>Sphenolithus belemnus</i>	G05-CB-700	1640.625	18.921 (2)
FO <i>Sphenolithus belemnus</i>	G05-CB-699	1629.375	
LO <i>Sphenolithus disbelemnus</i>	G05-CB-693	1611.125	
FO <i>Sphenolithus disbelemnus</i>	G05-CB-655	1541.375	
LO <i>Sphenolithus conicus</i>	G05-CB-655	1541.375	
LO <i>Sphenolithus dissimilis</i>	G05-CB-655	1541.375	
FO <i>Sphenolithus conicus</i>	G05-CB-600	1362.750	
LO <i>Sphenolithus ciproensis</i>	G05-CB-571	1314.375	24.75 (1)
LO <i>Sphenolithus distentus</i>	G05-CB-503	1211.375	
LO <i>Sphenolithus predistentus</i>	G05-CB-490	1192.125	27.500 (1)
FO <i>Sphenolithus compactus</i>	G05-CB-443	1082.875	
FO <i>Sphenolithus ciproensis</i>	G05-CB-394	994.625	29.100 (1)
FO <i>Sphenolithus distentus</i>	G05-CB-131	348.875	

Carmen de Bolívar, Estratigráfico 4 <i>Sphenolithus</i> Event	Sample	Depth (m)	Age (Ma)
TA <i>Sphenolithus heteromorphus</i>	E4/73.40 BIO	73.400	
BA <i>Sphenolithus heteromorphus</i>	E4/75.00 BIO	88.700	
FO <i>Sphenolithus heteromorphus</i>	E4/88.70 BIO	88.700	17.721 (2)
LO <i>Sphenolithus belemnus</i>	E4/96.30 BIO	96.300	17.973 (2)
FO <i>Sphenolithus belemnus</i>	E4/119.90 BIO	119.900	18.921 (2)
LO <i>Sphenolithus disbelemnus</i>	E4/125.78 BIO	125.780	22.760 (2)
FO <i>Sphenolithus disbelemnus</i>	E4/135.00	135.000	
LO <i>Sphenolithus conicus</i>	E4/140.00	140.000	
FO <i>Sphenolithus conicus</i>	E4/172.00	172.000	
LO <i>Sphenolithus capricornutus</i>	E4/208.00	208.000	23.700 (3)
LO <i>Sphenolithus calyculus</i>	E4/208.00	208.000	
FO <i>Sphenolithus capricornutus</i>	E4/239.00	239.000	
FO <i>Sphenolithus calyculus</i>	E4/239.00	239.000	
LO <i>Sphenolithus dissimilis</i>	E4/248.00	248.000	

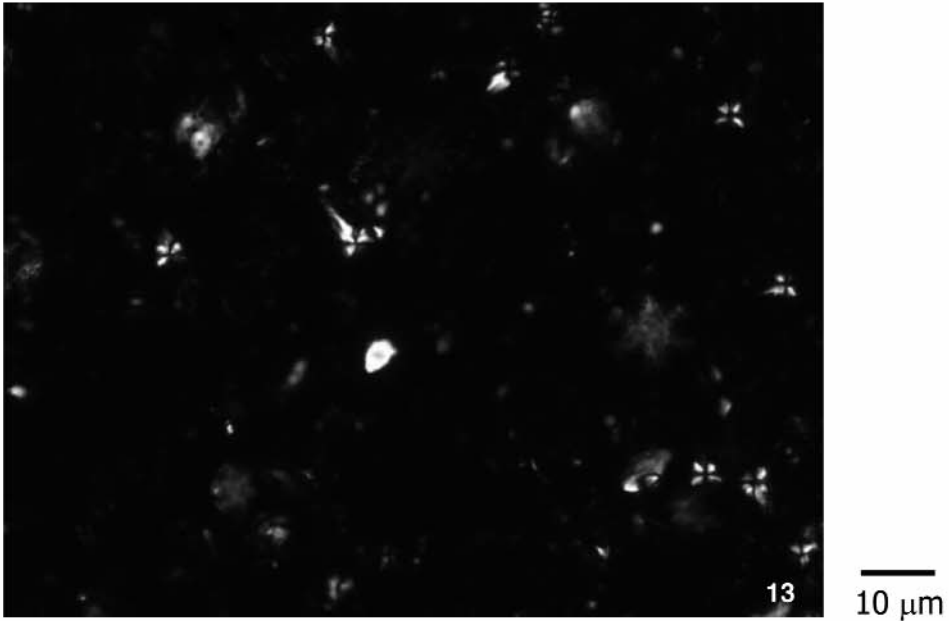
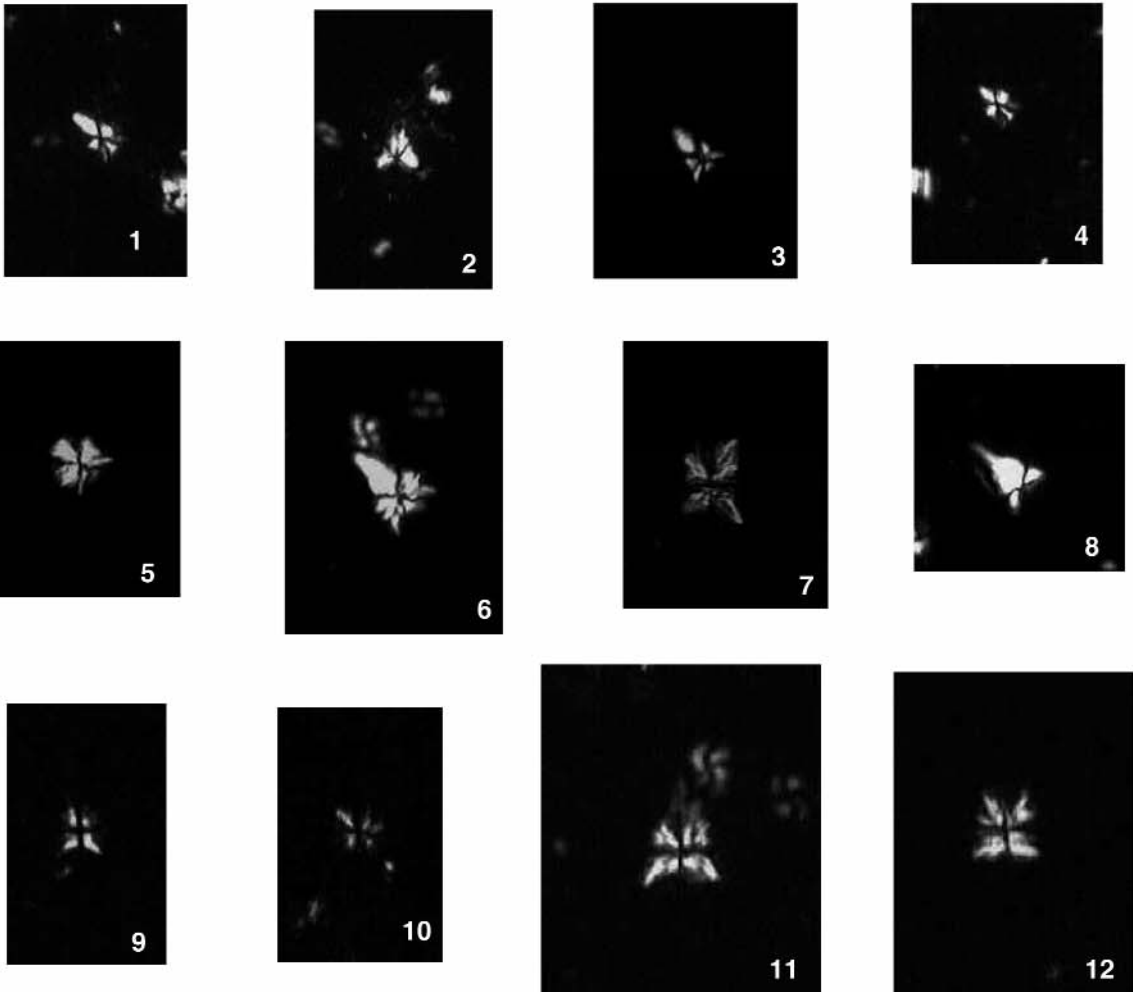
ODP 999 <i>Sphenolithus</i> Event	Core, section, interval (cm) Lower	Depth (mbsf)	Age (Ma)
FO <i>Sphenolithus abies</i>	30X-1, 140	269.40	
LO <i>Sphenolithus heteromorphus</i>	38X-1, 30	345.10	13.532 (2)
TA <i>Sphenolithus heteromorphus</i>	43X-1, 110	394.10	
BA <i>Sphenolithus heteromorphus</i>	45X-1, 110	413.20	
FO <i>Sphenolithus heteromorphus</i>	48X-1, 105	442.15	17.721 (2)
LO <i>Sphenolithus belemnus</i>	49X-1, 45	451.15	17.973 (2)
FO <i>Sphenolithus belemnus</i>	51X-1, 120	471.10	18.921 (2)
LO <i>Sphenolithus disbelemnus</i>	52X-1, 20	479.70	
FO <i>Sphenolithus disbelemnus</i>	52X-1, 105	480.55	22.760 (2)
LO <i>Sphenolithus delphix</i>	53X-1, 125	490.35	23.065 (2)
FO <i>Sphenolithus delphix</i>	55X-1, 5	508.35	23.328 (2)

Table 1. Standard and additional *Sphenolithus* events. Zonal boundaries according to the zonations of Martini (1971) and Bukry (1973, 1975) and Okada & Bukry (1980). Age of *Sphenolithus* horizons by 1, Berggren *et al.* (1985); 2, Raffi *et al.* (2006) and 3, Hüsing *et al.* (2007). FO: first occurrence. LO: last occurrence. BA: base of acme. TA: top of acme.

dances in *S. heteromorphus* were recorded for both the ODP 999 and the Carmen de Bolívar, Estratigráfico 4 sec-

Plate 1. All specimens x 1000 and in crossed nicols. Scale bar equals 10µm. Images 1- 8 from the Arroyo Alférez Section. Images 9-13 from the Carmen de Bolívar, Estratigráfico 4 section. 1, *Sphenolithus belemnus* Bramlette & Wilcoxon, 1967. 2, *Sphenolithus compactus* Backman, 1980. 3, *Sphenolithus conicus* Bukry, 1971. 4, *Sphenolithus disbelemnus* Fornaciari & Rio, 1996. 5, *Sphenolithus dissimilis* Bukry & Percival, 1971. 6, *Sphenolithus heteromorphus* Deflandre, 1953. 7, *Sphenolithus moriformis* (Bronnimann & Stradner, 1960) Bramlette & Wilcoxon, 1967. 8, *Sphenolithus predistentus* Bramlette & Wilcoxon, 1967. 9, *Sphenolithus calyculus* at 0° Bukry, 1985. 10, *Sphenolithus calyculus* at 45° Bukry, 1985. 11, *Sphenolithus heteromorphus* Deflandre, 1953. 12, *Sphenolithus moriformis* (Bronnimann & Stradner, 1960) Bramlette & Wilcoxon, 1967. 13, field of view of *Sphenolithus heteromorphus* SDI.

Plate 1



tions. Also, a very high abundance of *S. abies* was observed for ODP Site 999. Both *S. heteromorphus* and *S. abies* became the dominant component of the nannofossil assemblage during the mid-Miocene.

3.1 The Arroyo Alférez onshore section

The Arroyo Alférez section represents a shallow sequence in the area, mainly characterized by a foraminiferal assemblage probably indicative of a slope environment under the influence of dysoxic conditions (Fiorini & Jaramillo, 2006). The bottom is devoid of calcareous nannofossils (Fig. 3). Only small specimens of *S. moriformis* show a common abundance the record. The species identified in the late-Eocene interval were *S. distentus*, *S. moriformis* and *S. predistentus* (Plate 1). Their general abundance is common, except for *S. distentus*. The specimens are very small-to-moderate in size. In some intervals of the late Eocene the differences between *S. predistentus* and *S. distentus* are not evident. This is because *S. distentus* is normally rare and its diverging branches are partially or totally broken. Despite this, *S.*

distentus has a shorter main body and more birrefringent and less acute angle in the proximal cycle elements at cross nicols. In the Eocene/Oligocene transition [NP25 (CP19)/NN1 (CN1), Martini (1971), Okada & Bukry (1980)], its abundance increases slightly (Fig. 3) (see Appendix A).

Sphenolithus was more diverse and abundant during the Oligocene (Fig 4). The assemblage consists of *S. ciproensis*, *S. compactus*, *S. distentus*, *S. dissimilis*, *S. moriformis* and *S. predistentus*. This interval shows some transitional forms, probably directly related to the *S. predistentus-distentus-ciproensis* lineage. Particular difficulties in identifying transitional forms have been documented by other researchers (e.g Roth *et al.*, 1970; Haq, 1971; Moran & Watkins, 1988; Okada, 1990; Olafsson & Villa, 1992). Moderate-sized specimens are few-to-common in the record. However, an increase in *Sphenolithus* spp. can be noted at the end of the Oligocene (Fig 4). Small-to-medium sized specimens of *S. compactus* and *S. moriformis* are common (see Appendix A). The distribution of *S. ciproensis* and *S. predistentus* does not reveal important absences in the record, except at the beginning of the

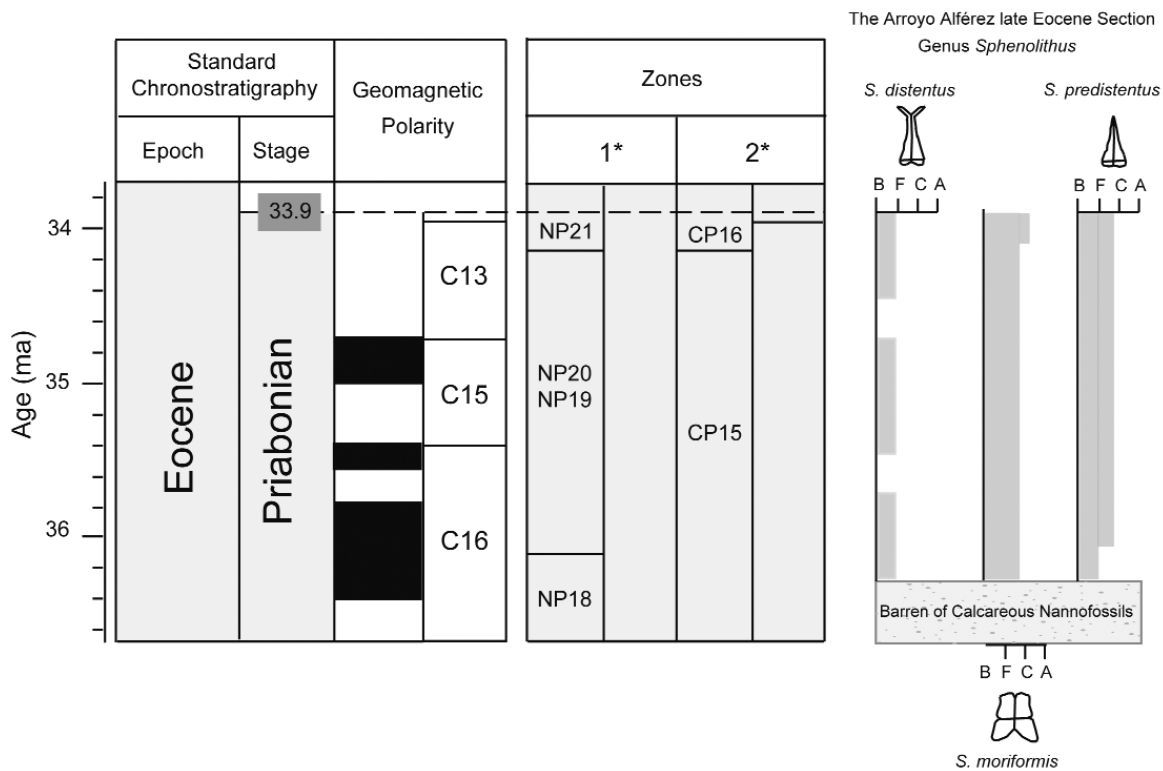


Figure 3. Distribution of *Sphenolithus* during the late Eocene in Arroyo Alférez section. A: Abundant, C: Common, F: Few, B: Barren/Absent (see text). Dotted grey bar correspond to calcareous nannofossil barren intervals.

Oligocene. The stratigraphic position of *S. ciproensis* was not hard to identify because the specimens are well preserved. *S. distentus* is rare in the record and is poorly preserved.

The distribution of *Sphenolithus* during the Miocene is characterized by slight peaks in abundance in some levels, but this genus is never the dominant component of the nannofossil assemblage. These taxa reach a maximum in the mid-

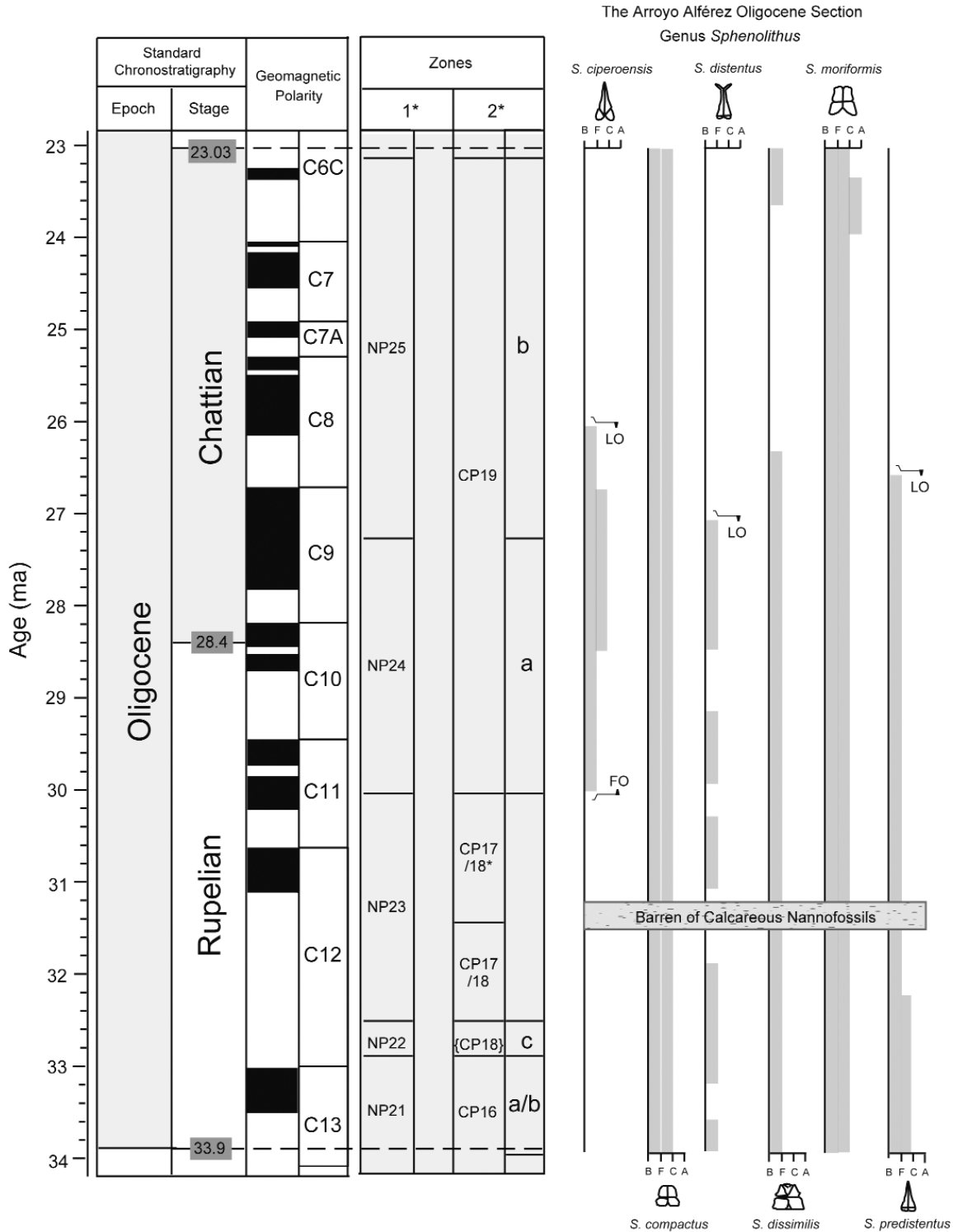


Figure 4. Distribution of *Sphenolithus* during the Oligocene in Arroyo Alferez section. A: Abundant, C: Common, F: Few, B: Barren/Absent (see text). Dotted grey bar correspond to calcareous nannofossil barren intervals.

Miocene (*S. heteromorphus* and *S. moriformis*) (Fig. 5). Few specimens of *S. belemnos*, *S. compactus*, *S. conicus*, *S. disbelemnos*, *S. dissimilis* are recorded. Less relevant peaks of abundance of small specimens of *S. moriformis* and *S. heteromorphus* are characteristic of the mid-late Miocene. We observed that *Sphenolithus* spp. were notably smaller than the original descriptions (lesser than 2-4µm). Exceptions occur at the beginning of the Miocene, where *S. moriformis* includes specimens larger than 12 µm, well preserved and strongly birrefringent (Fig. 5).

3.2 The Carmen de Bolívar, Estratigráfico 4 onshore section

The Carmen de Bolívar, Estratigráfico 4 section is located between the shallower sequence (Arroyo Alférez) and the open marine core (ODP 999). Pelagic and hemipelagic sediments from the Carmen de Bolívar, Estratigráfico 4 section were deposited in a deep-ocean environment (Caro & Spratt, 2003), covering an interval from the Oligocene/Miocene boundary to the mid-Miocene (Fig. 6). The species identi-

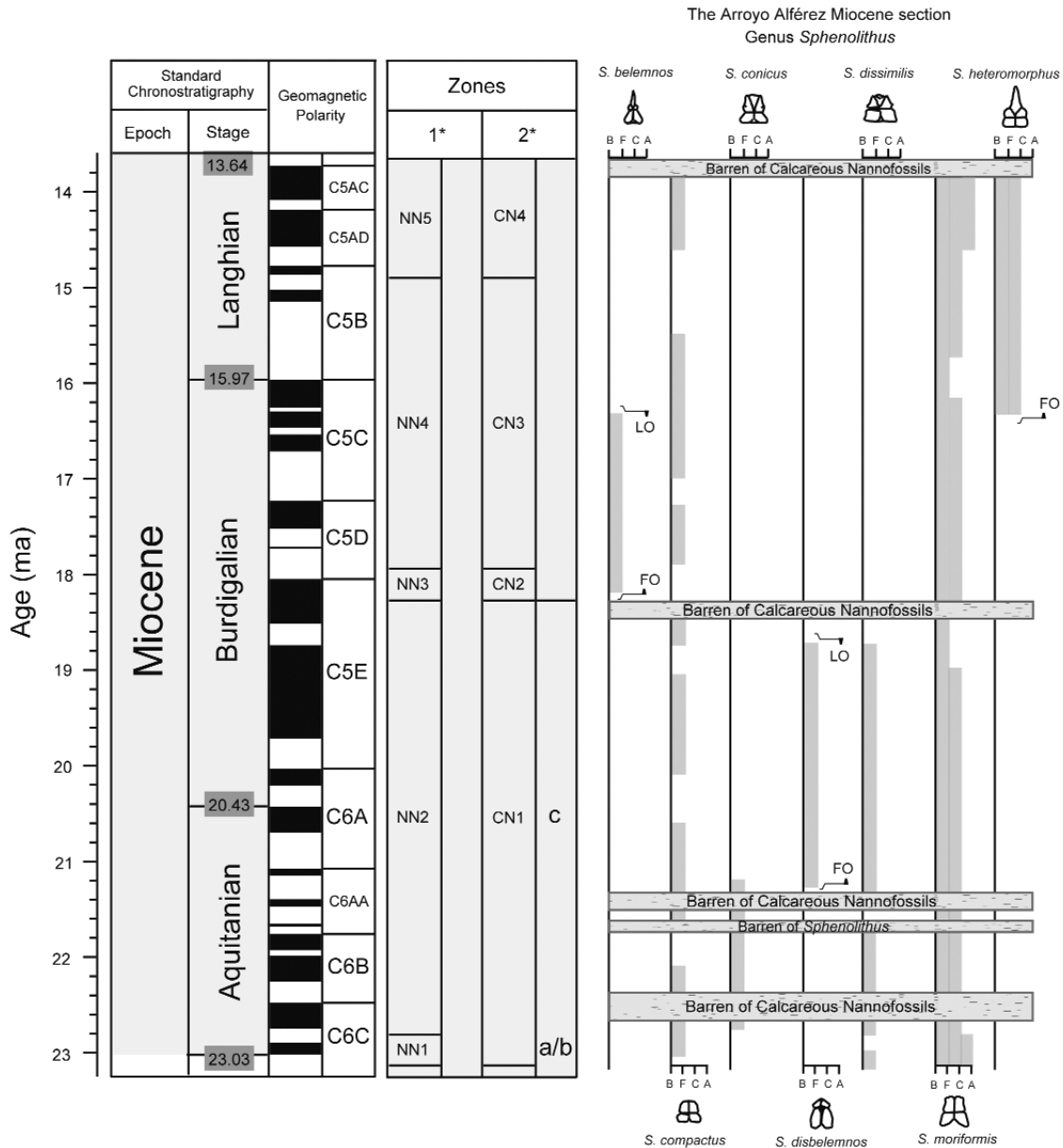


Figure 5. Distribution of *Sphenolithus* during the Miocene in Arroyo Alférez section. A: Abundant, C: Common, F: Few, B: Barren/Absent (see text). Dotted grey bar correspond to calcareous nannofossil barren intervals.

fied were *S. belemnus*, *S. calyculus*, *S. capricornutus*, *S. compactus*, *S. conicus*, *S. disbelemnus*, *S. dissimilis*, *S. moriformis* and *S. heteromorphus*. *S. moriformis* and the typical spined *S. heteromorphus* are abundant. The mean size of *Sphenolithus* coincides with the original descriptions (Appendix A). Some exceptions were observed in *S. moriformis* and *S. heteromorphus*, which are bigger in some intervals. In the lowermost early Miocene, we recognized small *S.*

capricornutus and *S. calyculus*. *S. capricornutus* occurs in low proportions, and its divergent apical spine is broken or notched. Irregular distributions (divergent apical spine broken or overgrown) are typical in *S. disbelemnus* and *S. conicus*. The most significant *Sphenolithus* event is located in Zone CN3 (NN4), characterized by an interval of high abundance of *S. heteromorphus* (acme zone) and a broad range of sizes (Fig. 6) (Plate 2).

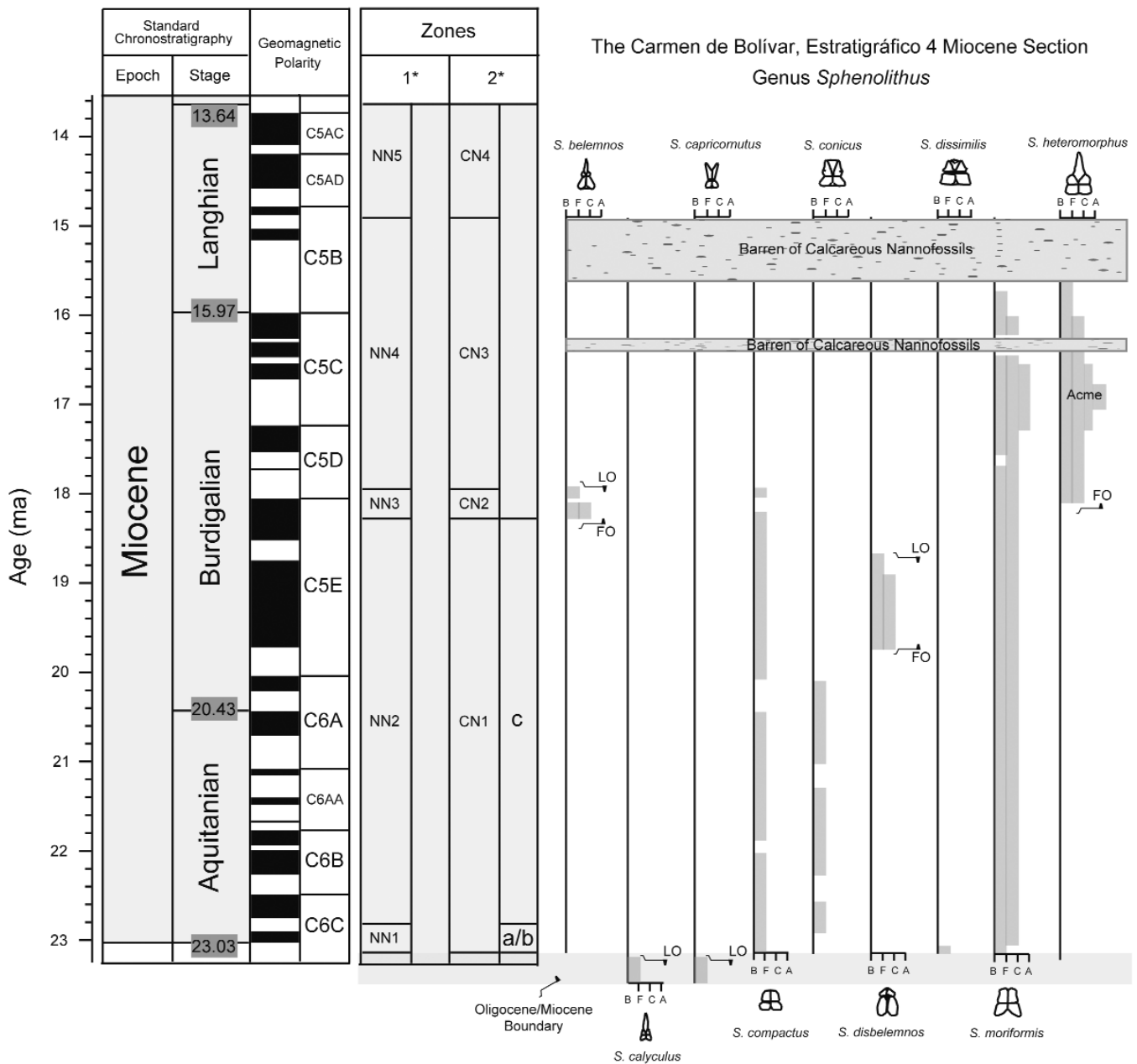


Figure 6. Distribution of *Sphenolithus* during the Miocene in Carmen de Bolívar, Estratigráfico 4 section. A: Abundant, C: Common, F: Few, B: Barren/Absent (see text). Dotted grey bar correspond to calcareous nannofossil barren intervals.

3.3 ODP Site 999

ODP Site 999 is located in the Colombian Basin, in the Mono Rise region, a surface area associated with open-ocean productivity. *Sphenolithus* is common, and the species identified are *S. abies*, *S. belemnos*, *S. compactus*, *S. conicus*, *S. delphix*, *S. disbelemnos*, *S. moriformis* and *S. heteromorphus* (Fig. 7). Two exceptional events were recognized: the high abundance intervals of *S. heteromorphus* (in the mid-Miocene) and those of *S. abies* (in the late Miocene). The size of *Sphenolithus* is normal or slightly larger (1-2 μm) than the original descriptions (Appendix A). In some intervals, poorly preserved specimens were frequent, coinciding with a marked decrease in total calcareous nannofossil abundance. *S. conicus*, *S. compactus* and *S. disbelemnos* were observed consistently, but in low abundances. The specimens of *S. moriformis* of normal size (4-7 μm) show a common abundance and exhibit a good preservation until its last occurrence in the late Miocene. Well preserved specimens of *S. belemnos* are common during its stratigraphic range (early Miocene). This species shows large, thin branches, sometimes partially broken (Plate 2, Appendix A).

4. EARLY MIOCENE TO LATE MIOCENE PALEOCEANOGRAPHIC EVOLUTION

The Cenozoic is characterized by a long-term global cooling trend from early Paleogene ice-free 'greenhouse' conditions towards the Neogene 'icehouse' regime (Zachos *et al.*, 2001). The mid-Miocene climate transition was a major cooling step in the Cenozoic climate (Zachos *et al.*, 2001). The warm phase of the early Miocene peaked in the Middle Miocene Climatic Optimum (MMCO; 17-14.5 Ma), followed by a long-term cooling trend (mid- to late-Miocene). The pronounced global cooling of the late Miocene marks a turning point in climate history (Shackleton & Kennett, 1975). The early- to mid-Pliocene represents the most recent period in the Earth's history of sustained global warmth (e.g. Dowsett *et al.*, 1992; Ravello & Andreasen, 2000; Billups & Schrag, 2002), preceding the dramatic cooling associated with the onset of Northern Hemisphere Glaciation (NHG) at 2.74 Ma (Raymo *et al.*, 1996; Dowsett *et al.*, 1999; Bartoli *et al.*, 2005).

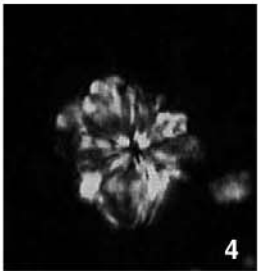
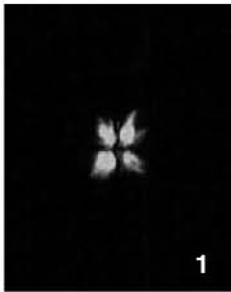
The calcareous nannofossil assemblages identified in the Caribbean sequences reflect variations in sea surface conditions and variations in the basins. Here, the relationship among *Sphenolithus* spp., *Reticulofenestra* <5 μm and *Discoaster* spp is considered. The Arroyo Alférez section, covering an interval between the late Eocene and the early Miocene, is not considered because of its discontinuity. Consequently, the oceanographic analysis is focused on the early Miocene to the late Miocene recorded in the Carmen de Bolívar, Estratigráfico 4 and Site ODP 999 sections.

4.1 Paleoproductivity proxies

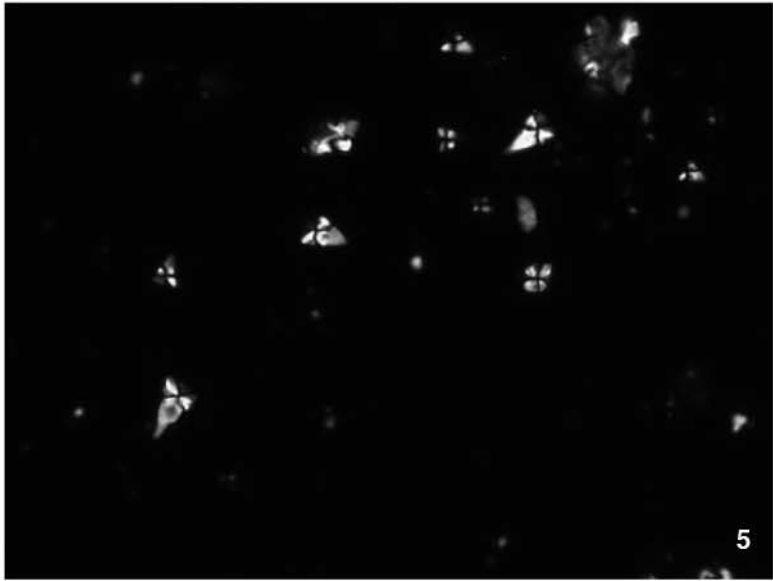
In the present work, the total number of nannoliths per gram of dry sediment is considered as a paleoproductivity proxy, although the absence of dry density data prevents the calculation of nannofossil fluxes (Flores *et al.*, 2005). Here, the exceptional abundance of *Sphenolithus* spp. is referred to as the SDI (*Sphenolithus* Dominance Interval). During the SDI, an extreme reduction in small reticulofenestrids (mainly *R. minuta* and *R. minutula*) occurred. Within this stratigraphic interval, *Discoaster* spp. was often strongly overgrown, preventing recognition at species level. At the same time, a reduction in the size of *Sphenolithus* spp took place (Figs 8 and 9).

From the paleoecological point of view, *Sphenolithus* is considered to be a genus confined to warm, well oxygenated surface waters and to open marine environments (Aubry, 1992; Fornaciari *et al.*, 1996); it is a reliable indicator of warm-temperature surface waters (Bukry, 1973; Wei & Wise, 1989; Marzouk & Soliman, 2004); it is characteristic in low-latitude warm water assemblages (Haq & Lohmann, 1976; Haq, 1980; Lohmann & Carlson, 1981), and it is more common in relatively shallow-water paleoenvironments (Perch-Nielsen, 1972, 1985). *Sphenolithus*

Plate 2. All specimens x 1000 and in crossed nicols. Scale bar equals 10 μm . All images from the ODP 999 core. 1, *Sphenolithus abies* Deflandre in Deflandre & Fert, 1954. 2, *Sphenolithus belemnos* Bramlette & Wilcoxon, 1967. 3, *Sphenolithus heteromorphus* Deflandre, 1953. 4, *Sphenolithus moriformis* (Bronnimann & Stradner, 1960) Bramlette & Wilcoxon, 1967. 5, field of view of *Sphenolithus heteromorphus* SDI. 6, field of view of *Sphenolithus abies* SDI.



10 μ m



10 μ m



10 μ m

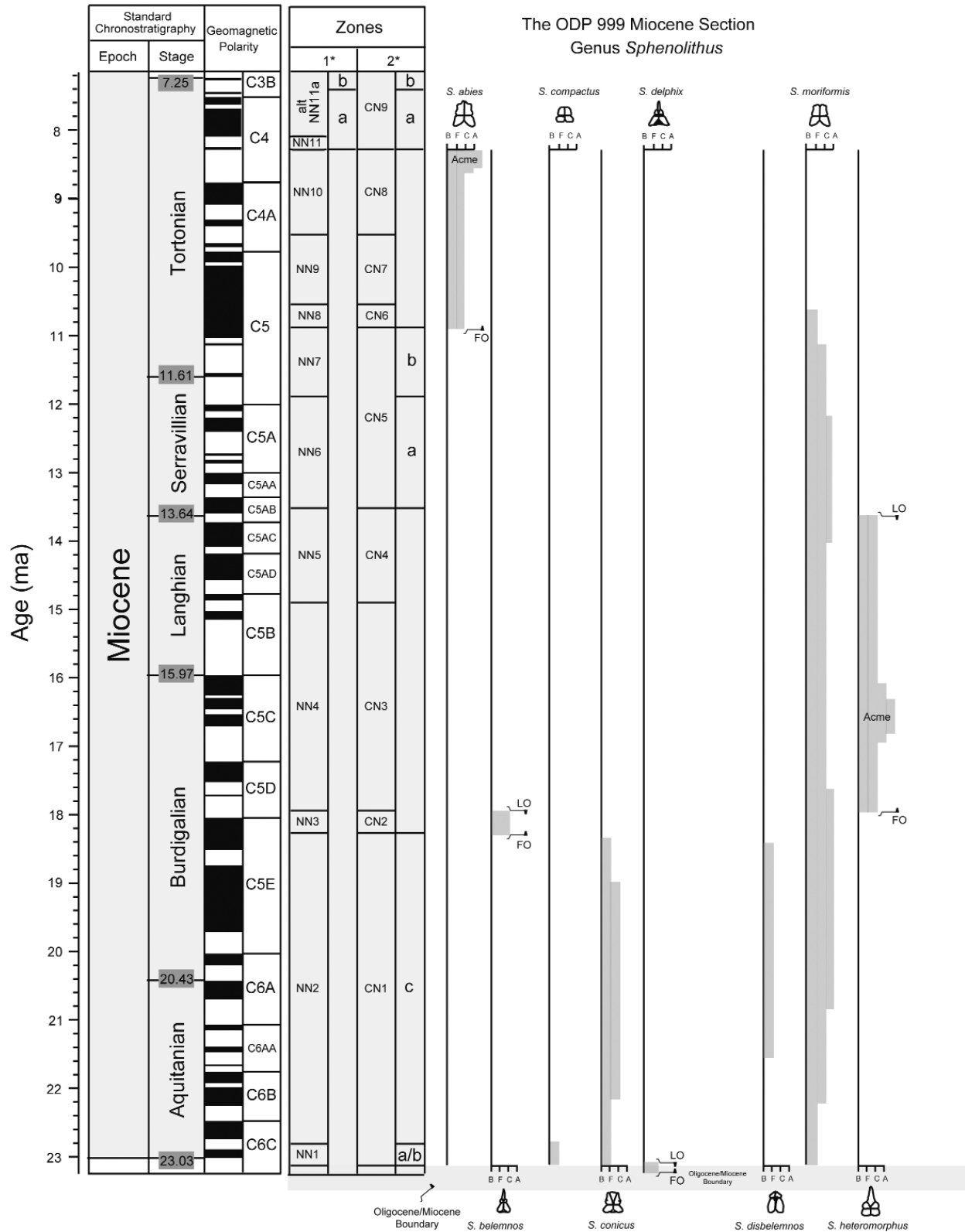


Figure 7. Distribution of *Sphenolithus* during the Miocene in ODP 999 section. A: Abundant, C: Common, F: Few, B: Barren/Absent (see text).

is scarce-to-rare in high latitudes (Edwards, 1971; Perch-Nielsen, 1985; Pospichal *et al.*, 1992), and is considered a k-selected (“specialist”) taxon adapted to oligotrophic and warm-water environments (Haq & Lohmann, 1976; Chepstow-Lusty *et al.*, 1992). This genus is considered to be a warm-oligotrophic one (Haq & Lohmann, 1976; Lohmann & Carlson, 1981; Flores & Sierro, 1987; Flores *et al.*, 1995; Castradori, 1998 and Flores *et al.*, 2005). Like *Sphenolithus*, *Discoaster* is more abundant in warmer conditions (Bukry, 1973; Haq & Lohmann, 1976; Haq, 1980; Lohmann & Carlson, 1981; Wei & Wise, 1989; Marzouk & Soliman, 2004).

Studies carried out on modern assemblages have reported the opportunistic behaviour of “small placoliths” (i.e. small reticulofenestrids, Okada & Honjo, 1973) in the Pacific Ocean. However, small Noelaerhabdaceae increase their abundance in upwelling regions (Okada & Honjo, 1973; Biekart, 1989; Okada & Wells, 1997; Negri & Villa 2000; Flores *et al.*, 2000) and during periods of high fertility (Biekart, 1989). In agreement with this, the small reticulofenestrid group is also considered a eutrophic taxon. In contrast, low abundances of reticulofenestrids are consistent with water stratification (Flores *et al.*, 2000).

4.2 Fluctuations in abundance patterns

The percentages of *Sphenolithus* in the Carmen de Bolívar, Estratigráfico 4 section varies from 1% (early Miocene) to ~20% (mid-Miocene). The maximum abundance of *S. heteromorphus* is recorded in the mid-Miocene (Fig. 8). Here, *S. heteromorphus* has percentages close to 80%. The dominance of small specimens of *S. heteromorphus* is observed at the acme interval (Fig. 8). *Reticulofenestra* <5µm is the most abundant taxon, with percentages close to 80%, except for two strong negative peaks (~2% and ~10%, respectively) recorded in the mid-Miocene. These low records are synchronous with the maxima of *S. heteromorphus*. The percentages of *Discoaster* spp. vary, ranging from 5% to 15%.

During the mid-Miocene to the end of the late Miocene, the total number of calcareous nannofossil per gram in the Carmen de Bolívar, Estratigráfico 4 section is low. This trend is well correlated with the increase in the percentages of *Sphenolithus* spp., *S. heteromorphus* and *Discoaster* spp. At the same time, the opposite trend is observed with *Reticulofenestra* <5µm. The maximum in total nannofossils per gram was reached in the early/mid-

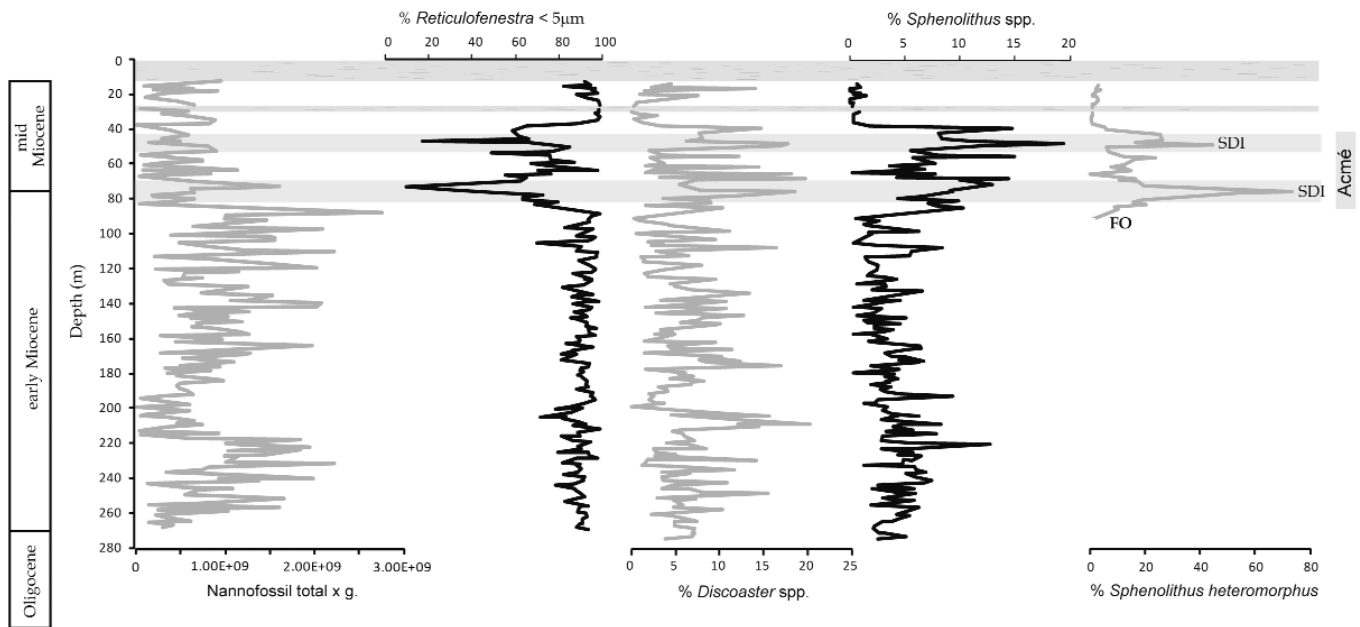


Figure 8. Percentages of *Reticulofenestra* <5µm, *Discoaster* spp., *Sphenolithus* spp., *Sphenolithus abies*, *Sphenolithus heteromorphus* and total nannofossils per gram in the Carmen de Bolívar, Estratigráfico 4. Grey bar correspond to calcareous nannofossil barren intervals. FO, first occurrence; SDI, *Sphenolithus* Dominance Interval.

Miocene transition, after the FO of *S. heteromorphus*. This maximum records a progressive decrease in *Reticulofenestra* <5µm and a slight increase in *Discoaster* spp. (~12%) and *Sphenolithus* spp. (~12%) (Fig. 8). During the SDI of *S. heteromorphus* the total number of nannofossil per gram is low

At ODP Site 999, the percentages of *Sphenolithus* spp. Vary from 1% to ~22% (Fig. 9). *Reticulofenestra* <5µm is the most abundant morphotype, showing percentages close to 70%, except in three levels of strong decrease, when the percentages falls to the minimum (1%). At the beginning of the mid-Miocene, two SDI (~60% and ~85%) of *S. heteromorphus* were observed (Fig. 9); simultaneously, an important decrease in *Reticulofenestra* <5µm was observed. *Discoaster* spp. Shows the same trend as that seen for *S. heteromorphus*, two positive peaks being identified (26% and ~36%) (Fig. 9). The interval between the top of the mid-Miocene to the late Miocene records the lowest abundances of *Sphenolithus* spp. (~1%) and *Discoaster* spp. (~2%). This is consistent with the maximum of *Reticulofenestra* <5µm (~98%). Another SDI of *S. abies* can be identified during the late Miocene. In this level, *Reticulofenestra* <5µm is almost absent (Fig. 9).

At ODP Site 999, the sediments have been described as nannofossil clay deposited continuously during the inter-

val studied (Sigurdsson *et al.*, 1997; Kameo & Bralower *et al.*, 2000). This allows us to assume that the accumulation rate did not undergo significant changes and, in view of the absence of siliceous and terrigenous materials, the total number of nannofossils per gram of dry sediment is a potential proxy for productivity. The most important peak in the total number of nannofossils per gram –at the beginning of the early Miocene- coincides with peaks in *Discoaster* spp. And *Sphenolithus* spp.; simultaneously *Reticulofenestra* <5µm decreases (Fig. 9). During the SDI episodes –in the mid-Miocene- the total number of nannofossil per gram is low. The minimum recorded at the top of mid-Miocene coincides with the increase in *Reticulofenestra* <5µm. This interval shows the poorest preservation. The maximum in the total number of nannofossils per gram occurs at the beginning of the late Miocene. This event corresponds to an SDI of *S. abies* and a dramatic reduction in *Reticulofenestra* <5µm.

4.3 Paleooceanographic evolution in Northern Colombia and the Caribbean Sea

Pulses in the abundance of *Sphenolithus* in the Carmen de Bolívar, Estratigráfico 4 and ODP 999 sections reflect supra-orbital intervals of oligotrophic conditions during the

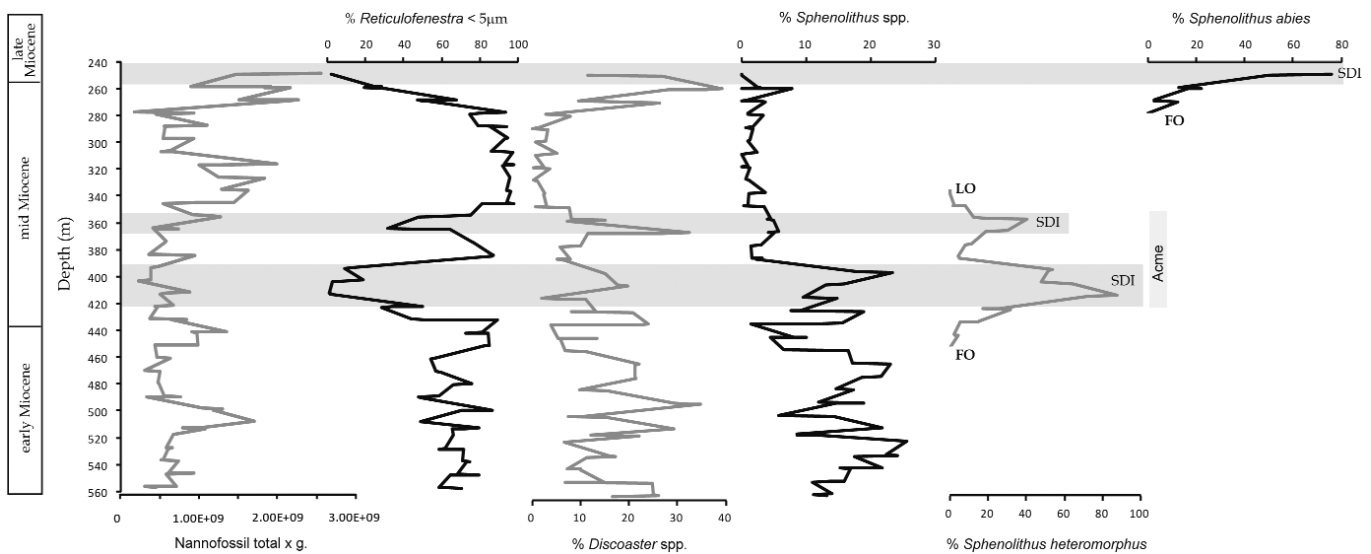


Figure 9. Percentages of *Reticulofenestra* <5µm, *Discoaster* spp., *Sphenolithus* spp., *Sphenolithus heteromorphus* and total of nannofossils per gram in ODP 999. FO: first occurrence; LO: last occurrence; SDI, *Sphenolithus* Dominance Interval.

mid- and late Miocene. This is supported by the opposite trend of *Reticulofenestra* <5µm (an “*r-selected*” species and a proxy for eutrophic conditions). However, no direct correlation between the abundances of *Discoaster* spp. With *Reticulofenestra* <5µm and *Sphenolithus* spp. Was observed. The correlation between the abundance of *Sphenolithus* and *Discoaster* during the SDI suggests a similar behaviour. Other SDI were observed in other species such as *S. distentus*, represented by small-to-medium-sized specimens and the absence of reticulofenestrads in the Oligocene of the Arabian sea (Flores *et al.*, in prep.). Raffi & Flores (1995) reported high-abundance intervals of *S. heteromorphus* in Miocene sediments from material recovered during ODP Leg 138 (Guatemala Basin).

The abundance of *Sphenolithus* in all the sequences corresponds to an increase in surface water temperatures and oligotrophy, related to the warming peak that occurred in the Middle Miocene Climatic Optimum (Flower & Kennett, 1994; Zachos *et al.*, 1994; Flower, 1999; Zachos *et al.*, 2001, Marzouk & Soliman, 2004; Zachos *et al.*, 2005). This episode occurred after the FO of *S. heteromorphus* and before the LO of *H. ampliaperta*, at 17.721 Ma and 14.914 Ma (Raffi *et al.*, 2006), respectively. According to this proposal, the SDI defined in the Northern Colombian and the Caribbean Sea sections during the Miocene represent episodes of warm and oligotrophic surface water conditions in both shallow and open water environments.

5. CONCLUSIONS

Sphenoliths are a major constituent of the Cenozoic nannofossil assemblages in the Caribbean Sea; they were more abundant during the Miocene and were common during the Paleogene. A total of 15 species of *Sphenolithus* has been identified, spanning from the late Eocene to the late Miocene. Few *Sphenolithus* Dominance Intervals (SDI), characterized by high abundances, are recognized in either shallow or open ocean sections.

The record of *Sphenolithus* is considered a proxy to monitor variations in temperature and water stratification, owing to its relationship with warm and oligotrophic conditions.

The mid-Miocene reflects supra-orbital shifts of eutrophic and oligotrophic conditions, marked by dramatic changes in *Reticulofenestra* <5µm and sphenolith abundances. Two SDI of *S. heteromorphus* have been identified in the Carmen de Bolívar, Estratigráfico 4 and ODP 999 sequences, corresponding to an intense oligotrophication of the basins, associated with the *Middle Miocene Climatic Optimum* (17-14.5 Ma). The end of the mid-Miocene is characterized by a sharp reduction in calcareous nannofossil abundance and poor preservation. This interval could be correlative with the mid-late Miocene “*carbonate crash*” (Farrell *et al.*, 1995; Lyle *et al.*, 1995; Pisias *et al.*, 1995).

At the beginning of the late Miocene, an SDI of *S. abies* can be identified in ODP Site 999, coinciding with a decrease in *Reticulofenestra* <5µm and interpreted as another relevant oligotrophic episode.

6. ACKNOWLEDGEMENTS

Valuable comments of Dr. Mario Cachão and Dra. Ornella Amore are gratefully acknowledged. The Instituto Colombiano del Petróleo-Ecopetrol, Colombian staff is thankfully acknowledged, especially Maria Carolina Vargas for their valuable effort in the development of this project. This research was supported by the Colombian Project Convenio de cooperación tecnológica USAL-ECOPETROL (001 de 2007). The samples used in this study were provided by the IODP (Integrated Ocean Drilling Program) and ICP-Ecopetrol, Colombia.

7. REFERENCES

- Abels, H.A., Hilgen, F.J., Krijgsman, W., Kruk, R.W., Raffi, I., Turco, E., and Zachariasse, W.J. 2005. Long-period orbital control on middle Miocene global cooling: integrated stratigraphy and astronomical tuning of the Blue Clay Formation on Malta. *Paleoceanography*, 20, PA4012.
- Acton, G.D., Galbrun, B., and King, J.W. 2000. Paleolatitude of the Caribbean Plate since the Late Cretaceous. Proceedings of the Ocean Drilling Program, Scientific Results, 149-173.
- Andrulleit, H. 1996. A filtration technique for quantitative studies of coccoliths. *Micropaleontology* 42, 403-406.
- Aubry, M.-P. 1992. Late Paleogene calcareous nannoplankton evolution:

- a tale of climatic deterioration. In: *The Eocene-Oligocene Climatic and Biotic Changes*. Prothero, D. & Berggren, W. A. (Eds). Princeton University Press, 272-309.
- Backman, J., and Shackleton, N.J. 1983. Quantitative biochronology of Pliocene and Early Pleistocene calcareous nannofossils from the Atlantic, Indian and Pacific oceans. *Marine Micropaleontology*, 8, 141-170.
- Bartoli, G., Sarnthein, M., Weinelt, M., Erlenkeuser, H., Garbe-Schönberg, D., and 2005. Final closure of Panama and the onset of northern hemisphere glaciation. *Earth and Planetary Science Letters*, 237 (1-2), 33-44.
- Benjamin, M., Johnson, N.M., and Naeser, C.W. 1987. Recent rapid uplift in the Bolivian Andes: evidence from fission-track dating. *Geology*, 15, 680-683.
- Berggren W. A., Kent D. V., Swisher C. C., and Aubry M. P. 1995. A revised Cenozoic geochronology and chronostratigraphy. In: *Geochronology, Time Scales and Global Stratigraphic Correlation* (W. Berggren, D. Kent, M. Aubry & J. Hardenbol, eds). Society for Sedimentary Geology Special Publications, 54, 129-212.
- Biekart, J.W. 1989. The distribution of calcareous nannoplankton in Late Quaternary sediments collected by the Snellius II Expedition in some southeast Indonesian basins. *Proceedings of the Koninklijke Nederlandse Akademie Van Wetenschappen Series B-Palaeontology Geology Physics Chemistry Anthropology*, 92, 77-141.
- Billups, K., and Schrag, D.P. 2002. Paleotemperatures and ice volume of the past 27 Myr revisited with paired Mg/Ca and $^{18}\text{O}/^{16}\text{O}$ measurements on benthic foraminifera. *Paleoceanography*, 17, 3-1.
- Bown, P.R. 1998. *Calcareous Nannofossil Biostratigraphy* (Paul Bown, ed). Chapman & Hall, 315 pp.
- Brand, L.E. 1994. Physiological ecology of marine coccolithophores. In: Winter, A. & Siesser, W. (Eds.), *Coccolithophores*. Cambridge University Press, Cambridge, 39-49.
- Bukry, D. 1973. Coccolith and silicoflagellate stratigraphy, Tasman Sea and Southern Pacific Ocean, Deep Sea Drilling Project Leg21. *Initial Report of the Deep Sea Drilling Project*, 21, 885-893.
- Bukry, D. 1975. Coccolith and silicoflagellate stratigraphy, northwestern Pacific Ocean, Deep Sea Drilling Project, Leg 32. *Initial Reports of the Deep Sea Drilling Project*, 32, 677-701.
- Caro, M., and Spratt, D. 2003. Tectonic evolution of the San Jacinto fold belt, NW Colombia. *Canadian Society of Exploration Geophysicists Recorder*, 36-43.
- Case, J.E., Shagam, R., and Giegengack, R.F. 1990. The geology of the northern Andes; an overview. In: Dengo, G. & Case, J.E (Eds.), *The Caribbean Region*. Geological Society of American, Geology of North America Series, H, 177-200.
- Castradori, D. 1998. Calcareous nannofossils in the basal Zanclean of the eastern Mediterranean Sea: remarks on Paleoceanography and sapropel formation. Proceedings of the Ocean Drilling Program, Scientific Results 160, 113-123.
- Chepstow-Lusty, A., Backman, J., Shackleton, N.J., 1992. Comparison of Upper Pliocene *Discoaster* abundance variations from the Atlantic, Pacific and Indian Oceans: the significance of productivity pressure at low latitudes. *Memoirs of Science Geological*, 44, 357-373.
- Di Stefano, A., Foresi, L.M., Lirer, F., Iaccarino, S.M., Turco, E., Amore, F.O., Morabito, S., Salvatorini, G., Mazzei, R., and Abdul Aziz, H. 2008. Calcareous plankton high resolution bio-magnetostratigraphy for the Langhian of the Mediterranean area. *Rivista Italiana di Paleontologia e Stratigrafia*, 114, 51-76.
- Dowsett, H.J., Cronin, T.M., Poore, R.Z., Thompson, R.S., Whatley, R.C., and Wood, A.M. 1992. Micropaleontological Evidence for Increased Meridional Heat Transport in the North Atlantic Ocean During the Pliocene. *Science*, 258, 1133-1135.
- Dowsett, H.J., Barron, J.A., Poore, R.Z., Thompson, R.S., Cronin, T.M., Ishman, S.E., and Willard, D.A. 1999. *Middle Pliocene paleoenvironmental reconstruction*. PRISM2, U.S. Geological Survey Open-File Report, 99-535, 13 pp.
- Duque-Caro, H. 1984. Structural Style, diapirism and accretionary episodes of the Sinú-San Jacinto terrane, southwestern Caribbean borderland. *Geological Society of America Memoir*, 162, 303-316.
- Edwards, A. R. 1971. A calcareous nannoplankton zonation of the New Zealand Paleogene. In: Farinacci, A. (Ed.), *Proceedings of the II Planktonic Conference*. Rome 1970, 1, 381-419.
- Farrell, J.W., Raffi, I., Janecek, T.R., Murray, D.W., Levitan, M., Dadey, K.A., Emeis, K-C, Lyle, M., Flores, J.-A., and Hovan, S. 1995. Late Neogene sedimentation patterns in the eastern equatorial Pacific Ocean. Proceedings of the Ocean Drilling Program, Scientific Results 138, 717-756.
- Fiorini, F., and Jaramillo, C.A. 2006. Paleoenvironmental reconstructions of the Oligocene-Miocene deposits of southern Caribbean (Carmen de Bolívar, Colombia) based on benthic foraminifera. *Boletín de Geología*, 29, 47-55.
- Flores, J. A., Bárcena, M. A., and Sierro, F. J., 2000. Ocean-surface and wind dynamics in the Atlantic Ocean off Northwest Africa during the last 140 000 years. *Palaeogeography, Palaeoclimatology, Palaeoecology*, 161, 459-478.
- Flores, J.A., and Sierro, F.J. 1987. Calcareous plankton in the Tortonian–Messinian transition series of the northwestern edge of the Guadalquivir basin. *Abhandlungen der Geologischen Bundesanstalt*, 39, 67-84.
- Flores, J.-A., and Sierro, F. J. 1997. Revised technique for calculation of calcareous nannofossil accumulation rates. *Micropaleontology*, 43, 321-324.
- Flores, J.A., Sierro, F. J., Filipelli, G., Barcena, M.A., Vázquez, A., and Utrilla, R. 2005. Surface water dynamics and phytoplankton communities during deposition of cyclic late Messinian sapropel sequences in the western Mediterranean. *Marine Micropaleontology*, 56, 50-79.
- Flores, J.A., Sierro, F.J., and Raffi, I. 1995. Evolution of the calcareous nannofossil assemblage as a response to the paleoceanographic changes in the eastern equatorial Pacific Ocean from 4 to 2 Ma (Leg 138, Sites 849 and 852). Proceedings of the Ocean Drilling Program, Scientific Results 138, 163-176.
- Flower, B.P. 1999. Warming without high CO₂? *Nature*, 399, 313-314.
- Flower, B.P., and Kennett, J.P. 1994. Middle Miocene ocean climate transition: High-resolution oxygen and carbon isotopic records from Deep Sea Drilling Project Site 588A, southwest Pacific. *Paleoceanography*, 8, 811-843.

- Fornaciari, E., and Agnini, C. 2008. Taxonomic note: *Sphenolithus pseudoheteromorphus*, a new Miocene calcareous nannofossil species from the equatorial Indian Ocean. *Journal of Nannoplankton Research*, 30, 97-101.
- Fornaciari, E., Di Stefano, A., Rio, D., and Negri, A. 1996. Middle Miocene quantitative calcareous nannofossil biostratigraphy in the Mediterranean region. *Micropaleontology*, 42, 37-63.
- Haq, B.U. 1971. Paleogene calcareous nanoflora, part III: Oligocene of Syria. *Stockholm Contributions in Geology*, 25, 99-127.
- Haq, B.U. 1980. Biogeographic history of Miocene calcareous nannoplankton and paleoceanography of the Atlantic Ocean. *Micropaleontology*, 25, 414-443.
- Haq, B.U., and Lohmann, G.P. 1976. Early Cenozoic calcareous nannoplankton biogeography of the Atlantic Ocean. *Marine Micropaleontology*, 1, 119-194.
- Hilgen, F.J. 1991a. Extension of the astronomically calibrated (polarity) time scale to the Miocene-Pliocene boundary. *Earth and Planetary Science Letters*, 107, 349-368.
- Hilgen, F.J. 1991b. Astronomical calibration of Gauss to Matuyama sapropels in the Mediterranean and implication for the geomagnetic polarity time scale. *Earth and Planetary Science Letters*, 104, 226-244.
- Hüsing S.K., Cascella, A., Hilgen F.J., Krijgsman W., Kuiper K.F., Turco E., and Wilson, D. 2010. Astrochronology of the Mediterranean Langhian between 15.29 and 14.17 Ma. *Earth and Planetary Science Letters*, 290, 254-269.
- Hüsing, S.K., Hilgen, F.J., Abdul Aziz, H., and Krijgsman, W. 2007. Completing the Neogene geological time scale between 8.5 and 12.5 Ma. *Earth and Planetary Science Letters*, 253, 340-358.
- Jordan, R. W., and Kleijne, A. 1994. A classification system for living coccolithophores. In: *Coccolithophores* (A. Winter & W.G. Siesser, Eds). Cambridge University Press, 83-105.
- Kameo, K., and Bralower, T.J. 2000. Neogene calcareous nannofossil biostratigraphy of Sites 998, 999, and 1000, Caribbean Sea. Proceedings of the Ocean Drilling Program, Scientific Results 165, 3-17.
- Maiorano, P., and Monechi, S. 1998. Revised correlations of Early and Middle Miocene calcareous nannofossil events and magnetostratigraphy from DSDP Site 563 (North Atlantic Ocean). *Marine Micropaleontology*, 35, 235-255.
- Margalef, R. 1967. The food-web in pelagic environment. *Helgolander Wiss Meeresunters*, 15, 548-559.
- Margalef, R. 1978. Life-forms of phytoplankton as survival alternatives in an unstable environment. *Oceanologica Acta*, 1, 493-509.
- Martini, E. 1971. Standard Tertiary and Quaternary calcareous nannoplankton zonation. In: Farinacci, A. (Ed.), *Proceedings of the II Planktonic Conference*. Rome 1970, 2, 739-785.
- Marzouk, A., and Soliman, S. 2004. Calcareous nannofossil biostratigraphy of the Paleogene sediments on an onshore-offshore transect of Northern Sinai, Egypt. *Journal of African Earth Sciences*, 38, 155-168.
- Mejía-Molina, A. E., Flores, J. A., and Torres, V. 2006. Nanofósiles Calcáreos de la Sección Arroyo Alférez (Carmen de Bolívar): una biozonificación preliminar para el Oligoceno-Mioceno medio del Norte de Colombia. *Boletín de Geología*, 29, 21-28.
- Mejía-Molina, A., Flores, J.A., Torres Torres, V., and Sierro, F.J., 2008. Análisis bioestratigráfico mediante Nanofósiles Calcáreos para el Oligoceno-Mioceno medio del norte de Colombia. Sección de superficie del Arroyo Alférez, Colombia. *Revista Española de Micropaleontología*, 40, 135-149.
- Moran, M.J., and Watkins, D.K. 1988. Oligocene calcareous nannofossil biostratigraphy from Ocean Drilling Program Site 628, Little Bahama Bank Slope. Proceedings of the Ocean Drilling Program, Scientific Results 101, 87-104.
- Negri, A., and Villa, G. 2000. Calcareous nannofossil biostratigraphy, biochronology and paleoecology at the Tortonian/Messinian boundary of the Faneromeni section (Crete). *Palaeogeography, Palaeoclimatology, Palaeoecology*, 156, 195-209.
- Langereis, C.G., and Hilgen, F.J. 1991. The Rosello composite: a Mediterranean and global reference section for the early to early late Pliocene. *Earth and Planetary Science Letters*, 104, 211-225.
- Lohmann, G.P., and Carlson, J.J. 1981. Oceanographic Significance of Pacific Late Miocene Calcareous Nannoplankton. *Marine Micropaleontology*, 6, 553-579.
- Lourens, L.J., Hilgen, F.J., Gudjonsson, L., and Zachariasse, W.J. 1992. Late Pliocene to early Pleistocene astronomically forced sea surface productivity and temperature variations in the Mediterranean. *Marine Micropaleontology*, 19, 49-78.
- Lyle, M., Dadey, K.A., and Farrell, J.W. 1995. The late Miocene (11-8 Ma) eastern Pacific carbonate crash: evidence for reorganization of deep-water circulation by the closure of the Panama gateway. Proceedings of the Ocean Drilling Program, Scientific Results 138, 821-838.
- Okada, H. 1990. Quaternary and Paleogene calcareous nannofossils, Leg 115. Proceedings of the Ocean Drilling Program, Scientific Results 115, 29-174.
- Okada, H., and Bukry, D. 1980. Supplementary modification and introduction of code numbers to the low-latitude coccolith biostratigraphic zonation (Bukry, 1973; 1975). *Marine Micropaleontology*, 5, 321-325.
- Okada, H., and Honjo, S. 1973. The distribution of oceanic coccolithophorids in the Pacific. *Deep Sea Research*, 20, 355-374.
- Okada, H., and Wells, P. 1997. Late Quaternary nannofossil indicators of climate change in two deep sea cores associated with the Leeuwin Current of Western Australia. *Palaeogeography, Palaeoclimatology, Palaeoecology*, 131, 413-432.
- Olafsson, G., and Villa, G. 1992. Reliability of *Sphenoliths* as zonal markers in Oligocene sediments from the Atlantic and Indian Oceans. In: Decima, F.P., Monechi, S., Rio, D. (Eds.), Proceedings of International Nannoplankton Association Conference, Firenze 1989. *Memorie di Scienze Geologiche*, XLII, 43, 237-259.
- Perch-Nielsen, K. 1972. Remarks on Late Cretaceous to Pleistocene coccoliths from the North Atlantic. *Initial Reports of the Deep Sea Drilling Project*, 12, 1003-1069.
- Perch-Nielsen, K. 1985. Mesozoic calcareous nannofossils. In: Bolli, H.M., Saunders, J.B., and Perch-Nielsen, K. (Eds.), *Plankton Stratigraphy*. Cambridge University Press, Cambridge, 329-426.
- Pisias, N.G., Mayer, L.A., and Mix, A.C. 1995. Paleoceanography of the eastern equatorial Pacific during the Neogene: synthesis of Leg 138

- drilling results. In: Pisias, N.G., Mayer, L.A., Janecek, T.R., Palmer-Julson, A. & van Andel, T.H. (Eds.). Proceedings of the Ocean Drilling Program, Scientific Results 138, 5-21.
- Pospichal, J., Wei, W., and Wise, S.W. Jr. 1992. Probing the limits of nanofossil stratigraphic resolution in the southern high latitudes. In: Decima, F.P., Monechi, S., Rio, D, eds. Proceedings of International Nannoplankton Conference, Firenze 1989. *Memorie di Scienze Geologiche*, XLII, 115-132.
- Raffi, I., and Flores, J-A. 1995. Pleistocene through Miocene calcareous from eastern equatorial Pacific Ocean (Leg 138). Proceedings of the Ocean Drilling Program, Scientific Results 138, 233-286.
- Raffi, I., Backman, J., Fornaciari, E., Pälike, H., Rio, D., Lourens, L.J., and Hilgen, F.J. 2006. A review of calcareous nanofossil astro-biochronology encompassing the past 25 Million years. *Quaternary Science Review*, 25, 3113-3137.
- Ravelo, A.C., and Andreasen, D.H. 2000. Enhanced circulation during a warm period. *Geophysical Research Letters*, 27, 1001-1004.
- Raymo, M.E., Grant, B., Horowitz, M., and Rau, G.H. 1996. Mid-Pliocene warmth: stronger greenhouse and stronger conveyor. *Marine Micropaleontology*, 27, 313-326.
- Roth, P. H., Franz, H.E., and Wise, S.W. Jr. 1970. Morphological study of the selected members of the genus *Sphenolithus* Deflandre (Icertae sedis, Tertiary). In: Farinacci, A. (Ed.), Proceedings of the II Planktonic Conference. Rome 1970, 2, 1099-1119.
- Shackleton, N.J., and Kennett, J.P. 1975. Paleotemperature history of the Cenozoic and the initiation of Antarctic glaciation: oxygen and carbon isotope analyses in DSDP sites 277, 279 and 281. Initial Reports of the Deep Sea Drilling Project 29, 743-755.
- Shagam, R. 1975. The northern termination of the Andes. In: Nairn, A.E.M. & Stehli, F.G, (Eds.), *The Ocean Basins and Margins, The Gulf of Mexico and the Caribbean* (Vol. 3). Plenum, New York, 325-420.
- Sigurdsson, H., Leckie, R.M., Acton, G.D., et al., 1997. Proceedings of the Ocean Drilling Program, Initial Reports, 165, 100 pp.
- Wei, W., and Wise, J.S.W. 1989. Paleogene calcareous nanofossil magnetobiochronology: Results from South Atlantic DSDP Site 516. *Marine Micropaleontology Plankton Biochronology*, 14, 119-152.
- Winter, A., and Siesser, W.G. 1994. *Coccolithophores*. Cambridge University Press, Cambridge, 242 pp.
- Young, J.R. 1994. Functions of coccoliths. In: Winter, A. and Siesser, W.G. (Eds.), *Coccolithophores*. Cambridge University Press, Cambridge, 63-82.
- Zachos, J.C., Pagani, M., Sloan, L., Thomas, E., and Billups, K. 2001. Trends, rhythms, and aberrations in global climate 65 Ma to present. *Science*, 292, 686-693.
- Zachos, J.C., Stott, L.D., and Lohmann, K.C. 1994. Evolution of early Cenozoic marine temperatures. *Paleoceanography*, 9, 353-387.
- Zachos, J. C., Röhl, U., Schellenberg, S. A., Sluijs, A., Hodell, D. A., Kelly, D. C., Thomas, E., Nicolo, M., Raffi, I., Lourens, L. J., McCarren, H., and Kroon, D. 2005. Rapid Acidification of the Ocean During the Paleocene-Eocene Thermal Maximum. *Science*, 308, 1611-1615.

MANUSCRITO RECIBIDO: 7 de abril, 2010

MANUSCRITO ACEPTADO: 8 de diciembre, 2010

Appendix A

Systematic description of *Sphenolithus*

Kingdom *Protist* Haeckel, 1866

Phylum *Prymnesiophyta* Hibberd, 1976

Class *Prymnesiophyceae* Hibberd, 1976

Order *Coccolithophorales* Schiller, 1926

Family Sphenolithaceae Deflandre in Grassé, 1952

Genus *Sphenolithus* Deflandre, 1952

(In Alphabetic Order of Generic Epithets)

AA: Arroyo Alférez; CB4: Carmen de Bolívar, Estratigráfico 4

Sphenolithus abies Deflandre in Deflandre & Fert, 1954

ODP 999: robust proximal column, conical shape, short lateral elements, blunt apical spine well preserved, size: 5 x 4 μm or lesser.

Sphenolithus belemnus Bramlette & Wilcoxon, 1967

AA: narrow, short body, apical spine robust, sometimes notched, size: 7-10 μm . CB4: narrow, dart-shaped, medium apical spine, size: 8-11 μm . ODP 999: narrow, dart-shaped, long, pointed apical spine, size: 9-12 μm .

Sphenolithus calyculus Bukry, 1985

Synonym: *Sphenolithus elongatus*

CB4: small size with slender apical spine, size: 4-7 μm .

Sphenolithus capricornutus Bukry & Percival, 1971

CB4: apical spine with two slender and diverging spines sometimes notched, size: 4-7 μm .

Sphenolithus ciperoensis Bramlette & Wilcoxon, 1967

AA: small and triangular outline, proximal column short, robust two-piece apical spine, size: 6-10 μm or lesser.

Sphenolithus compactus Backman, 1980

AA: very small, tightly packed, rounded compact apical spine, size: lesser than 3 μm . CB4: blocky proximal shield, compact apical spine, size: 2-3 μm . ODP 999: Small, tightly packed, rounded compact apical spine. Size: 2-3 μm or greater.

Sphenolithus conicus Bukry, 1971

AA: small, conical shape, blocky apical spine, size: 5-8 μm . CB4: medium size lateral elements, medium blocky apical spine, Size: 6-9 μm . ODP 999: conical shape, medium size, blocky apical spine, size: 7-12 μm .

Sphenolithus delphix Bukry, 1973

ODP 999: small to medium, triradiate shaped, lateral elements slightly elongated and sharpened, size: 6-10 μm .

Sphenolithus disbelemnus Fornaciari & Rio, 1996

Synonym: *Sphenolithus aubryae* De Kaenel & Villa (1996).

AA: dart-shaped, diminutive apical spine sometimes notched, size: 4-7 μm . CB4: narrow, dart-shaped, diminutive apical spine, size: 5-8 μm . ODP 999: dart-shaped, small apical spine, size: 6-9 μm .

Sphenolithus dissimilis Bukry & Percival, 1971

AA: small size, tripartite apical, size: 4-8 μm . ODP 999: medium size, tripartite apical, multi-element base wider than apex. Size: 5-10 μm .

Sphenolithus distentus (Martini, 1965) Bramlette & Wilcoxon, 1967

AA: small, poor preserved, triangular outline, apical spine composed of two segments that may bifurcate at the tip, usually notched. Size: 6-9 μm .

Sphenolithus heteromorphus Deflandre, 1953

AA: small to medium, pyramidal shape, short and robust apical spine sometimes notched, size: 7 x 5 µm. CB4: medium to very small, medium to short apical spine, sometimes overgrowth, size: 7 x 4 µm or lesser. ODP 999: large to very small, pyramidal shape, long to short apical spine, sometimes overgrowth, size: 10 x 5 µm or lesser.

Sphenolithus moriformis (Bronnimann & Stradner, 1960)
Bramlette & Wilcoxon, 1967

AA: small to large, pine-cone or beehive outline, size: 4-5 µm or greater than 12 µm. CB4: small to medium, bul-

bous, pine-cone outline, size: 4-7 µm. ODP 999: small to medium, pine-cone or beehive outline, size: 4-8 µm.

Sphenolithus neoabies Bukry & Bramlette, 1969

ODP 999: very small, conical shape, last of *Sphenolithus* lineage, size: 2-4 µm.

Sphenolithus predistentus Bramlette & Wilcoxon, 1967

AA: small, medium elongate apical spine composed of two thick segments that may bifurcate at the end, sometimes notched, size: 6-9 µm.

Calcareous nannofossils Upper Miocene biostratigraphy and biochronology at western equatorial Atlantic (ODP Site 999)

Yaned Margarita Buitrago-Reina^{1, 2}, José-Abel Flores¹ and Francisco Javier Sierro¹

¹ Departamento de Geología, Universidad de Salamanca. Plaza de La Merced s/n, 37008 Salamanca, España. margaritab@usal.es

² Instituto Colombiano del Petróleo - ICP-ECOPETROL S.A. Km. 7 vía Piedecuesta, Santander, Colombia.

Resumen

La perforación ODP 999 está localizada en la cuenca Caribe colombiana (Atlántico NW). Analizamos 154 muestras con edades comprendidas entre el Tortoniense (Mioceno superior) y el Zancleano (Plioceno inferior). La bioestratigrafía de este trabajo se basa en los esquemas zonales estándar para el Neógeno. Inicialmente determinamos las profundidades de los eventos de nanofósiles calcáreos que identificamos en este trabajo y posteriormente las edades para cada uno de ellos. Con este propósito, empleamos los datos del registro isotópico de ¹⁸O orbitalmente calibrado, obtenido para la perforación ODP 999. Finalmente, comparamos los resultados de las edades calibradas obtenidas en otras cuencas por diferentes autores, para determinar el grado de sincronismo o diacronismo. Obtuvimos las edades calibradas para 28 eventos y concluimos que 8 de ellos son sincrónicos, 8 diacrónicos y para 12 de ellos no existen datos para establecer las diferencias de edad.

Palabras clave: Cuenca Caribe, nanofósiles calcáreos, Mioceno, Tortoniense, Mesiniense, bioestratigrafía, biocronología.

Abstract

The ODP Site 999 is located in the Colombian Caribbean basin (Atlantic NW). We analyze 154 samples with ages ranging between Tortonian (Upper Miocene) until Zanclean (Lower Pliocene). The biostratigraphy of this work is based on the standard zonal schemes for the Neogene. Initially, we determine the depths of the calcareous nannofossil events that we identify in this work, and then the ages for each of them. For this purpose, we use the data of the orbitally tuned ¹⁸O isotope record of the ODP Site 999A. We compare the results of the calibrated ages obtained in other basins by different authors to determine the synchronism or diachronism. We achieve the calibrated ages for 28 events and we conclude that 8 of them are synchronic, 8 diachronic, and for 12 of them there are no data to establish age differences.

Key words: Caribbean basin, calcareous nannofossils, Miocene, Tortonian, Messinian, biostratigraphy, biochronology.

1. INTRODUCTION

The Ocean Drilling Program (ODP) Site 999 was drilled by the R/V JOIDES Resolution during the Leg 165 in the

Caribbean Sea (Figure 1). Leg 165 drilling was intended to address two major targets: the nature of the Cretaceous/Tertiary (K/T) boundary (65 Ma) of particular interest because of the relative proximity of the Kogi Rise to

the Chicxulub impact crater, and the influence of tropical seas on global ocean history and climate evolution. The drilling of five sites (998, 999, 1000, 1001 and 1002), allowed to the shipboard team to obtain data about the formation of the Caribbean Plate, discover several major episodes of explosive volcanism in the Caribbean region, and recover an important succession of submarine basaltic lava flows of the Caribbean Oceanic Plateau (Sigurdsson *et al.*, 1997).

The aims of this research were: 1) to achieve a high resolution calcareous nannofossils biostratigraphy and biochronology for Upper Miocene until Miocene/Pliocene interval boundary in the Caribbean; 2) to characterize the calcareous nannofossil assemblages in this region and period, and 3) to define alternative calcareous nannofossil events for the Tortonian/Messinian and the Miocene/Pliocene boundaries. Due to its location into the Colombian Caribbean Basin, it could be the reference framework for future correlations with sequences obtained in the continent.

1.1 Geologic and oceanographic setting

The Kogi Rise is a submarine promontory located on the Caribbean Plate that stands approximately 1000 meters above the relatively flat and featureless oceanic floor of the Colombian Caribbean Basin. It impedes the direct influence of the Amazonas and Orinoco Plumes, and of the turbidites from Magdalena Fan Complex and from Hess Escarpment (Burke *et al.*, 1984; Bowland, 1993; Sigurdsson *et al.*, 1997).

The formation and tectonic evolution of the Caribbean Plate has been studied by different authors, and some theories and models about the origin and evolution through the time have been suggested (Figure 2). The “Pacific” model establish that the Caribbean Plate was originated in the Mesozoic from a plate of the Pacific basin, most likely the Farallon Plate (e.g. Malfait & Dinkelman, 1972; Pindell & Dewey, 1982; Duncan & Hargraves, 1984; Pindell *et al.*, 1988; Burke, 1988; Pindell & Barrett, 1990; Pindell, 1994). The “intra-American” model state that the

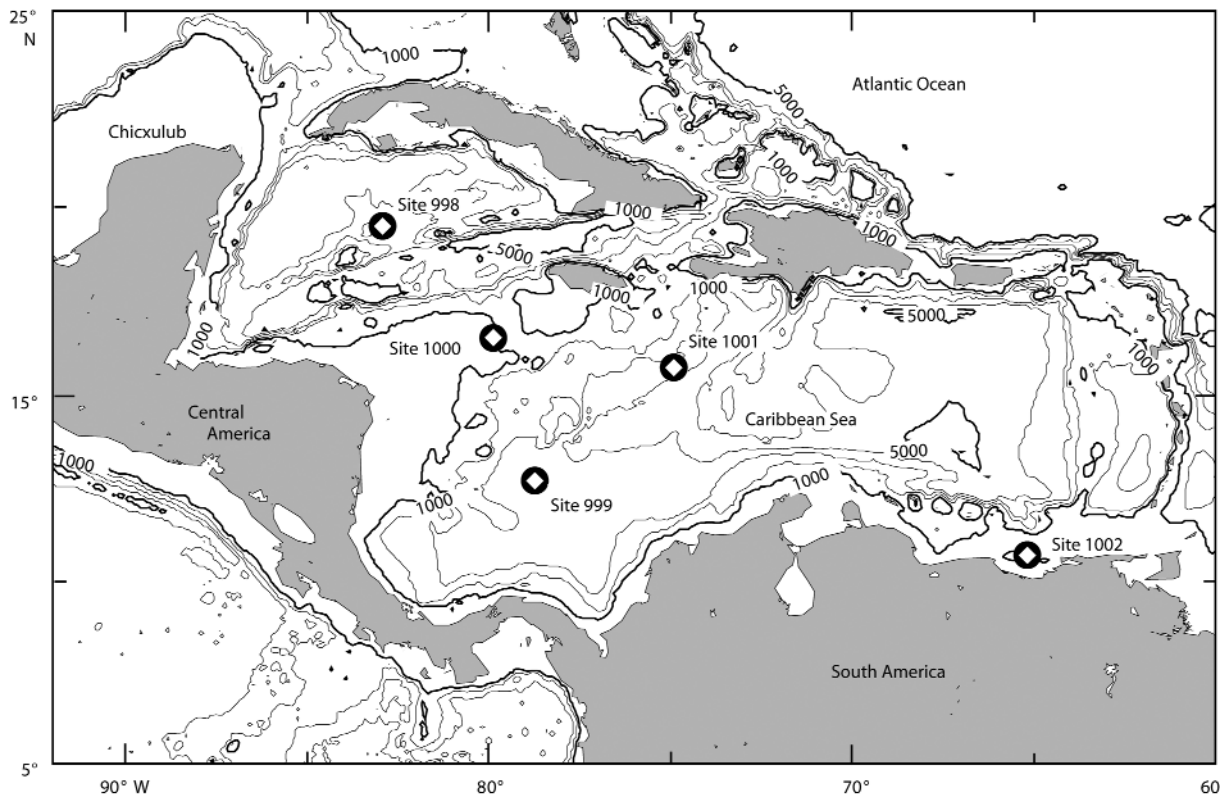


Figure 1. Location map of sites drilled during Leg 165 (Peters *et al.*, 2000).

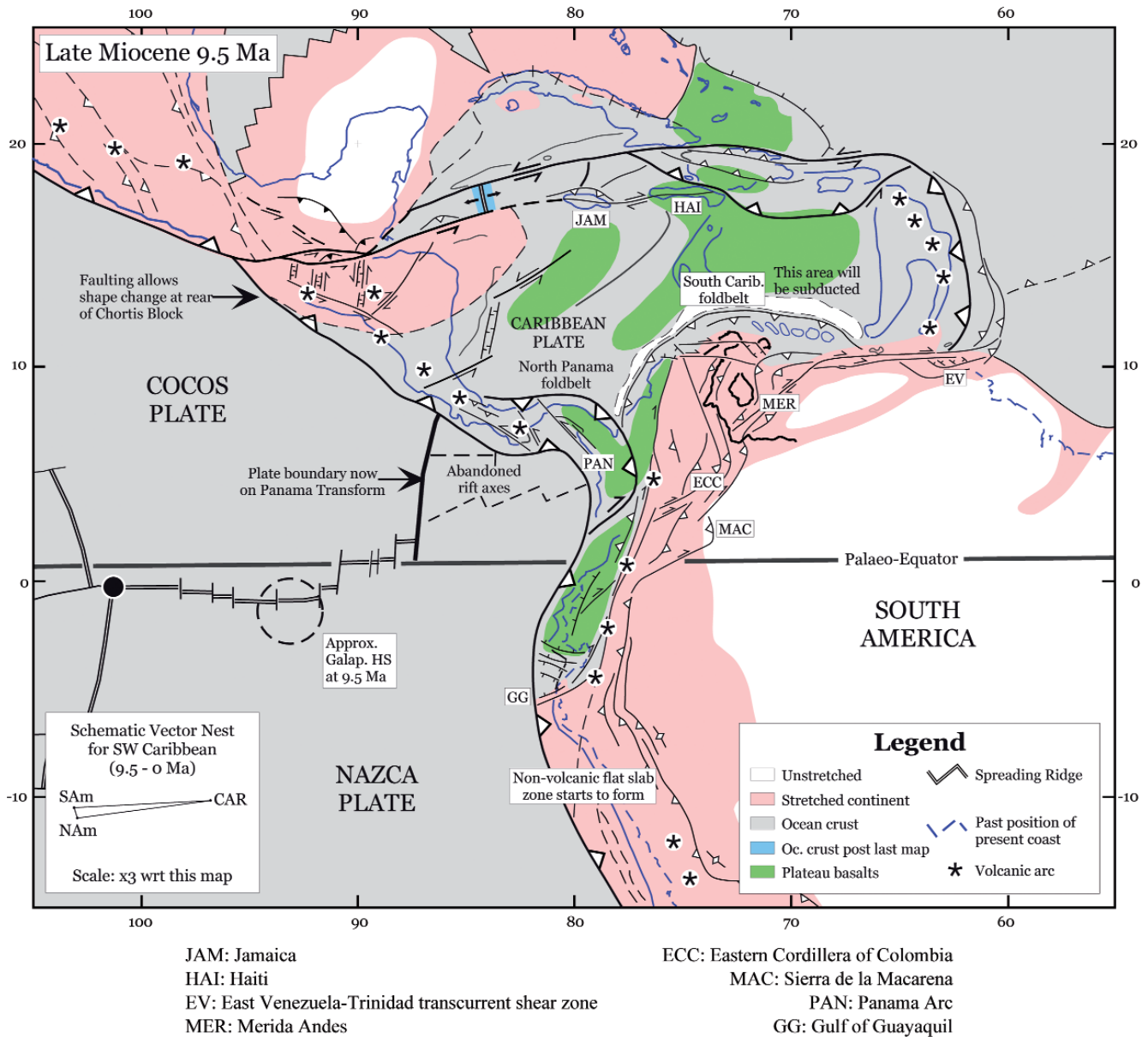


Figure 2. Late Miocene plate reconstruction (Pindell & Kennan, 2001).

origin of the Caribbean plate occurred between North and South America, west of its present day position (e.g., Klitgord & Schouten, 1986; Meschede & Frisch, 1998). Alternatively, “fixist” models indicate that the Caribbean plate has maintained roughly its current position (e.g., Morris *et al.*, 1990). This third type of model is incompatible with the paleomagnetic data from Acton *et al.* (2000), as well as with the opening history of the Atlantic Ocean (Pindell, 1994).

The Caribbean Basin was formed by the tectonic evolution of the Caribbean Plate, which originated the emer-

sion of the Antilles arc, several submarine ridges, sills and the subsequent formation of passages and trenches (Einslele, 1992; Guzmán, 2007). The islands arc and the sills between them are the sieves for the influx of water from Atlantic Ocean (Murphy *et al.*, 1999; Andrade & Barton, 2000). The Caribbean Basin topography present four major basins, from east to west: Venezuela, Colombia, Caiman and Yucatan (Tomczak & Godfrey, 2001). Researches carried out by Wüst (1964) and Gordon (1967), and observations and numerical models of Johns *et al.* (2002), indicates that the influx of water to the Caribbean

Sea occurs mainly through the Granada, San Vicente and Santa Lucia Passages (Windward Islands Passages), located southeast (Figure 3). This oceanic current in the Caribbean is an extension of the North and South Equatorial currents injected into the basin and flowing towards northwest of the Gulf of Mexico (Tomczak & Godfrey, 2001; Richardson, 2005). Currently, the Upper part of North Atlantic Deep Water (UNADW) and the Antarctic Intermediate Waters (AAIW) moves into the Caribbean Basin through Windward, Anegada, Mona, and Jungfern Passages (Roth *et al.*, 2000). Hence, the Caribbean is a semi-enclosed basin where the influx of waters from the Atlantic Ocean is permanent, and subsequently, reflects the oceanic changes as soon as they occur.

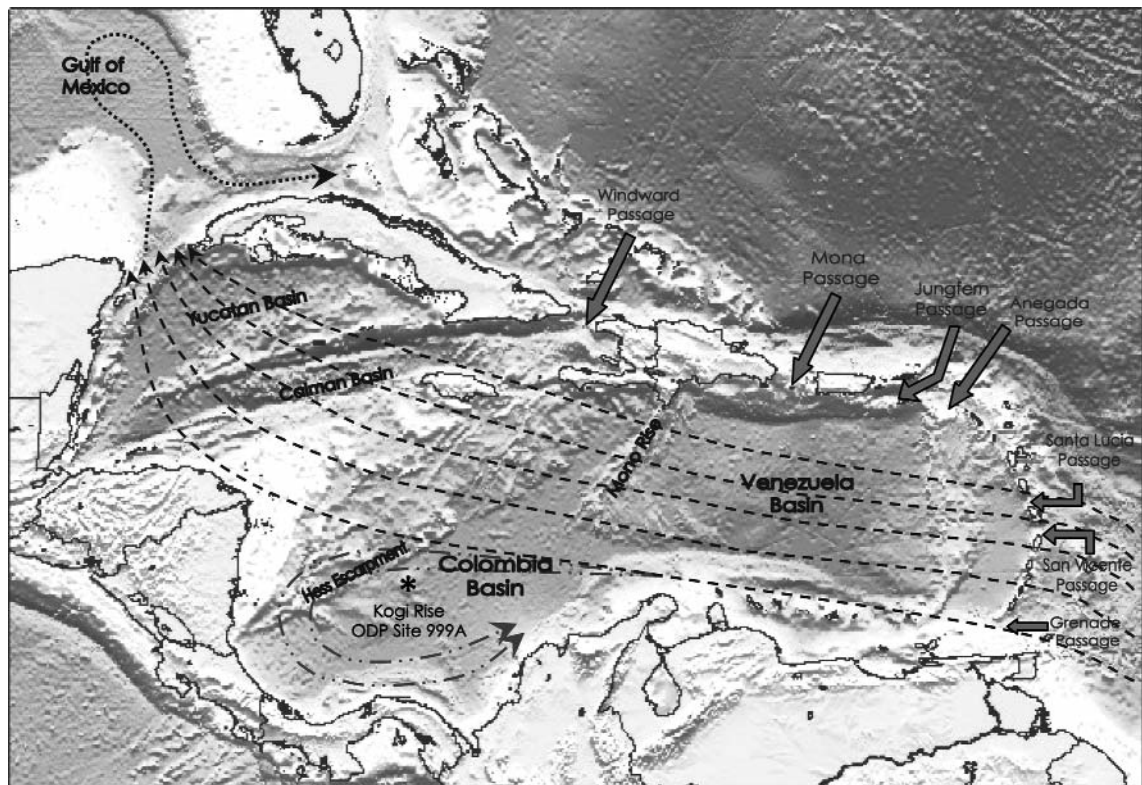
1.2 Material and methods

The ODP Site 999 was drilled in the western Colombian Caribbean Basin, at 12°44.639'N, 78°44.360'W, at 2827.9 m water depth, on “Kogi” Rise (named from the

indian tribe that inhabits the Sierra Nevada de Santa Marta, Colombia). The Site 999 was drilled in two holes: Hole A until a depth of 566.1 mbsf, with ages ranging from Lower Miocene to Pleistocene, and Hole B, until a depth of 1066.4 mbsf with ages ranging from Upper Cretaceous to Lower Miocene. Site 999A, was selected because it contains the sediments of Miocene and is placed in a crucial point to correlate with Colombian outcrops. The Kogi Rise is an isolated promontory, located out of the influence of turbidite deposition of the Magdalena fan complex and the Hess Escarpment (Sigurdsson *et al.*, 1997), allow recovering an undisturbed sedimentary sequence.

1.2.1 Lithology

The material was previously studied by Sigurdsson *et al.* (1997). They divided the whole sequence into six units, and the Upper Miocene interval corresponds to Unit I, consisting of clayey nannofossil mixed sediment with foraminifers and interbedded ash layers, massive and structureless. The Unit I was subdivided into three sub-



-----> Caribbean Current ———> Panama-Colombia Gyre > “Loop” Current

Figure 3. Basins and main currents in the Caribbean.

units (IA, IB and IC) based on the abundance of foraminifers, the occurrence of siliceous microfossils, and physical properties. The sediments of our interval correspond to the subunits IB (18X to 24H) characterized by the low abundance of foraminifers (>10%) and IC (25X to 27X) distinguishable from IB by the presence of significant amounts of biogenic siliceous material such as sponge spicules, radiolarians, and diatoms.

1.2.2 Techniques

A total of 154 samples were prepared from cores 18H to 27X using the decantation technique of Flores & Sierra (1997). Slides were observed with a polarized microscope at X1000 magnification. Additionally, several samples were studied under Scanning Electron Microscope (SEM) in order to check preservational aspects and details about nannofossil structures. For the Upper Miocene biostratigraphy, we have used semiquantitative analyses of presence-absence of the species and genus and obtaining the depths of the events. For biostratigraphic purposes, to determine when taxa became extinct or appear, we consider that is present if is recorded at least once in ten optical fields of view. The age of these events was orbitally calibrated after comparison with the benthic ^{18}O record (Bickert *et al.*, 2004).

Abbreviations to define events are as follows:

- FO: First occurrence: Appearance in the record of a species or morphotype, not always in a continuous and/or consistent distribution.
- LO: Last occurrence: End of the continuous and/or consistent distribution of a species or morphotype.
- T: Top (End)
- B: Base (Beginning)
- Paracme: Period when the species are absent in the record, or its abundance is lower than 1% of the assemblage.

1.2.3 Calcareous nannofossils preservation

The preservation of the calcareous nannofossils in this sequence is very good, with some minimal variations through the sequence. Overgrowth is frequent in *Discoaster* spp. and occasional in *Catinaster mexicanus*, *Coc-*

colithus pelagicus, *Helicosphaera carteri*, *Calcidiscus macintyreii*, and *Reticulofenestra minutula*. *Discoaster pentaradiatus* shows its tiny bifurcations and coccospheres of *C. pelagicus*, *C. leptoporus*, and *Reticulofenestra* spp. are common. Randomly, minimal dissolution was observed, mainly in *H. carteri*, and *Calcidiscus* spp.

2. BIOSTRATIGRAPHY AND BIOCHRONOLOGY

The calcareous nannofossil biostratigraphy at Site 999A was previously studied by Kameo & Bralower (2000) using zonal standard schemes for the Neogene and the Quaternary (Martini, 1971; Bukry, 1973, 1975; Okada & Bukry, 1980) and bioevent data by other authors (e.g. Raffi & Flores, 1995). For the time interval studied, we recognize the standard marker events of the zones and subzones of Martini (1971), Okada & Bukry (1980) and Raffi & Flores (1995), with slight variations in the assigned ages (Figure 4).

The time calibration was performed using the age vs. depth data of the orbitally tuned isotope record. Depth scale was corrected for the sediment expansion after recovery by a factor of 0.9 relative to the meters below seafloor level on top of each core. This age model was based on ^{18}O stratigraphy by correlation of benthic ^{18}O record at ODP 999 drilling (Bickert *et al.*, 2004), and the astronomically dated ^{18}O record from North Atlantic ODP Site 982 (Hodell *et al.*, 2001) and western equatorial Atlantic ODP Site 926 (Shackleton & Crowhurst, 1997; Shackleton & Hall, 1997). Ages were adjusted to the bioevents calibrated by Backman & Raffi (1997) based on the astronomically dated timescale of Shackleton & Crowhurst (1997) in western equatorial Atlantic ODP Site 926 (Table 1, Figures 5a, b).

The identified events are compared with ages obtained by Raffi & Flores (1995) at eastern equatorial Pacific (ODP Leg 138); Curry *et al.* (1995) and Backman & Raffi (1997) at western equatorial Atlantic (ODP Leg 154); Schneider (1995), Negri *et al.* (1999), Krijgsman *et al.* (1999), Hilgen *et al.* (2000a, b, c), Negri & Villa (2000), Raffi *et al.* (2003), Krijgsman *et al.* (2004) at Mediterranean sections; and finally Berggren *et al.* (1995), Lourens *et al.* (2004) and Raffi *et al.* (2006) for different points and basins.

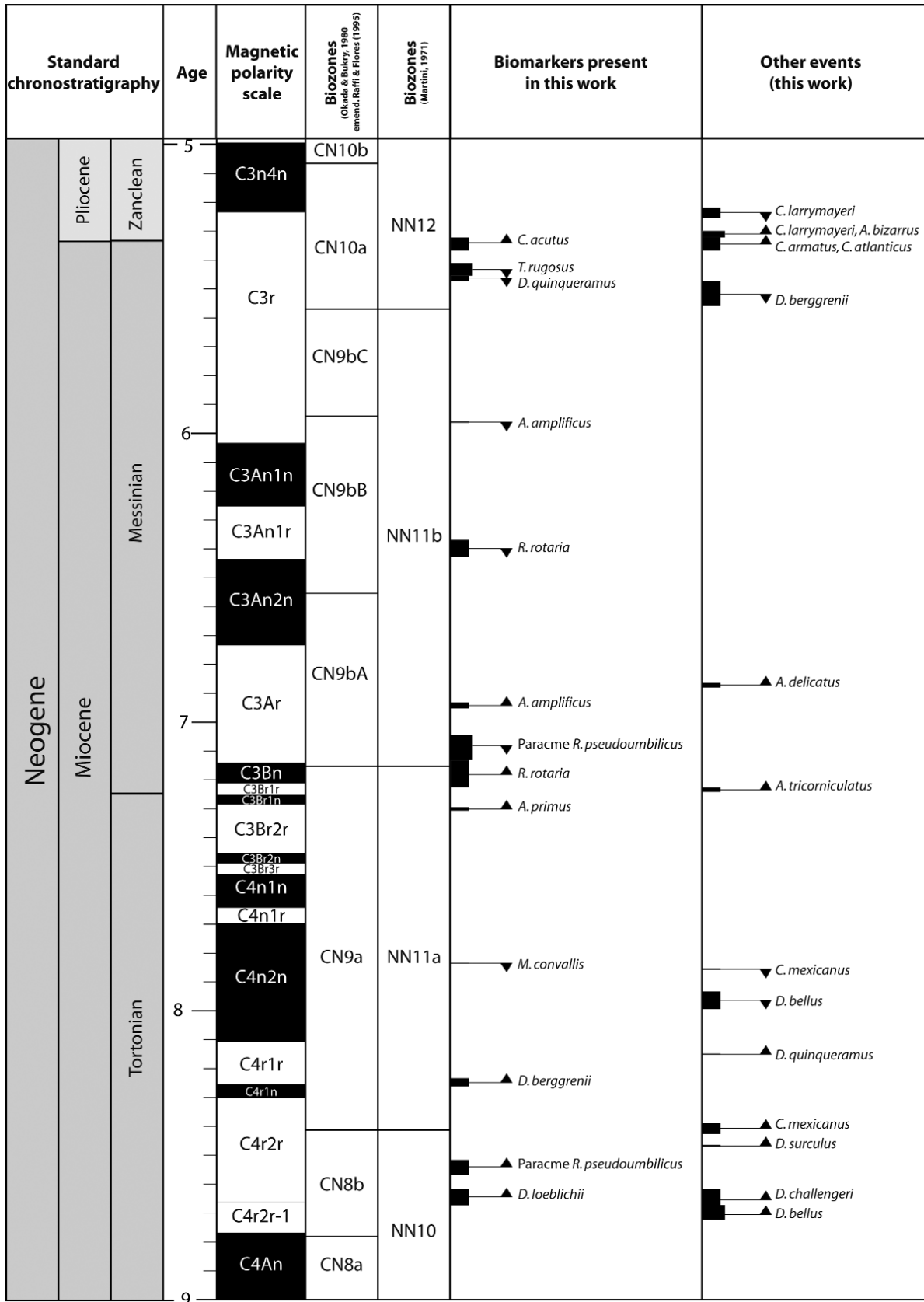


Figure 4. Chronostratigraphy and calcareous nannofossils biostratigraphy for ODP Site 999A.

Figure 5 (a, b) is the result of the integration of our biostratigraphic data with the sedimentation rate obtained by Bickert *et al.* (2004) and the calibration proposed by dif-

ferent authors (Table 1). Stripped squares represent ranges of ages assigned to each event in other basins. Black squares represent the interval of each event in this study.

Calcareous nannofossils events	Depth (mbsf)	Depth \otimes (rmbfsf*0.9)	Age (Ma) \otimes (This study)	Age (Ma) (other authors)	References
LO <i>C. larrymayeri</i>	159.60–158.50	159.595–158.495	5.255–5.219	NR	---
FO <i>A. bizarrus</i>	162.00–161.05	161.760–160.905	5.322–5.299	NR	---
FO <i>C. larrymayeri</i>	162.00–161.05	161.760–160.905	5.322–5.299	5.338±0.002	1
FO <i>C. atlanticus</i>	163.45–162.00	163.065–161.760	5.367–5.322	5.233±0.002	1*
FO <i>C. armatus</i>	163.45–162.00	163.065–161.760	5.367–5.322	NR	---
FO <i>C. acutus</i>	163.45–162.00	163.065–161.760	5.367–5.322	5.345	2
LO <i>T. rugosus</i>	166.23–165.00	165.572–164.460	5.453–5.410	5.279	1, 2
LO <i>D. quinqueramus</i>	166.73–166.23	166.017–165.572	5.473–5.453	5.54 – 5.59	1, 2, 3, 4
LO <i>D. berggrenii</i>	169.13–167.73	168.177–166.017	5.559–5.473	NR	---
LO <i>A. amplificus</i>	179.65–179.50	179.545–179.410	5.963–5.959	5.88 – 5.993	1, 2, 3, 4, 5
LO <i>R. rotaria</i>	192.80–191.80	192.330–191.430	6.426–6.370	6.760–6.771	6
FO <i>A. delicatus</i>	203.75–202.95 \otimes	200.368–200.008	6.880–6.864	7.134 – 7.250	5, 6
FO <i>A. amplificus</i>	203.05–202.05 \otimes	202.805–201.905	6.953–6.932	6.5 – 6.909	1, 2, 5, 7, 8, 9
T paracme <i>R. pseudoumbilicus</i>	209.10–207.35	208.250–206.675	7.132–7.044	7.077 – 7.170	1, 2, 5
FO <i>R. rotaria</i>	210.00–209.10	209.060–208.250	7.226–7.132	7.398–7.466	6, 10
FO <i>A. tricorniculatus</i>	210.35–210.00	209.375–209.060	7.242–7.226	NR	---
FO <i>A. primus</i>	210.60–210.45	210.570–210.435	7.306–7.295	7.362–7.449	1, 2, 6
LO <i>M. convallis</i>	220.05–219.95	220.035–219.945	7.836–7.833	7.8 – 8.685	5, 8
LO <i>C. mexicanus</i>	220.95–220.80	220.845–220.710	7.857–7.853	NR	---
LO <i>D. bellus</i>	225.10–223.65	224.580–223.275	7.994–7.933	NR	---
FO <i>D. quinqueramus</i>	229.65–229.55	229.635–229.545	8.152–8.148	NR	---
FO <i>D. berggrenii</i>	233.30–231.80	232.920–231.570	8.262–8.233	8.294 – 8.35	1, 2, 3
FO <i>C. mexicanus</i>	238.90–237.85	237.960–237.015	8.426–8.390	NR	---
FO <i>D. surculus</i>	240.15–240.00	239.205–239.056	8.470–8.465	NR	---
B paracme <i>R. pseudoumbilicus</i>	242.90–241.45	241.944–240.500	8.567–8.516	8.785	1, 2
FO <i>D. loeblichii</i>	245.90–244.30	244.932–243.339	8.673–8.617	8.43 – 8.7	3, 8
FO <i>D. challengerii</i>	245.90–244.30	244.932–243.339	8.673–8.617	NR	---
FO <i>D. bellus</i>	247.30–245.90	246.327–244.932	8.722–8.673	10.398 – 10.72	11, 12



From Bickert *et al.* (2004).

rmbfsf*0.9: Depth scale corrected for the sediment expansion after recovery by a factor of 0.9 relative to the meters below seafloor level on top of each core, from observations of multiple drilled sites were gaps on the order of 10% of the core length occurred.



Differences in depths are due to the change of the drilling system from APC to XCB (Depth data from the ODP Database)

* *Ceratolithus* sp. 1 (Backman & Raffi, 1997)

References:

1. Backman & Raffi, 1997; Shackleton & Crowhurst, 1997
 2. Raffi *et al.*, 2006; Lourens *et al.*, 2004
 3. Raffi & Flores, 1995; Schneider, 1995
 4. Krijgsman *et al.*, 2004
 5. Raffi *et al.*, 2003
 6. Negri *et al.*, 1999, Negri & Villa, 2000
 7. Krijgsman *et al.*, 1999
 8. Berggren *et al.*, 1995
 9. Curry *et al.*, 1995
 10. Hilgen *et al.*, 2000a
 11. Schneider, 1995; Raffi *et al.*, 1995
 12. Hilgen *et al.*, 2000c
- NR = Not reported

Table 1. Biostratigraphic events and calibrated ages for Upper Miocene at ODP Site 999A.

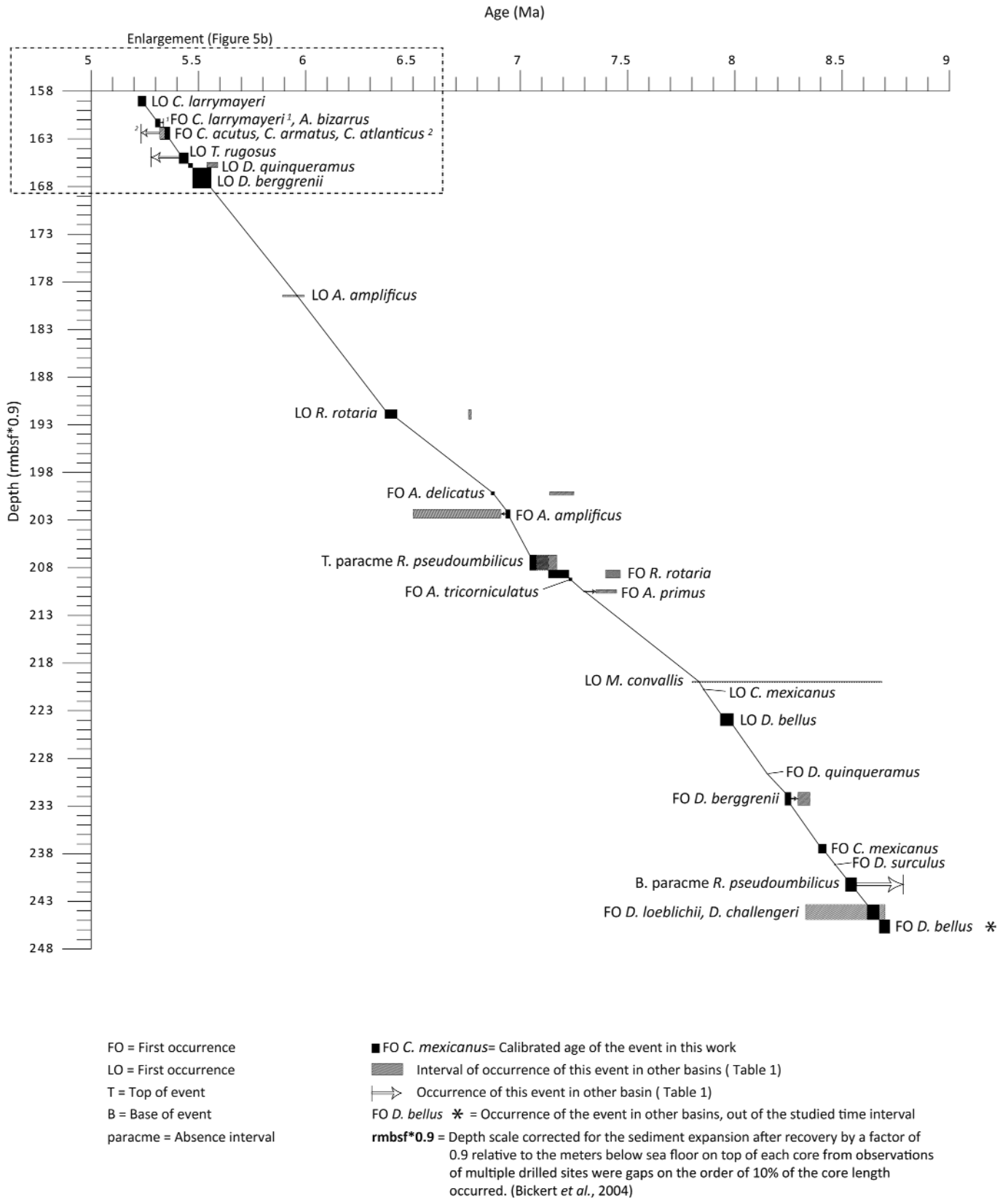
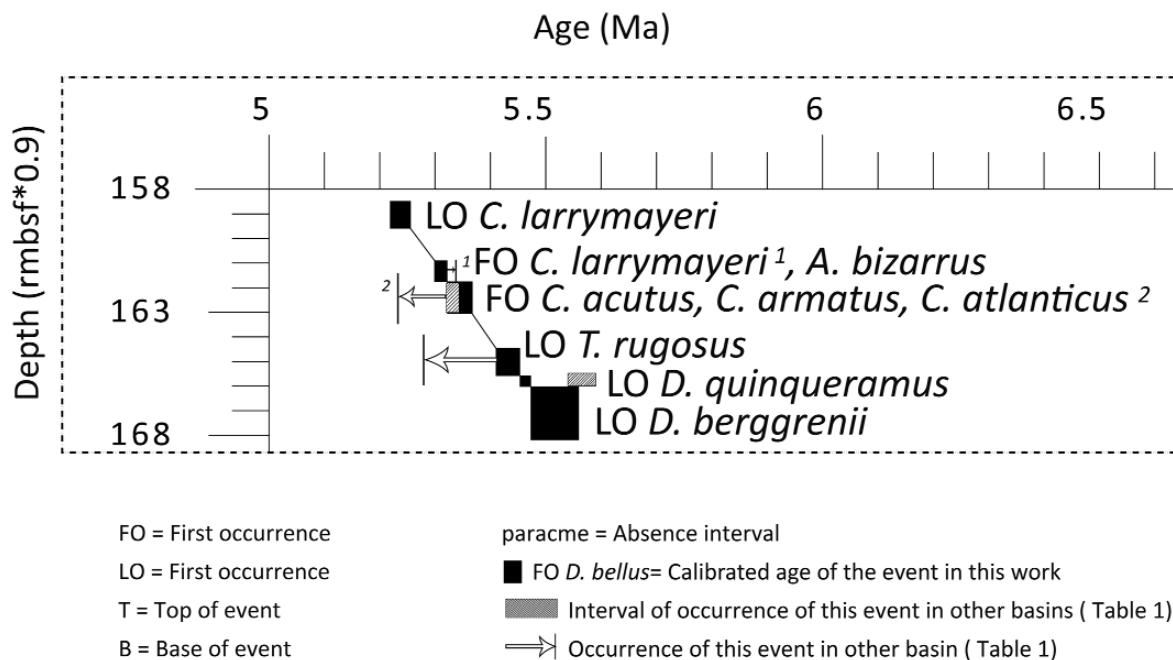


Figure 5a. Age Model for Upper Miocene at ODP Site 999A.



rmbfsf*0.9 = Depth scale corrected for the sediment expansion after recovery by a factor of 0.9 relative to the meters below sea floor on top of each core from observations of multiple drilled sites were gaps on the order of 10% of the core length occurred. (Bickert et al., 2004)

Figure 5b. Enlarged portion of Figure 5a (upper most record).

2.1 Miocene/Pliocene (M/P) boundary

2.1.1 Top of *Triquetrorhabdulus rugosus* - Base of *Ceratolithus acutus*

The Miocene/Pliocene (M/P) boundary is placed between the LO of *Triquetrorhabdulus rugosus* and the FO of *C. acutus* (*Ceratolithus* spp.). *T. rugosus* is recorded since Early Miocene and in this site its stratigraphic distribution is not always continuous. Around 7.2 Ma, near to the Tortonian/Messinian boundary, its presence is more regular, decreasing progressively until the LO at 5.452 - 5.410 Ma (CN10a/NN12, chron C3r-Gilbert). This age slightly diachronous respect to the western equatorial Pacific where the assigned age is 5.279 Ma (Backman & Raffi, 1997), and also regarding the proposal of Raffi & Flores (1995) in the eastern equatorial Pacific, who established that the LO of *T. rugosus* and the FO of *C. acutus* occur at 5.34 Ma.

Close to the Miocene/Pliocene boundary, *Ceratolithus* spp. appears in the record (*Ceratolithus acutus*) and begins its diversification.

The FO of *C. acutus* occurs at 5.367 - 5.322 Ma (subzone CN10a/Zone NN12, chron C3r-Gilbert). Raffi & Flores (1995) placed the age of this event at 5.34 Ma in the eastern equatorial Pacific, and Raffi *et al.* (2006) at 5.345 Ma in the equatorial Atlantic Ocean. Approximately at same age of the FO of *C. acutus*, the FO of *Ceratolithus armatus* and the FO of *Ceratolithus atlanticus* is observed. Briefly after is identified the FO of *Ceratolithus larrymayeri* and the FO of *Amaurolithus bizarrus* at 5.322 - 5.299 Ma (subzone CN10a/Zone NN12, chron C3r-Gilbert). The LO of *C. larrymayeri*, is placed at 5.255 - 5.219 Ma (subzone CN10a/Zone NN12, boundary between chronos C3n4n-Thvera and C3r-Gilbert).

2.2 Upper Miocene

For this interval all taxa are well preserved and total abundance is low, increasing its abundance towards the Miocene/Pliocene boundary. *Discoaster* spp. is the dominant taxa at Upper Miocene, specially five rayed aster-

oliths. *Discoaster loeblichii*, used by Raffi & Flores (1995) as a marker of CN8a/CN8b boundary at equatorial Pacific, is present in the sequence but it is less abundant and show small sizes. Alternatively, *C. mexicanus*, an endemic species, is very abundant. This taxon is a very useful marker to identify the late Tortonian in the Caribbean region. *Florisphaera profunda*, *Discoaster* spp. and *Reticulofenestra* spp. are very abundant through the Upper Miocene, even during the interval equivalent to the Messinian Salinity Crisis. At the lower part of the sequence the absolute abundance is low, but the relative abundances of *Sphenolithus abies* group (*S. abies*, *Sphenolithus moriformis*, *Sphenolithus verensis* and *Sphenolithus neoabies*), *F. profunda* and the small placoliths, are high. Specimens of *C. macintyreii* and *C. pelagicus* show relatively big sizes for this interval. At the end of the Tortonian and until the Messinian, the total abundance of the nanofossil record increased, reaching the higher values.

2.2.1 Top of *Discoaster quinqueramus*

The LO of *Discoaster quinqueramus* is noticeable because the decrease of this species since 5.921 Ma, when the abundances gradually became low until the extinction at 5.453 - 5.473 Ma (subzone CN10a/biozone NN12, chron C3r). This age corresponds to the younger part of the Upper Miocene and the event occurs before the Miocene/Pliocene boundary, with a very short difference with those established by Krijgsman *et al.* (2004) for the eastern equatorial Atlantic, and Backman & Raffi (1997) for the western equatorial Atlantic (Ceara Rise). *D. quinqueramus* shows an interval of very high abundance between 7.502 Ma and 6.814 Ma, being dominant over the other *Discoaster* species.

The LO of *Discoaster berggrenii* is identified at 5.559-5.473 Ma (base of subzones CN10a/NN12, chron C3r) and precedes the LO of *D. quinqueramus*.

2.2.2 Range of *Amaurolithus amplificus*

Amaurolithus amplificus is a robust species that probably is the result of the morphological evolution of *T. rugosus* (Raffi *et al.*, 1998). We observed some transitional forms between *T. rugosus* and *A. amplificus*, defined taxonomically as *Triquetrorhabdulus extensus* and *Triquetrorhabdulus finifer* (Theodoridis, 1984). At ODP Site 999 A.

amplificus is scarce and represented by several morphotypes, angular or rounded shaped. The FO of *A. amplificus* occurs at 6.953 - 6.932 Ma (subzones CN9bA/NN11b, chron C3Ar). Curry *et al.* (1995) report the age of this event in the western equatorial Atlantic at 6.5 Ma. Backman & Raffi (1997) found some problems to define the age of the FO of *A. amplificus* because the presence of evolutionary transitional forms, and placed the event at 6.840±0.003 Ma. Raffi & Flores (1995) defined the FO of *A. amplificus* at 6.50 Ma in the eastern equatorial Pacific, and Raffi *et al.* (2006), (according to the ATNTS2004 of Lourens *et al.*, 2004) assigned an age of 6.909 Ma at equatorial Atlantic and 6.684 Ma in the eastern Mediterranean.

After the FO of *A. amplificus* we observe the FO of *A. delicatus* at 6.880 - 6.864 Ma (subzones CN9bA/NN11b, chron C3Ar), and the LO of *Reticulofenestra rotaria* at 6.426 - 6.370 Ma (subzones CN9bB/NN11b, chron C3An1r).

The LO of *A. amplificus*, is identified at 5.963 - 5.959 Ma (subzones CN9bB/NN11b, chron C3r). Backman & Raffi (1997) obtained an age of 5.993±0.002 Ma in the western equatorial Atlantic. Krijgsman *et al.* (2004) assign an age of 5.976 - 5.972 Ma in sediments from eastern equatorial Atlantic (Morocco), and Raffi & Flores (1995) dated this event at 5.88±0.02 in the eastern equatorial Pacific.

2.3 Tortonian/Messinian boundary

The FO and the beginning of the diversification of *Amaurolithus* spp. mark the Tortonian/Messinian boundary. This interval is almost coincident with other four (4) events: the Upper Tortonian is marked by the FO of *Amaurolithus primus* followed by the FO of *Amaurolithus tricorniculatus*, and the Early Messinian is characterized by the FO of *R. rotaria* and the Top of the paracme of *R. pseudoubilicus*.

2.3.1 FO of *Amaurolithus* spp.

The first representatives of *Amaurolithus* in the record were horseshoe-shaped structures, malformed and tough, identified as *A. primus*, that at ODP Site 999A occurs at 7.306 - 7.295 Ma (subzone CN9a/NN11a, chron C3Br2r near to the boundary with C3Br1n). Backman & Raffi (1997),

Shackleton & Crowhurst (1997) and Raffi *et al.* (2006) proposed an age of 7.362 ± 0.004 Ma in the western equatorial Atlantic. Raffi *et al.* (2003), Hilgen *et al.* (1995, 2000a, 2000b), Krijgsman *et al.* (1997) and Negri & Villa (2000), estimated the age for this event for the Mediterranean at 7.424 Ma. The FO of *A. primus* is followed very closely by the FO of *A. tricorniculatus* estimated in 7.242 - 7.226 Ma (subzones CN9a/NN11a, chron C3Br1r).

2.3.2 Paracme of *Reticulofenestra pseudoumbilicus*

An interval of absence (paracme) of *R. pseudoumbilicus* ($>7\mu\text{m}$) was observed by Rio *et al.* (1990) in the equatorial Indian Ocean, Young (1990) in the western Indian Ocean and in the Red Sea, and afterwards by Takayama (1993) in the western equatorial Pacific. Raffi & Flores (1995) found this event since the limit of subzones CN8a/CN8b until CN9b. In the Indian Ocean it was interpreted as a regional feature reflecting oceanographic and climatic instability (Rio *et al.*, 1990). Gartner (1992) interpreted the decreasing of large placoliths in the North Atlantic as a possibly seasonal change in productivity (high productivity = low abundance of larger placoliths). At ODP Site 999A the paracme of *R. pseudoumbilicus* occurs at 8.567 - 8.516 Ma for the base, and 7.132 - 7.044 Ma for the top (from subzone CN8b/Zone NN10, chron C4r2r; until subzones CN9bA/NN11b, chron C3Ar). A marked decreasing or absence is abrupt and some specimens are present in the samples but always in proportions of less than 5%.

Other relevant event is the FO of *R. rotaria*. The age for this event is 7.226 - 7.132 Ma (subzones CN9a/ NN11a until CN9b/NN11b, chron C3Ar to C3Br1r).

2.4 Tortonian

2.4.1 FO of *Discoaster berggrenii* - LO of *Minylitha convallis*

The five rayed asteroliths appear at the Upper Miocene, and are one of the most important nannofossils of the assemblages. *Discoaster hamatus* and *D. bellus* were the oldest representatives of this group. *D. berggrenii* is the result of the evolution of *D. bellus* (Raffi *et al.*, 1998) from a not ornamented asterolith to one whose central area has

a protuberant five-rayed stellate knob. The development of this lineage possibly corresponds to an evolutionary adaptation that allows it to remain through the record until the higher Upper Miocene.

In our site, the FO of *D. berggrenii* was estimated at 8.262 - 8.233 Ma (subzones CN9a/NN11a, chron C4r1r/C4r1n). Raffi & Flores (1995) established an age of 8.35 ± 0.11 Ma in the eastern equatorial Pacific, and Shackleton & Crowhurst (1997) and Backman & Raffi (1997) proposed 8.281 ± 0.028 Ma for western equatorial Atlantic.

Raffi *et al.* (1998), based on morphological characters, proposed that *Discoaster quinqueramus* is a descendant in the lineage of *D. berggrenii* and *D. bellus*, which evolves from a simple central area and short rays until an ornamented central knob and long rays. Alternatively, *D. quinqueramus* shows radial symmetry. The FO of *D. quinqueramus* occurs at 8.152 - 8.148 Ma (subzones CN9a/NN11a, chron C4r1r), slightly after the FO of *D. berggrenii*. Shortly after of the FO of *D. quinqueramus*, occurs the LO of *D. bellus* at 7.994 - 7.933 Ma (subzones CN9a/NN11a, chron C4r2r).

The LO of *C. mexicanus* is placed at 7.857 - 7.853 Ma (subzones CN9a/NN11a, chron C4n2n). *C. mexicanus* was a taxon with geographical restriction that only has been reported at the Caribbean Sea (Kameo & Bralower, 2000) and the Gulf of Mexico (Bukry, 1971). Bukry (1973) suggests a possible derivation of *C. coalitus* and *C. mexicanus* from *Discoaster bollii* after the reduction of the rays.

The LO of *M. convallis* was estimated for this study at 7.836 - 7.833 Ma (subzones CN9a/NN11a, chron C4n2n). Raffi *et al.* (2003) reported an age of 8.685 ± 0.004 Ma in the Mediterranean, and Berggren *et al.* 7.8 Ma for several points and basins through the world.

2.4.2 Base of *Discoaster bellus* - Base of *Catinaster mexicanus*

In ODP Site 999A the FO of *D. bellus* occurs at 8.722 - 8.673 Ma (subzones CN8b/NN10, chron C4r2r). After this event start the diversification and the increase in the number of species of *Discoaster*. Nevertheless, *D. bellus* is not a common taxon. Schneider (1995), Raffi *et al.* (1995) and Raffi *et al.* (2006), report the FO of *D. bellus* at 10.72 Ma

in the eastern equatorial Pacific. Hilgen *et al.* (2000b, c) and Raffi *et al.* (2006), assign an age of 10.378 in the eastern Mediterranean. This interval is not studied here.

The FO of *D. loeblichii* is placed slightly after the FO of *D. bellus* at 8.673 - 8.617 Ma (subzones CN8b/NN10, chron C4r2r). Raffi & Flores (1995) used the FO of *D. loeblichii* to define the limit between subzones CN8a and CN8b estimating an age of 8.43±0.08 Ma. The FO of *D. challengerii* was recorded approximately at the same time that the FO of *D. loeblichii*. The FO of *D. surculus* occurs at 8.465 - 8.470 Ma (subzones CN8b/NN10, chron C4r2r).

For the FO of *C. mexicanus* we calculated 8.426 - 8.390 Ma (subzones CN8b/ NN10 until subzones CN9a/NN11a, chron C4r2r). The record of this species is continuous and abundant, but due to its geographical restriction it is not used as biostratigraphic marker in other regions. This species is a very useful marker for the Tortonian, not only for its continuity and abundance in the record, but for its short temporal range.

3. CONCLUSIONS

- We calibrated the age for 28 calcareous nannofossil events through Upper Miocene and Miocene/Pliocene boundary. This calibration is considered highly reliable, because we used the ¹⁸O stratigraphy, obtained by correlation with the astronomically dated ¹⁸O record from ODP Site 982 (North Atlantic) and western equatorial Atlantic ODP Site 926.
- The FO of *C. acutus* (5.367 - 5.322 Ma), the LO of *M. convallis* (7.836 - 7.833 Ma) and the FO of *Discoaster loeblichii* (8.673 - 8.617 Ma) are synchronic events; however the range of comparison of *M. convallis* is very wide (7.8 - 8.685 Ma; Berggren *et al.*, 1995 and Raffi *et al.*, 2003, respectively).
- The FO of *C. larrymayeri* (5.322 - 5.299 Ma), *C. atlanticus* (5.367 - 5.322 Ma), *A. amplificus* (6.953 - 6.932 Ma), *A. primus* (7.306 - 7.295 Ma), *D. berggrenii* (8.262 - 8.233 Ma), the LO of *T. rugosus* (5.452 - 5.410 Ma), *D. quinqueramus* (5.453 - 5.473 Ma), the top and the base of the paracme of *R. pseudoumbilicus* (8.567 - 8.516 Ma to 7.132 - 7.044 Ma) are slightly diachronic events.

- The LO of *R. rotaria* (6.426 - 6.370 Ma), and the FO of *A. delicatus* (6.880 - 6.864 Ma) and *R. rotaria* (7.226 - 7.132 Ma) are clearly diachronous (Table 1, Figures 5a, b).
- The Tortonian/Messinian boundary was established between the FO of *A. primus* and the FO of *A. tricorniculatus*, which is followed by the FO *R. rotaria* and the Top of the paracme of *R. pseudoumbilicus*.
- The Miocene/Pliocene boundary was defined by the FO of *C. acutus*, and the diversification of *Ceratolithus* genus (e.g. *C. armatus*, *C. atlanticus*).

4. ACKNOWLEDGEMENTS

The authors greatly acknowledge the *Instituto Colombiano del Petróleo-ICP-ECOPETROL* as sponsor of this research through the Cooperation Agreement subscribed with the *Universidad de Salamanca*. We thank Carlos Lancis and an anonymous referee for the reviewing of this article. Vladimir Torres Torres and María Carolina Vargas Fúquene, who made possible the cooperation agreement, were also acknowledged. This research used samples provided by the Ocean Drilling Program (ODP).

5. REFERENCES

- Acton, G.D., Galbrun, B. and King, J.W. 2000. Paleolatitude of the Caribbean Plate since the Late Cretaceous. In: Leckie, R.M., Sigurdson, H., Acton, G.D., and Draper, G. (Eds.), Proceedings of the Ocean Drilling Program, Scientific Results, 165: College Station, TX (Ocean Drilling Program), 149-173.
- Andrade, C.A. and Barton, E.D. 2000. Eddy development and motion in the Caribbean Sea. *Journal of Geophysical Research*, 105, 26 191-26 201.
- Backman, J. 1978. Late Miocene-Early Pliocene nannofossil biochronology and biogeography in the Vera Basin, SE Spain. *Stockholm Contributions in Geology*, 32, 93-114.
- Backman, J. 1980. Miocene-Pliocene nannofossils and sedimentation rates in the Hatton-Rockall Basin, NE Atlantic Ocean. *Acta Univ. Stockholm. Contrib. Geol.*, 36(1), 1-91.
- Backman, J., Schneider, D.A., Rio, D. and Okada, H. 1990. Neogene low-latitude magnetostratigraphy from Site 710 and revised age estimates of Miocene nannofossil datum events. In: Duncan, R.A., Backman, J., Peterson, L.C., *et al.*, Proceedings of the Ocean Drilling Program, Scientific Results, 115: College Station, TX (Ocean Drilling Program), 271-276. .

- Backman, J., and Raffi, I. 1997. Calibration of Miocene nannofossil events to orbitally tuned cyclostratigraphies from Ceara Rise. In: Shackleton, N.J., Curry, W.B., Richter, C., and Bralower, T.J. (Eds.), Proceedings of the Ocean Drilling Program, Scientific Results, 154: College Station, TX (Ocean Drilling Program), 83-99.
- Berggren, W.A., Kent, D.V., Swisher III, C.C., and Aubry, M.P. 1995. A revised Cenozoic Geochronology and Chronostratigraphy. In: *Geochronology, time scales and global stratigraphic correlation*. (Berggren, W.A. et al. Eds.) SEPM Special Publication, 54, 130-212.
- Bickert, T., Haug, G.H., and Tiedemann, R. 2004. Late Neogene benthic stable isotope record of Ocean Drilling Program Site 999: Implications for Caribbean paleoceanography, organic carbon burial, and the Messinian Salinity Crisis. *Paleoceanography*, 19, PA1023, doi: 10.1029/2002PA000799.
- Bowland, C.L. 1993. Depositional history of the western Colombian Basin, Caribbean Sea, revealed by seismic stratigraphy. *Geological Society of America Bulletin*, 105, 1321-1345.
- Bramlette, M.N., and Riedel, W.R. 1954. Stratigraphic value of discoasters and some other microfossils related to Recent coccolithophores. *Journal of Paleontology*, 28, 385-403.
- Bramlette, M.N., and Wilcoxon, J.A. 1967. Middle Tertiary calcareous nannoplankton of the Ciperó section, Trinidad, W.I. *Tulane Studies in Geology and Paleontology*, 5, 93-131.
- Brönnimann, P., and Stradner, H. 1960. Die Foraminiferen- und Discoasteriden-Zonen von Kuba und ihre interkontinentale Korrelation. *Erdöl-Zeitschrift für Bohr- und Fördertechnik*, 76, 364-369.
- Bukry, D. 1971. Cenozoic calcareous nannofossils from the Pacific Ocean. *San Diego Society of Natural History Transactions*, 16, 303-327.
- Bukry, D. 1973. *Low-latitude coccolith biostratigraphic zonation. Initial Reports of the Deep Sea Drilling Project*. Texas A&M University, Ocean Drilling Program, College Station, TX, United States, 15, 685-703.
- Bukry, D. 1975. *Coccolith and silicoflagellate stratigraphy, northwestern Pacific Ocean, Deep Sea Drilling Project, Leg 32. Initial Reports of the Deep Sea Drilling Project*. Texas A&M University, Ocean Drilling Program, College Station, TX, United States, 32, 677-701.
- Bukry, D., and Bramlette, M.N. 1969. *Initial Reports of the Deep Sea Drilling Project*, 1, 369-387.
- Bukry, D., and Percival, S.F. 1971. New Tertiary calcareous nannofossils. *Tulane Studies in Geology and Paleontology*, 8, 123-146
- Burke, K., Cooper, C., Dewey, J.F., Mann, P., and Pindell, J.L. 1984. Caribbean tectonics and relative plate motions. In Bonini, W.E., Hargraves, R.B., and Shagam, R. (Eds.). *The Caribbean-South American Plate Boundary and Regional Tectonics*. *Memoirs Geological Society of America*, 162, 31-63.
- Burke, K. 1988. Tectonic evolution of the Caribbean. *Annual Review of Earth and Planetary Sciences*, 16, 201-230.
- Burns, D.A. 1973. Structural analysis of flanged coccoliths in sediments from the South West Pacific Ocean. *Revista Española de Micropaleontología*, 5(1), 147-160.
- Clocchiatti, M., and Jerkovic, L. 1970. "*Cruciplacolithus tenuiforatus*", nouvelle espèce de Coccolithophoridae du Miocène d'Algérie et de Yougoslavie. *Cahiers de Micropaléontologie*, ser. 2, 2, 1-6.
- Curry, W.B., Shackleton, N.J., Richter, C., et al. 1995. Proceedings of the Ocean Drilling Program, Initial Reports, 154: College Station, TX (Ocean Drilling Program).
- Deflandre, G. 1942. Possibilités morphogénétiques comparées du calcaire et de la silice, à propos d'un nouveau type de microfossile calcaire de structure complexe, *Lithostromation perdurum* n. gen. n. sp. *Comptes Rendus des Seances de l'Académie des Sciences Paris*, 214, 917-19.
- Deflandre, G., and Fert, C. 1954. Observations sur les Coccolithophorides actuels et fossiles en microscopie ordinaire et électronique. *Annales de Paléontologie*, 40, 115-176.
- Duncan, R.A., and Hargraves, R.B. 1984. Plate tectonic evolution of the Caribbean region in the mantle reference frame. In: Bonini, W.E., Hargraves, R.B., and Shagam, R. (Eds.), *The Caribbean-South American Plate Boundary and Regional Tectonics*. *Memoirs Geological Society of America*, 162, 81-94.
- Einsele, G. 1992. *Sedimentary Basins. Evolution, Facies and Sediments Budget*. Springer Verlag, Berlin, 628 pp.
- Flores, J.-A. 1985. *Nanoplankton calcáreo en el Neógeno del borde noroccidental de la Cuenca del Guadalquivir (S.O. de España)*. Tesis Doctoral, Facultad de Ciencias, Universidad de Salamanca, 714 pp. (Inédita).
- Flores, J.-A., and Sierro, F.J. 1997. Revised technique for calculation of calcareous nannofossil accumulation rates. *Micropaleontology*, 43, 321-324.
- Flores, J.-A., Sierro, F.J., Filippelli, G.M., Bárcena, M.A., Pérez-Folgado, M., Vázquez, A., and Utrilla, R. 2005. Surface water dynamics and phytoplankton communities during deposition of cyclic late Messinian sapropel sequences in the western Mediterranean. *Marine Micropaleontology*, 56, 50-79.
- Gartner, S. 1967. Calcareous nannofossils from Neogene of Trinidad, Jamaica, and Gulf of Mexico. *University of Kansas Paleontological Contributions, Paper 29*, 1-7.
- Gartner, S. 1969. Correlation of Neogene planktonic foraminifera and calcareous nannofossil zones. *Transactions of the Gulf Coast Association of Geological Societies*, 19, 585-599.
- Gartner, S. 1992. Miocene nannofossil chronology in the North Atlantic, DSDP Site 608. *Marine Micropaleontology*, 18, 307-331.
- Gartner, S., and Bukry, D. 1974. *Ceratolithus acutus* Gartner and Bukry n. sp. and *Ceratolithus amplificus* Bukry and Percival - nomenclatural clarification. *Tulane Studies in Geology and Paleontology*, 11, 115-118.
- Gartner, S., and Bukry, D. 1975. *United States Geological Survey, Journal of Research*, 3, 451-465.
- Gordon, A.L. 1967. Circulation of the Caribbean Sea. *Journal of Geophysical Research*, 72, 6207-6223.
- Guzmán, G. 2007. *Stratigraphy and Sedimentary Environment and Implications in the Plato Basin and the San Jacinto Belt, Northwestern Colombia*. Ph.D. Thesis, University of Liège, Belgium, 487 pp.
- Haackel, E. 1894. *Systematische Phylogenie der Protisten und Pflanzen*.

- Reimer, Berlin, 400 pp.
- Haq, B.U. 1976. Coccoliths in cores from the Bellinghausen abyssal plain and Antarctic continental rise (DSDP Leg 35). *Initial Reports of the Deep Sea Drilling Project*, 35, 557-567.
- Haq, B.U., and Berggren, W.A. 1978. Late Neogene calcareous plankton biochronology of the Rio Grande Rise (South Atlantic Ocean). *Journal of Paleontology*, 52, 1167-1194.
- Hibberd, D.J. 1976. The ultrastructure and taxonomy of the Chrysophyceae and Prymnesiophyceae (Haptophyceae): a survey with some new observations on the ultrastructure of the Chrysophyceae. *Journal of the Linnean Society of London, Botany*, 72, 55-80.
- Hilgen, F.J., Krijgsman, W., Langereis, C.G., Lourens, L.J., Santarelli, A., and Zachariasse, W.J. 1995. Extending the astronomical (polarity) time scale into the Miocene. *Earth Planetary Science Letters*, 136, 495-510.
- Hilgen, F.J., Bissoli, L., Iaccarino, S., Krijgsman, W., Meijer, R., Negri, A., and Villa, G. 2000a. Integrated stratigraphy and astrochronology of the Messinian GSSP at Oued Akrech (Atlantic Morocco). *Earth and Planetary Science Letters*, 182, 237-251.
- Hilgen, F.J., Krijgsman, W., Raffi, I., Turco, E., and Zachariasse, W.J., 2000b. Integrated stratigraphy and astronomical calibration of the Serravallian/Tortonion boundary section at Monte Gibliscemi (Sicily, Italy). *Marine Micropaleontology*, 38, 181-211.
- Hilgen, F.J., Iaccarino, S., Krijgsman, W., Villa, A.G., Langereis, C.G., and Zachariasse, W.J., 2000c. The Global Boundary Stratotype Section and Point (GSSP) of the Messinian Stage (uppermost Miocene). *Episodes*, 23, 1-6.
- Hodell, D., Curtis, J., Sierro, F.J., and Raymo, M. 2001. Correlation of Late Miocene-to-Early Pliocene Sequences between the Mediterranean and North Atlantic. *Paleoceanography*, 16(2), 164-179.
- Jafar, S.A., Martini, E. 1975. *Senckenbergiana Lethaea*, 56, 381-397.
- Johns, W.E., Townsend, T.L., Fratantoni, D.M., and Wilson, W.D. 2002. On the Atlantic inflow to the Caribbean Sea. *Deep-Sea Research Part I*, 49, 211-243.
- Kameo, K., and Bralower, T.J. 2000. Neogene calcareous nannofossil biostratigraphy of Sites 998, 999, and 1000, Caribbean Sea. In: Leckie, R.M., Sigurdsson, H., Acton, G.D., and Draper, G. (Eds.), Proceedings of the Ocean Drilling Program, Scientific Results, 165: College Station, TX (Ocean Drilling Program). 3-17.
- Kamptner, E. 1948. Coccolithen aus dem Torton des Inneralpinen Wiener Beckens. *Akademie der Wissenschaften in Wien, Mathematisch-Naturwissenschaftliche Klasse; Abteilung I*, 157, 1-16.
- Kamptner, E. 1954. Untersuchungen über den Feinbau der Coccolithen. *Archiv für Protistenkunde*, 100, 1-90.
- Kamptner, E. 1963. Coccolithineen-Skelettreste aus Tiefseeablagerungen des Pazifischen Ozeans. *Annual Naturhistorisches Museum Wien*, 66, 139-204.
- Klitgord, K.D., and Schouten, H. 1986. Plate kinematics of the central Atlantic. In: Vogt, P.R., and Tucholke, B.E. (Eds.), *The Geology of North America (Vol. M): The Western North Atlantic Region*. Geological Society of America, 351-378.
- Krijgsman, W., Hilgen, F.J., Langereis, C.G., Santarelli, A., and Zachariasse, W.J. 1995. Late Miocene magnetostratigraphy, biostratigraphy and cyclostratigraphy in the Mediterranean. *Earth and Planetary Science Letters*, 136 (3-4), 475-494.
- Krijgsman, W., Hilgen, F.J., Negri, A., Wijbrans, J.R., and Zachariasse, W.J. 1997. The Monte del Casino section (northern Apennines, Italy): a potential Tortonion/Messinian boundary stratotype? *Palaeogeography, Palaeoclimatology, Palaeoecology*, 133 (1-2), 27-47.
- Krijgsman, W., Hilgen, F.J., Raffi, I., Sierro, F.J., and Wilson, D.S. 1999. Chronology, causes, progression of the Messinian salinity crisis. *Nature*, 400 (6745), 652-655.
- Krijgsman, W., Gaboardi, S., Hilgen, F.J., Iaccarino, S., de Kaenel, E., and van der Laan, E., 2004. Revised astrochronology for the Ain el Beida section (Atlantic Morocco): no glacio-eustatic control for the onset of the Messinian Salinity Crisis. *Stratigraphy*, 1, 87-101.
- Loeblich, A.R., and Tappan, H., 1978. The coccolithophorid genus *Calcidiscus* Kamptner and its synonyms. *Journal of Paleontology*, 52, 1390-1392.
- Lohmann, H. 1902. Die Coccolithophoridae, eine Monographie der Coccolithen bildenden Flagellaten, zugleich ein Beitrag zur Kenntnis des Mittelmeerauftriebs. *Archiv für Protistenkunde*, 1, 89-165.
- Lourens, L.J., Hilgen, F.J., Raffi, I., and Vergnaud-Grazzini, C. 1996. Early Pleistocene chronology of the Vrica section (Calabria, Italia). *Paleoceanography*, 11, 797-812.
- Lourens, L.J., Hilgen, F.J., Shackleton, N.J., Laskar, J., and Wilson, D. 2004. The Neogene Period. In: *A Geological Time Scale* (Gradstein, F. M., Ogg, J. G., Smith, A. G., eds.), Cambridge University Press, Cambridge, 409-440.
- Malfait, B.T., and Dinkelman, M.G. 1972. Circum-Caribbean tectonic and igneous activity and the evolution of the Caribbean plate. *Geological Society of America Bulletin*, 83, 251-272.
- Marino, M., and Flores, J.-A. 2002. Miocene to Pliocene Calcareous Nannofossil Biostratigraphy at ODP Leg 177 Sites 1088 and 1090. *Marine Micropaleontology*, 45, 291-307.
- Martini, E. 1971. Standard Tertiary and Quaternary calcareous nannoplankton zonation. In: Farinacci, A. (Ed.), *Proceedings of the II Planktonic Conference*. Ed. Tecnoscienza, Roma 1970, 2, 739-785.
- Martini, E., and Bramlette, M.N. 1963. Calcareous nannoplankton from the experimental Mohole Drilling. *Journal of Paleontology*, 37(4), 845-856.
- Meschede, M., and Frisch, W. 1998. A plate-tectonic model for the Mesozoic and Early Cenozoic history of the Caribbean plate. *Tectonophysics*, 296, 269-291.
- Morris, A.E.L., Taner, I., Meyerhoff, H.A., and Meyerhoff, A.A. 1990. Tectonic evolution of the Caribbean region: alternative hypothesis. In: Dengo, G., and Case, J.E. (Eds.), *The Caribbean Region*. Geol. Soc. Am., Geol. of North Am. Ser., H: 433-457.
- Muller, C., 1974. Calcareous nannoplankton, Leg 25 (Western Indian Ocean). *Initial Reports of the Deep Sea Drilling Project*, 25, 579-633.
- Murphy, S.J., Hurlburt, H.E., and O'Brien, J.J. 1999. The connectivity of eddy variability in the Caribbean Sea, the Gulf of Mexico, and the Atlantic Ocean. *Journal of Geophysical Research*, 98 (C5), 8389-8394.

- Murray, G., and Blackman, V.H. 1898. On the nature of the coccospheres and rhabdospheres. *Royal Society of London, Philosophical Transactions*, 190B, 427-441.
- Negri, A., Giunta, S., Hilgen, F. J., Krijgsman, W. and Vai, G. B. 1999. Calcareous nannofossil biostratigraphy of the Monte del Casino section (northern Apennines - Italy) and paleoceanographic conditions at times of late Miocene sapropel formation. *Marine Micropaleontology*, 36 (1), 13-30.
- Negri, A. and Villa, G. 2000. Calcareous nannofossil biostratigraphy, biochronology and paleoecology at the Tortonian/Messinian boundary of the Faneromeni section (Crete). *Palaeogeography, Palaeoclimatology, Palaeoecology*, 156, 195-209.
- Okada, H., and Honjo, S. 1973. The distribution of oceanic coccolithophorids in the Pacific. *Deep-Sea Research*, 20, 355-374.
- Okada, H., and Bukry, D. 1980. Supplementary modification and introduction of code numbers to the low-latitude coccolith biostratigraphic zonation (Bukry, 1973; 1975). *Marine Micropaleontology*, 5, 321-325.
- Perch-Nielsen, K. 1977. Albian to Pleistocene calcareous nannofossils from the Western South Atlantic, DSDP Leg 39. *Initial Reports of the Deep Sea Drilling Project*, 39, 699-823.
- Perch-Nielsen, K. 1985. Cenozoic calcareous nannofossils. In: Bolli, H.M., Saunders, J.B. and Perch-Nielsen, K. (Eds.), *Plankton Stratigraphy*. Cambridge University Press, Cambridge, 427-554.
- Peters, J.L., Murray, R.W., Sparks, J.W., and Coleman, D.S. 2000. Terrigenous matter and dispersed ash in sediment from the Caribbean Sea: results from Leg 165. In: Leckie, R.M., Sigurdsson, H., Acton, G.D., and Draper, G. (Eds.), *Proc. ODP, Sci. Results*, 165: College Station, TX (Ocean Drilling Program), 115-124.
- Pindell, J.L. 1994. Evolution of the Gulf of Mexico and the Caribbean, In: Donovan, S.K., and Jackson, T.A. (Eds.), *Caribbean Geology: An Introduction*. Jamaica (Univ. West Indies Publishers' Assoc.), 13-39.
- Pindell, J., and Dewey, J. 1982. Permo-Triassic reconstruction of western Pangea and the evolution of the Gulf of Mexico/Caribbean region. *Tectonics*, 1, 179-211.
- Pindell, J., Cande, S., Pitman, W., Rowley, D., Dewey, J., Labrecque, J., and Haxby, W. 1988. A plate-kinematic framework for models of Caribbean evolution. *Tectonophysics*, 155, 21-138.
- Pindell, J.L., and Barrett, S.F. 1990. Geological evolution of the Caribbean region: A plate-tectonic perspective. In: Dengo, G., and Case, J.E. (Eds.), *The Caribbean Region*. Geol. Soc. Am., Geol. North Am. Ser., H, 405-432.
- Raffi, I., and Flores, J.-A. 1995. Pleistocene through Miocene calcareous nannofossils from eastern equatorial Pacific Ocean. *Proceedings of the Ocean Drilling Program, Scientific Results*. College Station, TX (Ocean Drilling Program), 138, 233-286.
- Raffi, I., Rio, D., d'Atri, A., Fornaciari, E., and Rocchetti, S. 1995. Quantitative distribution patterns and biomagnetostratigraphy of middle and late Miocene calcareous nannofossils from equatorial Indian and Pacific oceans (Leg 115, 130, and 138). In: Pisias, N.G., Mayer, L.A., Janecek, T.R., Palmer-Julson, A., and van Andel, T.H. (Eds.), *Proceedings of the Ocean Drilling Program, Scientific Results*, 138: College Station, TX (Ocean Drilling Program), 479-502.
- Raffi, I., Backman, J., and Rio, D. 1998. Evolutionary trends of tropical calcareous nannofossils in the late Neogene. *Marine Micropaleontology*, 35, 17-41.
- Raffi, I., Mozzato, C.A., Fornaciari, E., Hilgen, F.J., and Rio, D. 2003. Late Miocene calcareous nannofossil biostratigraphy and astro-biochronology for the Mediterranean region. *Micropaleontology*, 49, 1-26.
- Raffi, I., Backman, J., Fornaciari, E., Pälike, H., Rio, D., Lourens, L., and Hilgen, F.J. 2006. A review of calcareous nannofossil astro-biochronology encompassing the past 25 million years. *Quaternary Science Reviews*, 25, 3113-3137.
- Richardson, P.L. 2005. Caribbean Current and eddies as observed by surface drifters. *Deep Sea Research Part II: Topical Studies in Oceanography*, 52 (3-4), 429-463.
- Rio, D., Fornaciari, E., and Raffi, I. 1990. Late Oligocene through early Pleistocene calcareous nannofossils from western equatorial Indian Ocean (Leg 115). In: Duncan, R.A., Backman, J., Peterson, L.C., et al., *Proceedings of the Ocean Drilling Program, Scientific Results*, 115: College Station, TX (Ocean Drilling Program), 175-235.
- Roth, J.M., Droxler, A.W., and Kameo, K. 2000. The Caribbean carbonate crash at the middle to late Miocene transition: linkage to the establishment of the modern global ocean conveyor. In: Leckie, R.M., Sigurdsson, H., Acton, G.D., and Draper, G. (Eds.), *Proc. ODP, Sci. Results*, 165: College Station, TX (Ocean Drilling Program), 249-273.
- Roth, P.H. 1970. Oligocene calcareous nannoplankton biostratigraphy. *Eclogae Geologicae Helveticae*, 63, 799-881.
- Schiller, J. 1930. Coccolithineae. In: L. Rabenhorst (Ed.). *Kryptogamen-Flora von Deutschland, Österreich und der Schweiz*. 10. Band, 2. Abt., 89-267.
- Schneider, D.A. 1995. Paleomagnetism of some Leg 138 sediments: detailing Miocene chronostratigraphy. In: Pisias, N.G., Mayer, L.A., Janecek, T.R., Palmer-Julson, A., van Andel, T.H. (Eds.). *Proceedings of the Ocean Drilling Program, Scientific Results*, 138. Ocean Drilling Program, College Station, TX, 59-72.
- Shackleton, N.J., Hall, M.A., and Pate, D. 1995a. Pliocene stable isotope stratigraphy of ODP Site 846. In: Pisias, N.G., Mayer, L.A., Janecek, T.R., Palmer-Julson, A., van Andel, T.H. (Eds.). *Proceedings of the Ocean Drilling Program, Scientific Results*, 138. Ocean Drilling Program, College Station, TX, 337-355.
- Shackleton, N.J., Crowhurst, S., Hagelberg, T., Pisias, N.G., and Schneider, D.A. 1995b. A new late Neogene time scale: application to Leg 138 sites. In: Pisias, N.G., Mayer, L.A., Janecek, T.R., Palmer-Julson, A., van Andel, T.H. (Eds.). *Proceedings of the Ocean Drilling Program, Scientific Results*, 138. Ocean Drilling Program, College Station, TX, 73-101.
- Shackleton, N.J., and Crowhurst, S. 1997. Sediment fluxes based on an orbitally tuned time scale 5 Ma to 14 Ma, Site 926. *Proceedings of the Ocean Drilling Program, Scientific Results*, 154, 69-82.
- Shackleton, N.J., and Hall, M.A. 1997. The late Miocene stable isotope record, Site 926. *Proceedings of the Ocean Drilling Program, Scientific Results*, 154, 367-374.
- Sigurdsson, H., Leckie, R.M., Acton, G.D., et al. 1997. Shipboard Scientific Party. Site 999. *Proceedings of the Ocean Drilling Program, Initial Reports*, 165: College Station, TX (Ocean Drilling Program),

131-230. .

- Takayama, T. 1993. Notes on Neogene calcareous nannofossil biostratigraphy of the Ontong Java Plateau and size variations of *Reticulofenestra* coccoliths. In: Berger, W.H., Kroenke, L.W., Mayer, L.A., et al. Proceedings of the Ocean Drilling Program, Scientific Results, 130: College Station, TX (Ocean Drilling Program), 179-229.
- Tan, S.H. 1927. . *Koninklijke Nederlandse Akademie van Wetenschappen, Proceedings; Sect. Sci.*, 30, 411-419.
- Theodoridis, S. A. 1984. Calcareous nannofossil biozonation of the Miocene and revision of the Helicoliths and Discoasters. *Utrecht Micropaleontological Bulletins*, 32, 271pp.
- Tomczak, M., and Godfrey, J.S. 2001. Regional Oceanography: An introduction. Pdf version 1.0, 391 pp.
- Wallich, G.C. 1877. Observations on the coccosphere. *Annals and Magazine of Natural History*, 19, 342-350.
- Wise, S.W. Jr. 1983. Mesozoic and Cenozoic calcareous nannofossils recovered by Deep Sea Drilling Project Leg 71 in the Falkland Plateau region, Southwest Atlantic Ocean. In: W.J Ludwig and V.A Krasheninnikov et al., Editors, Initial Reports of the Deep Sea Drilling Project 71, U.S. Government Printing Office, Washington, D.C., 481-550.
- Wüst, G. 1964. *Stratification and Circulation in the Antillean-Caribbean Basins, 1, Spreading and Mixing of the Water Types with an Oceanographic Atlas*. Columbia University Press, New York, 201 pp.
- Young, J.R. 1990. Size variation of Neogene *Reticulofenestra* coccolith from Indian Ocean DSDP cores. *Journal of Micropalaeontology*, 9, 71-86.

Web Pages:

Institute for Geophysics. University of Texas at Austin:
www.ig.utexas.edu/research/projects/caribbean

MANUSCRITO RECIBIDO: 23 de mayo, 2010

MANUSCRITO ACEPTADO: 10 de diciembre, 2010

Appendix 1

Calcareous Nannofossils considered in this study (in alphabetical order)

- Kingdom: **CHROMISTA** Cavalier-Smith, 1981
Phylum: **HAPTOPHYTA** Hibberd ex Cavalier-Smith, 1986
Class: **PRYMNESIOPHYCEAE** Hibberd, 1976
- Amaurolithus amplificus* (Bukry & Percival, 1971) Gartner & Bukry, 1975
Amaurolithus bizarrus (Bukry, 1973) Gartner & Bukry, 1975
Amaurolithus delicatus Gartner & Bukry, 1975
Amaurolithus primus (Bukry & Percival, 1971) Gartner & Bukry, 1975
Amaurolithus tricorniculatus (Gartner, 1967) Gartner & Bukry, 1975
Calcidiscus leptoporus (Murray & Blackman, 1898) Loeblisch & Tappan, 1978
Calcidiscus macintyreii (Bukry & Bramlette, 1969) Loeblisch & Tappan, 1978
Catinaster mexicanus Bukry, 1971
Ceratolithus acutus Gartner & Bukry, 1974
Ceratolithus armatus Müller, 1974
Ceratolithus atlanticus Perch-Nielsen, 1977
Ceratolithus larrymayeri Backman & Raffi, 1998
Coccolithus pelagicus (Wallich, 1877) Schiller, 1930
Coccolithus pelagicus var. *tenuiforatus* (Clocchiatti & Jerkovic, 1970) Wise, 1983
Discoaster asymmetricus Gartner, 1969
Discoaster bellus Bukry & Percival, 1971
Discoaster berggrenii Bukry, 1971
Discoaster brouweri Tan, 1927, emend. Bramlette & Riedel, 1954
Discoaster pentaradiatus Tan, 1927, emend. Bramlette & Riedel, 1954
Discoaster prepentarradiatus Bukry & Percival, 1971
Discoaster quinqueramus Gartner, 1969
Discoaster surculus Martini & Bramlette, 1963
Discoaster triradiatus Tan, 1927
Discoaster variabilis Martini & Bramlette, 1963
Dictyococcites antarcticus Haq, 1976
Dictyococcites productus (Kamptner, 1963) Backman, 1980
Florisphaera profunda Okada & Honjo, 1973
Geminolithella rotula (Kamptner, 1948) Backman 1980
Helicosphaera carteri (Wallich, 1877) Kamptner, 1954
Helicosphaera sellii (Bukry & Bramlette, 1969) Jafar & Martini, 1975
Lithostromation perdurum Deflandre, 1942
Minilytha convalis Bukry, 1973
Pontosphaera milepuncta Gartner, 1967
Pontosphaera multipora (Kamptner, 1948) Roth, 1970 emend. Burns, 1973
Reticulofenestra minuta Roth, 1970
Reticulofenestra minutula (Gartner, 1967) Haq & Berggren, 1978
Reticulofenestra pseudoumbilicus (Gartner, 1967) Gartner, 1969
Reticulofenestra rotaria Theodoridis, 1984
Scyphosphaera amphora Deflandre, 1942
Scyphosphaera apsteinii Lohmann, 1902
Scyphosphaera globulata Bukry & Percival, 1971
Sphenolithus abies Deflandre in Deflandre & Fert, 1954
Sphenolithus moriformis (Brönnimann & Stradner, 1960) Bramlette & Wilcoxon, 1967
Sphenolithus neoabies Bukry & Bramlette, 1969
Sphenolithus verensis Backman, 1978
Triquetrorhabdulus extensus Theodoridis, 1984
Triquetrorhabdulus finifer Theodoridis, 1984
Triquetrorhabdulus rugosus Bramlette & Wilcoxon, 1967

Appendix 2

Plates

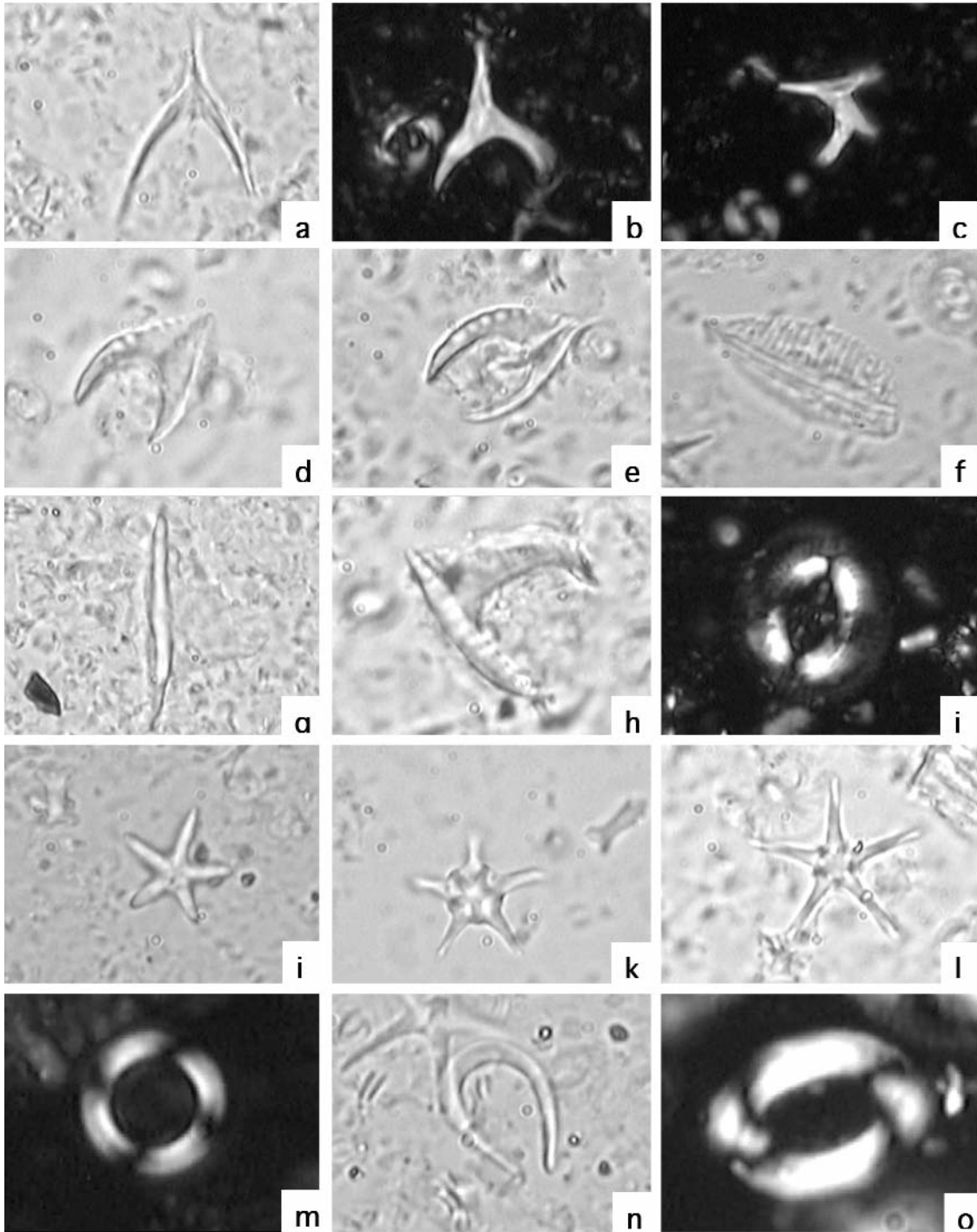


Plate 1. **a.** *C. larrymayeri*; **b.** *A. bizarrus*; **c.** *C. atlanticus*; **d.** *C. acutus*; **e.** *C. armatus*; **f.** *T. rugosus*; **g.** *T. extensus*; **h.** *A. amplificus*; **i.** *C. pelagicus*; **j.** *D. bellus*; **k.** *D. berggrenii*; **l.** *D. quinquerramus*; **m.** *R. rotaria*; **n.** *A. delicatus*; **o.** *R. pseudoumbilicus* >7 μ m.

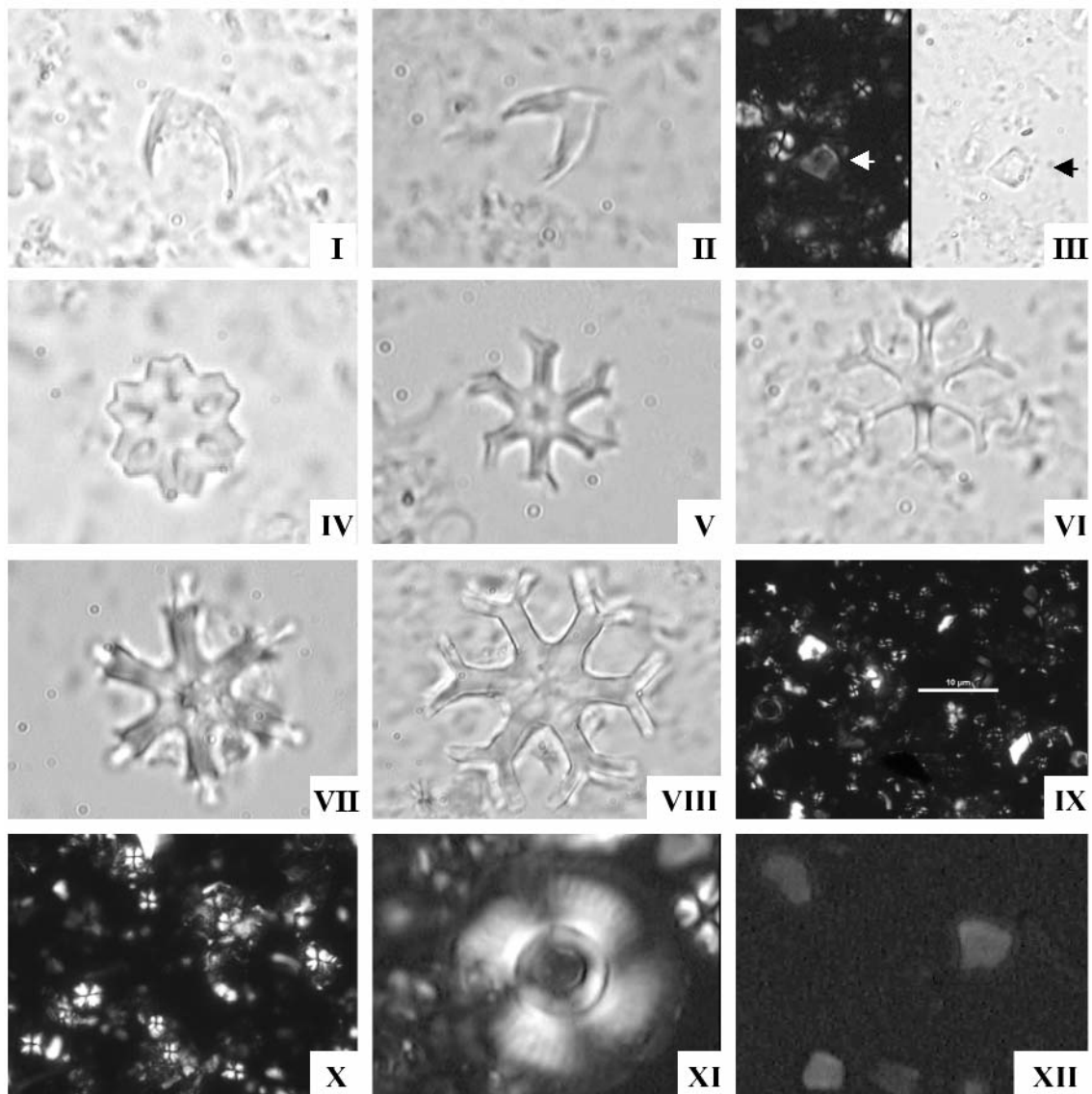


Plate 2. I. *A. tricorniculatus*; II. *A. primus*; III. *M. convallis* NX; IV. *C. mexicanus*; V. *D. loeblichii*; VI. *D. challengerii*; VII. *D. surculus*; VIII. *D. variabilis*; IX. Small placoliths (*R. minuta*); X. *Sphenolithus abies* group (*S. abies*, *S. moriformis*, *S. neoabies*); XI. *C. macintyreii*; XII. *F. profunda*.

Nannoplankton and planktonic foraminifera biostratigraphy of the eastern Betics during the Tortonian (SE Spain)

Carlos Lancis¹, José Enrique Tent-Manclús¹, Jesús Miguel Soria¹, Hugo Corbí¹,
Jaume Dinarès-Turell² and Alfonso Yébenes¹

¹ Universidad de Alicante, Departamento de Ciencias de la Tierra y del Medio Ambiente. Aptdo. 99.
03080 San Vicente del Raspeig, Alicante. Carlos.lancis@ua.es

² Istituto Nazionale di Geofisica e Vulcanologia, Via di Vigna Murata, 605, 00143 Roma, Italy.

Resumen

El final del Serravalliense y principio del Tortonense es un periodo de fuerte actividad tectónica en la Cordillera Bética. Además, existe un debate sobre la existencia de sedimentos de edad Tortonense inferior al no existir claras atribuciones fósiles en esa edad. Estos sedimentos se asignan a dicha edad por criterios indirectos, tanto estratigráficos como por la ausencia de contenido fósil más antiguo o más reciente. En este trabajo se describe la sección compuesta de *Les Moreres-Albatera*, que es probablemente una de las secciones más completas de edad Tortonense en la bibliografía de la Cordillera Bética, pese a tener un importante hiato de cerca de 1 Millón de años ligado a un evento tectónico intra-Tortonense. La sección presenta dos unidades litológicas calizas a la base (El Castellà) y al techo (Las Ventanas) y dos unidades intermedias margosas, la inferior, llamada Les Moreres, y la superior, Galería de los Suizos se encuentran separadas por el conglomerado de la Raya del Búho. Se han identificado las biozonas de nanofósiles calcáreos CN5b/NN7 a CN9a/NN11a (Okada & Bukry, 1980; Martini, 1971) y de foraminíferos planctónicos de MMi9 a MMi12a (Lourens *et al.*, 2004). La biostratigrafía de los primeros ha permitido identificar un hiato que incluye la parte alta de las biozonas CN7/NN9 hasta la parte baja de CN9a/NN11a (Okada & Bukry, 1980; Martini, 1971). La integración de los datos biostratigráficos con los paleomagnéticos en la sección *Albatera* permite la calibración del límite de los magnetocrones C4r.1r/C4n.2n.

Palabras clave: Cordillera Bética, Mioceno, Tortonense, Nanoplancton calcáreo, Foraminíferos planctónicos, Bioestratigrafía.

Abstract

The Serravallian-Tortonian boundary was a time of strong tectonic activity in the Betic Cordillera. The Early Tortonian sediments continue to be under debate because no clear fossil attributions are available. These sediments have been assigned an Early Tortonian age by indirect stratigraphic criteria or by the absence of fossil content older or younger in age. The present work documents the *Les Moreres-Albatera* composite section, probably the most complete section of the Tortonian age in the Betic Cordillera, despite a major time gap of about 1 Ma due to an intra-Tortonian tectonic event. The section has two limestone units at the bottom (El Castellà) and the top (Las Ventanas) and two intermediate marly units, the lower Les Moreres and the upper Galería de los Suizos divided by the Raya del Búho Conglomerate. The calcareous nannoplankton biozones from CN5b/NN7 to CN9a/NN11a (Okada & Bukry, 1980; Martini, 1971) have been identified, as have the planktonic foraminifera biozones from MMi9 to MMi12a (Lourens *et al.* 2004). The calcareous nannoplankton biostratigraphy has allowed the identification of a time gap that includes the upper part of the CN7/NN9 biozones to the lower part of the CN9a/NN11a (Okada & Bukry, 1980; Martini, 1971). The integrated palaeomagnetic and biostratigraphic study of *Albatera* section has allowed to calibrate the C4r.1r/C4n.2n chron boundary.

Key words: Betic Cordillera, Miocene, Tortonian, Calcareous nannoplankton, Planktonic foraminifera, Biostratigraphy.

1. INTRODUCTION

The convergence of Europe and Africa during the Cretaceous-Tertiary resulted in the narrowing and partial closure of the Atlantic-Mediterranean passages, and the building up of the Betic and Rif cordilleras to form an arc-shaped mountain belt lying at both sides of the Strait of Gibraltar (Fig. 1).

The Miocene is a crucial period for understanding the geodynamic evolution of the Betic Cordillera within the Western Mediterranean orogenic system. Those major orogenic events that shaped the Betic-Rif orogen occurred during the Early and Middle Miocene (Vera, 2004). A process of lithospheric reorganization of the Western Mediterranean took place due to the collisions of continental microplates against the passive Iberian and Africa margins. During the Late Miocene a new geodynamic period known as the neotectonic stage (Groupe de Recherches Néotectoniques de l'arc de Gibraltar, 1977) or post-orogenic stage (Viseras *et al.*, 2004) produced the Betic interior basins (e.g. Granada, Lorca, and Fortuna) caused by important post-orogenic isostatic readjustments as a consequence of the relative movement between Africa and Europe (plus Iberia). Recent reviews of the chronology of the Betic Cordillera and the Alboran Sea

sedimentary basins infill have shown a major time gap in the Early Tortonian (Rodríguez-Fernández *et al.*, 1999; Viseras *et al.*, 2004) registered as an extensive relative sea-level rise (transgressive and highstand phases). The complex network of these basins connected the Atlantic Ocean with the Mediterranean Sea, this being known as the Betic seaway. This seaway was closed during the latest Tortonian (Soria *et al.*, 1999), as has been registered in the Mediterranean affinity Betic basins such as Granada, Lorca, and Fortuna by evaporite precipitation and defined as the Tortonian Salinity Crisis (Krijgsman *et al.*, 2000), prior to the Messinian Salinity Crisis of the deep Mediterranean basin. The Tortonian Salinity Crisis has a clear relation with tectonics as in the Fortuna Basin (Tent-Manclús *et al.*, 2008). In other basins such as Guadix (central Betics), it corresponds to shallow clastic marine units (Soria *et al.*, 2003), or the Bajo Segura Basin by a major low-stand erosional surface (Tent-Manclús *et al.*, 2008).

Due to the relevance of the northern Atlantic-Mediterranean passage closure in the Mediterranean palaeogeographic evolution, the precise dating of the Betic Late Miocene sediments is needed in order to establish a stratigraphic framework for the different basins and thereby provide better knowledge of the progression of the tectonic deformation.

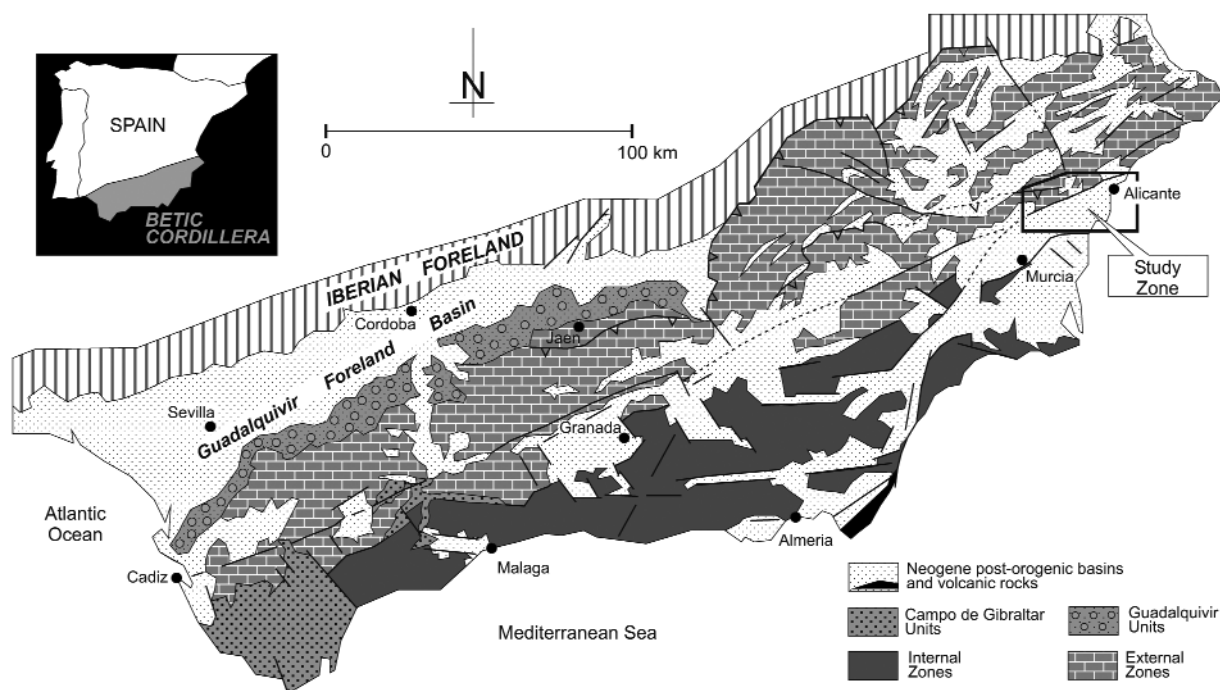


Figure 1. The Betic Cordillera geological sketch.

The aim of this paper is to present a nearly complete marine stratigraphic record of Tortonian age in the Betic Cordillera. This unusual record should allow a better estimate of the timing of the Late Miocene tectonic events. Our technique of smear slides made from centrifugated suspended sediments offers a precise calcareous nannoplankton biostratigraphy of the Tortonian sediments. Also it is completed with the planktonic foraminifera biostratigraphy, providing a more precise biostratigraphic scheme. This study is the first updated chronostratigraphic framework supported by calcareous nannofossils, and planktonic foraminifera bioevents following the tuned scale of Lourens *et al.* (2004), and completed by a magnetostratigraphic study of the Betic Cordillera Tortonian sediments.

2. SAMPLING AND METHODS

The Tortonian sediments are well exposed in two sections distributed along the Crevillente-Abanilla lineation (Fig. 2). The first one, the *Albatera* section is located in the western Alicante province about 8 km north of the Albatera village. It corresponds to a natural section of a creek west of the Albatera-Hondón de los Frailes road (CV-873). The second one, the *Les Moreres* section is located 2 km north of the Crevillente village in the *Les Moreres* valley.

In these two sections, the bedding is tilted towards the southeast.

The *Albatera* and *Les Moreres* sections (Fig. 2) have been sampled to study their nannofossil and planktonic foraminifera assemblages. A total of 99 samples were collected, 65 from the *Les Moreres* section (3.5-4 m interval), and 34 from the *Albatera* section (1-1.5 m interval), as shown in Figure 3. Each sample was wet sieved to collect the $>63\ \mu\text{m}$ and $>125\ \mu\text{m}$ fractions, whereupon the $>125\ \mu\text{m}$ fractions were studied. Then, to determine the coiling ratio of *Neogloboquadrina acostaensis*, the samples shown in the Figure 4 were sorted in Chapman slides and more than 200 individual planktonic foraminifera were counted per sample.

For the calcareous nannofossil study, four different smear slides were prepared for each sample, using the following method to increase the nannofossils to silt ratio (Lancis, 1998): For the first smear slide, 0.1 g of sediment was suspended in 10 ml distilled water (pH 7), extending on a 300 mm² surface, in one case, the direct suspension (without dilution) and in the other smear slide after a 1/3 dilution of the suspension with distilled water. In order to increase the smear slides quality, a second procedure was performed as follows. A 10-ml suspension of 0.1 g sediment in distilled water (pH 7) was centrifuged at 1800 rpm

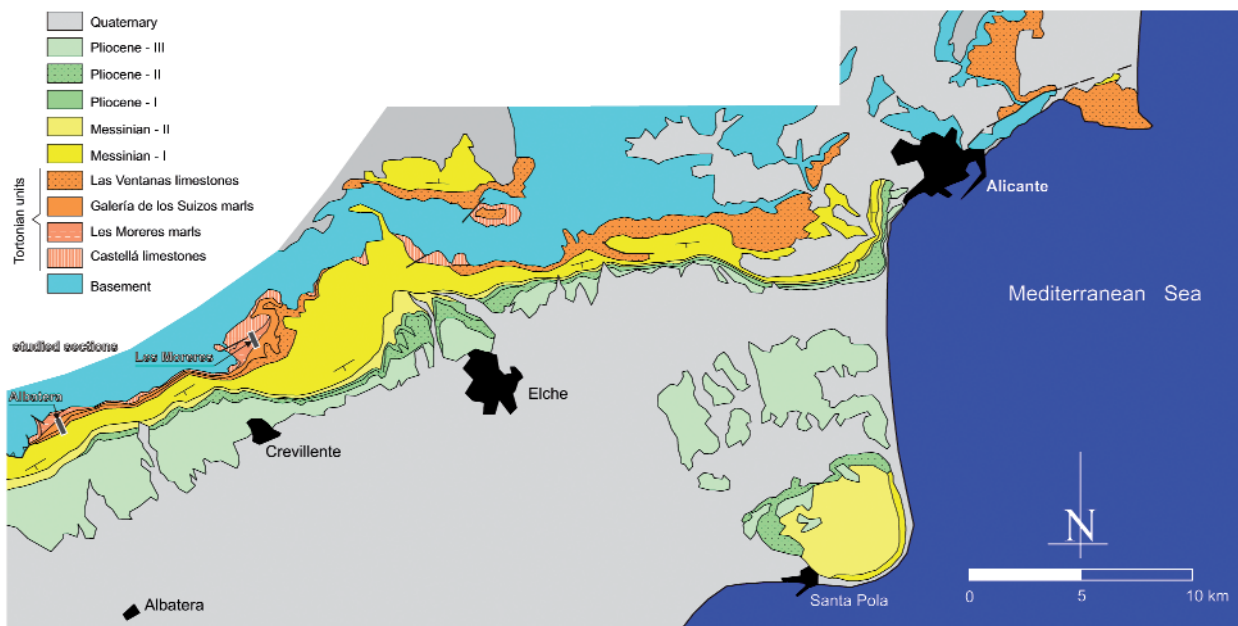


Figure 2. Simplified geological map of the study area with the locations of the *Albatera* and *Les Moreres* sections.

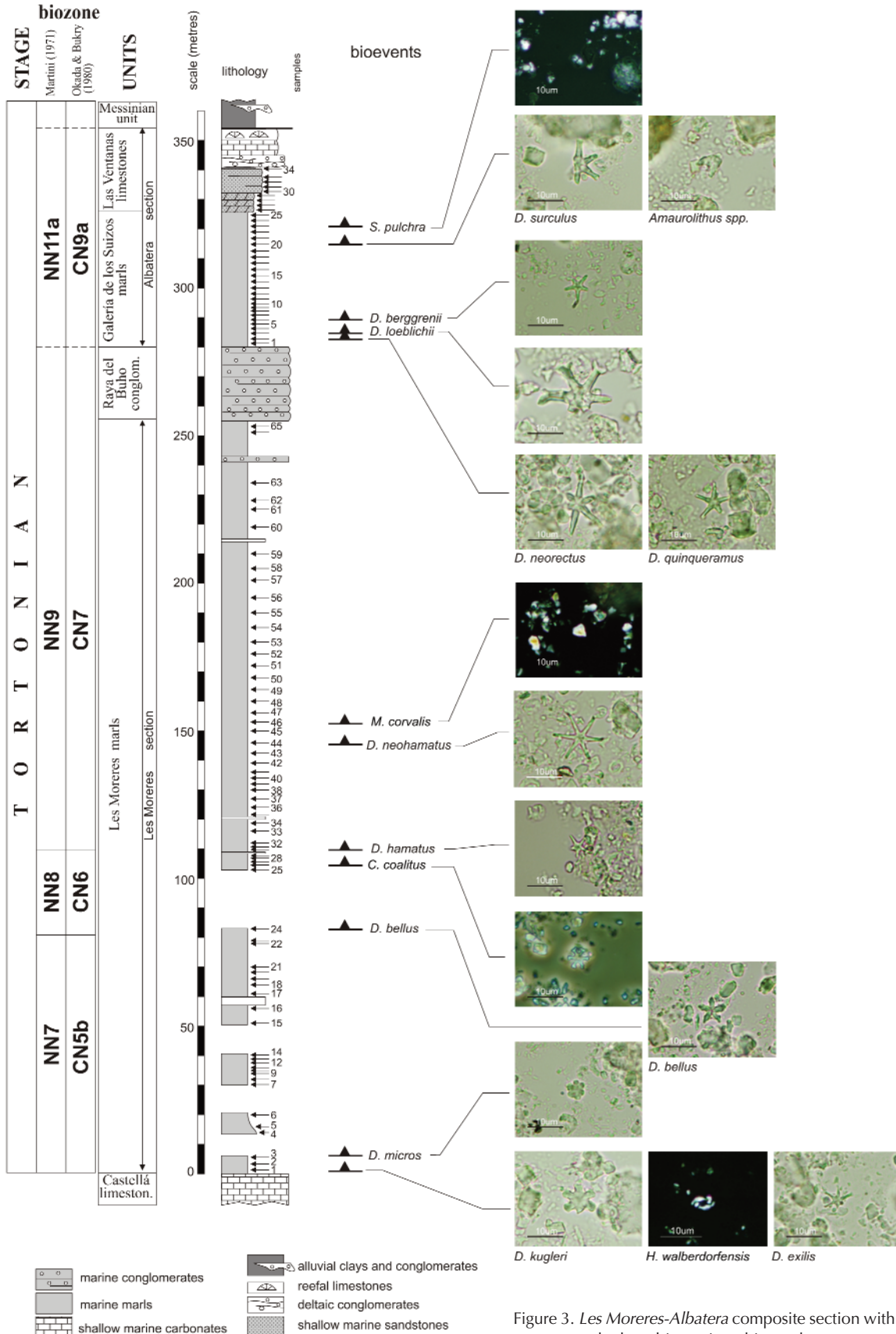


Figure 3. Les Morenes-Albatera composite section with the main calcareous nannoplankton biostratigraphic markers.

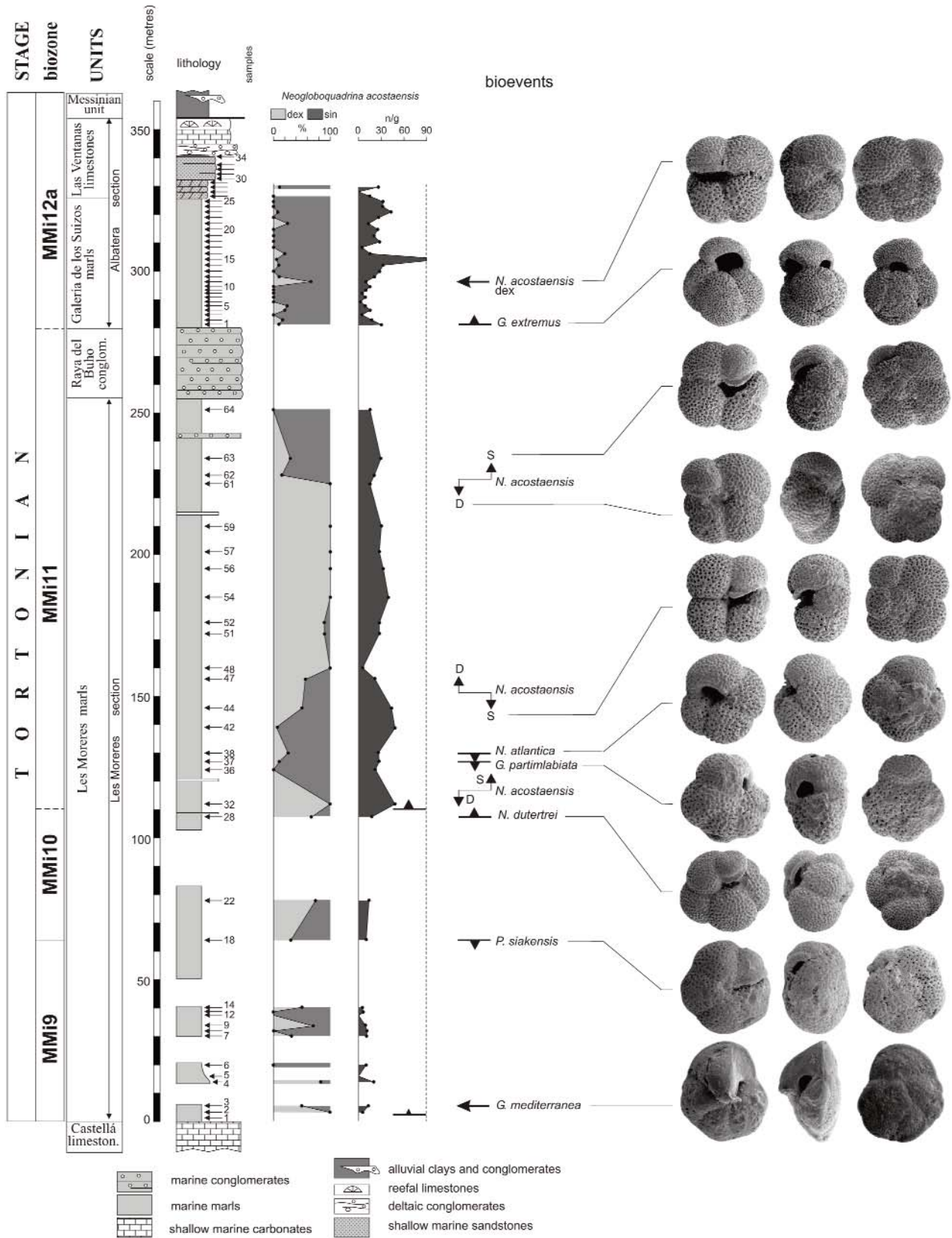


Figure 4. Planktonic foraminifera bioevents in the *Les Moreres-Albatera* composite section. The content of *Neogloboquadrina acostaensis* is expressed as the number of specimens per weight in grams of washed residue (n/g).

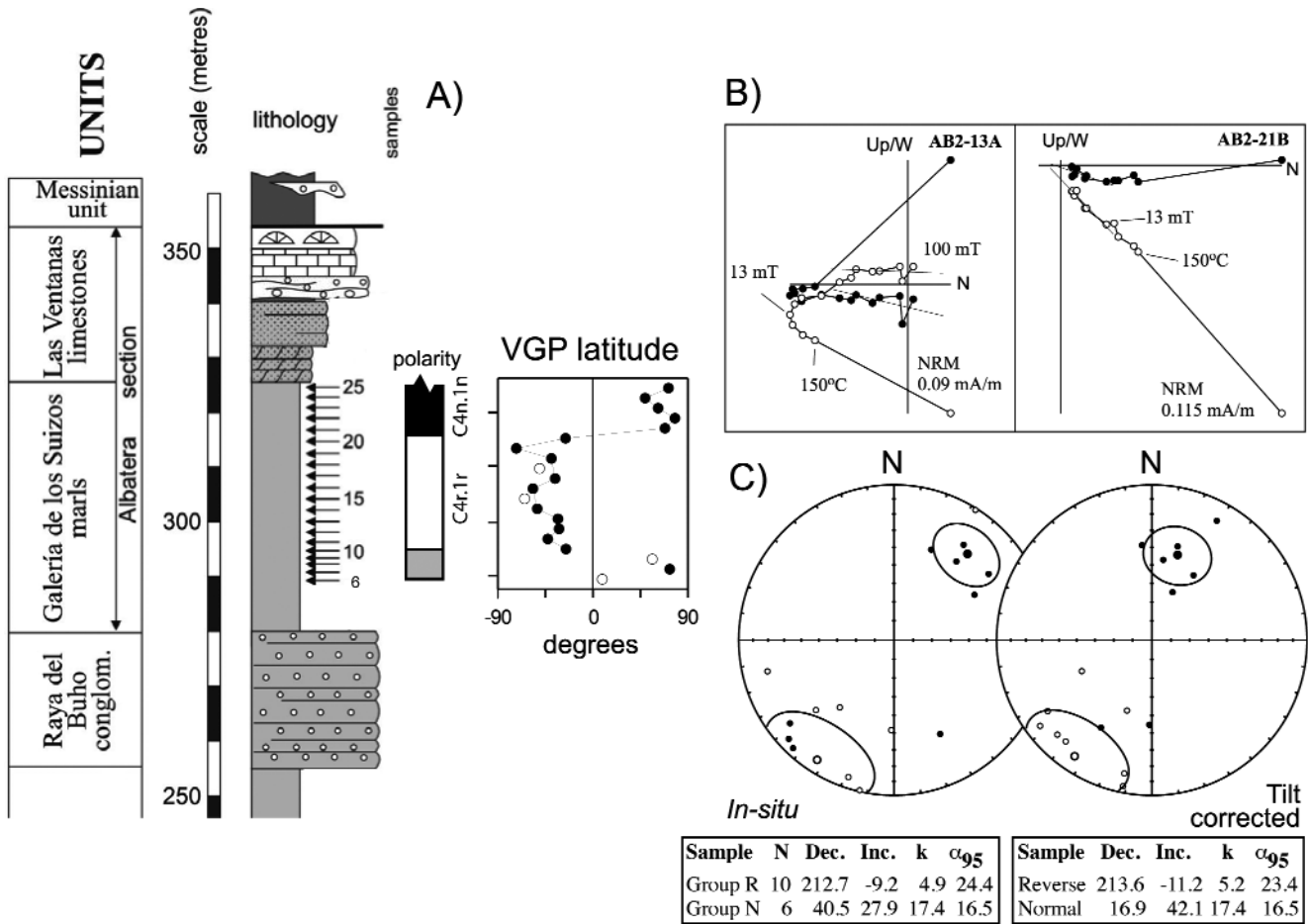


Figure 5. Paleomagnetic results and magnetostratigraphic interpretation of the *Albaterra* section. A) Stratigraphic log and polarity interpretation, VGP (virtual geomagnetic pole) (open circles: class B sites; closed circles: class A sites). B) Examples of orthogonal demagnetization diagrams representative of normal (AB2-21B) and reverse (AB2-13A) samples are given (open and closed symbols denote projections onto the vertical and horizontal planes, respectively). C) Stereographic projections of the ChRM components before (in situ) and after bedding correction (tilt corrected) are shown (open and closed symbols indicate projections onto the upper and lower hemisphere, respectively), together with the mean direction and statistics of normal and reverse polarity directions.

(450 g) for 2 min at room temperature. After discarding the supernatant, distilled water was added to the pellet to achieve 10 ml of suspension, and the new mixture was submitted to sonication for 8 seconds. This centrifugation-sonication procedure was repeated five times. Finally, 0.1 ml of the suspension was directly extended covering a 300 mm² surface on the slide, without dilution for the third smear slide and after 1/3 dilution with distilled water (pH 7) for the fourth one.

The four prepared smear slides of each sample were analysed at 100x, scanning the entire slide to find all the rare biostratigraphic markers. The mean values for nannofossil abundance were calculated using the number of coccoliths found in 30 visual fields counting around 500 nannoliths larger than 3 μm (Lancis, 1998). The percent-

age of *Reticulofenestra pseudoumbilicus* >7 μm was estimated considering only the nannoliths larger than 3 μm. For counting the “small reticulofenestrids” (< 3 μm), mean values were estimated counting around 3000 nannoliths in 30 visual fields and the percentages were calculated considering all the nannoliths. Finally, to determine the abundance of the asteroliths, nannoliths were counted in 600 visual fields. All values were then transformed into the number of nannoliths in 1 mm² of slide.

An initial pilot paleomagnetic study along the Les Moreres marls along the *Les Moreres* section indicated that the rocks are very weakly magnetic and unsuitable for magnetostratigraphic purposes. Paleomagnetic sampling was focussed to the more fresh marls after cleaning the outcrop. This study is, therefore, based on a total of 20

unique sampling sites, comprising 1 hand-sample per site from the Galeria de los Suizos Marls along the *Albatera* section (Fig. 5A). Hand-samples were oriented in situ with a compass and subsequently standard cubic specimens were cut in the laboratory for analysis. Natural remanent magnetization (NRM) and remanence through demagnetization were measured on a 2G Enterprises DC SQUID high-resolution pass-through cryogenic magnetometer (manufacturer noise level of 10^{-12} Am²) operated in a shielded room at the Istituto Nazionale di Geofisica e Vulcanologia in Rome, Italy. A Pyrox oven in the shielded room was used for thermal demagnetizations and alternating field (AF) demagnetization was performed with three orthogonal coils installed inline with the cryogenic magnetometer. Progressive stepwise AF demagnetization was routinely used and applied after a single heating step to 150°C. AF demagnetization included 14 steps (4, 8, 13, 17, 21, 25, 30, 35, 40, 45, 50, 60, 80, 100 mT). Characteristic remanent magnetizations (ChRM) were computed by least-squares fitting (Kirschvink, 1980) on the orthogonal demagnetization plots (Zijderveld, 1967). The ChRM declination and inclination were used to derive the latitude of the virtual geomagnetic pole (VGP) of each sample. This parameter was taken as an indicator of the original magnetic polarity, normal polarity being indicated by positive VGP latitudes and reverse polarity by negative VGP latitudes.

3. STRATIGRAPHY OF THE SOUTHERN ABANILLA-CREVILLENTE LINEATION

The Tortonian sediments studied seal the contact between the two major geological domains of the Betic Cordillera orogen (Fig. 1): the External Zone, the former South Iberian Palaeomargin (to the north), and the Internal Zone or Alborán Block that constitutes an allochthonous lithospheric fragment (Andrieux *et al.*, 1971), dominated by metamorphic rocks (to the south). Rocks from the Internal and External zones can be considered the basement. Over this basement, NW-SE basins formed during the Middle Miocene to the Tortonian (Tent-Manclús, 2003), and then, in the latest Tortonian the onset of the Trans-Alboran Shear Zone changed the palaeogeography developing the SW-NE Bajo Segura Basin (Tent-Manclús *et al.*, 2008). This change is marked by a calcareous sandstone unit includ-

ing coral-reef patches (Santisteban Bové, 1981), which deepens to the East. This unit was included by Montenat (1977) as the upper part of its Tortonian II unit, and was later named Las Ventanas Limestone by Tent-Manclús (2003).

3.1 Lithostratigraphic units

Montenat (1977) presented the first lithostratigraphic sketch of these basins, establishing over the basement the units: “Tortonian I”, to the sediments below the intra-Tortonian discontinuity, the “Tortonian II” to the marine sediments overlying the intra-Tortonian discontinuity, and the “Upper Miocene” to the continental sediments between the marine “Tortonian II” and “Pliocene I” sediments. Subsequently, Montenat *et al.* (1990), Alfaro García (1995), Soria *et al.* (2001), Tent-Manclús (2003), Tent-Manclús *et al.* (2004), and Soria *et al.* (2005) used many alternative lithological units, the relations of which are shown in Figure 6. For Montenat (1977) the older sediments over the basement in the southern flank of the Crevillente-Abanilla lineation were assigned to the Tortonian II unit. A brief description of the lithological units used in this study is provided below.

- a) El Castellà Limestone: dark grey to reddish bioclastic limestones.
- b) Les Moreres Marls: 300-m-thick white marls with some detrital intercalations near its bottom.
- c) Raya del Búho Conglomerate: a marine unit formed by balanid-encrusted metamorphic clasts of Internal Zone provenance, which in some outcrops erode the Moreres Marls.
- d) Galería de los Suizos Marls: a marly marine unit containing planktonic microfossils upwardly increasing in carbonate content.
- e) Las Ventanas Limestone: coral-reef limestone and yellowish calcareous sandstone, containing abundant fossils of corals (*Porites* and *Tarbellastrea*), bivalves, red algae, equinoderms, and *Dentalium*; laterally, this unit thins and disappears to the western Fortuna Basin (Azema and Montenat, 1975).
- f) Unconformably overlying the Las Ventanas limestone unit appears patches of marine conglomerates with clasts of the Crevillente Sierra sequences (External

UNITS This study	References			
	Montenat (1977)	Alfaro (1995)	Soria et al., (2001)	Tent-Manclús (2003) Tent-Manclús et al., (2004)
Messinian unit	Upper Miocene			Calcarenit. Shales and conglom.
Las Ventanas limestones	Tortonian II	MS-III	V	Las Ventanas limestones
Galería de los Suizos marls		MS-II	IV	Galería de los Suizos marls
Raya del Buño conglom.			III	Raya del Buño conglom.
Les Moreres marls			II	Les Moreres marls
El Castellá limeston.		Tortonian I	MS-I	I

Figure 6. The rock units names used by earlier works and the equivalences with the ones used in this study. The darker and light gray and white backgrounds are relative to the age assignment in the different works. The Tortonian deposits are in darker gray than the Messinian and the white background is the Serravallian assigned ages.

Zone and underlying tertiary) and some coral-reef which indicate the erosion of the Las Ventanas reef. Finally, at the top of the section is covered by a Messinian unit made by continental red beds.

4. BIOSTRATIGRAPHY OF CALCAREOUS NANNOFOSSILS

The nannofossil assemblages came from the two marly lithostratigraphic units, Les Moreres and Galería de los Suizos Marls. Figure 3 shows the main biostratigraphic events in the Tortonian age sediments studied. The preservation is fairly good and reworked nannoliths from the

Early Miocene, Paleocene, and Late Cretaceous are frequent.

4.1 Les Moreres Marls

The lowest levels of the Les Moreres Marls contain the following main calcareous nannoplankton assemblages: *Discoaster kugleri* (Fig. 7-1; 7-2; 7-3), *D. exilis* (Fig. 7-5; 7-6), *D. aulakos*, *D. micros* (Fig. 7-7), *D. prepentaradiatus*, *Coccolithus miopelagicus*, *C. pelagicus*, *Calcidiscus* spp., *Sphenolithus abies*, *Helicosphaera carteri*, *H. walberdorfensis* (Fig. 7-4) *Umbilicosphaera rotula*, *Dictyococcites antarcticus*, *Reticulofenestra pseudoumbilicus* (Fig. 7-9), *R. haqii*, *R. minutula*, and abundant "small reticulofenestrids" (*Reticulofenestra minuta* and *Dictyococcites productus*).

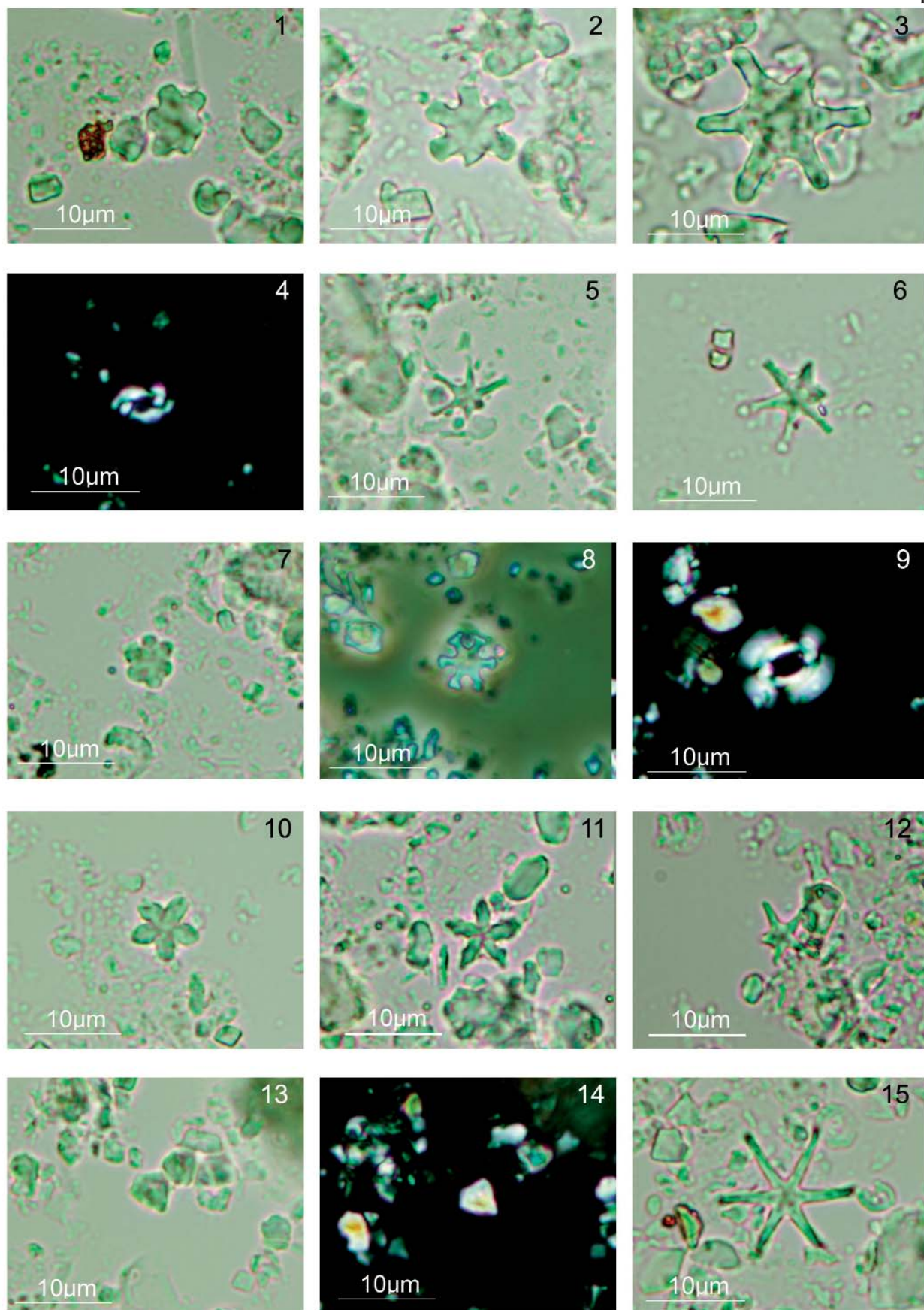
In the middle part of the *Les Moreres* section, sample 26, appear the first specimens of *Catinaster coalitus* (Fig. 7-8) and *Discoaster bellus* (Fig. 7-10, 7-11). In sample 31 the first *D. hamatus* (Fig. 7-12) was found, while *D. kugleri* and *H. walberdorfensis* had disappeared. Scarce specimens of *Discoaster calcaris*, *D. neohamatus*, and *D. pseudovariabilis* were also present and became more abundant in the upper part of the *Les Moreres* section. The first *Minilitha convalis* (Fig. 7-13, 7-14) were detected in the sample 46. The broken and overgrowth of nannofossils indicate some reworking in the samples.

4.2 Galería de los Suizos Marls

The lowest levels of the Galería de los Suizos Marls contain the following nannofossil assemblage: *Coccolithus pelagicus*, *Umbilicosphaera rotula*, *Calcidiscus macintyreii*, *C. leptoporus*, *Discoaster quinqueramus* (Fig. 8-4), *D. brouweri* (Fig. 8-1), *D. neorectus* (Fig. 8-3), *D. variabilis* (Fig. 8-8), *D. calcaris*, *D. pentaradiatus*, *D. pseudovari-*

Figure 7. **1-3-** *Discoaster kugleri* Martini & Bramlette, parallel light (PL): **1** sample 12 of *Les Moreres* section (Mor); **2** sample 19 Mor; **3** sample 22 Mor. **4-** *Helicosphaera walberdorfensis* Müller, crossed nicols (XN), sample 1 Mor. **5-6-** *Discoaster exilis* Martini & Bramlette, PL: **5** sample 22 Mor; **6** sample 1 Mor. **7-** *Discoaster micros* Theodoridis, PL, sample 20 Mor. **8-** *Catinaster coalitus* Martini & Bramlette, PL, sample 27 Mor. **9-** *Reticulofenestra pseudoumbilicus* Gartner, XN, sample 52 Mor. **10-11-** *Discoaster bellus* Bukry & Percival, PL: **10** sample 25 Mor; **11** sample 43 Mor. **12-** *Discoaster hamatus* Martini & Bramlette, PL, sample 60 Mor. **13-14.-** *Minylitha convalis* Bukry, sample 2 *Albatera* section (AB); **13** PL; **14** XN. **15-** *Discoaster neohamatus* Bukry & Bramlette, PL, sample 2 AB.

Figure 7



abilis, *D. loeblichii*, *D. intercalaris* (Fig. 8-11), *D. berggrenii* (Fig. 8-6), *Minilitha convalis* (Fig. 8-13; 8-14) *Sphenolithus abies*, *Sph. neoabies*, and *Scyphosphaera apsteinii* (Fig. 8-5). *Reticulofenestra pseudoumbilicus* > 7 µm, though present in almost all the samples of the *Albatera* section, represents less than 5% of the assemblage. *R. pseudoumbilicus* 5-7 µm, *R. haqii*, and *R. minutula* are also abundant and the "small reticulofenestrids" (*Reticulofenestra minuta* and *Dictyococcites productus*) show high percentages that in some cases approach 70%. In the highest part of the *Albatera* section, we found *Scyphosphaera intermedia* (Fig. 8-9), *Scy. conica* (Fig. 8-7), *Scy. amphora* (Fig. 8-10) and abundant *Pontosphaera multipora*. The first appearance of *Discoaster surculus* is in sample 15 but its First Common Occurrence (FCO) is from the sample 22 upwards. Some initial forms of *Amaurolithus* cf. *primus* were found in samples 20 and 23 (Fig. 8-13; 8-14) together with *Syracosphaera pulchra* (Fig. 8-15).

5. BIOSTRATIGRAPHY OF PLANKTONIC FORAMINIFERA

The Late Miocene planktonic foraminiferal microfossils in *Les Moreres* and the *Albatera* sections are mixed with a variable number of reworked Paleogene and Lower-Middle Miocene planktonic foraminifera. Preservation is fairly good both for the Late Miocene and reworked specimens. Washed residues in the 125-µm fraction were used to portray presence of Late Miocene marker species, in addition to the coiling patterns of *Neogloboquadrina acostaensis* (Fig. 4). In this study, we have considered the most typical species included in recent astronomically-calibrated biozonation charts, as that proposed by Lourens *et al.* (2004). Below, we follow the biozones established by these authors in order to describe the biostratigraphy of the studied section.

5.1 Les Moreres section

The first significant biostratigraphic horizon in the *Les Moreres* Marls is the LCO (Last Common Occurrence) of *Paragloborotalia siakensis* in sample 18, marking the upper boundary of the MMi9 biozone. *Neogloboquadrina*

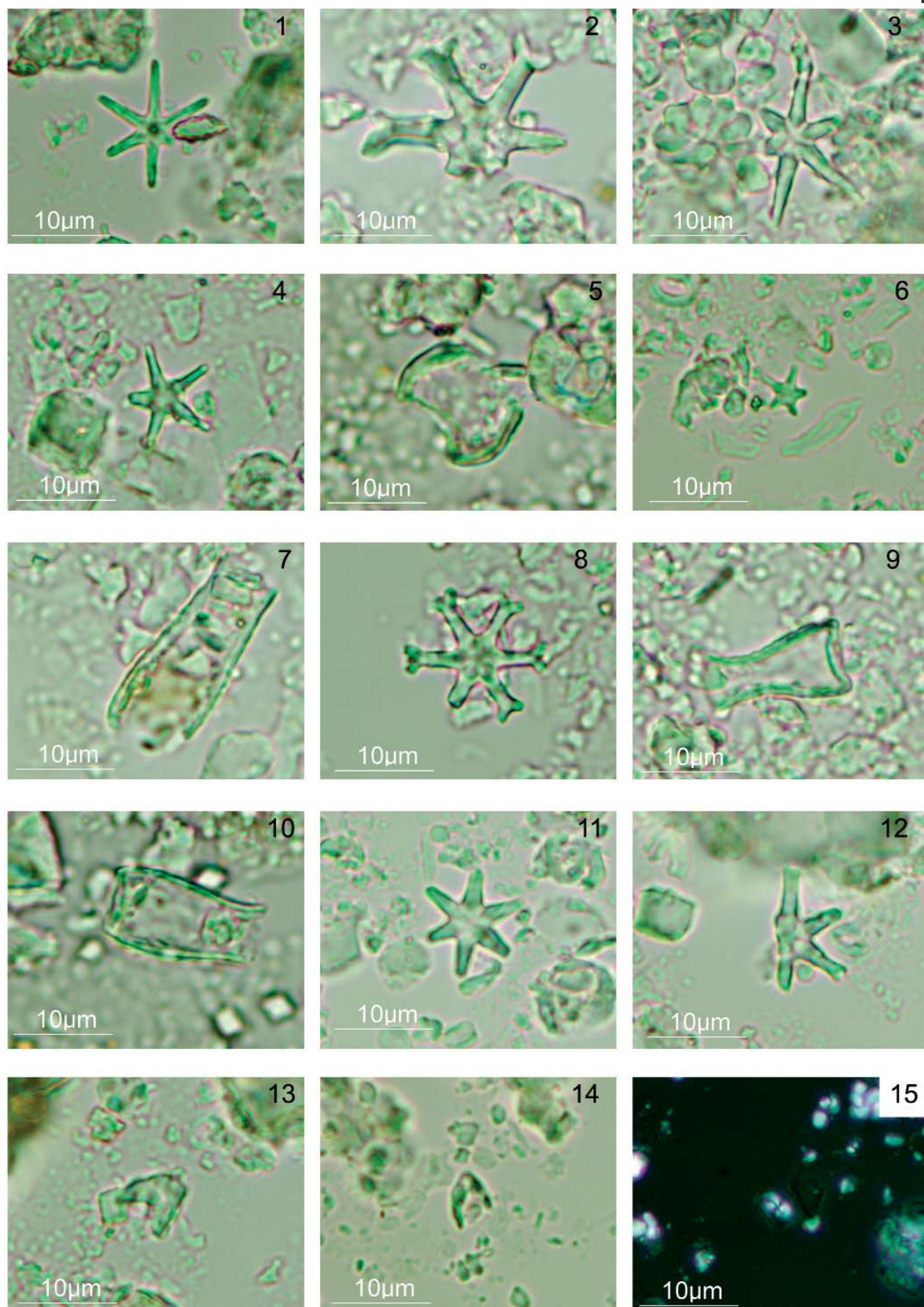
acostaensis is present from the extreme base to the top of the section; its content increases and is regularly recorded upward in sample 32, where the FCO of this species is located, marking the boundary between MMi10 and MMi11 biozones. From sample 32 to the top, the section can be assigned to the MMi11 biozone. Several noticeable intra-zonal bioevents are unambiguously correlated with other classical Mediterranean sections (e.g. the *Gibiliscemi* composite section in Sicily; Hilgen *et al.*, 2000). These events, from the bottom to the top of the biozone, are: 1) the dextral to sinistral coiling change of *Neogloboquadrinids* between samples 32 and 36; 2) the LCO of *Globorotalia partimlabiata* in sample 37; 3) the LCO of *Neogloboquadrina atlantica* (large- and small-sized forms) in sample 38; 4) the sinistral to dextral coiling change of *Neogloboquadrina acostaensis* between samples 44 and 47; and 5) the dextral to sinistral coiling change of *Neogloboquadrina acostaensis* between samples 59 and 61. This last event is located below and very close of the stratigraphic boundary between the *Les Moreres* Marls and the *Raya del Búho* Conglomerate. Also, it bears noting a brief influx of *Globorotalia mediterranea* at the base of the *Les Moreres* Marls, inside the MMi9 biozone. This constitutes the first report of this species in any Mediterranean section during the earliest Tortonian (Fig. 4).

5.2 Albatera section

From the bottom to the top of the *Galería de los Suizos* Marls, *Globigerinoides extremus* appears regularly; in addition, the joint presence of this species with dominant sinistral forms of *Neogloboquadrina acostaensis*, indicate the MMi12a biozone. In the lower half of this biozone (sample 11) an influx (ca. 70%) of dextral *Neogloboquad-*

Figure 8. **1-** *Discoaster brouweri* (Tan) Bramlette & Riedel, PL, sample 7 *Albatera* section (AB). **2-** *Discoaster loeblichii* Bukry, PL, sample 22 AB. **3-** *Discoaster neorectus* Bukry, PL, sample 15 AB. **4-** *Discoaster quinqueramus* Gartner, PL, sample 15 AB. **5-** *Scyphosphaera apsteinii* Lohmann, PL, sample 7 AB. **6-** *Discoaster berggrenii* Bukry, PL, sample 23 AB. **7-** *Scyphosphaera conica* Kämtner, PL, sample 22 AB. **8-** *Discoaster variabilis* Martini & Bramlette, PL, sample 15 AB. **9-** *Scyphosphaera intermedia* Deflandre, PL, sample 17 AB. **10-** *Scyphosphaera amphora* Deflandre, PL, sample 22 AB. **11-** *Discoaster intercalaris* Bukry, PL, sample 12 AB. **12-** *Discoaster surculus* Martini & Bramlette, PL, sample 22 AB. **13-14-** *Amaurolithus* spp. (A. cf. *primus*) (Bukry & Percival) Gartner & Bukry; **13** PL, sample 20 AB; **14** PL, sample 23 AB. **15-** *Syracosphaera pulchra* Lohmann, XN, sample 23 AB.

Figure 8



rina acostaensis occurs. This is a new and unreported event, until the present, in the Mediterranean Tortonian sections. The Las Ventanas Limestone, overlying the Galería de los Suizos Marls, contains no significant biostratigraphic planktonic foraminifera.

6. CALCAREOUS NANNOFOSSILS EVENTS

The distribution patterns of the selected calcareous nannofossil species are shown in the Figures 9, 10, 11, and 12. Most of them are index species for the Middle and Late Miocene in the Mediterranean and in the low-latitude oceans. The asteroliths are scarce and its preservation is poor in the *Les Moreres* section and best preserved in the *Albatera* section, Galería de los Suizos Marls. The occurrences and distribution patterns of the most important species are discussed below.

6.1 Presence of *Discoaster kugleri*

Bukry (1973) suggested as the secondary criterion of definition of the boundary CN5b/CN6 the LO (Last Occurrence) of *D. kugleri* join with the FO (First Occurrence) of *C. coalitus*. In addition, Zone CN5 is divided into two sub-zones (CN5b and CN5a) by the FO of *D. kugleri* (Bukry, 1973), which also defines the NN7/NN6 (Martini, 1971) zonal boundary. The recognition of this boundary has been debated, as *D. kugleri* is considered by many authors to be a weak marker (Gartner, 1992; Fornaciari *et al.*, 1990; Raffi & Flores, 1995; Fornaciari *et al.*, 1996). Although its interval of abundance has a wide geographic distribution (Raffi *et al.*, 1995; Backman & Raffi, 1997), *D. kugleri* is generally rare in the Mediterranean (Müller, 1978), and therefore it is not included as a (sub)zonal marker in the Middle Miocene Mediterranean zonation by Fornaciari *et al.* (1996).

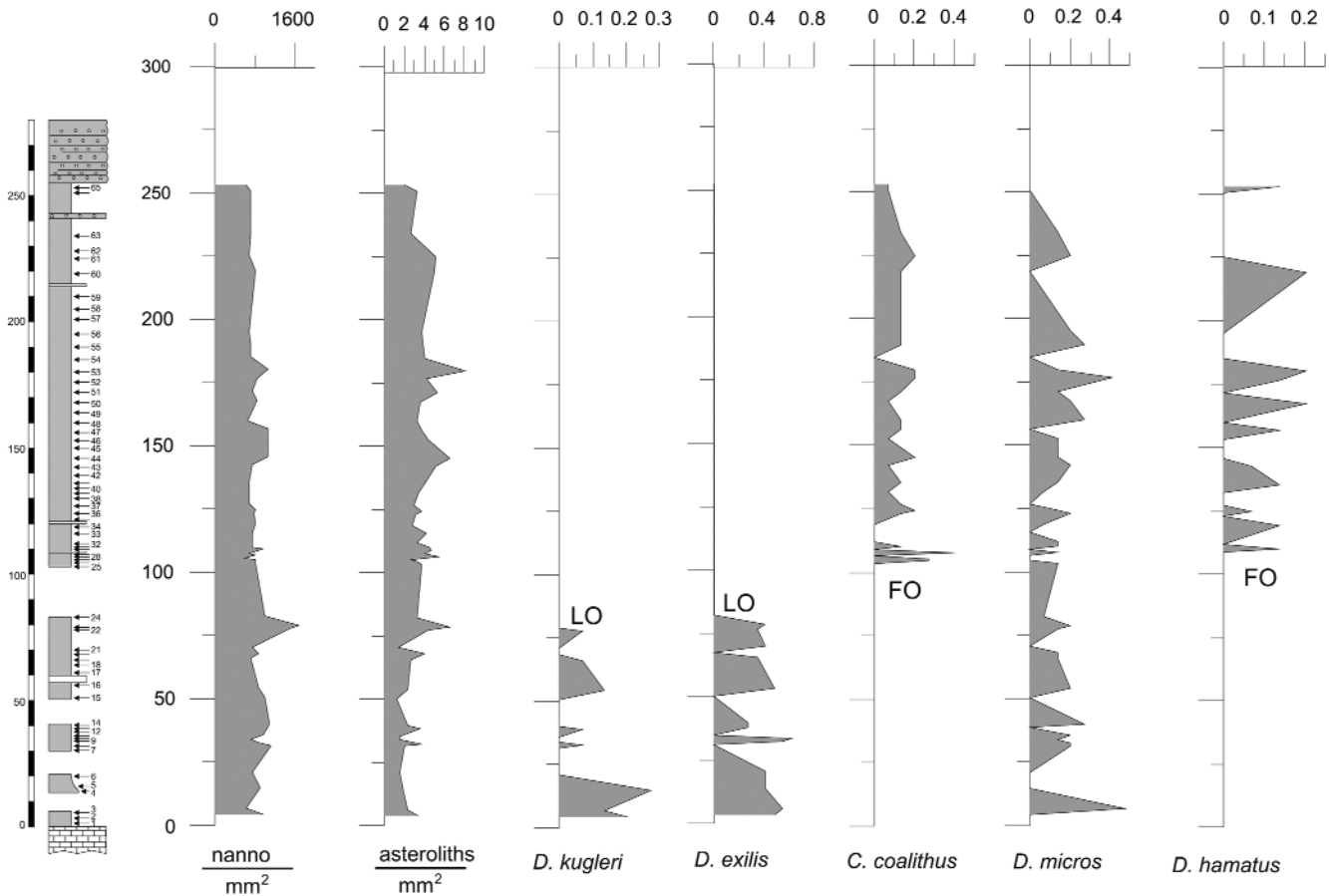


Figure 9. Quantitative distribution pattern of selected nannofossils in the *Les Moreres* section (as number of specimens per mm²). The following acronyms indicate bioevents: FO (First Occurrence); LO (Last Occurrence); FCO (First Common Occurrence); LCO (Last Common Occurrence). Please note differences in scaling.

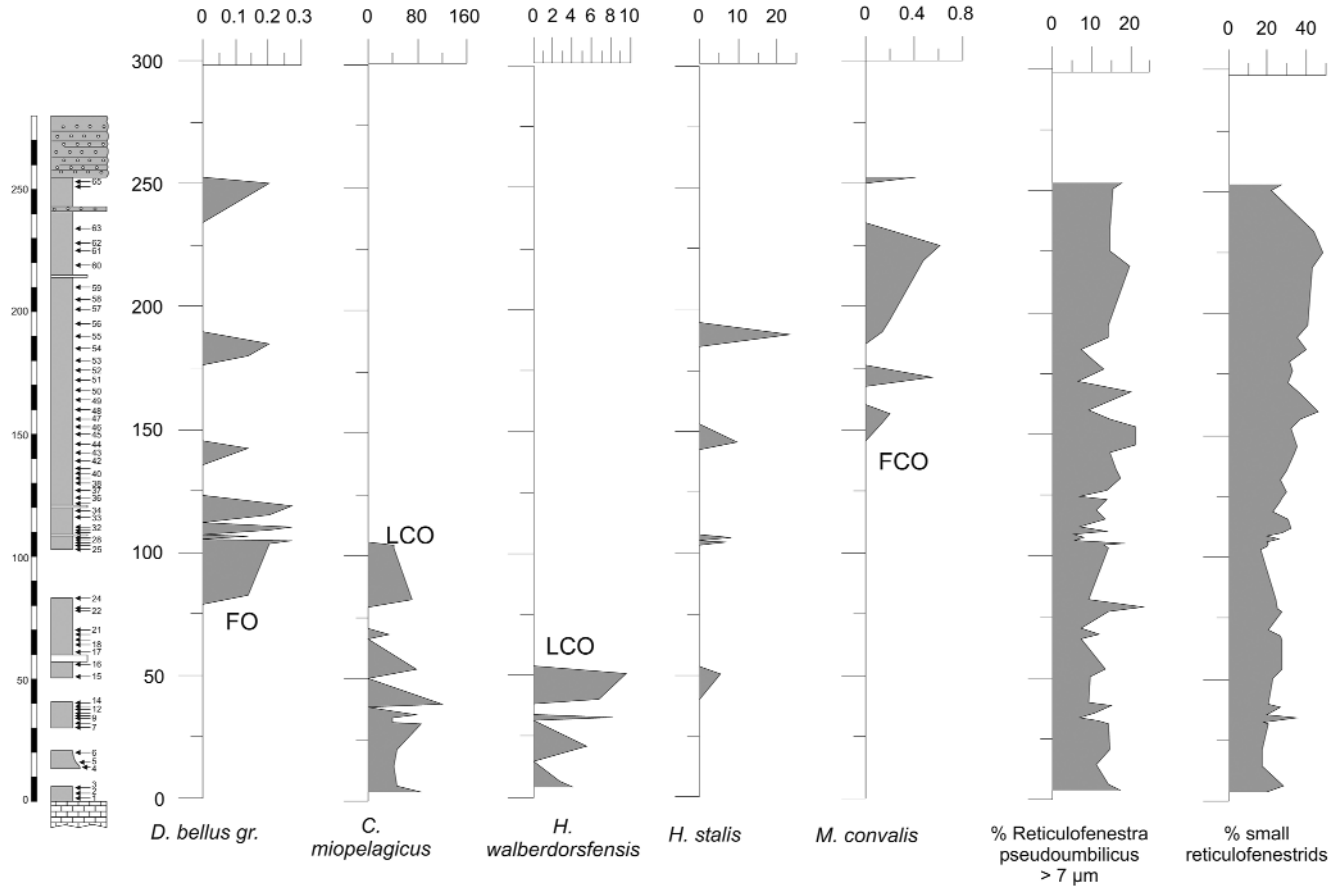


Figure 10. Quantitative distribution pattern of selected nannofossils in the *Les Moreres* section (as number of specimens per mm^2). The following acronyms indicate bioevents: FO (First Occurrence); LO (Last Occurrence); FCO (First Common Occurrence); LCO (Last Common Occurrence). Please note differences in scaling.

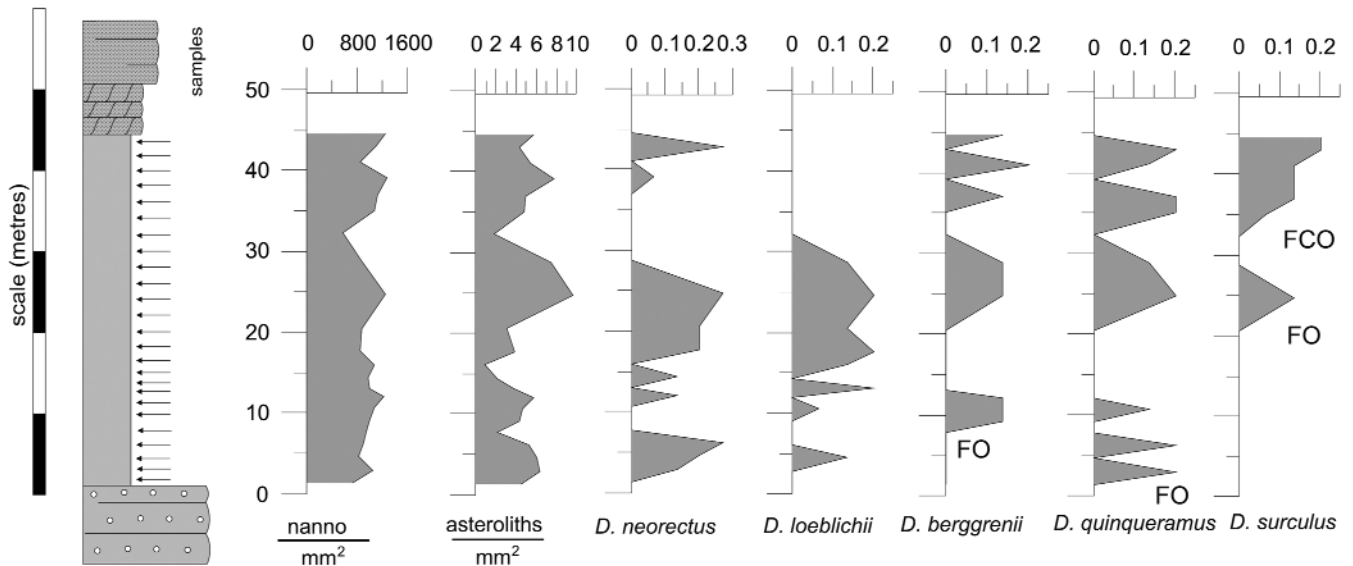


Figure 11. Quantitative distribution pattern of selected nannofossils in the *Albaterra* section (as number of specimens per mm^2). The following acronyms indicate bioevents: FO (First Occurrence); LO (Last Occurrence); FCO (First Common Occurrence); LCO (Last Common Occurrence). Please note differences in scaling.

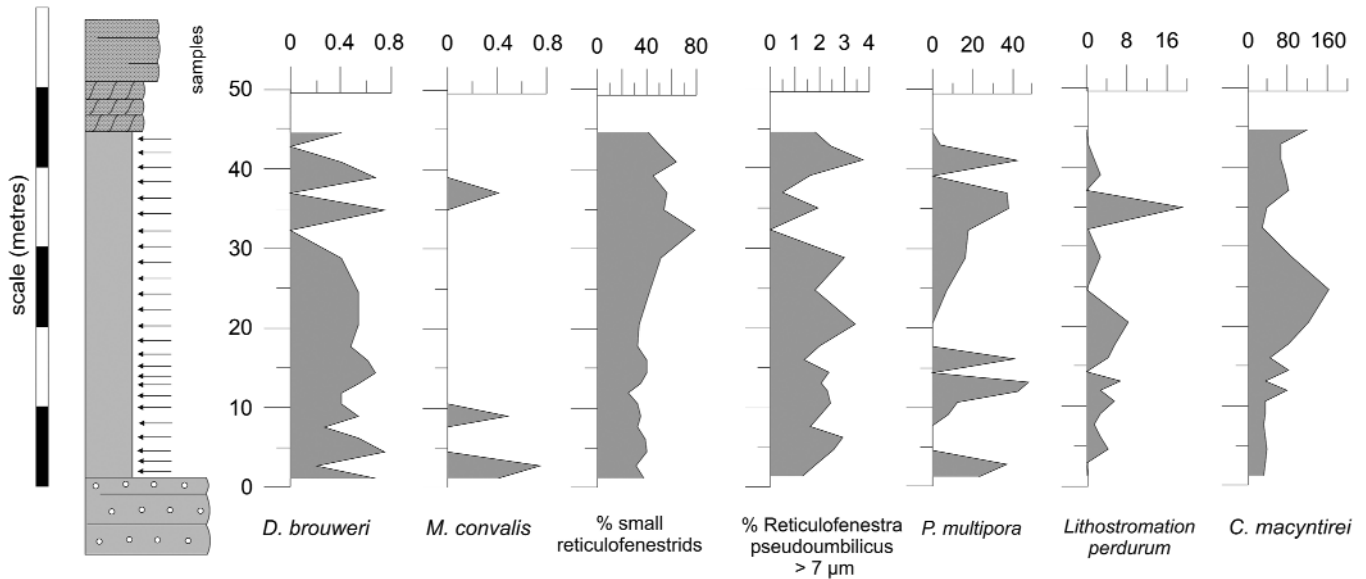


Figure 12. Quantitative distribution pattern of selected nanofossils in the *Albaterra* section (as number of specimens per mm²). The following acronyms indicate bioevents: FO (First Occurrence); LO (Last Occurrence); FCO (First Common Occurrence); LCO (Last Common Occurrence). Please note differences in scaling.

However, Hilgen *et al.* (2000), Hilgen *et al.* (2003), Foresi *et al.* (2002), Caruso *et al.* (2002) in the results of the analyses on the high-resolution samples of the Mediterranean basin show that the biostratigraphic signal provided by *D. kugleri* is clear and both the FCO and LCO are easily identified with astronomical ages also coincident with the same events in the low-latitude open oceans. In the western equatorial Atlantic, ODP sites 925 and 926 the FCO and LCO of *D. kugleri* were astronomically calibrated and dated at 11.863 and 11.578 Ma, respectively (Backman & Raffi, 1997; Shackleton & Crowhurst, 1997; Lourens *et al.*, 2004).

In the *Les Moreres* section, *D. kugleri* is scarce in the lowest samples, appears sporadically and then disappears before the FO of *Catinaster coalithus*. We cannot determine whether we are in the interval of continuous presence below the LCO or just above this level, which marks the Serravallian-Tortonian boundary.

6.2 LO of *Discoaster exilis*

Raffi *et al.* (1995) showed that the *D. exilis* LO occurs in an interval encompassing the appearance level of *D. hamatus* (between the top of biozone CN6 and the lower-

most part of Zone CN7) being an event controlled by environmental conditions and biogeography. Hilgen *et al.* (2000) in the Mediterranean found a distribution of *D. exilis* coincident with the data of the western equatorial Atlantic of Raffi *et al.* (1995). The distribution of *D. exilis* in *Les Moreres* section show a parallel distribution with *D. kugleri*, although the former is more abundant but seems to disappear just below the FO of *C. coalithus*.

6.3 LCO of *Helicosphaera walberdorfensis* and FCO of *H. stalis*

In the *Les Moreres* section, *Helicosphaera walberdorfensis* is present from the bottom of the section to sample 22. Although it is scarce, it coincides in distribution with *D. kugleri* and *D. exilis*. Hilgen *et al.* (2000) in the Mediterranean section of *Giblicsemi* found the LCO of *H. walberdorfensis* coinciding with the FCO of *H. stalis*, having an astronomically tuned age of between 10.743 and 10.717 Ma in agreement with the distributions reported by Fornaciari *et al.* (1996). In our samples, *H. stalis* is even scarcer than *H. walberdorfensis*, so that we could not specify the precise coincidence of the two events. *H. stalis* appears sporadically until the sample 55 of the *Les Moreres* section.

6.4 Presence of *Discoaster micros* and *Catinaster coalitus*

The bottom of the CN6 biozone (Okada & Bukry, 1980) and NN8 biozone (Martini, 1971) is defined by the FO of *C. coalitus* plus the LO of *D. kugleri*. *Catinaster coalitus* is consistently present in the low-latitude assemblages, whereas for Theodoridis (1984) and Fornaciari *et al.* (1996), it is scattered to absent at mid-latitudes and in the Mediterranean. However, Hilgen *et al.* (2000) observed in the Mediterranean *Giblissemi* section *C. coalitus* in two short intervals join with *D. micros*. Their astronomically tuned FO at 10.738 Ma is consistent with the data from the western equatorial Atlantic at 10.886 Ma (Backman & Raffi, 1997; Raffi *et al.*, 2006). In the investigated material, representatives of *Catinaster coalitus* (Fig. 7-8) are scarce but with a quite regular distribution between the samples 26 and 65 of the *Les Moreres* section. *Discoaster micros* (Fig. 7-7), a discoasterid from which the genus *Catinaster* is considered to have evolved (Raffi *et al.*, 1998), is also scarce and has a similar distribution. Integrated forms have also been found.

6.5 LCO of *Coccolithus miopelagicus*

The LCO of *C. miopelagicus* has been documented in the Mediterranean where the species is well represented. Fornaciari *et al.* (1996) found this event just below the disappearance level of *H. walberdorfensis*. Hilgen *et al.* (2000) consider LCO of *C. miopelagicus* coincident with the *D. hamatus* first occurrence. In the *Les Moreres* section we have found the LCO of *C. miopelagicus* just above the disappearance of *H. walberdorfensis* and the appearance of the first forms of *D. bellus* and slightly below the appearance of the first *D. hamatus*.

6.6 Presences of *Discoaster bellus*, *Discoaster hamatus*, *Discoaster calcaris* and *Discoaster neohamatus*

The appearances of the distinctive Neogene discoasterids *D. bellus* and *D. hamatus* (Fig. 7-10; 7-11; 7-12) constitute an important event that has been used in the open-ocean and Mediterranean biozones. *D. hamatus* is a marker of

both standard as well as Mediterranean zonation and its first and last occurrence define the bottom and top of the standard biozones NN9/CN7.

In the Indian Ocean, the two events (FO *D. bellus* gr. and FO *D. hamatus*) mainly coincide (Rio *et al.*, 1990). However, in the equatorial Pacific and western equatorial Atlantic, *D. bellus* gr. FO slightly precedes *D. hamatus* (Raffi *et al.*, 1995; Backman & Raffi, 1997; Raffi *et al.*, 2006). In the western equatorial Atlantic, *D. hamatus* FO was astronomically calibrated at 10.476 by Backman & Raffi, (1997) and afterwards re-tuned by Lourens *et al.* (2004) at 10.549. Hilgen *et al.* (2000) found *D. hamatus* sporadically in the Mediterranean *Giblissemi* section, assigning a 10.150 Ma age for the FO then recalibrated by Lourens *et al.* (2004) at 10.184 Ma. *Discoaster hamatus* is a scarce and discontinuous form in the *Les Moreres* section between samples 31 to 65, and also *D. bellus* between samples 24 to 64.

Discoaster neohamatus is also very scarce in both sections. Its FO is in the sample 44 of *Les Moreres* section, and its LO in the *Albatera* section is in sample 15. *Discoaster calcaris* also shows a similar distribution. *D. neohamatus* FO is a distinct event in some oceanic areas where the species is well represented and has been established in the western equatorial Atlantic at 10.521 Ma (Backman & Raffi, 1997; Lourens *et al.*, 2004; Raffi *et al.*, 2006). Hilgen *et al.* (2000) found rare sporadic specimens in the upper part of the Mediterranean *Giblissemi* section with an astronomically tuned age of 9.867 (Lourens *et al.*, 2004; Raffi *et al.*, 2006).

6.7 *Minylitha convallis* distribution range

The biostratigraphic significance of *M. convallis* has been documented in different deep-sea successions (Rio *et al.*, 1990; Gartner, 1992; Raffi *et al.*, 1995; Backman & Raffi, 1997) including the Mediterranean (Theodoridis, 1984; Fornaciari *et al.*, 1996; Hilgen *et al.*, 2000; Raffi *et al.*, 2003). The FO is slightly diachronic with an astronomically tuned age in the Mediterranean, of 10.733 Ma in *Giblissemi* section (Hilgen *et al.*, 2000) and 9.379 Ma in *Metochia* section, (Raffi *et al.*, 2003) and with a distribution range until the 8.685 Ma (Hilgen *et al.*, 1995; Raffi *et*

al., 2003; Lourens *et al.*, 2004; Raffi *et al.*, 2006). This range is shorter in the Mediterranean than in the tropical Indian Ocean, eastern equatorial Pacific and North Atlantic (Raffi *et al.*, 2003; Lourens *et al.*, 2004; Raffi *et al.*, 2006).

The species characterizes the assemblages of Zones NN9 upper part/CN7b and NN10/CN8. *Minylitha convallis* appears in the sample 46 of the *Les Moreres* section and is found continuously until the sample 2 of the *Albatera* section, after which it appears sporadically until the sample 21 of the *Albatera* section.

6.8 *Discoaster loeblichii* and *D. neorectus* distribution ranges

The FO of *D. loeblichii* and the FO of *D. neorectus* were two events used by Bukry (1973) to divide biozone CN8 into two subzones (CN8a and CN8b). *Discoaster loeblichii* is consistently present in sediments of Late Miocene age at low-latitude sites in the Pacific and in the mid-latitude Atlantic (from chron C4r to C4n/C3Bn reversal) (Bukry, 1971; Bukry, 1973; Gartner, 1992; Raffi *et al.*, 1995; Raffi & Flores, 1995). In the Mediterranean these are rare but have been registered in different sections (Theodoridis, 1984; Martín-Pérez, 1997; Lancis *et al.*, 2010) within the biozones CN8b and CN9a for *D. loeblichii* (Lancis *et al.*, 2010) and lasting to the biozone CN9b for *D. neorectus* (Martín-Pérez, 1997; Lancis, 1998; Lancis *et al.*, 2010).

6.9 Paracme interval of *Reticulofenestra pseudoumbilicus*

The quantitative evaluation of the *R. pseudoumbilicus* abundance in the composite section *Les Moreres-Albatera* enabled us to recognize the “Paracme interval”, from the bottom of the *Albatera* section, with percentages lower than the 5% in almost all the samples (Raffi *et al.*, 2003). This event, an interval of almost total absence of large specimens (>7µm) of *R. pseudoumbilicus*, was found for the first time by Rio *et al.* (1990) in the Late Miocene sediments from the tropical Indian Ocean. It was soon observed in other oceanic basins (Gartner, 1992, Raffi &

Flores, 1995; Backman & Raffi, 1997) and in the Mediterranean, though not as clearly defined as in oceanic areas due to the abundance of reworked forms (Lancis, 1998; Raffi *et al.*, 2003; Lancis *et al.*, 2010). The PB (Paracme Begin) has been astronomically calibrated in the western equatorial Atlantic at 8.785 Ma (Backman & Raffi, 1997; Lourens *et al.*, 2004; Raffi *et al.*, 2006) and in the Mediterranean *Metochia* section at 8.761 Ma (Raffi *et al.* 2003).

6.10 FO of the *Discoaster quinqueramus-Discoaster berggrenii*

The appearance of the species *D. berggrenii* and *D. quinqueramus* corresponds to the biostratigraphic boundary CN8/CN9 (Okada & Bukry, 1980) NN10/NN11 (Martini, 1971). These pentaradiated discoasterids are abundant in the open oceans. In the Mediterranean, they are absent in the sediments of the eastern area (Theodoridis, 1984; Raffi *et al.*, 2003) but can be recognized in the western (Rio *et al.*, 1976; Müller, 1978; Mazzei, 1985; Müller, 1990; Flores *et al.*, 1992; Martín Pérez, 1997; Lancis, 1998; Lancis *et al.*, 2010). The astronomically tuned age for the FO of *D. berggrenii* at the western equatorial Atlantic is 8.29 Ma (Backman & Raffi, 1997; Lourens *et al.*, 2004). *Discoaster berggrenii* and *D. quinqueramus* are scarce but continuous in our samples the FO of *D. quinqueramus* is in the sample 2 of the *Albatera* section and the FO of *D. berggrenii* is in the sample 3 but due to its scarcity both FO could be considered synchronous.

6.11 Bottom of the acme of “small reticulofenestrids”

This event is determined by an increase in the assemblage of small reticulofenestrids (having the long axis smaller than 3 µm) including *Reticulofenestra minuta* and *Dictyococcites productus* specimens. This assemblage has been observed by many authors (Backman, 1978; Flores, 1985; Flores & Sierro, 1987; 1989; Flores *et al.*, 1992; Lancis, 1998; Negri *et al.*, 1999; Negri & Villa, 2000; Raffi *et al.*, 2003; Wade & Bown, 2005; Lancis *et al.*, 2010) and is included in the CN9a subzone between the *D. berggrenii* and *A. primus* FO's. This increment was probably caused

by an ecological factor, given that these species predominate in the continental margins nannofloras assemblages (Haq, 1980). Flores *et al.* (1992) demonstrate that this was a synchronous event in some Mediterranean and north-Atlantic sections.

In the *Albatera* section the “small reticulofenestrids” are quite abundant throughout the section because the section was nearby the coast and nutrient-rich. The “small reticulofenestrids” flourish in such conditions, supporting the theory of high environmental stress (Aubry, 1992; Flores *et al.*, 1995; Flores *et al.*, 2005; Wade & Bown, 2005). The acme bottom cannot be precisely identified. However, from the bottom of the *Albatera* section and coinciding with the paracme of *R. pseudoumbilicus* the “small reticulofenestrids” become in general more abundant, with percentages as high as the 75% of the assemblage indicating that they are later than the acme beginning.

6.12 FO and FCO of *Discoaster surculus*

In general *D. surculus* (Figs 8-12) is scarce in the Mediterranean sections (Theodoridis, 1984; Raffi *et al.*, 2003) but its presence has been established in the western Mediterranean basins (Martín-Pérez, 1997; Lancis, 1998; Lancis *et al.*, 2010) in a good agreement with its biostratigraphic range in the equatorial Pacific (Gartner, 1992; Schneider, 1995; Lourens *et al.*, 2004).

Discoaster surculus is scarce in our samples. Its first appearance is in the sample 15 of the *Albatera* section (Galería de los Suizos Marls), and the FCO was established in the sample 20, which was used as a secondary marker for the upper part of the CN9a/NN11a.

6.13 FO of the Initial *Amaurolithus* spp. (*Amaurolithus* cf. *primus*)

The *Amaurolithus* spp. FO (*A. cf. primus*) (Fig. 8-13; 8-14) represents an useful evolutionary event for worldwide biostratigraphic framework (Raffi *et al.*, 1998). It marks the boundary between the subzones CN9a/CN9bA of Okada and Bukry (1980) emended by Raffi and Flores (1995), and NN11a/NN11b of Martini (1971). Some initial forms of

Amaurolithus spp. (*A. cf. primus*) appear sporadically in the uppermost part of the *Albatera* section from sample 20 to the top of the section and coinciding with the FCO of *D. surculus*; thus, these forms are older than thought from previous observations.

6.14 FO of the *Syracosphaera pulchra*

Syracosphaera pulchra (Fig. 8-15) is present in the sediments from the Miocene until today. Despite the fragility and small size of this coccolith, it has been cited sporadically in the Miocene to Pliocene Mediterranean sections (Müller, 1978; Lancis, 1998). It should be pointed out that peak abundance was observed in the nearby Fortuna basin coinciding with the FCO of *D. surculus* (Lancis *et al.*, 2010) and hence it would be considered a possible event to be evaluated in the future.

7. BIOSTRATIGRAPHIC CALIBRATION OF THE MAGNETOSTRATIGRAPHY DATA

7.1 Biostratigraphy

The Middle and Late Miocene index species in the Mediterranean do not always provide a robust biostratigraphic signal because they are scarce compared with the low-latitude oceans. However, we could recognize most of the events, as discussed in the previous section. The biohorizons of FO, FCO, LO and LCO identified in the composite *Les Moreres-Albatera* section provided a biozonal distribution pattern (Fig. 3) from the earliest to the latest Tortonian with a sedimentary gap marked by the Raya del Búho Conglomerates.

The bottom part of the *Les Moreres* section until the sample 23 can be assigned (Fig. 3) to the CN5b subzone (Okada & Bukry, 1980), equivalent to the NN7 of Martini (1971), by occurrence as the most significant species of the assemblage: *Discoaster kugleri*, *D. exilis*, *D. brouweri*, *D. aulakos*, *Helicosphaera walberdorfensis*, and *Coccolithus miopelagicus*. The FO of *Discoaster bellus* in sample 24, and the integrated forms *Discoaster micros/Catinaster coalitus* are considered to be the bottom of

the biozone CN6/NN8 (Okada & Bukry, 1980; Martini, 1971, respectively). Due to the scarcity of *Catinaster coalitus*, we have considered the subordinate FO events *D. bellus* and *D. micros*/*C. coalitus* to be sufficient to mark the base of the biozone (Lourens *et al.*, 2004; Raffi *et al.*, 2006). The first clear specimens of *Catinaster coalitus* appear in sample 26 and the first *D. hamatus* in the sample 31. The last FO marks the boundary between the biozone CN6/CN7 (Okada & Bukry, 1980) and NN8/NN9 (Martini, 1971). The upper part of the *Les Moreres* section show a uniform assemblage of the biozone CN7 (Okada & Bukry, 1980) and NN9 (Martini, 1971) by the presence of *Discoaster hamatus*, *D. bellus*, *D. micros*, *D. brouweri*, *D. variabilis*, *D. challengerii*, *D. bollii*, *D. neohamatus* (from the sample 44), *D. calacaris* (sample 43), *Catinaster coalitus*, *Reticulofenestra pseudoumbilicus*, *Coccolithus pelagicus*, *Calcidiscus macintyreii*, *C. leptoporus*, *Gemmilithella rotula*, *Dictyococcites antarcticus*, *Triquetrorhabdulus rugosus*, and *Minylitha convallis* (sample 46).

The *Albatera* section should be included in the CN9a subzone (Okada & Bukry, 1980)/NN11a subzone (Martini, 1971) because of the presence of *Discoaster quinqueramus* and *D. berggrenii* marking the biozone CN9a (Okada & Bukry, 1980) and NN11A (Martini, 1971). Also the entire section is included in the PB of *R. pseudoumbilicus* > 7 µm, which register values of less than 5% throughout the section (Raffi *et al.*, 2003). On the other hand, this section is above the acme of the small reticulofenestrids included in the CN9a subzone between the *D. berggrenii* and *A. primus* FO's (Backman, 1978; Flores *et al.*, 1992; Lancis, 1998; Negri *et al.*, 1999; Negri & Villa, 2000; Raffi *et al.*, 2003; Wade & Bown, 2005; Lancis *et al.*, 2010).

The highest part of the section (sample 15) can be assigned to upper part of the CN9a/NN11a (Raffi *et al.*, 2003) by the presence of *D. surculus* (FCO in the sample 20) used as a secondary marker for the upper part of the CN9a/NN11a. The upper boundary between CN9a/CN9b is marked by the *A. primus* FO; however, the scarce initial forms assigned to *Amaurolithus cf. primus* that are found to be almost coincident with the FCO of *D. surculus* are forms prior to the FO of *Amaurolithus primus* str. s. These initial forms should be considered to be included in the CN9a, and also a more detailed study is needed to clarify the earliest evolution of the ceratoliths.

Palaeocologically, we should highlight the scarcity of asteroliths and the abundance of small reticulofenestrids such as *Lithostromathion perdurum*, *Pontosphaera multipora*, and different forms of *Scyphosphaera* spp. that could be related to a shallow and high-productivity environment (Martini, 1965; Bukry, 1976; Siesser, 1977; Gartner *et al.*, 1979; Flores, 1985; Chesptow-Lusty *et al.*, 1992; Raffi & Flores, 1995; Lancis, 1998; Flores *et al.*, 2005; Wade & Bown, 2006; Lancis *et al.*, 2010).

7.2 Magnetostratigraphy

The intensity of the NRM is relatively weak in the studied rocks ranging between 0.05 mA/m and 0.15 mA/m. Upon stepwise demagnetization two components can normally be distinguished in addition to a small viscous component removed at the first demagnetization step likely related to handling and/or storage. A low-field components conforming to the present geomagnetic field is removed up to fields of 17-21 mT. Then, a characteristic remanent magnetization (ChRM) is removed up to the maximum field applied (100 mT) that trends toward the origin of the diagram and presents dual polarity (Fig. 5B). We have established a ranking attending the quality of the demagnetization trajectories. Class A includes samples for which the ChRM component can be calculate unambiguously. Class B denotes samples with ambiguous ChRM components. The VPG latitude derived from the class A ChRM directions yields a succession of two magnetozones, characterized by reverse polarity in the lower part of the succession and reverse polarity in the upper part (Fig. 5A). The lowermost part of the studied succession of the *Galeria de los Suizos* Marls (interval 290-295 m) include two unreliable class B samples and only one normal class A sample and therefore this interval is reported as of ambiguous polarity and depicted in gray colour on the polarity column of Fig. 5A.

7.3 Calibration of the magnetostratigraphy with the new biostratigraphic data

For a comprehensive biomagnetostratigraphic correlation previous magnetostratigraphic results from the nearby *Rio*

Chicamo section (Dinarès-Turell *et al.*, 1999, and Krijgsman *et al.*, 2000) need to be taken into account. The *Rio Chicamo* section has recently been biostratigraphically calibrated with nannofossil data (Lancis *et al.*, 2010), supporting the magnetostratigraphic correlation A of Dinarès-Turell *et al.* (1999). The lowest magnetozone of the *Rio Chicamo* section was interpreted as a normal chron encompassing chrons C3Br.1n and C3Bn, therefore lacking expression of the intermediate short reverse chron C3Br.1r, because the FO of *Amaurolithus primus* is known to be located in chron C3Br.2r (Hilgen *et al.*, 2000; 7.341-7.170 Ma) just below chron C3Bn. Consequently, the top of the *Albatera* section is clearly below chron C3Br.2r of *Amaurolithus primus* FO.

The nannofossil data presented herein offers two different calibration points (Fig. 5). First, the FCO of *D. surculus* appears in other sections in chron C4n.2n, then the *Reticulophenestra pseudumbilica* > 7 µm Paracme End occurs in the transition between C3Bn/C3Ar (Raffi *et al.*, 2006). Thus the *Albatera* section reverse and normal magneto-zones shown in Figure 5 can be calibrated as chrons C4r.1r and C4n.2n respectively. Also the ambiguous polarity magnetozone and depicted in gray color on the polarity column of Fig. 5A can point to chron C4r.1n but better samples are needed to confirm this.

8. DISCUSSION AND CONCLUSIONS

The sedimentation over the structured basement of the Crevillente Sierra started with the El Castellà limestone. As this unit has not been sampled, no direct dating is possible, but in the previous work of Tent-Manclús *et al.* (2004) some marly intervals are dated in a nearby section as Serravallian by the presence of *Discoaster heteromorphus* plus *D. kugleri*.

Then the sedimentation shifts to the Les Moreres Marls lithological unit, which yields abundant planktonic foraminifera and calcareous nannofossils. The lowest portion of the unit indicates by its microfossil content an interval near the Serravallian-Tortonian boundary (Fig. 13). The absence of planktonic foraminifera *Globigerinoides subquadratus* points to a Tortonian age but the presence of *D. kugleri* indicates the interval between the Serravallian-

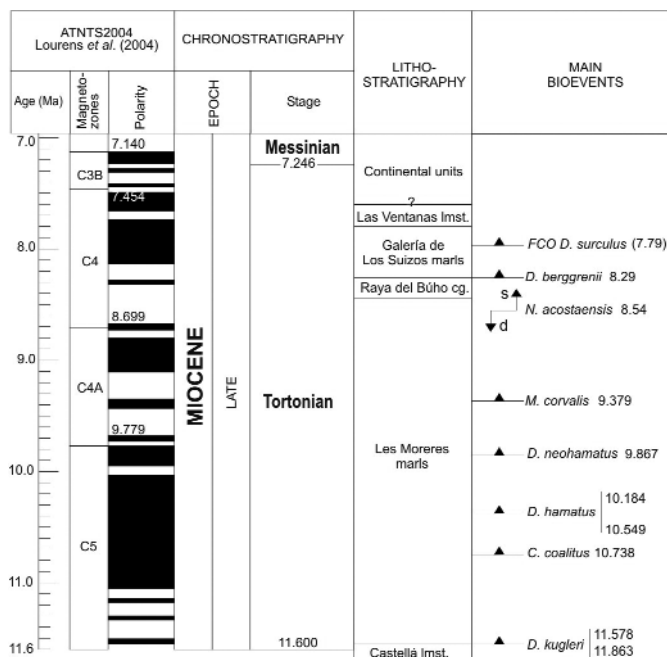


Figure 13. Summary of the positions of the biohorizons in the time interval 11.6 -7.8 Ma, relative to planktonic foraminifera and calcareous nannoplankton.

Tortonian boundary, and, depending on whether it is considered above or below the LCO, it could be assigned to the Tortonian or Serravallian, respectively. Thus the bottom part of the Les Moreres Marls is considered to be earliest Tortonian without ruling out a latest Serravallian age. The planktonic foraminifera and the calcareous nannofossils (Fig. 13) do not show any time gap from the bottom of the section assigned to the MMi9 planktonic foraminifera biozone (Lourens *et al.*, 2004) and CN5b/NN7 calcareous nannoplankton biozones (Okada & Bukry, 1980; Martini, 1971) to the to MMi11 planktonic foraminifera biozone (Lourens *et al.*, 2004) CN7/NN9 (Okada & Bukry, 1980; Martini, 1991). The top of the Les Moreres Marls can be calibrated by the dextral to sinistral change in *Neoglobobquadina acostaensis* estimated at 9.54 Ma by Lourens *et al.* (2004).

The Raya del Búho Conglomerate gradually overlies the Les Moreres Marls but the upper contact had developed an encrusted level interpreted as a possible time gap. This unit should be included in the MMi11 planktonic foraminifera biozone (Lourens *et al.*, 2004) and CN7/NN9 calcareous nannoplankton biozones (Okada & Bukry, 1980; Martini, 1971).

The bottom part of the Galería de los Suizos Marls in the *Albatera* section show a planktonic foraminifera assemblage included in the MMi12a biozone, and thus the foraminifera biozones do not have sufficient resolution to measure the time gap. However, the calcareous nannofossil assemblage with the FOs of *D. neorectus* and *D. quinqueramus* indicate the CN9a/NN11a biozones (Okada & Bukry, 1980; Martini, 1971) and can be calibrated by the FO of *D. berggrenii* as 8.29 Ma (Lourens *et al.*, 2004). The time gap between the Raya del Búho Conglomerate and the Galería de los Suizos Marls could be estimated at about 1.2 Ma. This discontinuity was caused by a NW-SE faulting tectonic event (Tent-Manclús, 2003). The Galería de los Suizos Marls fossilized those faults.

The *Albatera* section yields palaeomagnetic data shown in Figure 5 that can be calibrated as chrons C4r.1r and C4n.2n. The transition between those chrons was calibrated by Lourens *et al.* (2004) at 8.108 Ma. The top of the section is above the *D. surculus* FCO, calibrated at 7.79 Ma (Lourens *et al.*, 2004) which allows us to calibrate the bottom of the overlying Las Ventanas Limestones as younger than that age.

The composite *Les Moreres-Albatera* section should be considered as the most complete Tortonian section of the Betic Cordillera.

9. ACKNOWLEDGEMENTS

This work has been supported by the projects CGL2007-65832/BTE, PASUR CGL2009-08651 MCI, and CGL2009-07830 MCI, and the research group VIGROB-167. CL was funded by the research grant BEST/2010/068 GVA. We are indebted to David Nesbitt for correcting the English version of the paper.

10. REFERENCES

Alfaro García, P. 1995. *Neotectónica en la Cuenca del Bajo Segura (Extremo oriental de la Cordillera Bética)*. Ph. D. Thesis Univ. Alicante, Spain. 219 pp. (unpublished). <http://hdl.handle.net/10045/3176>

Aubry, M. P. 1992. Late paleogene calcareous nannoplankton evolution: a tale of climatic deterioration. In: *Eocene-Oligocene Climatic and Biotic Evolution* (Eds. D. R. Prothero and W. A. Berggren, W. A.). Princeton University Press, 272-309.

Azéma, J. and Montenat, C. 1975. *Mapa y memoria explicativa de la Hoja 892 (Fortuna) del Mapa Geológico Nacional a escala 1:50.000*. I.G.M.E., Madrid.

Backman, J. 1978. Late Miocene-Early Pliocene nannofossil biochronology and biogeography in the Vera basin, S.E. Spain. *Act. Univ. Stock. Contrib. Geol.*, 32, 2, 93-114.

Backman, J., Pestiaux, P., Zimmerman, H. and Hermelin, O. 1986. Paleoclimatic and Paleogeographic development in the Pliocene North Atlantic: *Discoaster* accumulation and coarse fraction data. In: North Atlantic Paleoclimatology (Eds. C. P. Summerhayes and N. J. Shackleton). *Geological Society Special Publication*, 21, 231-242.

Backman, J. and Raffi, I. 1997. Calibration of Miocene nannofossil events to orbitally-tuned cyclostratigraphies from Ceara Rise. In: (Eds. N. J. Shackleton, W. B. Curry, C. Richter, and T. J. Bralower), *Proceeding ODP, Scientific Results*, 154, 83-99. doi: 10.2973/odp.proc.sr.154.101.1997

Bukry, D. 1971. Cenozoic calcareous nannofossils from the Pacific Ocean. *Transactions of the San Diego Society of Natural History*, 16, 4, 303-328.

Bukry, D. 1973. Low-Latitude coccolith biostratigraphic zonation. In: (Eds. N. T. Edgar, J. B. Saunders, *et al.*), *Init. Repts. DSDP 15*, (U.S. Govt. Print. Off.), 685-703. doi: 10.2973/dsdp.proc.15.116.1973

Bukry, D. 1976. Coccolith stratigraphy of Manihiki Plateau, Central Pacific, Deep Sea Drilling Project, site 317. In: (Eds. S. O. Schlanger, E. D. Jackson, *et al.*), *Init. Repts. DSDP 33*, Washington (U. S. Govt. Print Off.), 493-499. doi: 10.2973/dsdp.proc.33.115.1976

Bukry, D. 1981. Cenozoic Coccoliths from the Deep Sea Drilling Project. *SEPM special publication*, 32, 335.

Bukry, D. and Percival, S. E. 1971. New Tertiary calcareous nannofossils. *Tulane Studies in Geology and Paleontology*, 8, 123-146.

Caruso, A., Sprovieri, M., Bonanno, A. and Sprovieri, R. 2002. Astronomical calibration of the Serravallian-Tortonian Case Pelacani section (Sicily, Italy). In: *Integrated Stratigraphy and Paleoclimatology of the Mediterranean Middle Miocene* (Ed. S. Iaccarino). *Riv. Ital. Paleontol. Stratigr.*, 108, 297-306.

Chesptow-Lusty, A., Shackleton, N.J. and Backman, J. 1992. Upper Pliocene *Discoaster* abundance from the Atlantic, Pacific, and Indian oceans: the significance of productivity pressure at low latitudes. *Mem. Sci. Geol.*, 44, 357-373.

Dinarès-Turell, J., Ortí, F., Playà, E. and Rossell, L. 1999. Palaeomagnetic chronology of the evaporitic sedimentation in the Neogene Fortuna Basin (SE Spain): early restriction preceding the 'Messinian Salinity Crisis'. *Palaeogeography, Palaeoclimatology, Palaeoecology*, 154, 161-178.

Flores, J. A. 1985. *Nanoplancton calcáreo en el Neógeno del borde noroccidental de la Cuenca del Guadalquivir (S.O. de España)*. Ph. D. Thesis, Univ. Salamanca, Spain.

Flores, J. A. and Sierro, F. J. 1987. Calcareous plankton in the Tortonian-Messinian transition of the Northwestern edge of the Guadalquivir Basin (SW Spain). *Abhandlungen der Geologischen Bundesanstalt*, 39, 64-87.

Flores, J. A. and Sierro, F. J. 1989. Calcareous nannoflora and planktonic foraminifera in the Tortonian/Messinian boundary interval of East At-

- lantic DSDP sites and their relation to Spanish and Moroccan sections. In: *Nannofossils and their applications* (Eds. S. Van Heck, and J. Crux). London: Ellis Horwood, 249-266.
- Flores, J. A., Sierro, F. J. and Glaçon, G. 1992. Calcareous plankton analysis in the pre-evaporitic sediments of the ODP site 654 (Tyrrhenian sea, Western Mediterranean). *Micropaleontology*, 38, 3, 279-288.
- Flores, J. A., Sierro, F. J. and Raffi, I. 1995. Evolution of the calcareous nannofossil assemblage as a response to the paleoceanographic changes in the eastern equatorial Pacific Ocean from 4 to 2 Ma (Leg 138, Sites 849 and 852). In: (Eds. N. G. Pisias, L. A. Mayer, T. R. Janecek, A. Palmer-Julson and T. H. van Andel). Proceedings ODP, Scientific Results 138, 163–176. doi: 10.2973/odp.proc.sr.138.108.1995
- Flores, J. A., Sierro F. J., Gabriel M. Filippelli G. M., Bárcena M. A., Pérez-Folgado M., Vázquez A. and Utrilla, R. 2005. Surface water dynamics and phytoplankton communities during deposition of cyclic late Messinian sapropel sequences in the western Mediterranean. *Marine Micropaleontology*, 56, 50–79.
- Fornaciari, E., Raffi, I., Rio, D., Villa, G., Backman, J. and Olafsson, G. 1990. Quantitative distribution patterns of Oligocene and Miocene calcareous nannofossils from the western equatorial Indian Ocean. In: (R. A. Duncan, J. Backman, L. C. Peterson *et al.*) Proceedings ODP, Sci. Results 115, 237-254.
- Fornaciari, E., Di Stefano, A. Rio, D. and Negri, A. 1996. Middle Miocene quantitative calcareous nannofossil biostratigraphy in the Mediterranean region. *Micropaleontology*, 42, 1, 37-63.
- Foresi, L.M., Bonomo, S., Caruso, A., Di Stefano, A., Di Stefano, E., Iaccarino, S.M., Lirer, F., Salvatorini, G. and Sprovieri, R. 2002. High-resolution calcareous plankton biostratigraphy of the serravallian succession of the Tremiti Islands (Adriatic Sea, Italy). In: Iaccarino, S. (Ed.), *Integrated Stratigraphy and Paleoceanography of the Mediterranean Middle Miocene*. *Rivista Italiana di Paleontologia e Stratigrafia*, 108, 257-273.
- Gartner, S. 1992. Miocene nannofossil chronology in the North Atlantic DSDP Site 608. *Marine Micropaleontology*, 18, 307-331.
- Gartner, S. and Bukry, D. 1975. Morphology and phylogeny of the Coccolithophyceae family Ceratolithaceae. *Journal Research. U. S. Geological Survey* 3, 4, 451-465.
- Gartner, S., Chen, M. P. and Stanton, R. J. 1979. Late Neogene history in the American Mediterranean. VII Int. Cong. Med. Neog. Athens. *Annales Géologiques des Pays Helléniques*, Tome Hors série, 1, 425-437.
- Groupe de Recherche Néotectonique de l'arc de Gibraltar (1977): L'histoire tectonique récente (Tortonien à Quaternaire) de l'Arc de Gibraltar et des bordures de la mer d'Alboran. *Bulletin Société Géologique de France*, 19, 575-614.
- Hilgen, F. J., Krijgsman, W., Langereis, C. G., Lourens, L. J., Santerelli, A. and Zachariasse, W. J. 1995. Extending the astronomical (polarity) time scale into the Miocene. *Earth Planetary Science Letters*, 136, 495–510.
- Hilgen, F.J., Krijgsman, W., Raffi, I., Turco, E. and Zachariasse, W. J. 2000. Integrated stratigraphy and astronomical calibration of the Serravallian/Tortonian boundary section at Monte Gibliscemi (Sicily, Italy). *Marine Micropaleontology*, 38, 182-211.
- Hilgen, F. J., Abdul Aziz, H., Krijgsman, W., Raffi, I. and Turco, E. 2003. Integrated stratigraphy and astronomical tuning of the Serravallian and lower Tortonian at Monte dei Corvi (Middle-Upper Miocene, northern Italy). *Palaeogeography, Palaeoclimatology, Palaeoecology*, 199, 229-264.
- Kirschvink, J. L. 1980. The least-square line and plane and analysis of paleomagnetic data. *Geophysical Journal of the Royal Astronomical Society*, 62, 699-718.
- Krijgsman, W., Garcés, M., Agustí, J., Raffi, I., Taberner, C. and Zachariasse, W. J. 2000. The 'Tortonian salinity crisis' of the eastern Betics (Spain). *Earth and Planetary Science Letters*, 181, 497-511.
- Lancis, C. 1998. *El nannoplancton calcáreo de las cuencas neógenas orientales de la Cordillera Bética*. Ph.D. Thesis, Univ. Alicante, Spain, 841 pp. <http://hdl.handle.net/10045/7944>
- Lancis, C., Tent-Manclús, J.E., Soria, J. M., Caracuel, J. E., Corbí, H., Dinarès-Turell, J., Estévez, A. and Yébenes, A. 2010. Nannoplankton biostratigraphic calibration of the evaporitic events in the Neogene Fortuna Basin (SE Spain). *Geobios*, 43, 201-217. doi: 10.1016/j.geobios.2009.09.007
- Lourens, L., Hilgen, F., Shackleton, N. J., Laskar, J. and Wilson, D. 2004. The neogene period. In: *A geologic Time Scale* (Eds. F. M. Gradstein, J. G. Ogg and A. G. Smith). Cambridge University Press, 409-440.
- Mazzei, R., 1985. The Miocene sequence of the Maltese islands: biostratigraphic and chronostratigraphic reference based on nannofossils. *Atti della Società Toscana di Scienze Naturali, Serie A*, 92, 165-197.
- Martín-Pérez, J. A. 1997. *Nannoplancton calcáreo del Mioceno de la Cordillera Bética (Sector Oriental)*. Ph. D. Thesis, Univ. Granada, Spain, 329 pp. (unpublished)
- Martini, E. 1965. Mid-Tertiary calcareous nannoplankton from Pacific deep-sea cores. In: *Submarine Geology and Geophysics* (Eds. W. F. Whittard and R. B. Bradshaw). Proc. 17th Symp. Colston Res. Soc. London, 393-411.
- Martini, E. 1971. Standard Tertiary and Quaternary calcareous nannoplankton zonation. Proc. II Planktonic conference, Tecnoscienza, Roma, 2, 736-785.
- Mazzei, R. 1985. The Miocene sequence of the Maltese islands: biostratigraphic and chronostratigraphic references based on nannofossils. *Atti della Società Toscana di Scienze Naturali, Memorie*, 42, 165-197
- Montenat, C. 1977. *Les bassins néogènes du levant d'Alicante et de Murcia (Cordillères bétiques orientales-Espagne)*. *Stratigraphie, paléogéographie et évolution dynamique*. Documents Laboratoire Géologie Faculté des Sciences de Lyon, 69, 345 pp.
- Montenat, C., Ott d'Estevou, Ph. and Coppier, G. 1990. Les bassins neogènes entre Alicante et Cartagena. In: *Les Bassins Néogènes du Domaine Bétique Orientale (Espagne)* (Ed. C. Montenat). Documents et Travaux, Institut Géologique Albert de Lapparent, 12-13, 313-368.
- Müller, C. 1978. Neogene calcareous nannofossils from the Mediterranean - Leg 42A of the Deep Sea Drilling Project. In: (Eds. K. J. Hsü, L. Montadert *et al.*). *Initial Reports DSDP*, 42 (Pt. 1), 727-751.
- Müller, C. 1990. Nannoplankton biostratigraphy and paleoenvironmental interpretations from the Tyrrhenian Sea, ODP Leg 107 (Western

- Mediterranean). In: Kastens, K. A., Mascle, J. et al., (Eds.), Proceedings ODP, Scientific Results, 107, 495-511.
- Negri, A., Giunta, S., Hilgen, F., Krijgsman, W. and Vai, G. B. 1999. Calcareous nannofossil biostratigraphy of the M. del Casino section (northern Apennines, Italy) and paleoceanographic conditions at times of Late Miocene sapropel formation. *Marine Micropaleontology*, 36, 1, 13-30.
- Negri, A. and Villa, G. 2000. Calcareous nannofossil biostratigraphy biochronology and paleoecology at the Tortonian/Messinian boundary of the Faneromeni section (Crete). *Palaeogeography, Palaeoclimatology, Palaeoecology*, 156, 195-209.
- Okada, H. and Bukry, D. 1980. Supplementary modification and introduction of code numbers to the low-latitude coccolith biostratigraphic zonation (Bukry, 1973; 1975). *Marine Micropaleontology*, 5, 321-325.
- Raffi, I. and Flores, J.A. 1995. Pleistocene through Miocene Calcareous nannofossils from eastern equatorial Pacific Ocean (Leg 138). In: (Eds. N. G. Pisias, L. A. Mayer, T. R. Janecek, A. Palmer-Julson and T. H. van Andel). Proceedings ODP, Scientific Results 138, 233-285. doi: 10.2973/odp.proc.sr.138.112.1995
- Raffi, I., Backman, J. and Rio, D. 1998. Evolutionary trends of calcareous nannofossils in the Late Neogene. *Marine Micropaleontology*, 35, 17-41.
- Raffi, I., Backman, J., Fornaciari, E., Pälike, H., Rio, D., Lourens, L. and Hilgen, F. 2006. A review of calcareous nannofossil astrobiochronology encompassing the past 25 million years. *Quaternary Science Reviews*, 25, 3113-3137. doi:10.1016/j.quascirev.2006.07.007
- Raffi, I., Mozzato, C., Fornaciari, E., Hilgen, F. J. and Rio, D. 2003. Late Miocene calcareous nannofossil biostratigraphy and astrobiochronology for the Mediterranean region. *Micropaleontology*, 49 (1), 1-26. doi:10.2113/49.1.1
- Raffi, I., Rio, D., d'Afri, A., Fornaciari, E. and Rochetti, S. 1995. Quantitative distribution patterns and biomagnetostratigraphy of Middle and Late Miocene calcareous nannofossils from equatorial Indian and Pacific Ocean (legs 115, 130 and 138). In: (Eds. N. G. Pisias, L. A. Mayer, T. R. Janecek, A. Palmer-Julson and T. H. van Andel). Proceedings ODP, Scientific Results, 138, 479-502. doi: 10.2973/odp.proc.sr.138.125.1995
- Rio, D., Mazzei, R. and Palmieri, G. 1976. The stratigraphic position of the Mediterranean Upper Miocene evaporites, based on nannofossils. *Memorie della Società Geologica Italiana*, 16, 261-276
- Rio, D., Fornaciari, E. and Raffi, I. 1990. Late Oligocene through early Pleistocene calcareous nannofossils from western equatorial Indian Ocean (Leg 115). In: (Eds. R. A. Duncan, J. Backman, L. C. Peterson, et al.). Proceedings ODP, Scientific Results, 115, 175-235. doi: 10.2973/odp.proc.sr.115.152.1990
- Rodríguez-Fernández, J., Comas, M. C., Soria, J., Martín-Pérez, J. A. and Soto, J. I. 1999. The Sedimentary record of the Alboran basin: an attempt at sedimentary sequence correlation and subsidence analysis. In: (Eds. R. Zahn, M. C. Comas and A. Klaus). Proceedings ODP, Scientific Results, 161, 69-76. doi:10.2973/odp.proc.sr.161.207.1999
- Santisteban Bové, C. 1981. *Petrología y sedimentología de los materiales del Mioceno superior de la cuenca de Fortuna (Murcia), a la luz de la crisis de salinidad*. Ph.D. Thesis, Univ. Barcelona, Spain. (unpublished)
- Schneider, D. A. 1995. Paleomagnetism of some ODP Leg 138 sediments: detailing Miocene magnetostatigraphy. In: (Eds. N. G. Pisias, L. A. Mayer, T. R. Janecek, A. Palmer-Julson and T. H. van Andel). Proceedings ODP, Scientific Results, 138, 59-72. doi: 10.2973/odp.proc.sr.138.105.1995
- Shackleton, N. J. and Crowhurst, S. 1997. Sediment fluxes based on an orbitally tuned time scale 5 Ma to 14 Ma, Site 926. In: (Eds. N. J. Shackleton, W. B. Curry, C. Richter and T. J. Bralower). Proceedings ODP, Scientific Results, 154, 69-82. doi:10.2973/odp.proc.sr.154.102.1997
- Siesser, W. G. 1997. Calcareous nannofossils as age and paleoenvironmental indicators. Electron van. Sudelike Afrika. In: Proc., 7. Elec. Micros. Soc. South Africa., 81-82.
- Soria, J. M., Alfaro, P., Fernández, J. and Viseras, C. 2001. Quantitative subsidence-uplift analysis of the Bajo Segura Basin (eastern Betic Cordillera, Spain): tectonic control on the stratigraphic architecture. *Sedimentary Geology*, 140, 271-289.
- Soria, J.M., Fernández, J. and Viseras, C. 1999. Late Miocene stratigraphic evolution of the intramontane Guadix Basin (Central Betic Cordillera, Spain): implications for an Atlantic-Mediterranean connection. *Palaeogeography, Palaeoclimatology, Palaeoecology*, 151, 255-266.
- Soria, J. M., Fernández, J., García, F. and Viseras, C. 2003. Correlative lowstand deltaic and shelf systems in the Guadix Basin (Late Miocene, Betic Cordillera, Spain): The stratigraphic record of forced and normal regressions. *Journal of Sedimentary Research*, 73, 6, 912-925. doi:1527-1404/03/073-912.
- Soria, J. M., Tent-Manclús, J. E., Caracuel, J. E., Yébenes, A., Lancis, A. and Estévez, A. 2005. La crisis de salinidad Tortonense: su registro en la zona de enlace entre las cuencas de Fortuna y del Bajo Segura. *Geo-Temas*, 8, 113-118.
- Tent-Manclús, J. E. 2003. *Estructura y estratigrafía de las sierras de Crevillente, Abanilla y Algayat: su relación con la Falla de Crevillente*. Ph.D. Thesis, Univ. Alicante, Spain, 957 pp. <http://hdl.handle.net/10045/10414>
- Tent-Manclús, J. E., Yébenes, A. and Estévez, A. 2005. ¿Por qué son tan diferentes las sierras de Crevillente y Abanilla? *Geogaceta*, 37, 71-74
- Tent-Manclús, J. E., Lancis, C., Soria, J. M., Dinarès-Turell, J., Estévez, A., Caracuel, J. E. and Yébenes, A. 2007. Primeros datos bioestratigráficos de los grupos evaporíticos de la Cuenca de Fortuna (Cordillera Bética). *Geogaceta*, 41, 231-234.
- Tent-Manclús, J. E., Lancis, C., Yébenes, A. and Estévez, A. 2004. Estratigrafía del Mioceno Medio y Superior al NW de Crevillente (Alicante). *Geo-Temas*, 7, 185-190.
- Tent-Manclús, J. E., Soria, J. M., Estévez, A., Lancis, C., Caracuel, J. E., Dinarès-Turell, J. and Yébenes, A. 2008. Tortonian Salinity Crisis and tectonics: A view from the Fortuna Basin (SE Spain). *Comptes Rendus Geoscience*, 340, 474-481. doi: 10.1016/j.crte.2008.05.003
- Theodoridis, S. A. 1984. Calcareous nannofossils biozonation of the Miocene and revision of the Helicoliths and Discoasters. *Utrecht Micropaleontological Bulletin*, 31, 271 pp.
- Viseras, C., Soria, J. M. and Fernández, J. 2004. Cuencas neógenas postorogénicas de la Cordillera Bética. In: *Geología de España* (Ed. J. A. Vera). SGE-IGME, Madrid, 576-581.

Vera, J. A. (Ed.) 2004. Cordillera Bética y Baleares. In: *Geología de España* (Ed. J. A. Vera). SGE-IGME, Madrid, 345-464.

Wade, B. S. and Bown, P. R. 2006. Calcareous nannofossils in extreme environments: The Messinian Salinity Crisis, Polemi Basin, Cyprus. *Palaeogeography, Palaeoclimatology, Palaeoecology*, 233, 271-286. doi:10.1016/j.palaeo.2005.10.007

Zijderveld, J. D. A. 1967. A.C. demagnetization of rock: analysis of results. In: *Methods in paleomagnetism* (Eds. D. W. Collinson, K. M. Creer, S. K. Runcorn). Elsevier, Amsterdam, 254-286.

MANUSCRITO RECIBIDO: 18 de mayo, 2010

MANUSCRITO ACEPTADO: 28 de noviembre, 2010

Appendix A

Taxonomic list of the calcareous nannoplankton considered in this work (see Young, 1998)

- Amaurolithus primus* (Bukry & Percival, 1971) Gartner & Bukry, 1975
- Calcidiscus macintyreii* (Bukry & Bramlette, 1969) Loeblich & Tappan, 1968
- C. leptoporus* (Murray & Blackman, 1898) Loeblich & Tappan, 1978
- Coccolithus pelagicus* (Wallich, 1871) Schiller, 1930
- C. miopelagicus* Bukry, 1971
- Catinaster coalitus* Martini & Bramlette, 1963
- Dictyococcites antarcticus* Haq, 1976 = *Reticulofenestra antarctica* Haq, 1976
- D. productus* (Kamptner, 1963) emend. Backman, 1980
- Discoaster aulakos* Gartner, 1967
- D. bellus* Bukry & Percival, 1971
- D. berggrenii* Bukry, 1971
- D. bolli* Martini & Bramlette, 1963
- D. brouweri* Tan Sin Hok, 1927 emend. Bramlette & Riedel, 1954
- D. calcaris* Gartner, 1967
- D. challengerii* Bramlette & Riedel, 1954
- D. exilis* Martini & Bramlette, 1963
- D. hamatus* Martini & Bramlette, 1963
- D. intercalaris* Bukry, 1971
- D. loeblichii* Bukry, 1971
- D. kugleri* Martini & Bramlette, 1963
- D. micros* Theodoridis, 1984
- D. neohamatus* Bukry & Bramlette, 1969
- D. neorectus* Bukry, 1971
- D. pentaradiatus* Tan Sin Hok, 1927 emend. Bramlette & Riedel, 1954
- D. prepentaradiatus* Bukry & Percival, 1971
- D. pseudovariabilis* Martini & Worsley, 1971
- D. quinquerramus* Gartner, 1969
- D. surculus* Martini & Bramlette, 1963
- D. tamalis* Kamptner, 1967
- D. triradiatus* Tan, 1927
- D. variabilis* Martini & Bramlette, 1963
- Geminolithella jafarii* (Müller, 1974) Backman, 1980
- G. rotula* (Kamptner, 1948) Backman, 1980
- Helicosphaera carteri* (Wallich, 1877) Kamptner, 1954
- H. rhomba* Bukry, 1971
- H. stalis* Theodoridis, 1984
- H. walberdorsfensis* Müller, 1974
- Lithostromation perdurum* Deflandre, 1942
- Pontosphaera multipora* (Kamptner, 1948) Roth, 1970
- Reticulofenestra gelida* (Geitzenauer, 1972) Backman, 1978
- R. haqii* Backman, 1978
- R. minuta* (Roth, 1970)
- R. minutula* Gartner, 1967
- R. pseudoumbilicus* (Gartner, 1967) Gartner, 1969
- Scyphosphaera amphora* Deflandre, 1942
- Scy. conica* Kamptner, 1955
- Scy. apsteinii* Lohmann, 1902
- Scy. intermedia* Deflandre, 1942
- Sphenolithus abies* Deflandre in Deflandre & Fert, 1954
- Sph. neoabies* Bukry & Bramlette, 1969
- Sph. moriformis* (Brönnimann & Stradner, 1960) Bramlette & Wilcoxon, 1967
- Syracosphaera pulchra* Lohmann, 1902
- Triquetrorhabdulus rugosus* Bramlette & Wilcoxon, 1967
- Small reticulofenestrads (nannolith size smaller than 3 µm, independently of central area properties: *Dictyococcites productus* (Kamptner, 1963) emend. Backman, 1980 plus *Reticulofenestra minuta* Roth, 1970)

Sea surface dynamics and coccolithophore behaviour during sapropel deposition of Marine Isotope Stages 7, 6 and 5 in Western Adriatic sea

Áurea Narciso¹, José-Abel Flores², Mário Cachão^{1,3}, Francisco Javier Sierra²,
Elena Colmenero-Hidalgo², Andrea Piva⁴ and Alessandra Asioli⁵

¹ Centre Geology University of Lisbon, 1749-016 Lisboa, Portugal. acnarciso@fc.ul.pt

² Department of Geology, University of Salamanca, 37008 Salamanca, Spain

³ Department of Geology, Fac. Sciences, University of Lisbon, 1749-016 Lisboa, Portugal

⁴ ISMAR, Consiglio Nazionale delle Ricerche, Via Gobetti 101, 40129 Bologna, Italy

⁵ IGG, Consiglio Nazionale delle Ricerche, Via Giotto 1, 35100 Padova, Italy

Resumen

Se presenta un análisis detallado de los nanofósiles calcáreos registrados en el testigo PRD1-2, recuperado durante la campaña PROMESS 1 con el objetivo de estudiar las variaciones en las asociaciones durante los MIS (Estadios Isotópicos Marinos) 7, 6 y 5, que integran capas equivalentes a los sapropeles S₈eq.–S₃eq. Los datos reflejan un descenso en la productividad de coccolitóforos, marcada por *Gephyrocapsa* spp., durante los MIS 7 y 6 en la capa equivalente al sapropel S₅eq. Por el contrario, *Florisphaera profunda* muestra picos en su abundancia en esos intervalos, reflejando una posición relativamente profunda de la nutriclina. En las dos capas equivalentes a sapropeles del MIS 5 (S₄eq. y S₃eq.) se observa lo opuesto. La sedimentación de esos sapropeles atípicos son concomitantes con la producción de agua profunda del Adriático y una subsecuente mezcla, como consecuencia de la actividad del viento Bora (noroeste), favoreciendo la eclosión de especies de zona fótica superior en relación a las de zona fótica inferior. Por otra parte, se ponen de manifiesto modelos de distribución similar entre especímenes retrabajados (Cretácico-Terciario), *Coccolithus pelagicus* y *Helicosphaera carteri*, con incremento importante en las capas equivalentes a sapropeles de los MIS 7 y 6 y durante la parte final del MIS 6, el más frío y seco. Debido al amplio rango de distribución de *C. pelagicus* (Paleoceno temprano-Reciente) y *H. carteri* (Mioceno-Reciente) los ejemplares procedentes del continente y vertidos a la cuenca Adriática, o redistribuidos por corrientes de fondo, son de particular importancia en ciertos intervalos (210-200, 145, 135, 110 y 85 ka). *Syracosphaera* spp., *Rhabdosphaera clavigera* y *Calciosolenia* spp., normalmente relacionadas con aguas cálidas y oligotróficas, no muestran relación con el registro isotópico. Sin embargo, su importante incremento hacia la parte superior o sobre la terminación de algunas capas equivalentes a sapropeles es coherente con el final de las condiciones secas y con el subsecuente de una situación oligotrófica y una redistribución de los nutrientes. Al mismo tiempo, el incremento de *Braarudosphaera bigelowii* coincidiría con una reducción en la salinidad durante S₈eq. y S₆eq., aun que su presencia puede corresponder también a aportes continentales, dado su amplio rango estratigráfico (Cretácico-Reciente).

Palabras clave: Nanofósiles calcareous, Coccolitóforos, Pleistoceno, Sapropeles, Adriático, Paleoceanografía, Paleoecología

Abstract

A detailed calcareous nannofossil analysis was performed in the core PRAD1-2, recovered in the Mid-Adriatic Deep during the PROMESS 1 Cruise, in order to show fluctuations of several species during the Marine Isotope Stages 7, 6 and 5, crossing the S₈eq.–S₃eq. sapropel-equivalent layers. This study reports a decrease in the coccolithophore productivity, given by *Gephyrocapsa* spp. abundance decreases, during the deposition of MIS 7 and MIS 6 sapropel-equivalent layers and also during S₅eq. *Florisphaera profunda*, on the contrary, shows abundance peaks within these intervals, reflecting a deeper position of the nutricline. Within the two last sapropel-equivalent layers of MIS 5 (S₄eq. and S₃eq.) the opposite can be observed. The deposition of these atypical sapropels may have been concomitant with some Adriatic Deep Water production and subsequent some water column mixing, in result of the activity of the north-easterly Bora wind, favouring the development of the upper photic zone species in relation to the lower photic zone

inhabitant *F. profunda*. Similar general abundance patterns are evidenced by reworked specimens (Cretaceous-Tertiary), *Coccolithus pelagicus* and *Helicosphaera carteri*, with important increases during the sapropel-equivalent layers of MIS 7 and MIS 6 and during the latest part of the glacial stage 6, the coldest and the driest one. Due to the extended fossil record of *C. pelagicus* (Early Paleocene-Recent) and *H. carteri* (Miocene-Recent), reworked placoliths and helicoliths from a continental source, by precipitation and runoff into the Adriatic basin, or from redistribution by bottom currents, are of particular importance at certain moments (210-200, 145, 135, 110 and 85 kyr). *Syracosphaera* spp., *Rhabdosphaera clavigera* and *Calciosolenia* spp., usually related to warm and oligotrophic water masses, do not show a clear correlation with the isotope record. However, their important increases at the top or above the termination of some sapropel-equivalent layers is consistent with the end of dryer conditions that feature the sapropel deposition, and with the subsequent reestablishment of the general oligotrophic state of the surface water with a nutrient redistribution. At the same time a salinity reduction should occur due to the simultaneous presence of *Braarudosphaera bigelowii*. During S_{8eq} and S_{6eq} the presence of *B. bigelowii* coupled with its stratigraphic range (Cretaceous-Recent), may also indicate a continental source for some pentoliths.

Key words: Calcareous nannofossils, Coccolithophores, Pleistocene, Sapropels, Adriatic, Paleoceanography, Paleoecology.

1. INTRODUCTION

Several studies have been performed on sapropel layers, a characteristic organic rich matter deposit commonly occurring in the Mediterranean Sea. Using sedimentological (Kroon *et al.*, 1998; Capozzi and Picotti, 2003; among others), geochemical (Bouloubassi *et al.*, 1999; Arnaboldi and Meyers, 2003; Gogou *et al.*, 2007; among others) and micropaleontological (Castradori, 1993; Rio *et al.*, 1997; Giunta *et al.*, 2003; Principato *et al.*, 2006; Marino *et al.*, 2007; Triantaphyllou *et al.*, 2009a, b, c; among others) techniques, most of these studies refer that sapropels are dark-coloured organic-rich layers interbedded in the normal pelagic (or hemipelagic) sediments of the Mediterranean Sea, related to climatic or oceanographic variations. The sapropel generation is associated to orbital scale oscillations under conditions of maximum summer insolation, corresponding to a minimum of the precession component of Earth's orbital with a periodicity of 21 kyr (Hilgen, 1991; Lourens *et al.*, 1996; Hilgen *et al.*, 1997; Sierro *et al.*, 1999). The maximum summer insolation is reflected by an increase in precipitation and runoff in the Mediterranean basin, responsible for an increased stratification of surface waters, while its reduction leads to a dry and cold climate, with the mixing of the bottom waters and, consequently, the reduction of organic matter (Hilgen, 1991; Sierro *et al.*, 1999; Flores *et al.*, 2005).

During the PROMESS 1 project several cores were recovered in the Adriatic Sea. The good quality record of the

sapropels in some sectors, as well as the moderately high sedimentation rates (20 cm/kyr) observed after the preliminary analyses, allowed the achievement of new material for study (Piva *et al.*, 2008).

Calcareous nannofossils, in which the Coccolithophore group is included, are an important component of sapropels and have been used mainly for biostratigraphic correlations and also for paleoceanographic reconstructions (Müller, 1985; de Kaenel and Villa, 1996; Negri *et al.*, 1999a, b; Negri and Villa, 2000; Flores *et al.*, 2005; Principato *et al.*, 2006; Triantaphyllou *et al.*, 2009a, b, c) by the knowledge of some parameters such as temperature, salinity, productivity, turbidity, depth, among others.

The present study addresses a time series that crosses several sapropel layers (S_3 , S_4 , S_5 , S_6 , S_7 and S_8) included in Marine Isotope Stages (MIS) 7, 6 and 5, between 199 and 81 kyr. Our sapropel layers are referred as sapropel-equivalent (e.g. S_{3eq}) because this numeric sequence was not specifically defined for the Adriatic ones, but for the sapropels of the Mediterranean in general (Piva *et al.*, 2008). They correspond to dark seldom laminated sediments bearing distinctive micropaleontological, geochemical and paleomagnetic parameters, indicating low oxygen conditions (Piva *et al.*, 2008). Based on micropaleontological content, this study allows to recognize the response of coccolithophore assemblages to climate variation during interglacial/glacial stages, and also to infer changes on several (paleo)ceanographic variables during the mentioned interval.

2. MATERIAL AND METHODS

2.1 Location of the studied area and material

For the present study, a borehole referred as PRAD1-2 was collected in the Mid-Adriatic Deep (LAT 42°40'34.7826''N; LONG 14°46'13.5565''E) in 185.5 m water depth (Figure 1). The coring device on board R/V Bavenit in the PROMESS1 Cruise provided a continuous sediment core of 71.2 m, with a recovery of 99.96 % (Piva *et al.*, 2008).

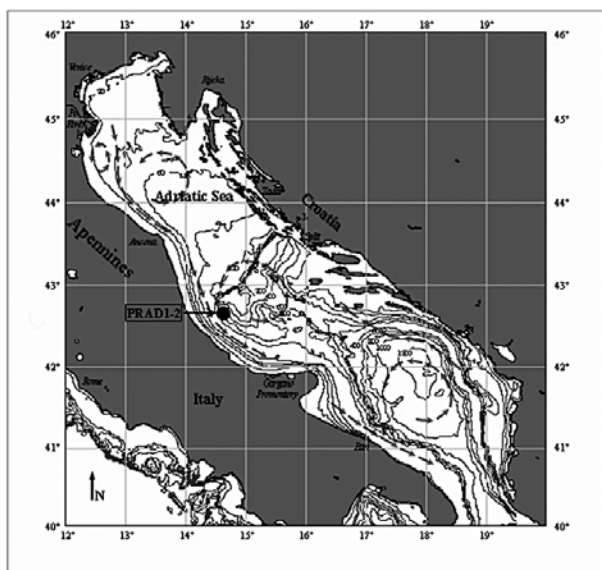


Figure 1. Map location of the borehole PRAD1-2 with coastline, topography and surface circulation (represented by arrows; based on Artegiani *et al.* (1997) and Cattaneo *et al.* (2003)).

A total of 234 samples, with an interval of 10 cm between contiguous samples, were analysed in what concerns the abundances of coccolithophore assemblages. The sequence selected for this study ranges between 21 to 43.7 mbsf (metres below surface), and includes the Marine Isotope Stages 7, 6 and 5 (Piva *et al.*, 2008).

2.2 Techniques

The study of coccolithophores involved the preview preparation of 234 slides according to Flores and Sierro (1997) decantation technique, followed by its observation under an optical polarizing microscope at 1250x magnification. In random fields of view up to 400 small coccoliths were counted, additionally with an independent counting of the larger coccoliths (> 5µm). When was not possible to find 400 small specimens, the counting was extended to a 24 random fields of view. The analysis based on absolute abundances (liths/g) was applied at first, however the related curves were indicative of clear dilution, revealing low significance. Therefore, the results are presented in percentage abundances (Figure 2).

Coccolithophore associations could reflect the nutrient content and its position in the water column, due to their ecological preferences. The relationship between small coccoliths and *F. profunda* (*N* ratio), which occur in the upper and in the lower photic zone, respectively, can be used to monitor the nutricline (and thermocline) fluctuations and, consequently, be used as a productivity proxy (Flores *et al.*, 2000). *N* ratio oscillates between 0 and 1, being the higher values indicative of higher productivity in the upper photic zone while the opposite is indicated by lower values.

Due to the high probability that certain coccoliths may be driven to the Adriatic basin reworked from surrounding on-shore Cenozoic formations, a simple statistical parameter named DELTA (Cachão, 1996) was computed as the standard difference between certain taxonomic groups, in this case the standardized abundance of the total of non-Quaternary coccoliths and nannoliths against the standardized abundance of two common Tertiary species: *Coccolithus pelagicus* and *Helicosphaera carteri*. The purpose is to statistically determine intervals when one variable prevails (has independent behaviour) over other (in the present case, reworking) that is recognized to strongly and directly influence most of the time the former (Figure 3).

2.3 Chronostratigraphic framework

The chronostratigraphic framework for PRAD1-2 is based on stable oxygen isotope stratigraphy, magnetostratigraphy, radiocarbon dates and bioevents (Piva *et al.*, 2008). The combination with additional control points corresponding to the ages of Termination midpoints (Lisiecki and Raymo, 2005) and to dated sub-stages relative maxima/minima values (Martinson *et al.*, 1987; Bassinot *et al.*, 1994) were also used. Concerning isotope oxygen stratigraphy, the $d^{18}O$ records were performed from the plank-

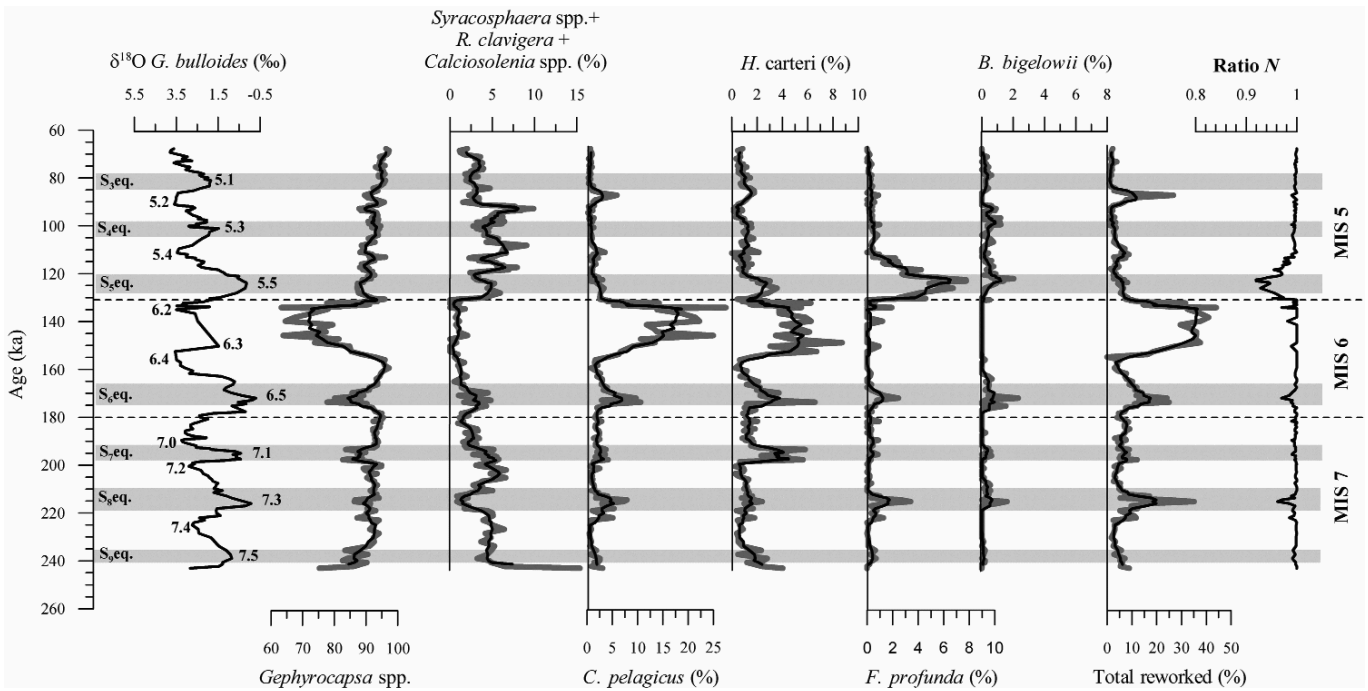


Figure 2. Relative abundances (percentages) of several coccolithophores and reworked specimens analysed in the borehole PRAD1-2, as well as the isotope curve based on *Globigerina bulloides* and the *N* ratio. A smooth line was applied to the abundance curves. Sapropel layers, isotopic stages and sub-stages are indicated. S₃eq.- Sapropel 3 equivalent; MIS-Marine Isotope Stage.

tic foraminifer *Globigerina bulloides*, which curve is illustrated in our results, and from the benthic foraminifer *Bulimina marginata*. The ages ascribed to sapropels in the mentioned borehole refer to the sapropel-based astronomical timescale for the last 1.1 Ma established in the Ionian Sea, eastern Mediterranean (Lourens, 2004). The sapropel layers can be detected by the decrease in reflectance index, by the oxygen isotope shift to lower values (Lourens, 2004), by the Oxygen Deficiency Stress curve, which reflects severe low-oxygen stress of the seafloor before totally azoic conditions (Rohling *et al.*, 1997), and by the quasi-absence in benthic foraminifera concentration (in Piva *et al.*, 2008).

The obtained age control points for the analysed core section are summarized in Table 1, concur in producing a refined age model (Figure 4).

3. SETTING

The Adriatic Sea is an elongated NW/SE orientated basin, located in the centre of the Mediterranean basin. The bathymetric features allow three subdivisions: a very shal-

low northern section, a central part in which water depth moderately increases, to reach at a depth of 1250 m in the south. Finally, the basin is limited by a sill, the Otranto strait, with a water depth of about 800 m (Ciabatti *et al.*, 1987) (Figure 1).

There are three principal water masses in the Adriatic Sea: the Adriatic Surface Water (0-30 m), the Levantine Intermediate Water (30-130 m) and the Adriatic Deep Water (> 130 m). The general circulation is cyclonic, driven by thermohaline currents, with a flow towards the northwest along the eastern side and a return flow towards the southeast along the western side. Into the three sub-basins the circulation is dominated by local cyclonic gyres, which are seasonally modulated (Orlic *et al.*, 1992; Artegiani *et al.*, 1997). The cold and dense Adriatic Deep Water is produced in the winter by the action of the cold and dry north-easterly Bora wind, which leads to deep water flow to the Mediterranean via the southern Adriatic Basin (Artegiani *et al.*, 1989).

The Adriatic Sea occupies the foreland of the Apennine and Dinaric thrust belts, originated by the collision of the African and the European plates (Geiss, 1987). The main clastic sources of the northern and central Adriatic appear

mbsf	Event	Age (ka B.P.)	Source
23.059	S3	81	Lourens [2004]
24.094	MIS 5.2	91	Martinson et al. [1987]
27.3	S4	101	Lourens [2004]
28	MIS 5.4	111	Martinson et al. [1987]
30.6	S5	124	Lourens [2004]
30.95	T II	130	Lisiecki and Raymo [2005]
32.5	MIS 6.2	135	Martinson et al. [1987]
33.581	MIS 6.4	152.5	Martinson et al. [1987]
35.3	S6	172	Lourens [2004]
37.32	IBE	188	Laj et al. [2006]
37.7	MIS 7.0	189.5	Martinson et al. [1987]
38.4	S7	195	Lourens [2004]
39.5	MIS 7.2	200.5	Martinson et al. [1987]
41.5	S8	216	Lourens [2004]
42.4	MIS 7.4	225	Martinson et al. [1987]
43.2	S9	239	Lourens [2004]

Table 1. Control points concurring in the definition of the age-depth model calculated for PRAD1-2 core (in Piva et al., 2008). S₃- Sapropel 3; MIS-Marine Isotope Stage; TII Termination II; IBE- Iceland Basin Excursion. Figure 2. Relative abundances (percentages) of several coccolithophores and reworked specimens analysed in the borehole PRAD1-2, as well as the isotope curve based on *Globigerina bulloides* and the *N* ratio. A smooth line was applied to the abundance curves. Sapropel layers, isotopic stages and sub-stages are indicated. S₃eq.- Sapropel 3 equivalent; MIS-Marine Isotope Stage.

located along its western side, being the catchment areas of this part of the Adriatic Sea associated to the drainage areas of the eastern Alpine rivers, the Po river catchment, and the eastern Apennine catchments north and south of the Gargano promontory (Cattaneo et al., 2003).

4. RESULTS

4.1 Coccolithophore assemblage description

The coccolithophore assemblage in the studied core is generally well preserved and abundant. ‘Small’ *Gephyrocapsa*, with the long axis < 3.5 mm according to Rio et al. (1990), and *Gephyrocapsa muelleriae* dominate the assemblages. *Gephyrocapsa oceanica* is also present in the studied core, but only during MIS 5/7 and in too low concentrations, while *Gephyrocapsa caribbeanica* is almost absent in the analysed samples. The large and subordinate taxa, by decreasing abundance order are: *Syracosphaera* spp. (dominated by *Syracosphaera pulchra*; with absolute abundances about 1.3x10¹⁰ liths/g in the total of samples), *Coccolithus pelagicus*, *Helicosphaera carteri*, *Rhab-*

dosphaera clavigera, *Florisphaera profunda* (dominated by *Florisphaera profunda* var. *profunda*; rare nanoliths of *Florisphaera profunda* var. *elongata*) *Calciosolenia* spp., *Braarudosphaera bigelowii*, *Calcidiscus leptoporus*, *Umbilicosphaera* spp., *Pontosphaera* spp. and *Umbellosphaera tenuis*. Due to the lower absolute abundances experienced by the last four taxa (< 1.4x10⁹ liths/g in the total of samples), they were not presented graphically. The abundances of *Syracosphaera* spp., *Rhabdosphaera clavigera* and *Calciosolenia* spp. were plotted together due to the similarity between their ecological preferences. ‘Small’ *Gephyrocapsa* and *G. muelleriae* are also presented together because are both indicative of productivity (moderate to high) in the upper photic zone (Bollmann, 1997; Wells and Okada, 1997; Flores et al., 2003; Boeckel et al., 2006). Cretaceous and Tertiary reworked specimens are always present, particularly during MIS 6. A complete list of the autochthonous taxa is given in the Appendix, including the less abundant species not mentioned above.

The results are presented in percentage abundances (Figure 2; the respective data matrix can be consulted in <http://mcprojectos.fc.ul.pt/papers/adriatic/Appendix1.pdf>).

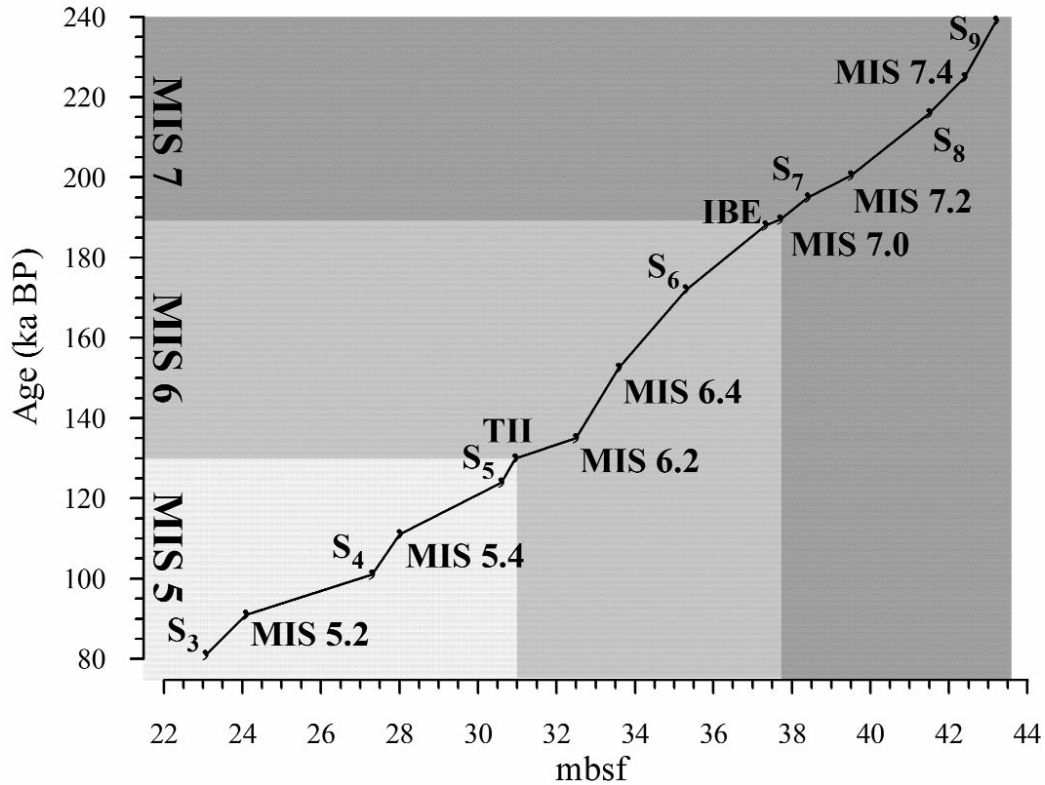


Figure 3. Age-depth model calculated for PRAD1-2 core (based on Piva *et al.*, 2008). Sapropel layers, isotopic stages and sub-stages are indicated. S₃- Sapropel 3; MIS-Marine Isotope Stage; TII- Termination II; IBE- Iceland Basin Excursion.

The analysis based on absolute abundances (liths/g) was applied at first, however, the related curves were indicative of clear dilution, revealing low significance.

The percentage abundance of *Gephyrocapsa* spp. ('small' *Gephyrocapsa* and *Gephyrocapsa muellerae*) exhibits clear decreases during the sapropel layers of MIS 7 (S₉eq.-S₇eq.) and MIS 6 (S₆eq.). However, the lowest abundances of these taxa are registered during the interval situated in the second half of the glacial stage, between the cold events 6.4 and 6.2. During MIS 5 these species decrease within S₅eq. and slightly increase within both S₄eq. and S₃eq. (Figure 2).

The abundance record of *Syracosphaera* spp., *Rhabdosphaera clavigera* and *Calciosolenia* spp. presents a decreasing trend from the base of MIS 7 until the top of MIS 6, recovering during the interglacial MIS 5 with moderate values. The comparison between the curves and the sapropel layers shows general decreases during the two first sapropel layers of MIS 7 (S₉eq. and S₈eq.) and the last two

of MIS 5 (S₄eq. and S₃eq.). During S₇eq., S₆eq. and S₅eq. abundance increases are observed. Peaks of these taxa are also registered at the top or above the MIS 5 sapropel layers (Figure 2).

A very close pattern is observed between *C. pelagicus* and reworked specimens, with abundance increases during the sapropel layers of MIS 7 (S₉eq. – S₇eq.; more pronounced within S₈eq.) and MIS 6 (S₆eq.), and a very slight increase during S₅eq. The highest abundances are observed, however, during the second half of the glacial stage, between the cold events 6.4 and 6.2. A similar pattern is also observed between the last two forms (*C. pelagicus* and reworked specimens) and *Helicosphaera carteri*, which present increases coincident with the sapropel layers of MIS 7 (S₉eq. – S₇eq.; more pronounced within S₇eq.), MIS 6 (S₆eq.), and the highest abundances during the second half of MIS 6, between the cold events 6.4 and 6.2. During MIS 5, the *H. carteri* abundance increases are essentially within the sapropel layers S₅eq. and S₄eq. (Figure 2).

The abundance peaks of *Florisphaera profunda* show clear association with almost all sapropel layers that cross the isotope stages 7 (S₉eq. – S₇eq.), 6 (S₆eq.), and 5 (S₅eq.), being its record particularly important during S₅eq. (Figure 2).

Braarudosphaera bigelowii (Figure 2) record is more significant during MIS 5, with higher abundances mostly indicative of the end of sapropel deposition, and also within the sapropel layer of MIS 6 (S₆eq.).

The *N* ratio presents lower values during several sapropel layers, reflected by higher abundances of *F. profunda* and lower abundances of *Gephyrocapsa* spp. during their deposition.

4.2 The DELTA parameter

The relatively high proportion of reworked forms recommended the use of the statistical parameter DELTA to determine their influence in the abundance pattern of specific taxa, *C. pelagicus* and *H. carteri* in this case. Figure 3 shows that during most of the time interval the DELTA parameter varies close to 0, indicating that the two variables in analysis have similar behaviour, either co-variante or both less represented. However, there are discrete moments where reworked forms are statistically much more significant than the two species: 210-200, 145, 135, 110 and 85 kyr. These moments do not have a direct relation to the sapropel equivalent intervals, except for S₈eq. *C. pelagicus* displays four prominent maxima in the second half of MIS 6, none directly related to sapropel layers. *H. carteri* discloses five preferential moments of development: at the base, just before S₉eq.; during S₇eq.; at the beginning of S₆eq.; at around 150 kyr (MIS 6); and during S₅eq.

5. DISCUSSION

The analysis of the coccolith records for the entire core shows discrepancies between the marine isotope stages 7, 6 and 5. As shown in Figure 2, the overall reduction of *Gephyrocapsa* spp. (*Gephyrocapsa muelleriae* and 'small' *Gephyrocapsa*) across the sapropel layers of MIS 7 and

MIS 6 reproduces the relative abundance pattern of the total autochthonous calcareous nannofossils, since its percentages are always above 60 %. During MIS 5, the record of *Gephyrocapsa* spp. is a little bit different, with an abundance decrease within S₅eq. and slight increases within S₄eq. and S₃eq. The calcareous nannofossil reduction at the beginning of sapropel layers had already been detected by other authors (Negri *et al.*, 1999a, b; Negri and Villa, 2000; Negri and Giunta, 2001; Negri *et al.*, 2003), who also speculated that the general decrease could be a consequence of an increase of the primary siliceous productivity (*r*-strategist species), which in turn would not be preserved in sediment because of the high silica unsaturation of the Mediterranean waters. The slight abundance increases observed during the deposition of S₄eq. and S₃eq., may reflect different depositional conditions that feature the marine isotope stage 5 when compared to the previous stages.

The comparison of *Florisphaera profunda* and *Gephyrocapsa* spp. curves shows opposite trends between these two taxa, although two exceptions can be observed, in S₄eq. and S₃eq. again. *F. profunda* is a lower photic layer inhabitant of tropical and subtropical waters in the present day ocean (Okada and McIntyre, 1977; Molfino and McIntyre, 1990). Considering the ecological preferences of *F. profunda* and *Gephyrocapsa* spp., opposite trends between their records should be expected. If we imagine a mechanism which favours the water column stratification, the consequent deeper position of the nutricline would lead to a productivity drop in the upper photic zone, given by *Gephyrocapsa* spp. decreases, and to a productivity raise in the lower photic zone, given by *F. profunda* increases. *N* ratio, constructed through the relationship between the upper and lower productivity layer species reflects exactly that. The *N* curve shows negative peaks, which reproduce the dominance of *F. profunda*, coincident with the sapropel layers of MIS 7 (although during S₇eq. this is not so evident), MIS 6, and with S₅eq. Other authors had already reported this positive correlation between *F. profunda* abundances and sapropel layers (Negri *et al.*, 1999a; Negri and Giunta, 2001; Principato *et al.*, 2006; Thomson *et al.*, 2004), considering the increase of this taxon also an excellent tool to indicate the Deep Chlorophyll Maximum (Castradori, 1993) and to infer paleonutricline dynamics (Molfino and McIntyre, 1990; Castradori, 1993; Marino *et al.*, 2008).

The variation in the intensity of the cold and dry north-easterly Bora wind, responsible for the production of the Adriatic Deep Water (ADW) during winter (Artegiani *et al.*, 1989), may trigger or not the generation of sapropels. When there is a tendency for normal winter conditions the continuous production of the ADW is expected and the subsequent mixing of the water column, which in turn leads to the oxidation of the organic matter in the deep sea sediments. Under these conditions no sapropels are formed in the Adriatic Sea. However, when there is a tendency for a reduction in the intensity of the Bora wind, the less deep water production leads to the stagnation of deep waters and the subsequent preservation of organic matter and sapropel generation. The gradual decrease of *F. profunda* above S_5 eq. and until the event 5.4 reflects the gradual fresh water input and water column mixing in response to the Bora wind activity. At the beginning of S_4 eq., and also of S_3 eq., a reduction in the Bora wind intensity occurred changing the main paleoceanographic conditions. However, characteristics of these two last sapropels of MIS 5 that are not observed in the others, like the slight abundance increase of *Gephyrocapsa* spp. and the scarce presence of *F. profunda*, may reflect a rise in coccolithophore productivity synchronous with the sapropel deposition due to a shallower nutricline. In this way, during the deposition of these atypical sapropel layers at the present site, the reduction of the winter north-easterly Bora wind has not been so intense, allowing some deep water formation that prevented the total stratification of the water column and bottom stagnation.

The similarity between the records of *C. pelagicus*, *H. carteri* and reworked specimens has already been mentioned. If on the one hand the record of *C. pelagicus* could be useful, providing us information about eutrophication and sea surface temperature, if we are referring to small morphotype (Geisen *et al.*, 2002), or about turbulence and nutrient availability, if we are referring to intermediate morphotype (Cachão and Moita, 2000), on the other hand the similarity between the records of the total *C. pelagicus* and reworked specimens can not guarantee an autochthonous origin for the *C. pelagicus* placoliths. In addition, since reworked specimens recognized in this work range from Cretaceous to Tertiary (Piva *et al.*, 2008) and *C. pelagicus* is known in the geological record since Early Palaeocene (Perch-Nielsen, 1985), there is a strong probability that a significant proportion of their placoliths has

been transported into the Adriatic basin. The high correlation between *C. pelagicus* and reworked specimens is confirmed by a correlation coefficient of 0.94, for the entire data set. DELTA parameter, however, discloses a sequence of short term preferential developments of this species towards the end of MIS 6, with no direct relation to sapropel equivalent time intervals. This possibly could indicate time slices of a productivity increase in the basin at the end of the cold period.

Concerning *H. carteri*, the interpretation of its record must also be carefully done, since the presence of *H. carteri* helicoliths may also result from the Apennine source. In fact, the stratigraphic range of this taxon (Early Miocene-Recent; in Perch-Nielsen, 1985) and the similar abundance pattern with reworked specimens ($r = 0.73$), especially during MIS 7 and 6, corroborates this assumption. However, the information provided by DELTA indicates abundance peaks of autochthonous *H. carteri* just before S_9 eq., during S_7 eq., at the beginning of S_6 eq., during mid MIS 6 and during S_5 eq. *H. carteri* is considered a coastal taxon, indicative of moderately elevated nutrient conditions and turbidity (Giraudeau, 1992; Ziveri *et al.*, 1995; Ziveri *et al.*, 2000; Colmenero-Hidalgo *et al.*, 2004; Malinverno *et al.*, 2009), and proliferates between 40 to 70 m water depth close to the chlorophyll maximum (Cros *et al.*, 2000; Cros, 2002). Other authors suggest that high frequencies of *H. carteri* indicate an increase in productivity and/or a decrease in salinity (Pujos, 1992; Flores *et al.*, 2005; Triantaphyllou *et al.*, 2009c). During S_7 eq. our data suggest two hypotheses for the proliferation of *H. carteri*: a reduction in surface salinity due to enhanced continental runoff and higher nutrient availability in the middle part of the photic zone, since a nutrification in the lower part, inferred by *F. profunda*, and in the upper part of the photic zone, inferred by *Gephyrocapsa* spp., is not so evident.

During the latest part of the glacial stage 6, the coldest and the driest one (Bard *et al.*, 2002), the subsequent sea-level fall (Siddall *et al.*, 2006) with the shortening of the distance between the continental source and the depositional area was responsible for the terrigenous input increase and, consequently, for calcareous nannofossils assemblages strongly composed by reworked specimens. During most of the analysed time interval, reworked coccoliths, including *C. pelagicus* and *H. carteri*, were trans-

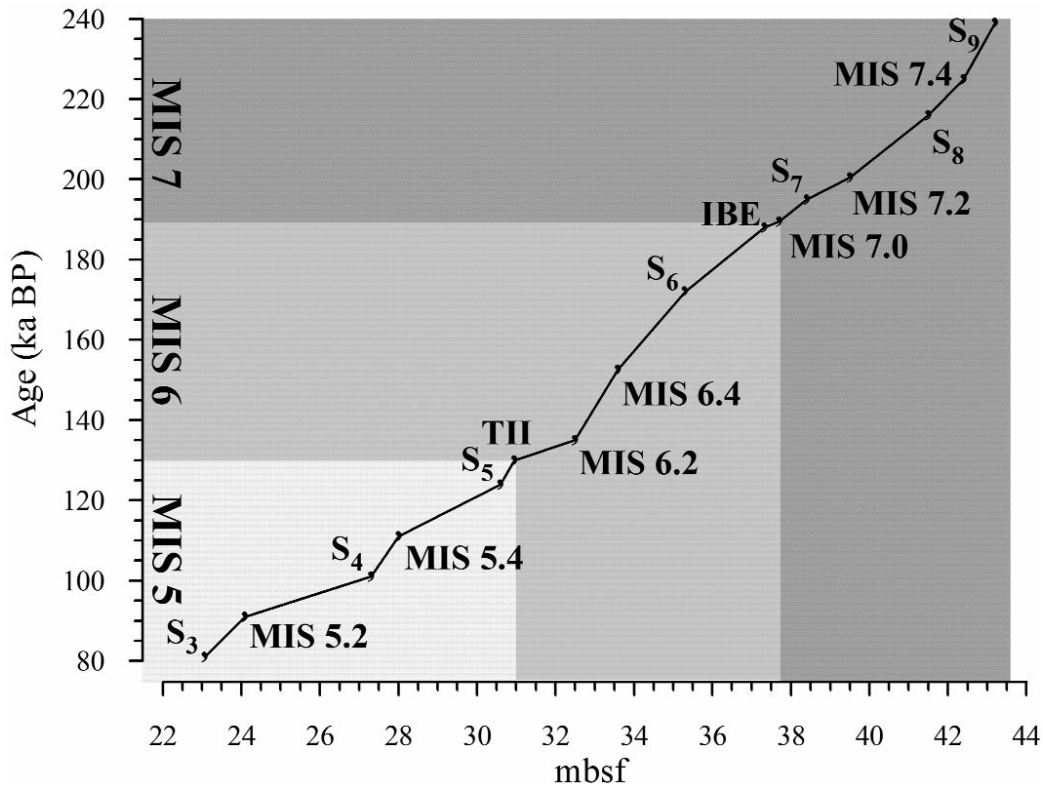


Figure 4. The parameter DELTA or the difference between the standardized abundance of the total non-Quaternary coccoliths and nanoliths, and the standardized abundance of two Tertiary species: *Coccolithus pelagicus* and *Helicosphaera carteri*. The light arrows indicate the most significant predominance of reworked specimens whereas the dark arrows indicate the most significant predominance of autochthonous *C. pelagicus* and *H. carteri*.

ported into the Adriatic Sea by rivers or/and re-distributed from material already deposited by bottom currents, and finally deposited together with autochthonous specimens in the studied site. However, at certain moments (see Figure 3), sediment delivery mainly from the Cretaceous areas led to a strong dominance of coccoliths from other species. These episodes occurred during MIS 7, at the onset of S_8 eq., and also during MIS 6 or MIS 5, although without a relation to sapropels.

Syracosphaera spp. and *Rhabdosphaera clavigera* are upper-middle photic zone taxa preferring warmer and low nutrient environments (McIntyre *et al.*, 1972; Ziveri *et al.*, 2004; Maiorano *et al.*, 2008; Dimiza *et al.*, 2008; Malinverno *et al.*, 2009; among others). The same ecological preferences are assumed for *Calciosolenia* spp., which is plotted together with the last two taxa (Figure 2). Our data show that the record of these forms follows a complex pattern with general decreases during S_9 eq., S_8 eq., S_4 eq. and S_3 eq., and general increases during S_7 eq., S_6 eq. and S_5 eq.

Considering that the onset of sapropel deposition is driven by cold and mixed surface waters, also suggested by Negri *et al.* (2003), this first eutrophic phase would lead to nutrient depleted waters, favouring k-strategist species in a second phase. If on the one hand this fact is reflected in our data by the abundance increases during some sapropel layers, on the other hand another explanation is needed for the abundance decreases registered within the other sapropels. During S_8 eq., for instance, the reduction of oligotrophic species occurs simultaneously with the most important increase of reworked specimens, which in turn may reflect climatic conditions probably more severe than in the other sapropel layers. In this way, the development of the k-strategist species should have been inhibited by the higher turbidity of the surface waters, in response to a more intensive runoff and higher terrigenous input during this time slice. The patterns observed during S_4 eq. and S_3 eq. are consistent with water masses still too productive for the predominant development of k-strategist species. This suggests, as already mentioned, a water

mass stratification not very strong or not well marked during these time slices. A simple correlation between this oligotrophic cluster and the temperature inferred from the isotope record is difficult to establish, although the better development of these taxa is related to interglacial isotope stages.

Concerning *Braarudosphaera bigelowii*, although in low abundance across the entire core, it has some importance during MIS 5, being associated with the end of sapropel deposition and appearing sometimes above these terminations. This fact establishes a relation between this taxon development and low salinity waters in result of increased fluvial runoff, which in turn led to the reestablishment of the general oligotrophic state of the surface water. Although only few studies report the presence of this species in sapropels, our results show moderate abundances of *B. bigelowii* within S₈eq. (MIS 7) and S₆eq. (MIS 6), in which concomitant increases of reworked specimens are also registered. Since the First Occurrence of *B. bigelowii* is dated from Cretaceous (Perch-Nielsen, 1985), we can suggest that the identified specimens could correspond to reworked material from the Apennines, transported by fluvial runoff. However, the subsequent development of hyposaline and nutritive waters may also have promoted the autochthonous development of *B. bigelowii* during these same sapropel layers.

6. CONCLUSIONS

The results based on core PRAD1-2 allowed concluding the existence of fluctuations in the calcareous nannofossils content between the interglacial stages 7 and 5, and also between these and the glacial stage 6, revealing a transition between different paleoceanographic conditions across the analysed interval. The most similar features were observed among S₉eq., S₈eq., S₇eq. and S₆eq., and also between the last two sapropel layers of MIS 5, S₄eq. and S₃eq.

In particular our study is indicative that:

- There is a coccolithophore productivity decrease during the deposition of S₉eq., S₈eq., S₇eq., S₆eq. and S₅eq., given by the abundances of *Gephyrocapsa* spp.

This productivity decrease, which occurs in the upper photic zone, is accompanied by an increase of *F. profunda* (extremely high within S₅eq.) in the lower photic zone, allowing to understand the nutricline dynamics for each moment. S₄eq. and S₃eq. are atypical sapropel layers, in which slight abundance increases of *Gephyrocapsa* spp. and scarce abundances of *F. profunda* are observed;

- The sapropel layers of MIS 7 (S₉eq., S₈eq. and S₇eq.), MIS 6 (S₆eq.) and the first one of MIS 5 (S₅eq.) were formed during winters characterised by a reduction in the north-easterly Bora wind, which in turn limited the production of the Adriatic Deep Water. Thus, the subsequent strong stratification of the water column and the low oxygen content at the bottom, favoured the preservation of the organic matter. During the deposition of the last sapropel layers of MIS 5, S₄eq. and S₃eq., the reduction of the winter north-easterly Bora wind has not been so intense, allowing some ADW production and some subsequent mixing of the water column;
- The increase of reworked specimens abundance is another feature of MIS 7 and MIS 6 sapropel layers, indicating fluvial runoff events with terrigenous input synchronous with the sapropel deposition. However, the most important increases are observed during the latest part of MIS 6, which is associated with a remarkable sea-level fall, probably due to the action of bottom currents in material already deposited;
- The stratigraphic range of *C. pelagicus* and *H. carteri* and the similarity between their records and the record of reworked specimens, could reflect an Apennine source for the most part of *C. pelagicus* and *H. carteri* coccoliths by precipitation and runoff into the Adriatic basin. However, the information provided by DELTA indicates in situ developments of *C. pelagicus* during the second half of MIS 6, and in situ preferential developments of *H. carteri* just before S₉eq., during S₇eq., at the beginning of S₆eq., during mid of MIS 6 and during S₅eq.;
- There is not a clear relation between the cluster *Syracosphaera* spp., *R. clavigera* and *Calciosolenia* spp. and warm and oligotrophic waters. However, the de-

velopment of these taxa at the top or above the termination of some sapropel layers, is consistent with the end of dryer conditions that feature the sapropel deposition, and with the subsequent reestablishment of the general oligotrophic state of the surface water with a nutrient redistribution. At the same time a salinity reduction should occur due to the simultaneous presence of *B. bigelowii*. On the other hand, the presence of *B. bigelowii* within some sapropel layers of MIS 7 and MIS 6, together with its stratigraphic range, may indicate also a continental source for some pentoliths.

7. ACKNOWLEDGEMENTS

The authors wish to thank to the PROMESS 1 crew and EU, EPROMESS (MEC) CGL2006-10593 and GRACCIE (CONSOLIDER-INGENIO CSD 2007-00067), which allowed the recovery of the PRAD1-2 core and provided the analysed samples. This research was supported by a grant of the Foundation for Science and Technology of Portugal. This is ISMAR-Bologna (CNR) contribution n° 1629.

8. REFERENCES

- Arnaboldi, M., and Meyers, P. 2003. Geochemical evidence for paleoclimatic variations during deposition of two Late Pliocene sapropels from the Vrica section, Calabria. *Palaeogeography, Palaeoclimatology, Palaeoecology*, 190, 257-271.
- Artegiani, A., Azzolini, R., and Salusti, E. 1989. On dense water in the Adriatic Sea. *Oceanologica Acta*, 12 (2), 151-160.
- Artegiani, A., Bregant, D., Paschini, E., Pinardi, N., Raicich, F., and Russo, A. 1997. The Adriatic Sea general circulation. Part II: baroclinic circulation structure. *Journal of Physical Oceanography*, 27, 1515-1532.
- Bard, E., Antonioli, F., and Silenzi, S. 2002. Sea-level during the penultimate interglacial period based on a submerged stalagmite from Argentano la Cave (Italy). *Earth and Planetary Science Letters*, 196(3-4), 135-146.
- Bassinot, F., Labeyrie, L., Vincent, E., Quidelleur, X., Shackleton, N., and Lancelot, Y. 1994. The astronomical theory of climate and the age of the Brunhes Matuyama magnetic reversal. *Earth and Planetary Science Letters*, 126, 91-108.
- Boeckel, B., Baumann, K.-H., Henrich, R., and Kinkel, H. 2006. Coccolith distribution patterns in South Atlantic and Southern Ocean surface sediments in relation to environmental gradients. *Deep-Sea Research I*, 53, 1073-1099.
- Bollmann, J. 1997. Morphology and biogeography of the genus *Gephyrocapsa* coccoliths in Holocene sediments. *Marine Micropaleontology*, 29, 319-350.
- Bouloubassi, I., Rullkotter, J., and Meyers, P. 1999. Origin and transformation of organic matter in Pliocene-Pleistocene Mediterranean sapropels: organic geochemical evidence reviewed. *Marine Geology*, 153, 177-197.
- Cachão, M. 1996. *Nanofósseis calcários em Biostratigrafia, Paleoecologia e Paleoceanografia. Exemplos do Neogénico do Algarve (Portugal), do Mar Tirreno (ODP 653), e a problemática de Coccolithus pelagicus*. PhD thesis, University of Lisbon, 356 pp.
- Cachão, M., and Moita, T. 2000. *Coccolithus pelagicus*, a productivity proxy related to (moderate) fronts. *Marine Micropaleontology*, 39, 131-156.
- Capozzi, R., and Picotti, V. 2003. Pliocene sequence stratigraphy, climatic trends and sapropel formation in the Northern Apennines (Italy). *Palaeogeography, Palaeoclimatology, Palaeoecology*, 190, 349-371.
- Castradori, D. 1993. Calcareous nanofossils and the origin of eastern Mediterranean sapropels. *Paleoceanography*, 8, 459-471.
- Cattaneo, A., Correggiari, A., Langone, L., and Trincardi, F. 2003. The late-Holocene Gargano subaqueous delta, Adriatic shelf: sediment pathways and supply fluctuations. *Marine Geology*, 193, 61-91.
- Ciabatti, M., Curzi, P.V., and Lucchi, F. R. 1987. Quaternary sedimentation in the Central Adriatic Sea. *Giornale di Geologia*, 49, 113-125.
- Colmenero-Hidalgo, E., Flores, J.-A., Sierro, F.J., Bárcena, M.A., Lowe-mark, L., Schönfeld, J., and Grimalt, J. 2004. Ocean surface water response to short-term climate changes revealed by coccolithophores from the Gulf of Cadiz (NE Atlantic) and Alboran Sea (W Mediterranean). *Palaeogeography, Palaeoclimatology, Palaeoecology*, 205, 317-336.
- Cros, M.L. 2002. *Planktonic Coccolithophores of the NW Mediterranean*. Publicacions de la Universitat de Barcelona, Barcelona.
- Cros, M.L., Kleijne, A., Zeltner, A., Billard, C., and Young, J. 2000. New examples of holococcolith-heterococcolith combination coccospheres and their implications for coccolithophorid biology. *Marine Micropaleontology*, 39, 1-34.
- De Kaenel, E., and Villa, G. 1996. Oligocene-Miocene calcareous nanofossil biostratigraphy and paleoecology from the Iberia abyssal plain. *Proc. Ocean Drill. Program Sci. Results*, 149, 79-105.
- Dimiza, M., Triantaphyllou, M., and Dermizakis, M. 2008. Seasonality and ecology of living coccolithophores in Eastern Mediterranean coastal environments (Andros Island, Middle Aegean Sea). *Micropaleontology*, 54(2), 159-175.
- Flores, J.-A., and Sierro, F.J. 1997. Revised technique for calculation of calcareous nanofossil accumulation rates. *Micropaleontology*, 43, 321-324.
- Flores, J.-A., Bárcena, M., and Sierro, F.J. 2000. Ocean-surface and wind dynamics in the Atlantic Ocean off Northwest Africa during the last 140 000 years. *Palaeogeography, Palaeoclimatology, Palaeoecology*, 161, 459-478.
- Flores, J.-A., Marino, M., Sierro, F.J., Hodell, D.A., and Charles, C.D. 2003. Calcareous plankton dissolution pattern and coccolithophore

- assemblages during the last 600 kyr at ODP Site 1089 (Cape Basin, South Atlantic): paleoceanographic implications. *Palaeogeography, Palaeoclimatology, Palaeoecology*, 196, 409-426.
- Flores, J.-A., Sierro, F.J., Filippelli, G., Bárcena, M., Pérez-Folgado, M., Vázquez, A., and Utrilla, R. 2005. Surface water dynamics and phytoplankton communities during deposition of cyclic late Messinian sapropel sequences in the western Mediterranean. *Marine Micropaleontology*, 56, 50-79.
- Geisen, M., Billard, C., Broerse, A., Cros, L., Probert, I., and Young, J. 2002. Life-cycle associations involving pairs of holococcolithophorid species: intraspecific variation or cryptic speciation? *European Journal of Phycology*, 37, 531-550.
- Geiss, E. 1987. A new compilation of crustal thickness data for the Mediterranean area. *Annales Geophysicae*, 5B, 623-630.
- Giraudeau, J. 1992. Distribution of Recent nannofossils beneath the Benguela system: southwest African continental margin. *Marine Geology*, 108, 219-237.
- Giunta, S., Negri, A., Morigi, C., and Capotondi, L. 2003. Coccolithophorid ecostratigraphy and multi-proxy paleoceanographic reconstruction in the Southern Adriatic Sea during the last deglacial time (Core AD91-17). *Palaeogeography, Palaeoclimatology, Palaeoecology*, 190, 39-59.
- Gogou, A., Bouloubassi, I., Lykousis, V., Arnaboldi, M., Gaitani, P., and Meyers, P. 2007. Organic geochemical evidence of Late Glacial-Holocene climate instability in the North Aegean Sea. *Palaeogeography, Palaeoclimatology, Palaeoecology*, 256, 1-20.
- Hilgen, F.J. 1991. Astronomical calibration of Gauss to Matuyama sapropels in the Mediterranean and implication for the Geomagnetic Polarity Time Scale. *Earth and Planetary Science Letters*, 104, 226-244.
- Hilgen, F.J., Krijgsman, W., Langereis, C.G., and Lourens, L.J. 1997. Breakthrough made in dating of the geological record. *EOS, Transactions, American Geophysical Union*, 78, 286-289.
- Kroon, D., Alexander, I., Little, M., Lourens, L.J., Matthewson, A., Robertson, A., and Sakamoto, T. 1998. Oxygen isotope and sapropel stratigraphy in the Eastern Mediterranean during the last 3.2 million years. *Proc. ODP Sci. Res.*, 160, 181-189.
- Lisiecki, L., and Raymo, M. 2005. A Pliocene-Pleistocene stack of 57 globally distributed benthic $d^{18}O$ records. *Paleoceanography*, 20, PA1003.
- Lourens, L. 2004. Revised tuning of Ocean Drilling Program Site 964 and KC01B (Mediterranean) and implications for the $d^{18}O$, tephra, calcareous nannofossil, and geomagnetic reversal chronologies of the past 1.1 Myr. *Paleoceanography*, 19, PA3010.
- Lourens, L., Antonarakou, A., Hilgen, F.J., Van Hoof, A.A.M., Vergnaud Grazzini, C., and Zachariasse, W.J. 1996. Evaluation of the Plio-Pleistocene astronomical timescale. *Paleoceanography*, 11, 391-413.
- Maiorano, P., Aiello, G., Barra, D., Di Leo, P., Joannin, S., Lirer, F., Marino, M., Pappalardo, A., Capotondi, L., Ciaranfi, N., and Stefanelli, S. 2008. Paleoenvironmental changes during sapropel 19 (i-cycle 90) deposition: Evidences from geochemical, mineralogical and micropaleontological proxies in the mid-Pleistocene Montalbano Jonico land section (southern Italy). *Palaeogeography, Palaeoclimatology, Palaeoecology*, 257, 308-334.
- Malinverno, E., Triantaphyllou, M., Stavrakakis, S., Ziveri, P., and Lykousis, V. 2009. Seasonal and spatial variability of coccolithophore export production at the South-Western margin of Crete (Eastern Mediterranean). *Marine Micropaleontology*, 71, 131-147.
- Marino, M., Maiorano, P., and Lirer, F. 2008. Changes in calcareous nannofossil assemblages during the Mid-Pleistocene Revolution. *Marine Micropaleontology*, 69, 70-90.
- Marino, G., Rohling, E., Rijpstra, W., Sangiorgi, F., Schouten, S., and Damsté, J. 2007. Aegean Sea as driver of hydrographic and ecological changes in the eastern Mediterranean. *Geology*, 35, 675-678.
- Martinson, D., Pisias, N., Hays, J., Imbrie, J., Moore, T., and Shackleton, N. 1987. Age dating and the orbital theory of the ice ages: development of a high-resolution 0 to 300,000-year chronostratigraphy. *Quaternary Research*, 27, 1-29.
- McIntyre, A., Ruddiman, W.F., and Jantzen, R. 1972. Southward penetrations of the North Atlantic Polar Front: faunal and floral evidence of large-scale surface water mass movements over the last 225,000 years. *Deep-Sea Research*, 19, 61-77.
- Molfino, B., and McIntyre, A. 1990. Precessional forcing of nutricline dynamics in the Equatorial Atlantic. *Science*, 249, 766-769.
- Müller, C. 1985. Late Miocene to recent Mediterranean biostratigraphy and paleoenvironments based on calcareous nannoplankton. In: Stanley, J., Wezel, F.C. (Eds.), *Geological Evolution of the Mediterranean Basin*. Springer-Verlag, New York, 471-485.
- Negri, A., and Giunta, S. 2001. Calcareous nannofossil paleoecology in the sapropel S1 of the eastern Ionian sea: paleoceanography implications. *Palaeogeography, Palaeoclimatology, Palaeoecology*, 169, 101-112.
- Negri, A., and Villa, G. 2000. Calcareous nannofossil biostratigraphy, biochronology and paleoecology at the Tortonian/Messinian boundary of the Faneromeni section (Crete). *Palaeogeography, Palaeoclimatology, Palaeoecology*, 156, 195-209.
- Negri, A., Capotondi, L., and Keller, J. 1999a. Calcareous nannofossils and planktic foraminifera distribution patterns in Late Quaternary-Holocene sapropel of the Ionian Sea. *Marine Geology*, 157, 89-103.
- Negri, A., Morigi, C., and Giunta, S. 2003. Are productivity and stratification important to sapropel deposition? Microfossil evidence from late Pliocene insolation cycle 180 at Vrica, Calabria. *Palaeogeography, Palaeoclimatology, Palaeoecology*, 190, 243-255.
- Negri, A., Giunta, S., Hilgen, F., Krijgsman, W., and Vai, G.B. 1999b. Calcareous nannofossil biostratigraphy of the M. del Casino section (northern Apennines, Italy) and paleoceanographic conditions at times of Late Miocene sapropel formation. *Marine Micropaleontology*, 36, 13-30.
- Okada, H., and McIntyre, A. 1977. Modern coccolithophores of the Pacific and North Atlantic Oceans. *Micropaleontology*, 23(1), 1-55.
- Orlic, M., Gacic, M., and La Violette, P.E. 1992. The currents and circulation of the Adriatic Sea. *Oceanologica Acta*, 15, 109-122.
- Perch-Nielsen, K. 1985. Mesozoic calcareous nannofossils & Cenozoic calcareous nannofossils chapters. In: Bolli, H. M., Saunders, J. B., Perch-Nielsen, K. (Eds.), *Plankton Stratigraphy*. Cambridge University Press, Cambridge, 329-554.

- Piva, A., Asioli, A., Schneider, R., Trincardi, F., Andersen, N., Colmenero-Hidalgo, E., Dennielou, B., Flores, J.-A., and Vigliotti, L. 2008. Climatic cycles as expressed in sediments of the PROMESS1 borehole PRAD1-2, central Adriatic, for the last 370ka: 1. Integrated stratigraphy. *Geochem. Geophys. Geosyst.*, 9, 1-21.
- Principato, M., Crudeli, D., Ziveri, P., Slomp, C., Corselli, C., Erba, E., and de Lange, G. 2006. Phyto- and zooplankton paleofluxes during the deposition of sapropel S1 (eastern Mediterranean): Biogenic carbonate preservation and paleoecological implications. *Palaeogeography, Palaeoclimatology, Palaeoecology*, 235, 8-27.
- Pujos, A. 1992. Calcareous nannofossils of Plio-Pleistocene sediments from the Northwestern margin of tropical Africa. In: Summerhayes, C.P., Prell, W.L., Emeis, K.C. (Eds.), *Upwelling Systems: Evolution since the Early Miocene*. Geological Society of London Special Publications, 64, 343-356.
- Rio, D., Sprovieri, R., and Channell, J. 1990. Pliocene-early Pleistocene chronostratigraphy and the Tyrrhenian deep-sea record from site 653. *Proc. ODP, Sci. Results*, 107, 705-714.
- Rio, D., Channell, J., Bertoldi, R., Poli, M., Vergerio, P., Raffi, I., Sprovieri, R., and Thunell, R. 1997. Pliocene sapropels in the northern Adriatic area: chronology and paleoenvironmental significance. *Palaeogeography, Palaeoclimatology, Palaeoecology*, 135, 1-25.
- Rohling, E., Jorissen, F., and de Stigter, H. 1997. 200 year interruption of Holocene sapropel formation in the Adriatic Sea. *Journal of Micropaleontology*, 16, 97-108.
- Siddall, M., Bard, E., Rohling, E., and Hemleben, C. 2006. Sea-level reversal during Termination II. *Geology*, 34, 817-820.
- Sierro, F.J., Flores, J.-A., Zamarreño, I., Vázquez, A., Utrilla, R., Francés, G., Hilgen, F.J., and Krijgsman, W. 1999. Messinian pre-evaporite sapropels and precession-induced oscillations in the Western Mediterranean climate. *Marine Geology*, 153, 137-146.
- Thomson, J., Crudeli, D., de Lange, G.J., Slomp, C.P., Erba, E., Corselli, C., and Calvert, S.E. 2004. Florisphaera profunda and the origin and diagenesis of carbonate phases in eastern Mediterranean sapropel units. *Palaeogeography, Palaeoclimatology, Palaeoecology*, 19, 1-19.
- Triantaphyllou, M., Antonarakou, A., Dimiza, M., and Anagnostou, C. 2009a. Calcareous nannofossil and planktonic foraminiferal distributional patterns during deposition of sapropels S6, S5 and S1 in the Libyan Sea (Eastern Mediterranean). *Geo-Marine Letters*, 30, 1-13.
- Triantaphyllou, M., Antonarakou, A., Kouli, K., Dimiza, M., Kontakiotis, G., Papanikolaou, M., Ziveri, P., Mortyn, P., Lianou, V., Lykousis, V., and Dermitzakis, M. 2009b. Late Glacial-Holocene ecostratigraphy of the south-eastern Aegean Sea, based on plankton and pollen assemblages. *Geo-Marine Letters*, 29, 249-267.
- Triantaphyllou, M., Ziveri, P., Gogou, A., Marino, G., Lykousis, V., Bou-loubassi, I., Emeis, K.-C., Kouli, K., Dimiza, M., Rosell-Melé, A., Papanikolaou, M., Katsouras, G., and Nunez, N. 2009c. Late Glacial-Holocene climate variability at the south-eastern margin of the Aegean Sea. *Marine Geology*, 266, 182-197.
- Wells, P., and Okada, H. 1997. Response of nannoplankton to major changes in sea-surface temperature and movements of hydrological fronts over Site DSDP 594 (south Chatham Rise, southeast New Zealand), during the last 130 kyrs. *Marine Micropaleontology*, 32, 341-363.
- Ziveri, P., Thunell, R.C., and Rio, D. 1995. Export production of coccolithophores in an upwelling region: results from San Pedro Basin, Southern California Borderlands. *Marine Micropaleontology*, 24, 335-358.
- Ziveri, P., Rutten, A., de Lange, G.J., Thomson, J., and Corselli, C. 2000. Present-day coccolith fluxes recorded in the central eastern Mediterranean sediment traps and surface sediments. *Palaeogeography, Palaeoclimatology, Palaeoecology*, 158, 175-195.
- Ziveri, P., Baumann, K.-H., Boeckel, B., Bollmann, J., and Young, J. 2004. Biogeography of selected Holocene coccoliths in the Atlantic Ocean. In: Thierstein, H.R., Young, J.R. (Eds.), *Coccolithophores from Molecular Processes to Global Impact*. Springer, Berlin, 403-428.

MANUSCRITO RECIBIDO: 20 de marzo, 2010

MANUSCRITO ACEPTADO: 27 de noviembre, 2010

Taxonomic appendix

- Braarudosphaera bigelowii* (Gran and Braarud, 1935) De-
flandre, 1947
Calcidiscus leptoporus (Murray and Blackman, 1898) Loe-
blich and Tappan, 1978
Calciosolenia murrayi Gran, 1912
Ceratolithus telesmus Norris, 1965
Coccolithus pelagicus (Wallich, 1877) Schiller, 1930
Coccolithus pelagicus braarudii (Gaarder 1962a) Geisen
et al. (2002)
Coccolithus pelagicus pelagicus (Wallich, 1877) Schiller,
1930
Florisphaera profunda var. *elongata* Okada and McIntyre,
1980
Florisphaera profunda var. *profunda* Okada and Honjo,
1973
Gephyrocapsa caribbeanica Boudreaux and Hay, 1967
Gephyrocapsa muelleri Bréhéret, 1978
Gephyrocapsa oceanica Kamptner, 1943
Gephyrocapsa ericsonii McIntyre and Bé, 1967
Gephyrocapsa aperta Kamptner, 1963
Helicosphaera carteri (Wallich, 1877) Kamptner, 1954
Helicosphaera carteri var. *carteri* (Wallich, 1877) Kampt-
ner, 1954
Helicosphaera carteri var. *hyalina* (Gaarder, 1970) Jordan
and Young, 1990
Helicosphaera carteri var. *wallichii* (Lohmann, 1902)
Theodoridis, 1984
Pontosphaera discopora Schiller, 1925
Pontosphaera multipora (Kamptner, 1948) Roth, 1970
emend. Burns, 1973
Rhabdosphaera clavigera Murray and Blackman, 1898
Syracosphaera pulchra Lohmann, 1902
Umbellosphaera tenuis (Kamptner, 1937) Paasche, in
Markali and Paasche, 1955
Umbilicosphaera sibogae (Weber-van Bosse, 1901)
Gaarder, 1970
Umbilicosphaera hulburtiana Gaarder, 1970

Coccolithophore biogeography in the Mediterranean Iberian margin

M. Carmen Álvarez^{1*}, F. Ornella Amore², Lluïsa Cros³, Belén Alonso³ and Javier Alcántara-Carrió¹

¹Instituto de Investigación en Medio Ambiente y Ciencia Marina, Universidad Católica de Valencia, Guillem de Castro 94, 46003 Valencia, Spain. carmen.alvagar@gmail.com, javier.alcantara@ucv.es

²Dipartimento di Studi Geologici e Ambientali, Università degli Studi del Sannio, Via Dei Mulini 59/A, 82100 Benevento, Italy. f.amore@unisannio.it

³Instituto de Ciencias del Mar (CSIC), Passeig Marítim de la Barceloneta, 37-49, 08003 Barcelona, Spain. lluisa@icm.csic.es, belen@icm.csic.es

*Present address: Centro Universitario de Investigaciones Oceanológicas, Universidad de Colima, Carretera Manzanillo-Barra de Navidad km 19.5, Colonia El Naranjo, C.P 28860, Manzanillo, Colima, Mexico.

Resumen

En este trabajo se estudió la distribución de cocolitos en muestras de sedimentos superficiales del margen ibérico mediterráneo. Se calculó la abundancia total y se representó en un mapa de distribución. La mayor abundancia de cocolitos se registró en tres muestras situadas en los alrededores de las islas Baleares y se relacionó con los aportes de las aguas atlánticas modificadas más modernas (Modified Atlantic Water, MAW). La menor abundancia total se registró cerca de la costa, en el área de acción de la corriente del Norte (NC) y del frente Catalán y se ha relacionado principalmente con los aportes terrígenos del río Ebro. Las abundancias relativas muestran que los pequeños placolitos (*Emiliana huxleyi*, *Gephyrocapsa aperta* y *Gephyrocapsa ericsonii*) son las formas dominantes de la asociación de cocolitos en el Mediterráneo occidental, disminuyendo su abundancia con la distancia a la costa y relacionándolas con concentraciones de nutrientes. La distribución de *Gephyrocapsa oceanica* y *Gephyrocapsa muelleræ* parece estar relacionada con la MAW de las proximidades del estrecho de Gibraltar y con alguno de los remolinos costeros generados por la corriente de Argelia (AC), respectivamente. *Syracosphaera* spp. y *Helicosphaera* spp. también alcanzan una abundancia significativa mostrando una distribución concéntrica en el mar Catalano-Balear. La distribución de *Florisphaera profunda*, que mostró algunos valores más altos al sur del delta del Ebro, también puede ser de interés biogeográfico.

Palabras clave: Cocolitóforos, sedimentos superficiales, biogeografía, Mediterráneo occidental, margen ibérico mediterráneo.

Abstract

The distribution of coccoliths in surface sediments from the Mediterranean Iberian Margin is shown in the present study. Total abundance was recorded and represented in a distribution map. Higher abundance was recorded in three samples located in the surroundings of the Balearic Islands related to the contribution of the recent Modified Atlantic Waters (MAW). The lowest total abundance was recorded close to the Iberian shoreline under the influence of the Northern Current (NC) and the Catalan Front and mainly related to the terrigenous runoff of the Ebro River. Relative abundance reveals that the small placoliths (*Emiliana huxleyi*, *Gephyrocapsa aperta* and *Gephyrocapsa ericsonii*) are the dominant group in the Western Mediterranean; decreasing in percentage with distance from the coast and related to nutrient concentrations. *Gephyrocapsa oceanica* and *Gephyrocapsa muelleræ* distributions seem to be related to the recent MAW close to the Strait of Gibraltar and to some of the coastal eddies generated from the Algerian Current (AC), respectively. *Syracosphaera* spp. and *Helicosphaera* spp. also reach significant abundances, having a concentric distribution in the Catalano-Balearic Sea. The distribution of *Florisphaera profunda*, which has higher values to the south of the Ebro Delta, may also be of biogeographic interest.

Key words: Coccolithophore, core-tops, biogeography, Western Mediterranean, Mediterranean Iberian Margin.

1. INTRODUCTION

Biogeographic studies are essential for the understanding of the nature of each species with regard to the ecosystem or environment, but can also be useful in other aspects of science such as: in the provision of the information necessary for sustainable use and conservation of species, for example in agriculture and fisheries; in environmental assessment by helping to ensure minimum impact on the natural environment; in making possible a comparison between taxa and other features (physical, chemical or biological) to establish dependence/influence relationships; in quantitative palaeoceanography to calculate palaeotemperatures and palaeosalinities (Spellerberg & Sawyer, 1999, Boeckel *et al.*, 2006; Saavedra-Pellitero *et al.*, 2010; Saavedra-Pellitero *et al.*, in press).

Coccolithophores are planktic, single-celled golden-brown algae which produce coccoliths, biomineralised calcified plates (Geisen *et al.*, 2002; de Vargas *et al.*, 2007). Coccolithophores are important components of the phytoplankton in Western Mediterranean waters (Margalef, 1969; Estrada, 1980; Arin *et al.*, 2002) and coccoliths are abundant and well preserved in the surface sediments of the Western Mediterranean (Knappertsbusch, 1993). The distribution of coccoliths in surface sediments reflects the environmental parameters of the overlying water masses and may be successfully used to improve palaeoclimatic reconstructions (Findlay & Giraudeau, 2002; Andrúleit *et al.*, 2004), to locate the different surface water masses (Eide, 1990), as well as to assess ecological and preservational factors and highlight their role as carbonate producers (Boeckel & Baumann, 2004).

Several biogeographic studies of coccoliths have been carried out in different parts of the Mediterranean Sea on live assemblages, in surface sediments and ancient sediments (Bartolini, 1970; Violanti *et al.*, 1987; Rio, 1982; Rio *et al.*, 1990; Kleijne, 1991; Knappertsbusch, 1993; Roth, 1994; Winter *et al.*, 1994; Cros, 1995; Ziveri *et al.*, 2000; Cros, 2001). This work presents the biogeographic study of coccoliths in a belt of surface samples selected from along the Mediterranean Iberian Margin from the south of the Gulf of Lyon to the Strait of Gibraltar. This study has been undertaken in order to define the differences between the Iberian and Balearic Margin coccolithophore assemblages and their possible relation to water masses in terms of abundance and distribution.

2. OCEANOGRAPHIC SETTING

Semi-enclosed seas, such as the Mediterranean, improve the signal recorded in the sedimentary record making palaeoclimatic events more evident (von Grafenstein *et al.*, 1999; Pérez-Folgado *et al.*, 2003). The Western Mediterranean is a boundary between this marginal sea and the Atlantic Ocean. The study of sediments in the Western Mediterranean provides information about the features in both areas and the connection between them.

In the Western Mediterranean, more specifically in the Mediterranean Iberian Margin, it is possible to distinguish two main sub-basins (Fig. 1): the Catalano-Balearic Sea, located to the north between the Iberian Peninsula and the Balearic Islands; and the Alboran Sea, located to the south between the Iberian Peninsula and Africa.

2.1 The Catalano-Balearic Sea

Surface circulation in the Catalano-Balearic Sea is mainly characterised by the Northern Current (NC) flowing to the south along the continental slope (Fig. 1). The water mass associated with the NC is the old Modified Atlantic Water (MAW) which arrives in the Catalano-Balearic Sea after traversing the Western Mediterranean. A branch of the NC is diverted when it reaches the proximity of the Alboran Sea because it comes into contact with the recent MAW (36.5) merging into its path towards the Western Mediterranean. The recent MAW also arrives in the Catalano-Balearic Sea carried by the Algerian Current (AC) from the south and entering through the Balearic channels (La Violette *et al.*, 1990; Salat, 1996; Millot, 1999). The AC runs along the northern coast of Africa between 0° and 2°E, and then meanders, generating coastal eddies and upwellings (López-García *et al.*, 1994; Benzohra & Millot, 1995; Millot, 1999; Pascual *et al.*, 2002).

Globally considered, the Mediterranean Sea has low productivity. Nevertheless two geostrophic fronts, related to the continental slope and originated by the density difference between different water masses, develop very important mixing processes, favouring primary productivity (Estrada, 1996) and an increase of suspended organic matter (Calafat *et al.*, 1996) in the Catalano-Balearic Sea. One of these is the Catalan Front, extending from the Gulf of

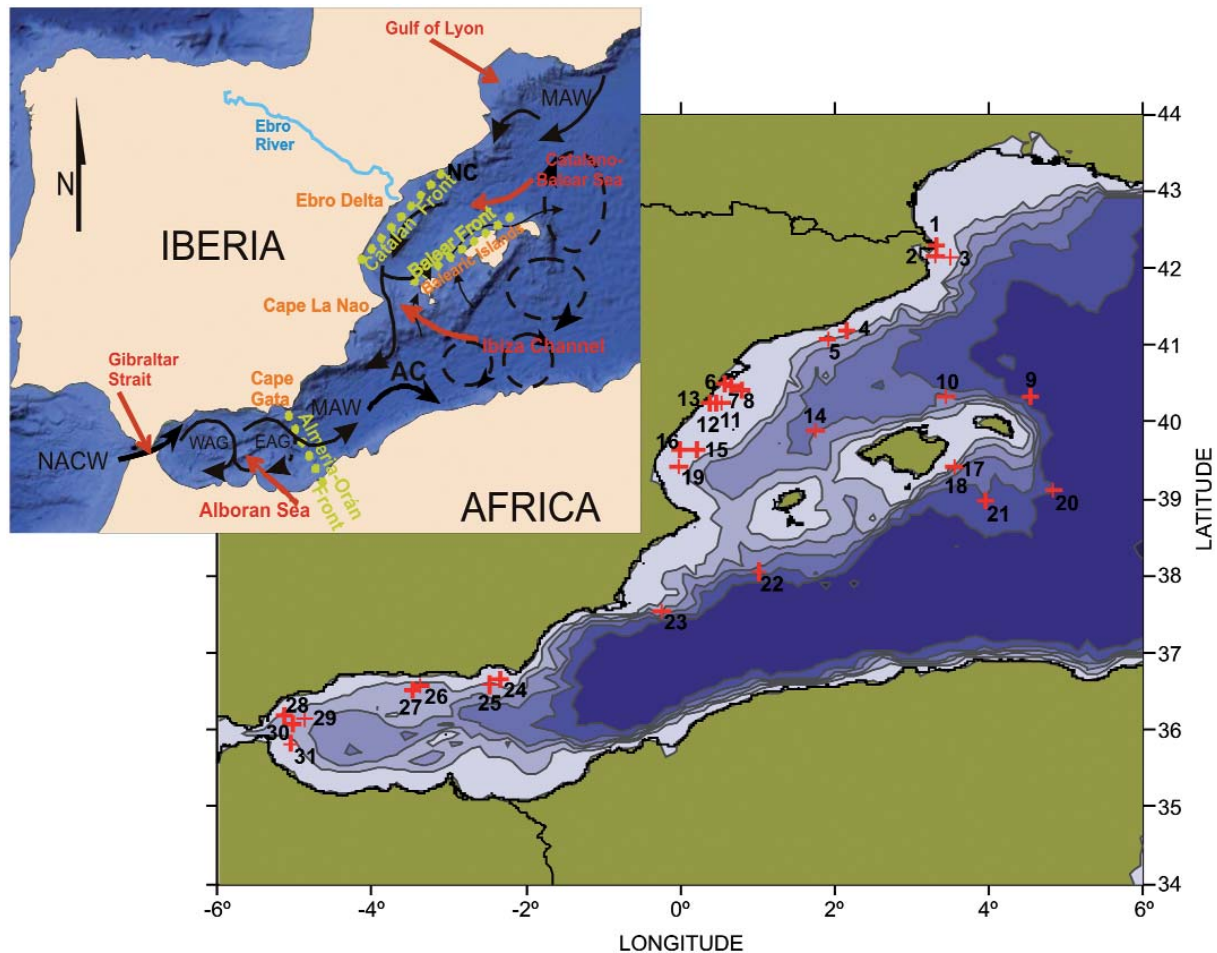


Figure 1. Study area map showing main oceanographic features and core-top locations (+). NC: Northern Current, AC: Algerian Current, NACW: North Atlantic Central Water, MAW: Modified Atlantic Water, WAG: Western Alboran Gyre, EAG: Eastern Alboran Gyre.

Lyon to the Ebro Delta, which acts as border between the shelf waters of lower salinity (<37.5) and the open sea waters of higher salinity (>38.0) (Font *et al.*, 1988). The other is the Balearic Front which separates colder Mediterranean waters from warmer waters of recent MAW (Font *et al.*, 1988; Pinot *et al.*, 1994). Moreover, a high contribution of nutrients in the zone is developed between the two fronts (Estrada & Margalef, 1988); this intermediate zone consists of the permanent presence of dense waters arising from a divergent structure (Font *et al.*, 1988).

2.2 Alboran Sea

The most characteristic surface feature of the Alboran Sea is the recent MAW, a modification of the North Atlantic Central Water (NACW) (Fig. 1). Recent MAW enters the

Mediterranean Sea through the Strait of Gibraltar and is progressively modified along its flow trajectory by mixing with intermediate waters (López-García *et al.*, 1994; Benzohra & Millot, 1995; Millot, 1999). Recent MAW describes two anticyclonic gyres flowing eastwards: the Western Alboran Gyre (WAG) and the Eastern Alboran Gyre (EAG) (Millot *et al.*, 1997; Millot, 1999; Vargas-Yáñez *et al.*, 2002).

The Alboran Sea has two high productivity surface zones developed from the mixing of two different water masses, the NACW and the MAW. The westernmost productivity zone is called the Alboran Front (Cheney, 1978) and shows high biological activity (Bárcena & Abrantes, 1998) related to an upwelling developed close to the northern border of the WAG. The origin of the Alboran Front seems to be related to the instability developed between the Atlantic Water, the Intermediate Water and the deep sea topogra-

phy contact (Perkins *et al.*, 1990). The other productivity zone is the Almeria-Oran Front (AOF) defined by the connection between the Mediterranean Water and the Atlantic Water close to Cabo de Gata (Tintoré *et al.*, 1988) and which is controlled by the size and position of the EAG.

3. MATERIALS AND METHODS

Thirty-one core-tops taken from along the Mediterranean Iberian Margin and surrounding the Balearic Islands were studied (Fig. 1). Information on geographic location as well as a description of the sedimentary material are reported

in Table I. Gravity cores were recovered in different oceanographic cruises between 1973 and 1996 by personnel from the Institute of Marine Sciences (CSIC). The sedimentary rate was diverse (Medialdea *et al.*, 1986; Alonso & Maldonado, 1992; Ercilla *et al.*, 1995; Bozzano *et al.*, 2009) among the different samples, reflecting the sedimentary environment. However, taking into account the age model of the different cores in the study area (Flores *et al.*, 1997; Cacho *et al.*, 1999; Colmenero *et al.*, 2004; Sierro *et al.*, 2005; Bozzano *et al.*, 2009), the sediments of surface samples are Holocene from conditions comparable to those of the present. The core-tops studied are considered as representative of current sediment deposition.

SAMPLE NUMBER	SAMPLE CODE	LATITUDE (°)	LONGITUDE (°)	WATER DEPTH (m)	SEDIMENT DESCRIPTION
1	GC-88-1, TR-70 (A)	42.2973	3.3184	72	SANDY-MUD WITH <i>Turritella</i>
2	TG6TR-12/GC-88-1	42.1546	3.3078	100	MUD
3	TG-15 (sec 1d2) (A)/GC-88-1	42.1369	3.4993	196	MUD
4	K-104/CL-83-1 (sec 1d3) (A)	41.1847	2.1514	265	BROWN MUD
5	TC-35 (A)/GC-93-1	41.0731	1.9154	567	GREY HOMOGENEOUS MUD
6	TG-1 (A)/GC-92-1	40.4906	0.5664	17.9	MUD WITH MONOSULPHIDES
7	TG-6 (A)/GC-92-1	40.4583	0.6617	36	MUD WITH MONOSULPHIDES
8	K-30 (sec 1) (A)/79KEB	40.4100	0.7933	66	COMPACT YELLOW MUD
9	K-37 (sec 1) (A)/CO-80-4	40.3339	4.5413	2400	HEMIPELAGIC MUD
10	K-39 (sec 1) (A)/CO-80-4	40.3306	3.4423	1210	GREY MUD
11	TK-61/80-CL (sec unica) (A)	40.2519	0.5333	60	BEIGE SILTY-MUD
12	TK-60/80-CL (sec 1) (A)	40.2506	0.4689	48	BEIGE SILTY-MUD
13	TK-59 (sec 1) (A)/80-CL	40.2503	0.3844	31	BEIGE SILTY-MUD
14	KF-4/VALSIS (1-2)	39.8786	1.7538	1510	MUD
15	TK-30/80-CL (A)	39.6333	0.2172	140	GREY CLAY
16	TK-33/80-CL (sec 1) (A)	39.6333	-0.0011	73	BEIGE MUD
17	35411 (pilot)/E-3D-78	39.4200	3.5533	730	HEMIPELAGIC MUD
18	35411 (sec 1)/E-3D-78	39.4200	3.5533	730	HEMIPELAGIC MUD
19	K-2/CO-80-3 (A)	39.4167	-0.0200	105	OLIVE GREEN CLAY
20	K-33 (sec 1) (A)/CO-80-4	39.1150	4.8350	2350	HEMIPELAGIC MUD
21	K-30 (sec 1) (A)/CO-80-4	38.9700	3.9487	1920	MUD WITH FORAMS
22	K-10 (sec 1) (A)/CO-80-4	38.0500	1.0150	1957	HEMIPELAGIC MUD
23	K-4 (sec 1) (A)/CO-80-4	37.5403	-0.2431	1260	GREY CLAY WITH FORAMS
24	ALM22 (sec 1d2) (A)/MAYC-96	36.6640	-2.3328	467	GREY MUD
25	ALM19 (sec 1d2) (A)/MAYC-96	36.5898	-2.4805	500	GREY SANDY MUD
26	MTL18 (sec 1d2) (A)/MAYC-96	36.5818	-3.3763	743	MUD WITH LAYERS OF SILT
27	MTL2 (sec 1d1) (A+RX)/MAYC-96	36.5260	-3.4740	753	MUD WITH MILLIMETRIC LEVELS OF SANDS OR COARSE SILTS
28	GDR4 (sec 1d2)/MAYC-96	36.1822	-5.1418	621	GREY MUD
29	TG-16 (sec 1d2) (A) /GC-90-1	36.1461	-4.8736	889	MUD
30	TG-13/STR-93 (sec 1d2)	36.0678	-5.0169	857	MUD
31	TG-8 (sec 1d2)/STR-93	35.8181	-5.0522	408	GREY AND BEIGE MUD

Table I. Core-top information. Sample numbers correspond to the number assigned in the map in figure 1. Sample identification code, location and textural description are as appear in the repository of the Institute of Marine Sciences (CSIC, Barcelona). For detailed information see: <http://www.icm.csic.es/gma/en/content/marine-sample-repository>.

3.1 Sampling and sample preparation

The samples were made by taking approximately the first cubic centimetre of sediment from each gravity core, at the Institute of Marine Sciences (CSIC, Barcelona).

Slides were prepared at the Catholic University of Valencia following the technique of Flores & Sierro (1997). This technique allows the homogeneous distribution of coccoliths on the slide in order to calculate subsequent coccolith total abundances.

3.2 Coccolith preservation

Coccolith preservation in the studied samples can be considered as good-to-moderate according to the preservation ranking of Roth & Thierstein (1972) and Flores & Marino (2002). The presence of delicate forms, such as small placoliths, and the rim of the shield in large taxa, confirm the good preservation of coccoliths.

3.3 Counting and data plotting

Observations were made at the University of Sannio using a Nikon cross-polarising light microscope (1000x) and counting around 500 coccoliths per slide (Fatela & Taborada, 2003). In addition software (*LUCIA* Measurement Version 4.61), adapted to calcareous nannoplankton research, was used in the routine counting. *LUCIA* was very useful in enabling the discrimination of different species by the application of biometric criteria.

Data were plotted as contour maps using the software “Golden Software Surfer 8” and the “kriging gridding” method of interpolation (Matheron, 1960; Wackernagel, 1995).

4. RESULTS

The total abundances (Fig. 2) and relative abundances of different coccolithophore taxa (Fig. 3) have been calculated for each sample studied.

SAMPLE NUMBER	SAMPLE CODE	TOTAL abundance (coccoliths/g)
1	GC-88-1, TR-70 (A)	1.54E+09
2	TGóTR-12/GC-88-1	5.89E+08
3	TG-15 (sec 1d2) (A)/GC-88-1	5.85E+08
4	K-104/CL-83-1 (sec 1d3) (A)	1.07E+09
5	TC-35 (A)/GC-93-1	2.01E+09
6	TG-1 (A)/GC-92-1	1.08E+08
7	TG-6 (A)/GC-92-1	2.83E+08
8	K-30 (sec 1) (A)/79KEB	8.74E+08
9	K-37 (sec 1) (A)/CO-80-4	8.62E+09
10	K-39 (sec 1) (A)/CO-80-4	7.47E+09
11	TK-61/80-CL (sec unica) (A)	8.81E+08
12	TK-60/80-CL (sec 1) (A)	4.78E+08
13	TK-59 (sec 1) (A)/80-CL	2.43E+08
14	KF-4/VALSIS (1-2)	6.45E+08
15	TK-30/80-CL (A)	3.57E+08
16	TK-33/80-CL (sec 1) (A)	7.62E+08
17	35411 (pilot)/E-3D-78	4.95E+09
18	35411 (sec 1)/E-3D-78	4.88E+09
19	K-2/CO-80-3 (A)	1.71E+09
20	K-33 (sec 1) (A)/CO-80-4	4.03E+09
21	K-30 (sec 1) (A)/CO-80-4	1.33E+09
22	K-10 (sec 1) (A)/CO-80-4	1.01E+10
23	K-4 (sec 1) (A)/CO-80-4	4.82E+09
24	ALM22 (sec 1d2) (A)/MAYC-96	2.17E+09
25	ALM19 (sec 1d2) (A)/MAYC-96	3.14E+09
26	MTL18 (sec 1d2) (A)/MAYC-96	2.79E+09
27	MTL2 (sec 1d1) (A+RX)/MAYC-96	1.06E+09
28	GDR4 (sec 1d2)/MAYC-96	1.49E+09
29	TG-16 (sec 1d2) (A) /GC-90-1	4.03E+09
30	TG-13/STR-93 (sec 1d2)	1.87E+09
31	TG-8 (sec 1d2)/STR-93	1.61E+09

Table II. Coccolithophore assemblage total abundance (coccoliths/g). Values are expressed to the powers of eight, nine and ten.

In the studied samples, the total abundances of coccoliths range from 5×10^8 to 9.5×10^9 coccoliths/g of dry sediment with average values of around 2.5×10^9 coccoliths/g. The total abundance map (Fig. 2) shows the highest values located around the Balearic Islands (8×10^9 to 9.5×10^9 coccoliths/g) whilst the lowest values are located close to the Iberian margin shore line (5×10^8 to 1×10^9 coccoliths/g).

According to the relative abundances, small placoliths (*Emiliania huxleyi*, *Gephyrocapsa aperta* and *Gephyrocapsa ericsonii*) were the dominant group in the assemblages with percentage values of over 60% reaching almost 90% in some locations. Small placoliths are dis-

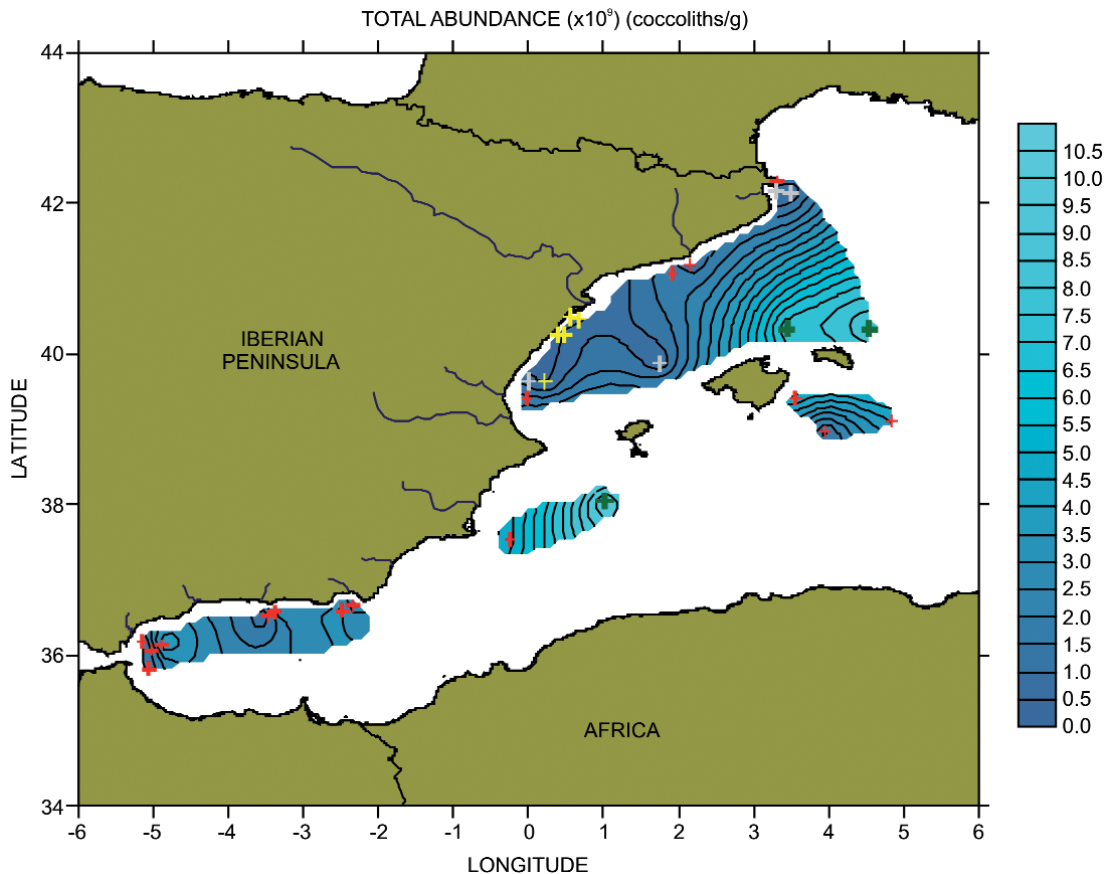


Figure 2. Total abundance distribution map and core-top locations (+). Samples coloured in green show total abundances over 8×10^9 (coccoliths/g). Samples coloured in yellow and grey show total abundances lower than 0.5 and 1×10^9 (coccoliths/g) respectively. Samples coloured in red show intermediate values between 1 and 8×10^9 . In the right-hand column of values, the colour ranges from dark blue (low values) to turquoise (high values).

tributed throughout the studied area showing their highest abundance close to the shore and the lowest off shore line (Fig. 3a).

Gephyrocapsa oceanica has a relative abundance of 10% close to the Strait of Gibraltar (3b) and *Gephyrocapsa muelleri* reaches 27% east of the Balearic Islands (3c).

Syracosphaera spp. reaches 10% with a specific and very concentric distribution northwest of the Balearic Islands (3d).

Helicosphaera spp., *Rhabdosphaera* spp. and *Umbilicosphaera* spp. show the lowest relative abundances in the assemblage, with around 3%, 2.5% and 2% respectively, each having a distinct distribution pattern. *Helicosphaera* spp. is found in a north-south band with the highest relative abundances spread out northwest of the Balearic Islands (3e), similar to the distribution of *Syracosphaera* spp. (3d). Two other specific, concentric areas

of lower relative abundance are located northeast of the Balearic Islands and south of Cabo de Gata. *Rhabdosphaera* spp. shows two clear positions: the first, more spatially concentrated and with high percentages, is south of the Gulf of Lyon, while the other is more widely distributed and located between the south of the Balearic Islands and Cape La Nao (3e). *Umbilicosphaera* spp. has no prevailing concentration point and is distributed throughout the sampling area, although lower distributions were seen in three areas: south of the Gulf of Lyon, south of the Ebro River Delta and east of the Balearic Islands (3g).

Florisphaera profunda is more abundant in the southern proximities of the Ebro River Delta reaching a value of 6% in one sample from this area (3h).

In two specific locations, the south of the Gulf of Lyon and the Ebro River Delta (3i), reworked coccoliths reach significant abundances of around 10%.

SAMPLE NUMBER	SAMPLE CODE	Small Placoliths %	G. oceanica %	G. muellerae %	Syracosphaera spp. %	Helicosphaera spp. %	Rhabdosphaera spp. %	Umbilicosphaera spp. %	F. profunda %	REWORKED COCCOLITHS %
1	GC-88-1, TR-70 (A)	82.09	0.79	0.79	2.17	0.98	0.79	0.00	1.77	0.98
2	TGóTR-12/GC-88-1	88.05	0.00	0.60	0.80	0.40	0.20	0.40	1.39	1.59
3	TG-15 (sec 1d2) (A)/GC-88-1	79.64	0.40	0.40	2.17	0.40	2.37	0.59	1.98	4.94
4	K-104/CL-83-1 (sec 1d3) (A)	83.10	0.20	1.19	1.39	1.39	0.20	0.00	2.19	0.40
5	TC-35 (A)/GC-93-1	80.55	0.79	0.39	0.79	1.96	0.00	1.57	0.59	1.96
6	TG-1 (A)/GC-92-1	70.64	0.00	0.00	2.75	0.00	0.92	0.00	2.75	6.42
7	TG-6 (A)/GC-92-1	81.51	1.51	0.00	3.77	0.75	1.13	0.00	1.89	4.53
8	K-30 (sec 1) (A)/79KEB	79.56	0.00	0.00	1.98	0.20	0.00	0.40	4.17	5.75
9	K-37 (sec 1) (A)/CO-80-4	73.86	1.19	2.77	0.99	1.58	0.00	0.79	0.79	0.00
10	K-39 (sec 1) (A)/CO-80-4	70.48	2.10	1.90	1.52	0.95	0.57	0.19	0.95	0.00
11	TK-61/80-CL (sec unica) (A)	87.30	0.00	0.60	0.60	0.40	0.00	0.40	1.98	1.39
12	TK-60/80-CL (sec 1) (A)	80.36	0.22	0.00	1.79	0.45	0.22	0.22	3.35	7.37
13	TK-59 (sec 1) (A)/80-CL	67.53	0.43	1.73	2.16	0.43	0.87	0.00	6.49	9.96
14	KF-4/VALSIS (1-2)	74.70	1.00	1.59	10.76	3.19	0.00	0.80	1.20	3.98
15	TK-30/80-CL (A)	68.79	0.61	1.82	0.61	0.00	0.61	0.30	4.24	1.82
16	TK-33/80-CL (sec 1) (A)	82.47	0.40	1.20	0.00	0.81	0.00	0.00	0.80	2.59
17	35411 (pilot)/E-3D-78	70.00	0.98	1.18	0.78	0.20	0.78	1.96	1.96	0.00
18	35411 (sec 1)/E-3D-78	65.61	3.78	23.86	1.39	0.20	0.20	0.00	0.20	0.00
19	K-2/CO-80-3 (A)	89.39	0.79	0.39	1.38	0.20	0.20	0.20	0.98	0.59
20	K-33 (sec 1) (A)/CO-80-4	66.67	0.59	26.67	0.59	0.39	0.00	0.00	1.57	0.39
21	K-30 (sec 1) (A)/CO-80-4	68.79	0.40	5.57	3.18	0.20	0.99	0.00	0.40	0.20
22	K-10 (sec 1) (A)/CO-80-4	69.42	1.15	1.92	2.12	1.92	1.15	1.15	1.35	0.00
23	K-4 (sec 1) (A)/CO-80-4	75.00	0.98	2.17	1.77	0.39	1.38	0.79	0.98	0.59
24	ALM22 (sec 1d2) (A)/MAYC-96	76.34	6.36	3.58	1.19	0.40	0.20	0.60	2.19	0.80
25	ALM19 (sec 1d2) (A)/MAYC-96	82.25	3.16	4.93	2.76	1.78	0.20	1.18	0.20	0.39
26	MTL18 (sec 1d2) (A)/MAYC-96	84.52	4.96	2.78	1.39	0.00	0.00	0.79	1.19	0.99
27	MTL2 (sec 1d1) (A+RX)/MAYC-96	76.29	9.76	5.58	1.00	0.60	0.20	1.00	0.80	1.00
28	GDR4 (sec 1d2)/MAYC-96	74.35	10.34	5.96	0.80	0.40	0.20	0.80	1.19	2.78
29	TG-16 (sec 1d2) (A) /GC-90-1	66.47	6.86	0.98	3.14	0.39	0.00	0.39	0.98	0.00
30	TG-13/STR-93 (sec 1d2)	71.29	5.74	6.34	1.39	0.00	0.20	0.79	1.78	1.19
31	TG-8 (sec 1d2)/STR-93	73.41	5.95	3.97	1.98	0.40	0.20	0.60	0.40	2.58

Table III. Relative abundance (%) of each coccolithophore taxa.

5. DISCUSSION

Geographic variability in the study area was very evident after plotting the three points, in the surroundings of the Balearic Islands, which had the highest coccolith total abundances of all sampling points (green crosses in Fig. 2). Previous studies also registered the area as richer in coccoliths than others in the Western Mediterranean Sea (Knappertsbusch, 1993; Cros, 1995, 2002; Flores *et al.*,

1997; Amore *et al.*, 2000, 2004; Colmenero-Hidalgo *et al.*, 2005). This area is mainly characterised by two oceanographic features: firstly, the action of the recent MAW, and secondly, the presence of the Balearic front (Font *et al.*, 1988; La Violette *et al.*, 1990; Salat, 1996). Recent MAW is characterised by warmer waters which reach the area through the Ibiza and inter-island channels. It was estimated that about 14% of the nutrients reaching the area come from inflowing Atlantic surface waters

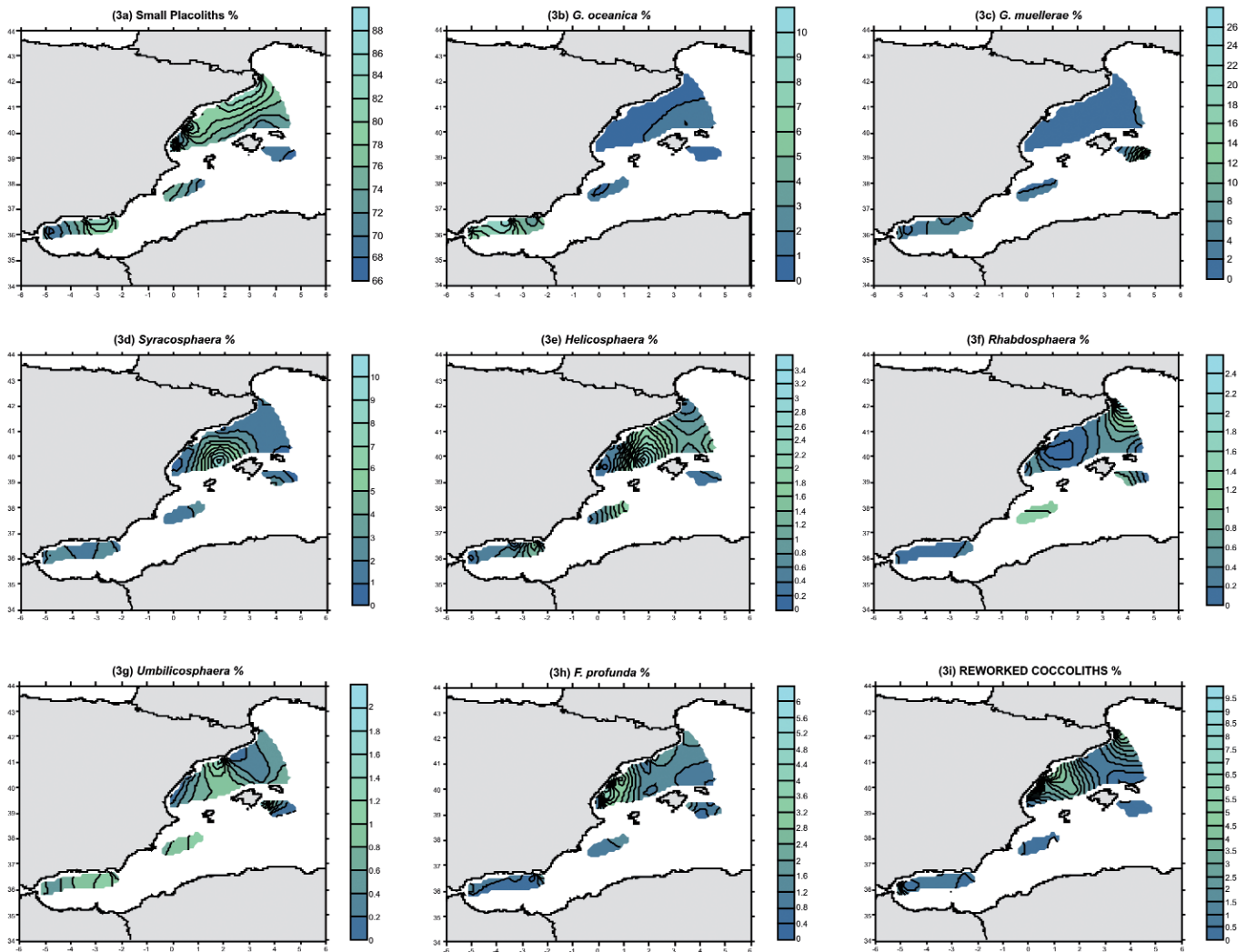


Figure 3. Relative abundance (%) distribution map of the different coccolithophore taxa. The colour, in the right-hand column, fluctuates from dark blue (low values), to green (medium values) and turquoise (high values).

(Estrada & Margalef, 1988). We consider recent MAW to play an important role as it provides optimum conditions for the development of the highest abundances of coccolithophores in the studied region.

Contrastingly, the lowest total abundance of coccoliths was recorded in five samples concentrated to the south of the Ebro Delta (yellow crosses in Fig. 2). It may be possible to extend this area if the other four samples in which lower abundance was seen are also considered (grey crosses in Fig. 2). It is necessary to point out that these samples could be influenced by the Ebro River runoff, which can be identified as far as the southern margin of the Ebro continental shelf, in the northern sector of the Gulf of Valencia, and also in the central area of the basin (Forcén-Vázquez *et al.*, 2010). Another important factor linked to the Ebro River

runoff could be a dilution of the coccolith signal in sediments due to the effect of the high terrestrial input (at present, the sediment discharge of the Ebro River is between 1 and 1.5×10^5 tons per year (Guillén & Palanques, 1992). The whole area is under the influence of the ancient MAW driven by the NC to the south-west along the continental slope (Salat, 1996; Millot, 1999). The shelf/slope and nutrient-rich Catalan Front are also located here (Estrada & Salat, 1989; Salat, 1996; Millot, 1999).

Intermediate total abundance values characterise the last nineteen samples which complete the locations studied (red crosses in Fig. 2). Taking into account these intermediate values, it would be possible to establish a preliminary quantification to estimate standard coccolith palaeoproductivity in the Western Mediterranean.

Small placoliths (*E. huxleyi*, *G. aperta* and *G. ericsonii*) are the dominant taxa in Western Mediterranean coccolith assemblages showing relative abundances which decrease as distance to the coast increases (Fig. 3a). Small placoliths have been considered as ubiquitous taxa (McIntyre & Bé, 1967; Okada & McIntyre, 1979) while their joint appearance in an assemblage has been reported as indicative of upwelling conditions or high primary productivity periods (Okada & Honjo, 1973; Kleijne *et al.*, 1989; Wells & Okada, 1997). Taking into account the data from this study, a link with high nutrient concentrations can also be suggested, which is consistent with the work of Bárcena *et al.* (2004) in the Alboran Sea.

The relationship of *Gephyrocapsa* with the stratified and warmer water masses of Atlantic origin was reported by Knappertsbusch (1993) and Cros (1995) who described *G. oceanica* as a tracer for Atlantic surface waters in the Mediterranean Sea. The distribution of *G. oceanica* in the Alboran Sea, close to the Strait of Gibraltar, shows a very obvious relationship with the inflow of slightly modified waters of Atlantic origin in accordance with the data of Knappertsbusch (1993). In addition to this, we also suggest a probable relationship with the dynamics of the WAG. The distribution of *G. muellerae* is not coincident with that of *G. oceanica* and is probably related to high nutrient concentrations linked to some of the coastal eddies generated by the AC (eastward 0–2°E) (Lohrenz *et al.*, 1988; Moran *et al.*, 2001; Bárcena *et al.*, 2004).

Syracosphaera spp. and *Helicosphaera* spp. show a very interesting concentric distribution in the area to north-west of the Balearic Islands. This concentric distribution seems to be related to the MAW and the dome-shaped fertilised area, generated by instabilities of the Catalan and Balearic fronts and characterised by an isopycnal dome with high oxygen concentrations, low temperatures and nutrient-rich waters rising with respect to the surrounding area (Margalef & Estrada, 1987; Estrada & Margalef, 1988; Font *et al.*, 1988; Estrada & Salat, 1989; Salat, 1996). *Syracosphaera* spp. has been defined as a ubiquitous genus (Okada & McIntyre, 1977) inhabiting the middle photic zone (Weaver & Pujol, 1988; Winter *et al.*, 1994). It has also been related to water upwelling in Benguela (Giraudeau *et al.*, 1993). *Helicosphaera* spp. has been described in high-productivity waters (Pujos, 1992; Flores *et al.*, 1995). The increase in abundance of both taxa (*Syra-*

cosphaera spp. and *H. carteri*) has been reported under surface water stratification (Colmenero-Hidalgo *et al.*, 2004; Álvarez *et al.*, 2005). The *Syracosphaera* spp. and *Helicosphaera* spp. data in the Catalano-Balearic Sea seem to be related to the isopycnal doming of dense water between the Catalan and Balearic fronts (Font *et al.*, 1988; Salat, 1996). However, *Helicosphaera* spp. was also found in two further locations: on north eastern side of the Balearic Islands and in the Alboran Sea, close to the Almeria-Oran Front. In these cases, *Helicosphaera* spp. seems to be responding to high chlorophyll concentrations linked to local upwelling zones (Estrada & Margalef, 1988; Estrada & Salat, 1989; Sánchez-Vidal *et al.*, 2004).

Rhabdosphaera spp. and *Umbilicosphaera* spp. were defined as warm-water taxa (Okada & Honjo, 1973; Winter *et al.*, 1994; Flores *et al.*, 1997). The distribution shown by the warmer taxa could be specifically related to the MAW located in the Algerian Basin.

The distribution of *F. profunda*, with three values higher than 3% to the south of the Ebro Delta may reflect the influence of river discharge, which agrees with the observations of Bárcena *et al.* (2004); who linked *F. profunda* to maximum rainfall and river discharge in the Alboran Sea.

Reworked Cretaceous to Neogene coccoliths have been identified with relative abundances reaching 9.96 % in one sample from the south of the Ebro Delta; this percentage is higher than those reported by Knappertsbusch (1993). The distribution of reworked coccoliths shows an obvious link to terrigenous input from the main rivers in the zone, the Ebro and Rhone, and may provide a very good proxy for the input of continental elements as previously reported by Flores *et al.* (1997) and Colmenero-Hidalgo *et al.* (2004).

6. CONCLUSIONS

Total abundance coccolith distribution data show areas of higher (the Balearic Island surroundings with a belt connecting to the Gibraltar area) and lower values (Iberian side of the Catalano-Balearic sea, especially southwards of the Ebro Delta). Recent MAW is considered to play an important role, contributing to the development of coccolithophores in the area. The lower total abundances match

well with the path of the NC current. Terrigenous runoff could be involved in the dilution of the coccolith signal in sediments close to the Ebro Delta.

The percentage coccolith distribution data show that:

- 1) The small placoliths are the dominant taxa in the coccolith assemblages, decreasing in relative abundance with distance from the coast. This distribution is interpreted as related to nutrient concentrations.
- 2) *G. oceanica* distribution in the west of the Alboran Sea is related to the dynamics of the recent MAW and WAG. *G. muelleræ* distribution in the Algerian Basin is related to high nutrient concentrations linked to the coastal eddies generated by the AC.
- 3) The relative abundance of *Syracosphaera* spp. and *Helicosphaera* spp. in the Catalano-Balearic Sea is linked to the central divergent structure. However, the distribution of *Helicosphaera* spp. close to the Balearic Islands and the Almeria-Oran Front is linked to local upwelling zones.
- 4) *F. profunda* distribution close to the Ebro Delta and its southern proximities could be related to the influence of river discharge.
- 5) Higher percentages of Cretaceous to Neogene reworked coccoliths were located mainly in areas of terrigenous river runoff.

From the results of this biogeographic study it can be seen that the general distribution of coccoliths, understood as synoptic remains of past environmental events, can be basic useful tools for other disciplines related to marine resources.

7. ACKNOWLEDGEMENTS

This study was supported by a grant from the regional government of Valencia (Generalitat Valenciana) to M.C.A. and was undertaken within the framework of the MONTERA project (Ref: CTM-14157-C02-02-MAR) and CONTOURIBER project (Ref: CTM2008-06399-C04-04/MAR). We are grateful to the anonymous referees for their valuable comments and M.A. Díaz Flores (UNAM) and M.A. Galicia Pérez (UCOL) for the useful comments on physical oceanography.

8. REFERENCES

- Alonso, B. and Maldonado, A. 1992. Plio-Quaternary margin growth patterns in a complex tectonic setting: northeastern Alboran Sea. In: A. Maldonado (Ed.), *The Alboran Sea. Geo-Marine Letters*, Special Volume 2-3, 137-143.
- Amore, F.O., Ciampo, G., Di Donato, V., Esposito, P., Russo-Ermolli, E. and Staiti, D. 2000. An integrated micropaleontological approach applied to Late Pleistocene-Holocene paleoclimatic and paleoenvironmental changes (Gaeta Bay, Tyrrhenian Sea). In: *Climates: Past and Present*. (Ed. Hart M.B.), Royal Geol. Soc. London Special Publication, 181, 95-111.
- Amore, F.O., Caffau, M., Massa, B. and Morabito, S. 2004. Late Pleistocene-Holocene paleoclimate and related paleoenvironmental changes as recorded by calcareous nannofossils and planktonic foraminifera assemblages in the southern Tyrrhenian Sea (Cape Palinuro, Italy). *Marine Micropaleontology*, 52, 255-276.
- Álvarez, M.C., Flores, J.A., Sierro, F.J., Diz, P., Francés, G., Pelejero, C. and Grimalt, J. 2005. Millennial surface water dynamics in the Ría de Vigo during the last 3000 years as revealed by coccoliths and molecular biomarkers. *Palaeogeography, Palaeoclimatology, Palaeoecology*, 218, 1-13.
- Andrulleit, H., Rogalla, U. and Stäger, S. 2004. From living communities to fossil assemblages: origin and fate of coccolithophores in the northern Arabian Sea. *Micropaleontology*, 50 (1), 5-21. doi: 10.2113/50.Supp_1.5
- Arin, L. Morán, X.A.G. and Estrada, M. 2002. Phytoplankton size distribution and growth rates in the Alboran Sea (SW Mediterranean): short term variability related to mesoscale hydrodynamics. *Journal of Plankton Research*, 24 (10), 1019-1033.
- Bárcena, M.A. and Abrantes, F. 1998. Evidence of a high-productivity area off the coast of Málaga from studies of diatoms in surface sediments. *Marine Micropaleontology*, 35, 91-103.
- Bárcena, M.A., Flores, J.A., Sierro, F.J., Pérez-Folgado, M., Fabres, J., Calafat, A. and Canals, M. 2004. Planktonic response to main oceanographic changes in the Alboran Sea (Western Mediterranean) as documented in sediment traps and surface sediments. *Marine Micropaleontology*, 53, 423-445.
- Bartolini, C. 1970. Coccoliths from sediments of the western Mediterranean. *Micropaleontology*, 16, 129-154.
- Benzohra, M. and Millot, C. 1995. Hydrodynamics of an open sea Algerian eddy. *Deep-Sea Research I*, 42 (10), 1831-1847.
- Boeckel, B. and Baumann, K-H. 2004. Distribution of coccoliths in surface sediments of the south-eastern South Atlantic Ocean: ecology, preservation and carbonate contribution. *Marine Micropaleontology*, 51 (3-4), 301-320. doi:10.1016/j.marmicro.2004.01.001
- Boeckel, B., Baumann, K-H., Henrich, R. and Kinkel, H. 2006. Coccolith distribution. *Research I*, 53, 1073-1099.
- Bozzano, G., Alonso, B., Ercilla, G., Estrada, F. and García, M. 2009. Late Pleistocene and Holocene depositional facies of the Almeria Channel (Western Mediterranean). In: B. Kneller, O.J. Martinsen, B. Mc Caffrey (Eds.), *External Controls on Deep Water Depositional Systems*. London Geological Society, SEPM Special Publication, 92, 199-297.

- Cacho, I., Grimalt, J.O., Pelejero, C., Canals, M., Sierro, F.J., Flores, J.A. and Shackleton, N.J. 1999. Dansgaard-Oeschger and Heinrich event imprints in the Alboran Sea paleotemperatures. *Paleoceanography*, 14 (6), 698-705.
- Calafat, A.M., Casamor, J.L., Canals, M. and Nyffeler, F. 1996. Distribution and elemental composition of the suspended particulate matter in the Catalan-Balearic Sea. *Geogaceta*, 20 (2), 370-373.
- Cheney, R.E. 1978. Recent observations of the Alboran Sea frontal system. *Journal of Geophysical Research*, 83, 4593-4597.
- Colmenero-Hidalgo, E., Flores, J.A., Sierro, F.J., Bárcena, M.A., Lfwe-mark, L., Schinfeld, J. and Grimalt, J.O. 2004. Ocean surface water response to short-term climate changes revealed by coccolithophores from the Gulf of Cadiz (NE Atlantic) and Alboran Sea (W Mediterranean). *Palaeogeography, Palaeoclimatology, Palaeoecology*, 205, 317-336.
- Colmenero-Hidalgo, E., Flores, J.A., Sierro, F.J. and Grimalt, J.O. 2005. Sea surface temperature reconstruction in the southeastern Iberian Margin during the Last Glacial period by means of coccolithophore analyses. *Geogaceta*, 38, 195-198.
- Cros, L. 1995. Calcareous nannoplankton in surficial sediments of the Catalano-Balearic Sea. (Northwestern Mediterranean). In: 5th INA Conference in Salamanca 1993. (Eds. J.A. Flores, F.J. Sierro). Proceedings, Universidad de Salamanca, 47-59.
- Cros, L. (2001) 2002. *Planktonic Coccolithophores of the NW Mediterranean*. PhD. Thesis. Publicaciones de la Universidad de Barcelona, 181 pp.
- De Vargas, C., Aubry, M.P., Probert, I. and Young, G. 2007. Origin and Evolution of Coccolithophores: From coastal Hunters to Oceanic Farmers. In: *Evolution of Primary Producers in the Sea*. (Eds. P. Falowski, A. Knoll). Elsevier Academic Press, London, 251-285.
- Eide, L.K. 1990. Distribution of coccoliths in surface sediments in the Norwegian-Greenland Sea. *Marine Micropaleontology*, 16 (1-2), 65-75. doi:10.1016/0377-8398(90)90029-L
- Ercilla, G., Díaz, J.I., Alonso, B. and Farrán, M. 1995. Late Pleistocene-Holocene evolution of the northern Catalanian continental shelf (Northwestern Mediterranean Sea). *Continental Shelf Research*, 15 (11/12), 1435-1451.
- Estrada, M. 1980. Composición taxonómica del fitoplancton en una zona próxima a la desembocadura del río Besós (Barcelona), de Octubre de 1978 a marzo de 1979. *Investigación Pesquera*, 44 (2), 275-289.
- Estrada, M. and Margalef, R. 1988. Supply of nutrients to the Mediterranean photic zone along a persistent front In: *Océanographie pélagique méditerranéenne* (Eds. Minas, H.J., Nival, P.). *Oceanologica Acta*, SP, 133-142.
- Estrada, M. and Salat, J. 1989. Phytoplankton assemblages of deep and surface water layers in a Mediterranean frontal zone. In: *Topics in Marine Biology* (Ed. Ros, J.D.). *Scientia Marina*, 53 (2-3), 203-214.
- Estrada, M. 1996. Primary production in the northwestern Mediterranean. In: *The European anchovy and its environment*, (Eds. Palomera, I., Rubiés, P.). *Scientia Marina*, 60 (2), 55-64.
- Fatela, F. and Taborda, R. 2003. Confidence limits of species proportions in microfossil assemblages. *Marine Micropaleontology*, 45, 169-174.
- Flores, J.A., Sierro, F.J. and Raffi, I. 1995. Evolution of the calcareous nannofossil assemblage as a response to the paleoceanographic changes in the Eastern equatorial Pacific from 4 to 2 Ma (Leg 138, Sites 849 and 852). *ODP Proceedings, Initial Reports*, 138, 163-176.
- Flores, J.A. and Sierro, F.J. 1997. Revised technique for calculation of calcareous nannofossil accumulation rates. *Micropaleontology*, 43, 321-324.
- Flores, J.A., Sierro, F.J., Francés, G., Vázquez, A. and Zamarreño, I. 1997. The last 100,000 years in the Western Mediterranean: Sea surface water and frontal dynamics as revealed by Coccolithophores. *Marine Micropaleontology*, 29, 351-366. doi:10.1016/S0377-8398(96)00029-1
- Flores, J.A. and Marino, M. 2002. Pleistocene calcareous nannofossil stratigraphy for ODP Leg 177 (Atlantic sector of the Southern Ocean). *Marine Micropaleontology*, 45, 191-224.
- Font, J., Salat, J. and Tintoré, J., 1988. Permanent features of the circulation in the Catalan sea. *Oceanologica Acta*, 9, 51-57.
- Forcén-Vázquez, A., Alcántara-Carrió, J. and Pelegrí, J.L. 2010. Descripción de las masas de agua en la plataforma continental del golfo de Valencia: Influencia de las masas de agua de origen continental y de borde de plataforma. Libro de Resúmenes del I Encuentro Oceanografía Física Española, 64.
- Geisen, M., Billard, C., Broerse, A.T.C., Cros, L., Probert, I. and Young, J.R. 2002. Life-cycle associations involving pairs of holococcolithophorid species: intraspecific variation or cryptic speciation? *European Journal of Phycology*, 37, 531-550.
- Giraudeau, J., Monteiro, P.M.S. and Nikodemus, K. 1993. Distribution and malformation of living coccolithophores in the northern Benguela upwelling system off Namibia. *Marine Micropaleontology*, 22, 93-110.
- Guillén, J. and Palanques, A. 1992. Sediment dynamics and hydrodynamics in the lower course of a river highly regulated by dams: the Ebro River. *Sedimentology*, 39, 567-579.
- Kleijne, A., Kroon, D. and Zeveboom, W. 1989. Phytoplankton and foraminiferal frequencies in northern Indian Ocean and Red Sea surface waters. *Netherlands Journal of Sea Research*, 24, 531-539.
- Kleijne, A. 1991. Holococcolithophorids from the Indian Ocean, Red Sea, Mediterranean Sea and North Atlantic Ocean. *Marine Micropaleontology*, 17, 1-76.
- Knappertsbusch, M. 1993. Geographic distribution of living and Holocene coccolithophores in the Mediterranean Sea. *Marine Micropaleontology*, 21, 219-247.
- La Violette, P.E., Tintoré, J. and Font, J. 1990. The surface circulation of the Balearic Sea. *Journal of Geophysical Research*, 95 (C2), 1559-1567.
- López-García, M.J., Millot, C., Font, J. and García-Ladona, E. 1994. Surface circulation variability in the Balearic Basin. *Journal of Geophysical Research*, 99 (C2), 3285-3296. doi: 10/1029/93JC02114
- Lohrenz, S.E., Wiesenburg, D.A., De Palma, I.P., Johnson, K.S. and Gustafson, D.E. 1988. Interrelationships among primary production, chlorophyll, and environmental conditions in frontal regions of the western Mediterranean Sea. *Deep-Sea Research*, 35, 793-810.

- LUCIA Measurement Version 4.61. digital analysis software:
<http://www.laboratory-imaging.com/>
- Margalef, R. 1969. Composición específica del fitoplancton de la costa catalano-levantina (Mediterraneo occidental) en 1962-1967. *Investigación Pesquera*, 33(1), 345-380.
- Margalef, R. and Estrada, M. 1987. Synoptic distribution of summer phytoplankton (Algae and Protozoa) across the principal front in the Western Mediterranean. *Investigación Pesquera*, 51, 121-140.
- Matheron, G. 1960. *Krigeage d'un panneau rectangulaire par sa périphérie*. Note géostatistique, Ecole des Mines de Paris, Paris.
- McIntyre, A. and Bé, A.W.H. 1967. Modern coccolithophores of the Atlantic, I. Placoliths and Cyrtoliths. *Deep-Sea Research*, 14, 561-597.
- Medialdea, J., Maldonado, A., Alonso, B., Farrán, M., Giró, S., Díaz, J.I. and Vázquez, A. 1986. *Mapa Geológico de la Plataforma Continental Española y Zonas Adyacentes. E. 1:200.000. Memoria y Hoja nº 41 y 42. Tarragona*. Instituto Geológico y Minero de España, Madrid, vol 1, 79 pp.
- Millot, C., Benzohra, M. and Taupier-Letage, I. 1997. Circulation off Algeria inferred from the Médiprod-5 current meters. *Deep Sea Research I*, 44 (9-10), 1467-1495.
- Millot, C. 1999. Circulation in the Western Mediterranean Sea. *Journal of Marine Systems*, 20, 423-442.
- Moran, Xoxé Anxelu G., Taupier-Letage, I., Vázquez-Domínguez, E., Ruiz, S., Arin, L., Raimbault, P. and Estrada, M. 2001. Physical-Biological coupling in the Algeria Basin (SW Mediterranean): Influence of mesoscale instabilities on the biomass and production of phytoplankton and bacterioplankton. *Deep-Sea Research I*, 48 (2), 405-437.
- Okada, H. and Honjo, S. 1973. The distribution of oceanic coccolithophorids in the Pacific. *Deep-Sea Research*, 20, 355-374.
- Okada, H. and McIntyre, A. 1977. Modern coccolithophores of the Pacific and North Atlantic Oceans. *Micropaleontology*, 23, 1-55.
- Okada, H. and McIntyre, A. 1979. Seasonal distribution of modern coccolithophores in the western North Atlantic Ocean. *Marine Biology*, 54, 319-328.
- Pascual, A., Buongiorno Nardelli, B. Larnicol, G., Emelianov, M. and Gomis, D. 2002. A case of an intense anticyclonic eddy in the Balearic Sea (western Mediterranean). *Journal of Geophysical Research*, 107(C11), 3183. doi:10.1029/2001JC000913.
- Pérez-Folgado, M., Sierro, F.J., Flores J.A., Cacho, I., Grimalt J.O., Zahn, R. and Shackleton, N. 2003. Western Mediterranean planktonic foraminifera events and millennial climatic variability during the last 70 kyr. *Marine Micropaleontology*, 48, 49-70.
- Perkins, H., Kinder, T.H. and La Violette, P.E. 1990. The Atlantic inflow in the northwestern Alborán Sea. *Journal of Physical Oceanography*, 20, 242-263.
- Pinot, J.M., Tintoré, J. and Gomis, D. 1994. Quasi-synoptic mesoscale variability in the Balearic Sea. *Deep Sea Research I*, 41, 897-914.
- Pujos, A. 1992. Calcareous nanofossils of Plio-Pleistocene sediments from the northwestern margin of tropical Africa. In: *Upwelling Systems: Evolution Since the Early Miocene* (Eds. Summerhayes, C.P., Prell, W.L., Emeis, K.C.). Special Publication-Geological Society, London, 64, 343-359.
- Rio, D. 1982. The fossil distribution of coccolithophore genus *Gephyrocapsa* Kamptner and related Plio-Pleistocene chronostratigraphic problems. In: DSDP. (Eds. Prell, W.L., Gardner, J.V., et al.). Initial Reports, 68, 325-343.
- Rio, D., Raffi, I. and Villa, G. 1990. Pliocene-Pleistocene calcareous nanofossil distribution patterns in the Western Mediterranean. In: Proceedings of the Ocean Drilling Program. (Eds. Kastens, K.A., Mascle, J., et al.). Scientific Results, 107, 513-533. doi:10.2973/odp.proc.sr.107.164.1990
- Roth, P.H. and Thierstein, H. 1972. Calcareous nannoplankton: Leg 14, Deep Sea Drill. Project. In: Hayes, D.E., Pimm, A.C. (Eds.), Initial Reports of the Deep Sea Drilling Project 14. U.S. Government Printing Office, Washington, 421-485.
- Roth, P.H. 1994. Distribution of coccoliths in oceanic sediments. In: *Coccolithophores*. (Eds. Winter, A., Siesser, W.G.). Cambridge University Press, Cambridge, 199-218.
- Saavedra-Pellitero, M., Flores, J.A., Baumann, K-H. and Sierro F.J. 2010. Coccolith distribution patterns in surface sediments of Equatorial and Southeastern Pacific Ocean. *Geobios*, 43, 131-149.
- Saavedra-Pellitero, M., Flores, J.A., Lamy, F., Sierro, F.J. and Cortina, A. in press. Coccolithophore estimates of paleotemperature and paleoproductivity changes in the Southeast Pacific over the past ~27 kyr. *Paleoceanography*, doi:10.1029/2009PA001824.
- Salat, J. 1996. Review of hydrographic environmental factors that may influence anchovy habitats in northwestern Mediterranean. *Scientia Marina*, 60 (2), 21-32.
- Sánchez-Vidal, A., Calafat, A., Canals, M. and Fabres, J. 2004. Particle fluxes in the Almeria-Oran front: control by coastal upwelling and sea surface circulation. *Journal of Marine Systems*, 52 (1-4), 89-106.
- Sierro, F.J., Hodell, D.A., Curtis, J.H., Flores, J.A., Reguera, I., Colmenero-Hidalgo, E., Bárcena, M.A., Grimalt, J.O., Cacho, I., Frigola, J. and Canals, M. 2005. Impact of iceberg melting on Mediterranean thermohaline circulation during Heinrich events. *Paleoceanography*, 20, PA2019, doi:10.1029/2004PA001051.
- Spellerberg, I.F. and Sawyer, J.W.D. 1999. Biogeography: the nature of the subject, its history and its applications. In: *An introduction to applied biogeography* (Eds. I.F. Spellerberg, J.W.D. Sawyer). University Press, Cambridge, 1-22.
- Tintoré, J., La Violette, P.E., Bladé, I. and Cruzado, A. 1988. A study of an intense density front in the eastern Alborán Sea: The Almería-Orán front. *Journal of Physical Oceanography*, 18, 1384-1397.
- Vargas-Yáñez, M., Plaza, F., García-Lafuente, Sarhan, J.T., Vargas, J.M. and Vélez-Belchi, P. 2002. About the seasonal variability of the Alboran Sea circulation. *Journal of Marine Systems*, 35, 229-248.
- Violanti, D., Parisi, E. and Erba, E. 1987. Fluttuazioni climatiche durante il Quaternario nel Mar Tirreno, Mediterraneo occidentale (carota PC-19 Ban 80). *Rivista Italiana di Paleontologia e Stratigrafia*, 92, 515-570.
- Von Grafenstein, R., Zahn, R., Tiedeman, R. and Murat, A. 1999. Planktonic $\delta^{18}O$ record at sites 976 and 977, Alboran Sea: stratigraphy, forcing, and paleoceanographic implications, In: Proc. Ocean Drill.

- Prog. (Eds. R. Zahn, M.C. Comas, A. Klaus). *Sci. Res.*, 161, 469-479. doi:10.2973/odp.proc.sr.161.233.1999
- Wackernagel, H. 1995. *Multivariate Geostatistic*. Springer-Verlag, Heidelberg, 256.
- Weaver, P.P.E. and Pujol, C. 1988. History of the Last Deglaciation in the Alboran Sea (Western Mediterranean) and adjacent North Atlantic as revealed by Coccolith floras. *Palaeogeography, Palaeoclimatology, Palaeoecology*, 64, 35-42.
- Wells, P. and Okada, H. 1997. Response of nannoplankton to major changes in sea-surface temperature and movements of hydrological fronts over Site DSDP 594 (south Chatham Rise, southeastern New Zealand), during the last 130 kyr. *Marine Micropaleontology*, 32, 341-363.
- Winter, A., Jordan, R.W. and Roth, P. 1994. Biogeography of living coccolithophores in ocean waters. En: *Coccolithophores*. (Eds. Winter, A., Siesser, W.G.). Cambridge University Press, Cambridge, 161-177.
- Ziveri, P., Rutten, A., de Lange, G.J., Thomson, J. and Corselli, C. 2000. Present-day coccolith fluxes recorded in central eastern Mediterranean sediment traps and surface sediments. *Palaeogeography, Palaeoclimatology, Palaeoecology*, 158, 175-195. doi:10.1016/S0031-0182(00)00049-3

MANUSCRITO RECIBIDO: 15 de mayo, 2010

MANUSCRITO ACEPTADO: 12 de diciembre, 2010

Palynomorphs and foraminifera from Colombia housed in the systematic collections of Ecopetrol-ICP

Diana Espitia¹, María Carolina Vargas², José E. Arenas³, Carlos A. Jaramillo⁴,
Milton J. Rueda⁵ and Hermann Duque-Caro⁶

¹DTH-EOS Ltda., Bucaramanga, Colombia. despitiav@gmail.com

²Instituto Colombiano del Petróleo-ECOPETROL SA.-ICP, Km 7 vía Piedecuesta, Santander, Colombia.
maria.vargas@ecopetrol.com.co.

³Instituto Colombiano de Geología y Minería-INGEOMINAS, Bogotá, Colombia.

⁴Smithsonian Institute of Tropical Research-Panamá, Panamá.

⁵Paleoflora Ltda. Bucaramanga, Colombia.

⁶Duque Caro & Cia. Ltda., Bogotá, Colombia.

Resumen

Numerosos estudios palinológicos y micropaleontológicos (foraminíferos) realizados por ECOPETROL S.A. a través de investigaciones desarrolladas en diversas cuencas sedimentarias colombianas, han permitido entender la distribución vertical y horizontal de varios taxones incrementando tanto la resolución bioestratigráfica como la interpretación biofacial de las secuencias sedimentarias. Con el objetivo de estandarizar la taxonomía y preservar todo el conocimiento generado, el Instituto Colombiano del Petróleo (ICP) de ECOPETROL S.A creó las colecciones sistemáticas de palinomorfos y foraminíferos, las cuales contienen morfoespecies que abarcan desde el Cretácico hasta el Holoceno. Las colecciones están organizadas por morfoespecies y por asociaciones regionales. La colección de palinomorfos está constituida por 814 morfoespecies (83% polen y esporas, 13% dinoflagelados y 4% representados por elementos preservados en preparaciones palinológicas), de las cuales 368 han sido formalmente descritas y 345 son informales mientras que la colección de foraminíferos, comprende más de 600 morfoespecies entre formas planctónicas (35 %) y bentónicas (65%). Ambas colecciones –palinomorfos y foraminíferos– están indexadas en bases de datos por medio del software *FileMaker Pro*, migrando a MySQL con una interface de usuario cakephp la cual permite acceder a la herramienta por medio de la web. Estas bases de datos contienen descripciones y fotomicrografías del material depositado en ellas así como del material tipo original. Las colecciones son actualizadas permanentemente por los conservadores por medio de revisiones constantes, discusiones y mejoras en las técnicas de preservación. Este material es consultado de manera continua por los miembros del Grupo de Bioestratigrafía-ICP y por estudiantes así como por expertos internacionales, como en el caso de la colección de palinomorfos. Por estas razones, consideramos nuestras colecciones y sus bases de datos como herramientas eficaces para estandarizar la taxonomía y preservar el conocimiento bioestratigráfico del norte de Suramérica así como un repositorio potencial para nuevos holotipos que provengan de investigaciones futuras en Colombia y áreas adyacentes.

Palabras clave: Colecciones micropaleontológicas, Cretácico, Cenozoico, Colombia, dinoflagelados, esporas, polen, foraminíferos.

Abstract

Numerous palynological and foraminiferal studies made by ECOPETROL S.A. in several Colombian sedimentary basins have enabled us to understand the vertical and horizontal distribution of several taxa increasing both the biostratigraphic resolution and biofacial interpretation of these sequences. In order to standardise the taxonomy and preserve all the generated knowledge, the Colombian Pe-

troleum Institute (ICP) of ECOPETROL S.A built palynomorph and foraminiferal systematic collections comprising morphospecies from the Cretaceous to the Holocene. These collections are organised by taxa and by regional location, according to Colombian sedimentary basins. The palynomorph collection consists of 814 morphospecies (83% pollen and spores, 13% dinoflagellate cysts, and 4% elements preserved in palynological slides), 368 described and 345 informal morphospecies whilst the foraminiferal collection holds over 600 morphospecies of foraminifera among planktonic (35 %) and benthic forms (65%). Both collections - palynomorph and foraminiferal - are indexed in *FileMaker Pro* databases, and they are currently being migrated to MySQL employing a cakephp user interface which allows to access the tool through the web. These databases contain descriptions and photomicrographs of the material deposited in them as well as of the original types. These collections are updated regularly by the curators, by means of constant revisions, discussions and improvements of preservation techniques. This material is currently not only in constant use by members of the Biostratigraphy Team at ICP and students but also by international experts, as in the case of the palynomorph collection. For these reasons, we consider our collections and their databases as effective tools to standardise the taxonomy and preserve the biostratigraphical knowledge of northern South America as well as a potential repository of new holotypes derived from future research in Colombia and adjacent areas.

Key words: Micropalaeontological collections, Cretaceous, Cenozoic, Colombia, dinoflagellate cysts, pollen, spores, foraminifera.

1. INTRODUCTION

The systematic collections at ICP began as an effort to preserve and consolidate the biostratigraphical information which had been acquired during several years of oil exploration by ECOPETROL S.A-ICP. As a result, the collection of palynomorphs (pollen, spores and dinoflagellate cysts) was created in 2004 by the palynologist Carlos Jaramillo. The preservation of the slides revealed the necessity to standardise the taxonomy of tropical palynomorphs and an electronic database using *FileMaker Pro* (Jaramillo *et al.*, 2004) was then created. The main purpose was to have a quick reference to the tropical morphospecies described for northern South America, especially the ones present in Colombian continental sedimentary sequences. All this knowledge was then successfully used in exploratory oil wells (on-site) as applied biostratigraphy (Jaramillo *et al.*, 2004; Rueda *et al.*, 2005; Pulido *et al.*, 2006; Vargas *et al.*, 2007, 2008; Torres *et al.*, 2008). The same process was subsequently employed for the construction of the foraminiferal collection by micropalaeontologists at ICP with the permanent advice and revision of the stratigrapher and micropalaeontologist Hermann Duque-Caro, with material from marine sedimentary sequences of northern Colombia (Jaramillo *et al.*, 2004; Rueda *et al.*, 2005; Pulido *et al.*, 2006; Espitia & Arenas, 2006; Espitia, 2007, 2008; Espitia *et al.*, 2008).

2. METHODS

Hundreds of rock samples not only from wells (wet and dry ditch cutting samples) but also from outcrop sections and stratigraphic wells from several Colombian sedimentary basins were analysed on the basis of their microfossil content over a period of about five years as a result of multiple projects related to oil exploration research at ECOPETROL SA.-ICP. From these analyses, several key marker palynomorph and foraminifera morphospecies were selected taking into account the concept of an index fossil: a taxon with easily recognizable morphological characteristics, with a widespread geographical distribution and with a short geologic time range. In some cases though, several morphospecies which do not have a short stratigraphic range, as in the case of benthic foraminifera, were selected because they were significant biostratigraphic events of a given stratigraphic level in a regional scale by means of their first and/or and last occurrences. Once selected, each morphospecies was taxonomically revised –based on classic literature- and validated by experts of each fossil group before entering into the collections formally.

After that, a unique code was generated for each slide and in the case of palynomorphs the position of the specimen on the slide was defined using the England Finder System. For foraminiferal slides, where the specimens can be picked

and mounted on a single cardboard-slide commonly 3 of a single morphospecies the slides were properly labelled including not only a unique code but also key information such as morphospecies' name, author, locality, age, depth and collector's name, among a few others. Next, optical and/or SEM photomicrographs were taken and loaded into the database where descriptions and biostratigraphic information relating to the taxa were also entered.

3. RESULTS

The palynomorph and foraminiferal systematic collections at ECOPETROL S.A-ICP constitute the organised arrangement of taxa which are consulted permanently by palynologists and micropalaeontologists. Based on their morphological characteristics and biostratigraphical value they represent reference material for proper and accurate identification of organic, calcareous and agglutinated microfossils.

These collections constituted reference collections holding more than 1400 morphospecies among foraminifera and palynomorphs. Currently, the palynomorph collection consists of 814 morphospecies. The material is mainly composed of pollen (68%), spores (15%) and dinoflagellate cysts (13%) with 549, 125 and 107 morphospecies respectively. The additional 4% are constituted of algae, acritarchs, fungal remains and foraminiferal inner linings. The foraminiferal collection is constituted of 640 foraminiferal morphospecies, including both planktonic (226) and benthic (414) forms. The latter group encompasses 310 calcareous, 1 pseudochitinous, and 103 agglutinated specimens.

3.1 Status of the material

The foraminiferal collection is predominantly composed of secondary type specimens, i.e., 686 homeotypes, 20 topotypes, and 118 morphotypes. From the former group 37 morphospecies of planktonic foraminifera are illustrated in Rincón *et al.* (2007). Recently, the first holotype entered the collection. It is an agglutinated benthic foraminifera from the Colombian Caribbean Sea (continental slope). Along with the holotype, 10 paratypes are

also deposited in this collection. It is worth mentioning that another paratype of this morphospecies is deposited in the collection of foraminifera at the Smithsonian National Museum of Natural History in Washington. The complete taxonomic information of this form is addressed in Fiorini (2009). On the other hand, the palynomorph collection is made up of 29 holotypes (Yepes, 2001; Jaramillo *et al.*, 2007; Jaramillo *et al.*, in press), 29 paratypes, 38 homeotypes, the last one selected from workshops on the bases of publications (Jaramillo & Yepes, 1994; Jaramillo & Dilcher, 2001; Jaramillo *et al.*, 2007; Silva-Caminha *et al.*, 2010), 101 morphotypes and 345 "informal" morphospecies, that is, morphospecies which have not been formally proposed.

3.2 Repository

The collections are located in the biostratigraphy section of the ICP. The palynomorph collection currently contains 1214 "reference slides" and 27000 slides of the regional collection. The foraminiferal collection is composed of more than 6000 micropalaeontological slides (see Fig. 1). The slides of this latter collection are arranged either by morphospecies name for quick reference to a single morphospecies or according to the basin where the microfossil assemblage comes from, namely morphospecies and regional collections (see Fig. 2). Each slide of the regional collection contains the picked and/or sorted microfauna of the analysed stratigraphic level (see Figs 2 and 3). Apart from foraminifera, these slides contain, where available, ostracods, microbivalves, microgastropods, diatoms, radiolaria and remains of echinoderms and fish (teeth, denticles and otoliths).

3.3 Geological interval

The foraminifera from these collections cover the range from the Cretaceous (Cenomanian) to the Quaternary (Holocene). The Cenozoic specimens comprise 89% of the collection whilst the Cretaceous microfauna comprise about 11 %. In the case of palynomorph taxa, the oldest forms correspond to the Maastrichtian (Cretaceous) and the younger ones to Pleistocene, with a proportion of 76% of palynomorphs covering the Cenozoic and 24% the Cretaceous.



Figure 1. Repository of the systematic collections at ICP. 1. Palynomorph collection a. Morphospecies collection, b. Regional collection; 2. Foraminiferal collection a. Morphospecies collection, b. Regional collection.

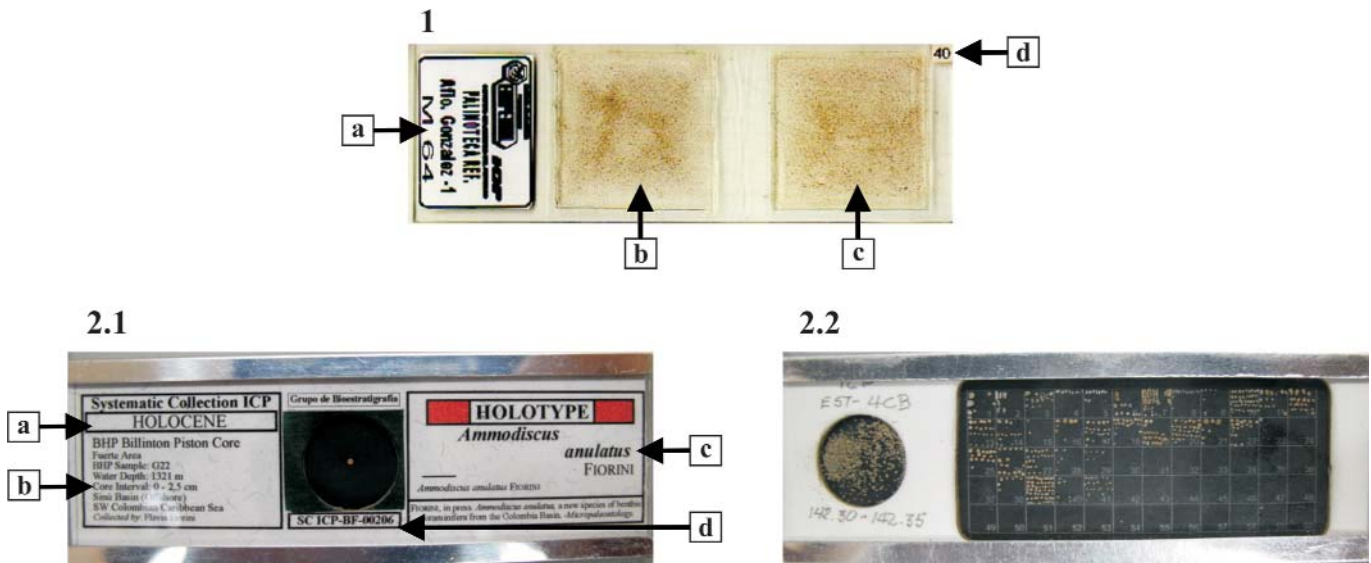


Figure 2. Slides. 1. Palynological slide. a. General information, b and c. Assemblages. The slide has two preparations, with (c) and without (b) oxidation methods, in order to compare the recovery of palynomorphs, d. Slide code. 2. Foraminiferal slides. 2.1. Morphospecies collection a. Age, b. General information, c. Species name, d. Slide code; 2.2 Regional collection. Note the complete assemblage of foraminifera within the slide.

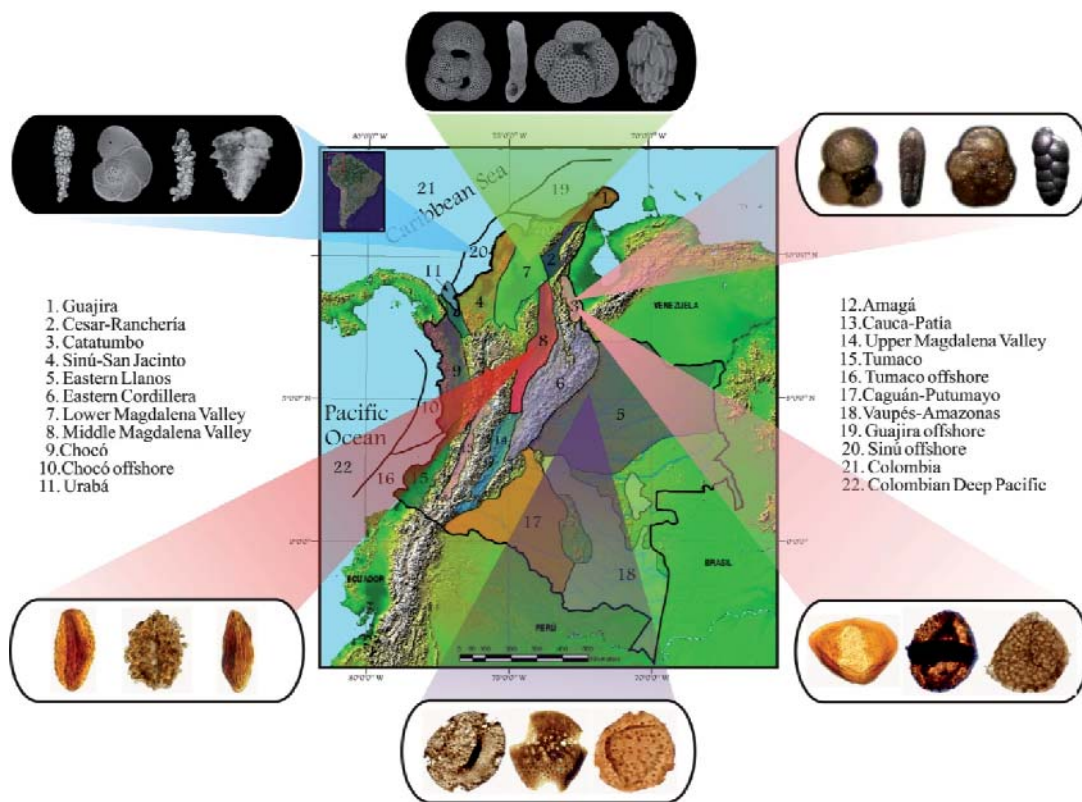


Figure 3. Colombian sedimentary basins. Modified from ANH (2007). Note the palynological (below) and foraminiferal (above) assemblages of five basins.

4. DATABASE

The physical collections are linked to databases built in *File Maker Pro 8* software, and they are currently being migrated to MySQL employing a cakephp user interface which allows to access the tool through the web (<http://biogeodb.stri.si.edu/jaramillo/palynomorph/pollen>). In this manner they constantly feed the electronic record which is consulted by palynologists and micropalaeontologists not only at the Colombian Petroleum Institute (ICP) but also those working on biostratigraphic control on-site at exploratory wells where the response of the biostratigrapher must be fast and effective. Certainly these databases have proven to be quite useful tools to achieve this goal.

The structure of the databases consists of multiple panels which are connected to each other through several easy-to-use links which help the user to find a given morphospecies with a simple search. The information contained in the databases includes morphological description of each

morphospecies, remarks and comparison with related forms, biostratigraphic range and distribution, optical and/or SEM photomicrographs, bibliographic references and also information on the location within the physical collection in order to have quick access to any slide for direct consultation using the microscope or stereomicroscope (Figs 4 and 5). In those cases where there are no homeotypes or topotypes for physical reference of certain morphospecies, the original description of the holotypes and/or paratypes as well as their photomicrographs are included for reference. That is why the biostratigraphers and mainly the curators are continually in search of these morphospecies and related assemblages within the material from Colombian basins through numerous taxonomic revisions, discussions and final validation with the aim of having more complete reference collections which constitute the basis of a better understanding of the regional distribution of these microfossils in time and space and its relation to the geologic, stratigraphic, and tectonic evolution of northern South America.

a → **Pollen** Spores Dinoflagellates Publications

Logged in as: cvarges [Log out]

A Morphological Electronic Database of Cretaceous-Tertiary and Extant pollen and spores from Northern South America

Jaramillo, C., Rueda, M., and de la Parra, F. 2010.

Sponsored by Colombian Petroleum Institute-Ecopetrol S.A., Smithsonian Tropical Research Institute, and the Smithsonian National Museum of Natural History.

ecopETROL

Note: The Extant data is derived from the digitalization of the 25,000 species of the **Alan Graham Palynological Collection**.

The **Alan Graham Palynological Collection** is the best collection of neotropical pollen in the world. This collection comprises over 25,000 pollen slides of modern taxa, mostly from the neotropics, and thousands of pollen slides from Dr. Graham's work on the geological history of the forests of Central America. The collections began as part of an early palynology laboratory set up in the herbarium of the University of Texas in 1954, and expanded with original preparations and exchanges with numerous laboratories throughout the world. One special value of the modern reference component is that all original preparations are vouchered to a specific herbarium collection allowing identification of fossil material and spore specimens used in taxonomic studies to be verified. This priceless collection has been donated to the Smithsonian Institution thanks to the generosity of Alan Graham, Professor Emeritus at the Kent State University and current curator at the Missouri Botanical Garden.

Database has been produced with the collaboration of Verne Sagun, Enrique Moreno, Giovanni Bedoya, Millerlandy Romero, Diana Ochoa, Carlos Sanchez, Guillermo Rodríguez, Lineth Contreras, Paula Mejía, Pilar López, Silvana Da Silva, Carlos Santos, Carolina Vargas, Francy Carvajal, Fatima Leite, Pi Williamson, Andrés Pardo, Patricia Brenac and the access to the palynological collections of PETROBRAS, PDVSA, University of Amsterdam, Smithsonian Museum of Natural History, Museum of Natural History of Paris, Jan Du Chene collection, Florida Museum of Natural History, British Museum of Natural History, and GNS Science.

b → **Name** **Examiner**

Bombacacidites annae, picture 1

c → **Pollen** Spores Dinoflagellates Publications

Logged in as: cvarges [Log out]

Chronostratigraphy: Bombacacidites annae

Ref.	Period FAD	Epoch FAD	Age FAD			
Show	Tertiary	late	Paleocene	early	Selandian	Delete
Show	Tertiary	late	Paleocene			Delete
Show	Tertiary	late	Paleocene			Delete

Ref.	Period LAD	Epoch LAD	Age LAD			
Show	Tertiary	late	Paleocene			Delete
Show	Tertiary	late	Paleocene	late	Thanetian	Delete
Show	Tertiary	late	Paleocene			Delete
Show	Tertiary	late	Paleocene			Delete

d → **Pollen** Spores Dinoflagellates Publications

Logged in as: cvarges [Log out]

Publications

New Reference

Id	Reference	First Author
Show 57	Leideimyer, P. 1966 The Paleogene and Lower Eocene pollen flora of Guyana. Leidse Geologische Mededelingen 38: 49-70	Leideimyer, 1966

Figure 4. Slide shots of the palynomorph MSQl database. a. Morphological information, b. Photomicrographs, c. Biostratigraphic information, d. References cited.

These collections are accessible to micropalaeontologists and palynologists who are interested in the field of Biostratigraphy, Micropalaeontology, Palaeobotany, Palaeoecology and also to international scientists.

5. ACKNOWLEDGEMENTS

The authors would like to thank to Biostratigraphy Team at ECOPETROL S.A.-ICP for extensive taxonomic discussions and input for each collection. We also thank Flavia Fior-

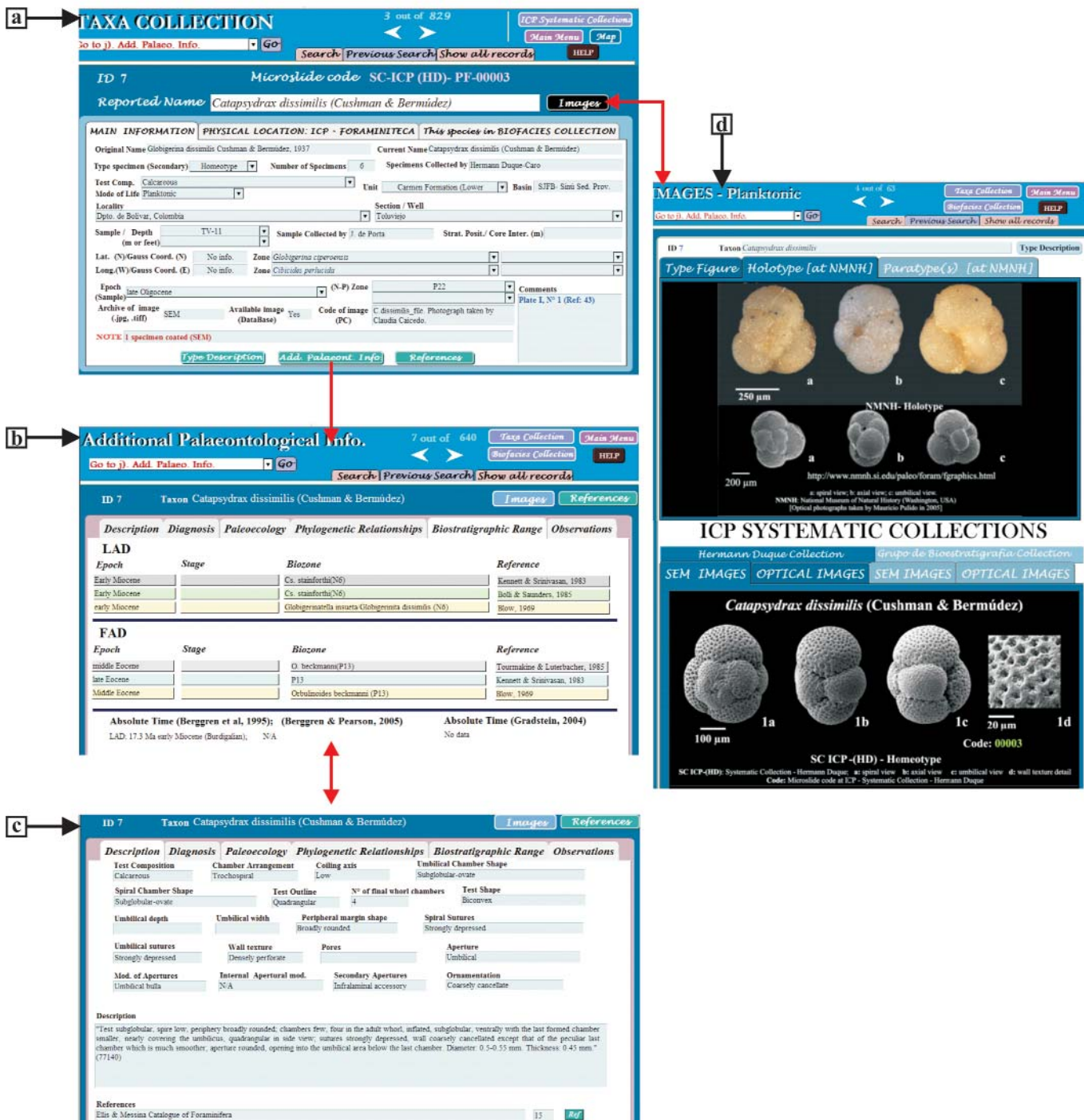


Figure 5. Slide shots of the foraminiferal Filemaker Pro-8 database. a. General information and physical location, b. Biostratigraphic information, c. Morphological characteristics, d. Optical and SEM photomicrographs.

ini for choosing our foraminiferal collection as repository of her new morphospecies and also for her discussions about agglutinated benthic taxa. We are grateful to Olga Lucia Celis Guzmán for constant assistance with *File-Maker Pro* software. The authors also thank the reviewers, Dr. Gary Rosemberg and an anonymous reviewer for their

helpful comments and suggestions which improved the manuscript. This research was supported by the Colombian Petroleum Institute (ICP) of ECOPETROL S.A. Partial funding toward this research was given by the Smithsonian Institute of Tropical Research (Panama).

6. REFERENCES

- Agencia Nacional de Hidrocarburos (ANH) 2007. *Colombian Sedimentary Basins: Nomenclature, boundaries and Petroleum Geology, a New Proposal*. ANH and B&M Exploration Ltda. Bogotá, 92 pp.
- Espitia, D. and Arenas, J. 2006. *Colección de Referencia de Foraminíferos del Instituto Colombiano del Petróleo ECOPEPOTROL-ICP: Foraminífera Versión 1 Fase 1 –Base de Datos Versión 1 Diciembre de 2006*. Internal Report N° 35-06.
- Espitia, D. 2007. *Colecciones de Referencia de Foraminíferos del Instituto Colombiano del Petróleo ECOPEPOTROL-ICP: Foraminífera Versión 2 –Base de Datos Versión 4 Noviembre de 2007*. Internal Report N° 32-07.
- Espitia, D. 2008. *Colecciones de Referencia de Foraminíferos del Instituto Colombiano del Petróleo ECOPEPOTROL-ICP: Foraminífera Versión 3 –Base de Datos Versión 7 Noviembre de 2008*. Internal Report N° 26-08.
- Espitia, D., Duque-Caro, H., Arenas, J.E., Caicedo, C., Duarte, J.A., Fiorini, F., Giraldo, V., Mantilla, O., Molinares, C., Patarroyo, G., Pulido, M. and Celis, O.L. 2008. Foraminiferal Collections from Colombian basins and Caribbean areas. *33rd International Geological Congress*. Oslo, Norway, August 6-14.
- Fiorini, F. 2009. *Ammodiscus anulatus*, a new species of benthic foraminifera from the Colombian Basin. *Micropaleontology*, 55 (1), 94-96.
- Jaramillo, C. and Yepes, O. 1994. Palinoestratigrafía del Grupo Oliní (Coniaciano-Campaniano), Valle Superior del Magdalena. In: *Estudios geológicos del Valle Superior del Magdalena* (Ed. F. Etayo-Serna). Universidad Nacional, Bogotá, XVII, 1-17.
- Jaramillo, C. and Dilcher, D. 2001. Middle Paleogene palynology of Central Colombia, South America: A study of pollen and spores from tropical latitudes. *Palaeontographica B*, 285, 87-213.
- Jaramillo, C., Rueda, M., Pulido, M., Muñoz, F., De la Parra, F., Cárdenas, A., Molinares, C., Celis, O.L. and Vargas, M.C. 2004. *Proyecto Cronología de las Secuencias Bioestratigráficas del Cenoico del Piedemonte Llanero – Paleoceno*. ECOPEPOTROL – ICP. Internal Report.
- Jaramillo, C., Pardo, A., Rueda, M., Torres, V., Harrington, G. and Mora, G. 2007. The palynology of the Cerrejón Formation (Upper Paleocene) of northern Colombia. *Palynology*, 31, 153-189.
- Jaramillo, C., Rueda, M. and Torres, V. in press. A palynological zonation for the Cenozoic of the Llanos and Llanos Foothills of Colombia. *Palynology*.
- Pulido, M., Rodríguez, G., Torres, V., Vargas, M.C., Jaramillo, C., Fiorini, F., Cardona, A., Bayona, G., Rueda, M., Rincón, D. and Arenas, J. 2006. *Proyecto Cronología de las Secuencias Bioestratigráficas del Cenoico del Piedemonte Llanero. Fase 4-Mioceno*. Ecopetrol ICP – Smithsonian Tropical Research Institute (STRI).
- Rincón, D. A., Arenas, J.E., Cuartas, C. H., Cárdenas, A. L., Molinares, C. E., Caicedo, C. and Jaramillo, C. 2007. Eocene-Pliocene planktonic foraminifera biostratigraphy from the continental margin of the south-west Caribbean. *Stratigraphy*, 4 (4), 261-311.
- Rueda, M., Jaramillo, C., Torres, V., Pulido, M., Rincón, D., Cárdenas, A., Celis, O. and Vargas, M.C. 2005. *Proyecto cronología de las secuencias bioestratigráficas del Cenoico del Piedemonte Llanero. Fase 3-Oligoceno*. Ecopetrol ICP – Smithsonian Tropical Research Institute (STRI).
- Silva-Caminha, S., Jaramillo, C. and Absy, M.L. 2010. Neogene palynology of the Solimões Basin, Brazilian Amazonia. *Palaeontographica B*, 283, 1-67.
- Torres, V., Rueda, M., Jaramillo, C. and Vargas, M.C. 2008. A Pollen and spore Reference Collection for Northern South America: A key tool for talking a common language in applied biostratigraphy. III Colombia Oil & Gas Investment Conference. Cartagena, Colombia.
- Vargas, M.C., Torres V., Rueda, M. and Jaramillo, C. 2008. A Reference Collection for fossil pollen of the Neotropics. XII International Palynological Congress. Bonn, Germany, August 30 – September 6.
- Vargas, M.C., Rueda, M., Torres, V., Jaramillo, C., Romero, M., Celis, O.L., Arenas, J.E., Espitia, D., and Duque-Caro, H. 2007. Colecciones de Referencia de Palinomorfos y Foraminíferos del Norte de Suramérica: Un Patrimonio Científico de ECOPEPOTROL S.A.- I Simposio Venezolano de Paleontología y Bioestratigrafía. Los Teques, Venezuela, May 7-11.
- Yepes, O. 2001. Maastrichtian-Danian dinoflagellate cyst biostratigraphy and biogeography from two equatorial sections in Colombia and Venezuela. *Palynology*, 25, 217-249.

MANUSCRITO RECIBIDO: 18 de mayo, 2010

MANUSCRITO ACEPTADO: 26 de noviembre, 2010

Erratum to “An attempt of classification of the Palaeozoic *incertae sedis* Algospongia”.

Revista Española de Micropaleontología 42 (2010) 129-241

Daniel Vachard¹ and Pedro Cózar²

¹Université de Lille 1, FRE 3298 du CNRS: Géosystèmes, Bâtiment SN 5, 59655 Villeneuve d'Ascq, France.
Daniel.Vachard@univ-lille1.fr

² UEI y Departamento de Paleontología, Instituto de Geología Económica CSIC-UCM, Facultad de Ciencias Geológicas, José Antonio Novais 2, 28040 Madrid, Spain. pcozar@geo.ucm.es

During the final stage of production of the issue containing the above article the authors became aware that there were further corrections which still needed to be carried out and, in addition to this, certain figures and captions had inadvertently changed from the original files. Unfortunately, as the issue was already in print, modifications are presented below.

Name of some suprageneric categories are misspelled through the text, where is written Moravamininidae should be written Moravaminidae, Analiporaceae should be replaced by Anatoliporaceae, where is written Beresellinae should be Beresellina.

In figure 15, some stratigraphic ranges have to be modified, as *Wetheredella* last occurs in the Baskhirian, as well as *Uraloporella* [the publication of Choh & Kirkland, 2008, contains errors in the figure caption, but revision of Ph.D. of Choh, 2004, shows *Uraloporella* in the Bashkirian, and no *Trinodella*], *Evlania* should be extended up to the Viséan, and *Labyrinthoconus* should be restricted to the Givetian.

The reference to Fig. 2.5 in the genus *Exvotarisella* should be replaced by Fig. 2.7.

Captions of Figures 2 and 3 are incorrect, and should be as follow:

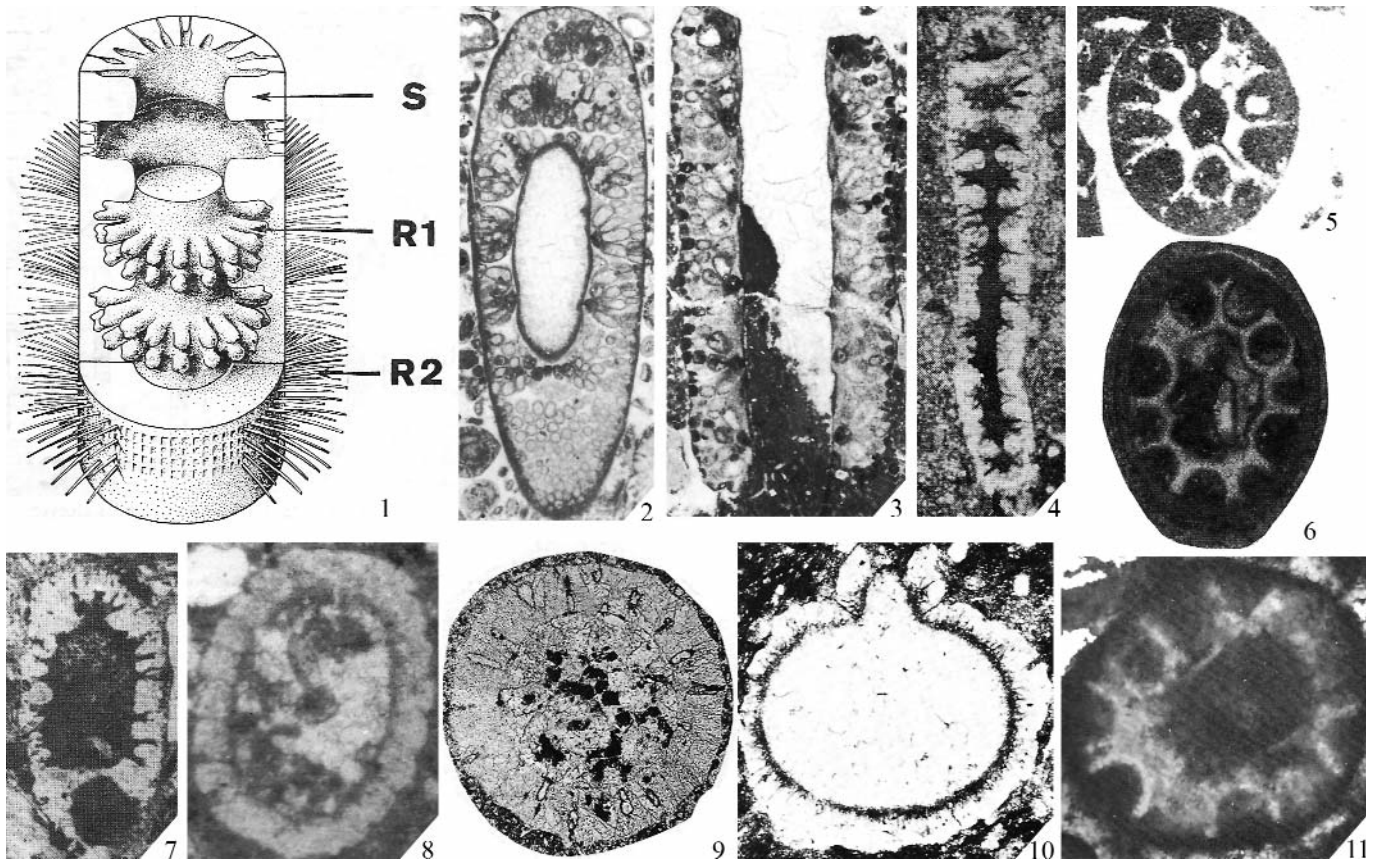


Figure 2. Comparison with the algae Dasycladales. Comparison of the pseudo-tufts of *Exvotarissella* (1, 4, 7) and true tufts of *Eodasycladus barrabei* (Lebouché & Lemoine) (2-3). **1**, Reconstruction after Skompski, 1987, text-fig. 2 p. 26; S = wall, R1 = irregular superficie of the chamber, R2 = perforations through the wall, allowing the passage of cytoplasmic branchlets from chamber to external environment (to compare with Fig. 1.10 and Figs 2.2-2.3). **2-3**, True metaspondyl tufts of the dasycladale *Eodasycladus barrabei* (Lebouché & Lemoine) according to Barattolo *et al.*, 1994, pl. 2, figs 1-2; both from Middle Lias of Saint-Chinian, southern France; x 25. **4, 7**, *Exvotarissella* in Skompski, 1986, pl. 8, figs 8 (x 100) and 1 (x 90), respectively, Lublin basin, Poland, late Viséan. **5**, *Cyliindroporella sudgeni* Elliott (after Bassoullet *et al.*, 1978, pl. 8, fig. 3 after type material of Elliott); Early Cretaceous, Fahud (Oman), x 54. **6**, *Atractyliopsis* sp. (*sensu* Sebbar & Mamet, 1999) (pl. 2, fig. 10) (Early Bashkirian and early Moscovian respectively; Bechar Basin, Algeria; x 40) (compare with Figs 2.5, 2.11). **8-10**, Different Charophytes. **8**, Cenozoic or Mesozoic Characeae of Sebbar *et al.* (2000, pl. 9, fig. 1), Aouinet-Legraa section, Tindouf Basin, Algeria, x 50; misinterpreted as late Viséan "Sycidiales". **9**, True *Sycidium* illustrated by Langer (1976, pl. 25, fig. 12; the wall and organization differ absolutely from Fig. 2.8), Devonian of Eifel (Germany), x 90. **10**, *Chovanella burgessi* Peck & Eyer after Eyer (1971, pl. 5, fig. 5), also different from Fig. 2.9; Cedared Formation, Devonian of British Columbia (Canada), x 75. **11**, *Cyliindroporella* cf. *arabica* Elliott (after Elliott, 1975, pl. 50, fig. 5); oblique-transverse section, Great Oolite (Bathonian) of Gloucestershire (England), x 100. This alga, which belongs in fact to *Holosporella siamensis* (= *Sarfatella dubari*) (Granier, pers. comm., October, 2010) represents another assignment for the false *Atractyliopsis* Sebbar & Mamet, 1999 (see above Fig. 2.6). (References are all included in Vachard & Cózar, 2010).

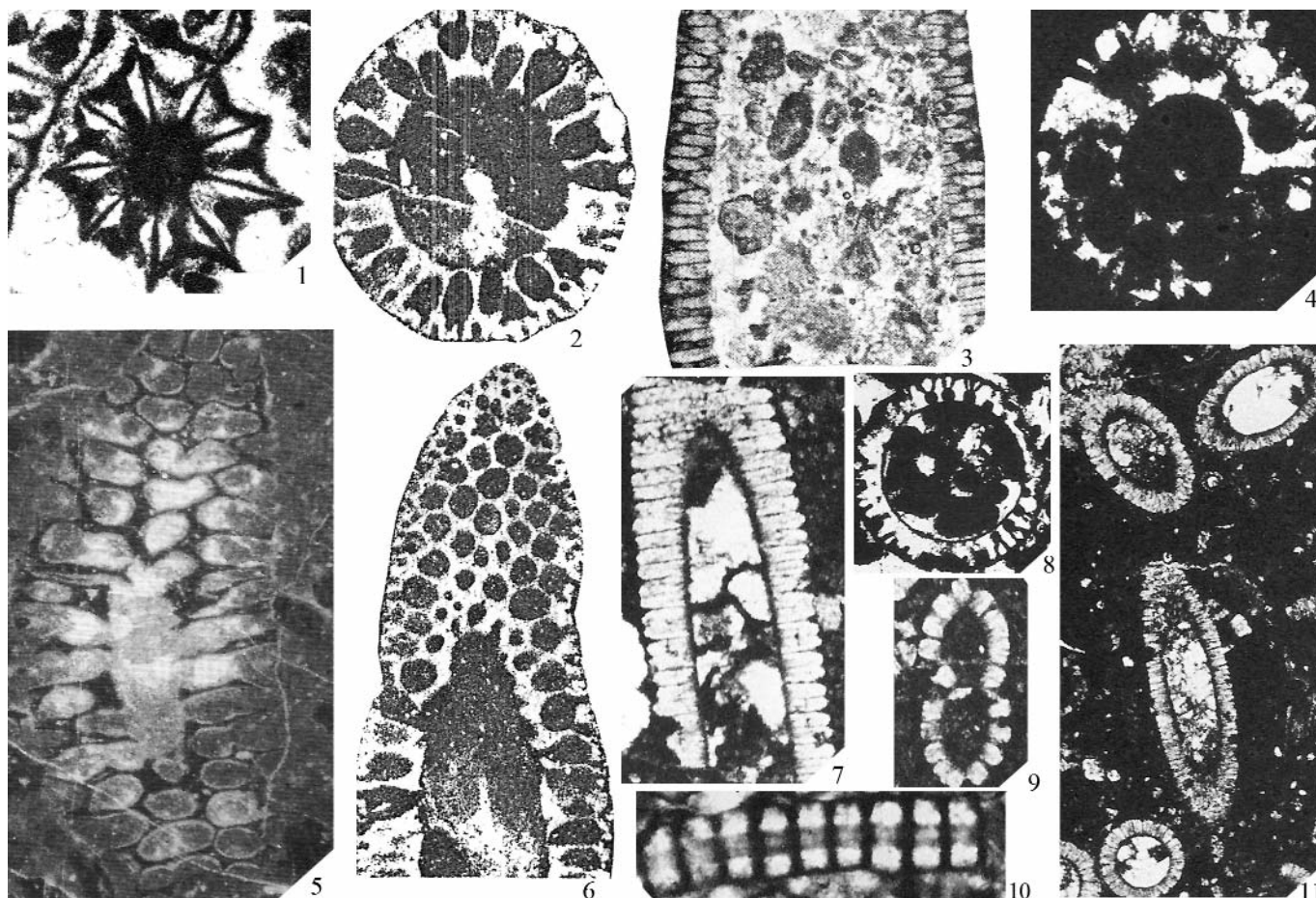


Figure 3. Atypical "dasycladales", Lazarus issinellids and possible misinterpretations of *Zergabriella* and *Koninckopora*. **1**, *Clypeina jurassica* Favre (this specimen should be quoted as *C. sulcata*, according to Granier, pers. comm., October, 2010); bilayered atypical "dasycladale", after Bassoullet *et al.*, 1978, pl. 4, fig. 5; Berriasian, Val de Fier, France, x 107. **2, 6**, *Hoegenites kringla* Nitecki & Spjelnaes; after Nitecki & Spjelnaes, 1989 (figs 2.2 and 2.10 respectively); this "Ordovician tubular microproblematica" (*sic*) is evidently something similar to *Cymopolia*, the paragon of Cenozoic-Recent dasycladales (compare with Fig. 3.4); Helgøya (9 km north of Oslo, Norway); indicated as Caradocian (Ordovician) in age. x 32.5. **3**, *Koninckopora pruvosti* Güvenç (*sensu* Mamet & Roux, 1975a, pl. 3, fig. 1; part) third bilayered atypical "dasycladale". Early Asbian, Great Britain, x 19. **4**, *Cymopolia barberae* Elliott, 1968, pl. 8, fig. 2; transverse section, Palaeocene/Early Eocene, Iraq, x 50. **5**, *Zergabriella embergeri* Bouroullec & Deloffre; oblique section of another bilayered atypical "dasycladale", after Granier (1989, pl. 1, fig. 6), Berriasian, Provence (France), x 60. **7, 9, 11**, *Hensonella cylindrica* Elliott questioned here as an issinellid Lazarus effect, after Elliott, 1968, pl. 22, figs 3, 5, 1 respectively; Early Cretaceous, Qamchuqa Formation, Iraq, 7, x 45, 9, x 45, 11, x 27. **8**, *Dissocladella savitriæ* Pia, after Elliott, 1968, pl. 11, fig. 1, Palaeocene, Sinjar Formation, Iraq, x 25; another dasycladale similar to *Hoegenites*. **10**, *Salpingoporella apenninica* Sartoni & Crescenti, after Elliott, 1968, pl. 20, fig. 5, Late Jurassic, Najmah Formation, Kirkuk well, Iraq, x 45 (*S. apenninica* is a junior synonym of *S. annulata*, according to Granier, pers. comm., October, 2010); true euspondyl dasycladale confused with *Hensonella*. The shape is similar, but the wall is different. (References are all included in Vachard & Cózar, 2010).

REFERENCES

Choh, S.-J. S. 2004. *Microfacies and Depositional Environments of Selected Pennsylvanian Calcareous Algal Deposits from Southern U.S.A. and Application of Information Technology for Sedimentary Petrology Teaching and Research*. Ph. D. University of Texas at Austin, 168 p. (unpublished).

Vachard, D. and Cózar, P. 2010. An attempt of classification of the Palaeozoic incertae sedis Algospongia. *Revista Española de Micropaleontología*, 42 (2), 129-241.

REVISTA ESPAÑOLA DE MICROPALAEONTOLOGÍA, 42 (3), 2010

SUMARIO

MICROFOSSILS, STRATIGRAPHY AND ENVIRONMENTS

Special Editor: José-Abel Flores

- ALEJANDRA MEJÍA-MOLINA, JOSÉ-ABEL FLORES, VLADIMIR TORRES TORRES AND FRANCISCO JAVIER SIERRO
Distribution of calcareous nannofossils in Upper Eocene-Upper Miocene deposits from northern Colombia and the Caribbean sea..... 279-300
- YANED MARGARITA BUITRAGO-REINA, JOSÉ-ABEL FLORES AND FRANCISCO JAVIER SIERRO
Calcareous nannofossils Upper Miocene biostratigraphy and biochronology at western equatorial Atlantic (ODP Site 999) 301-319
- CARLOS LANCIS, JOSÉ ENRIQUE TENT-MANCLÚS, JESÚS MIGUEL SORIA, HUGO CORBÍ, JAUME DINARÈS-TURELL AND ALFONSO YÉBENES
Nannoplankton and planktonic foraminifera biostratigraphy of the eastern Betics during the Tortonian (SE Spain)..... 321-344
- ÁUREA NARCISO, JOSÉ-ABEL FLORES, MÁRIO CACHÃO, FRANCISCO JAVIER SIERRO, ELENA COLMENERO-HIDALGO, ANDREA PIVA AND ALESSANDRA ASIOLI
Sea surface dynamics and coccolithophore behaviour during sapropel deposition of Marine Isotope Stages 7, 6 and 5 in Western Adriatic sea 345-358
- M. CARMEN ÁLVAREZ, F. ORNELLA AMORE, LLUÏSA CROS, BELÉN ALONSO AND JAVIER ALCÁNTARA-CARRIÓ
Coccolithophore biogeography in the Mediterranean Iberian margin 359-371
- DIANA ESPITIA, MARÍA CAROLINA VARGAS, JOSÉ E. ARENAS, CARLOS A. JARAMILLO, MILTON J. RUEDA AND HERMANN DUQUE-CARO
Palynomorphs and foraminifera from Colombia housed in the systematic collections of Ecopetrol-ICP 373-380
- DANIEL VACHARD AND PEDRO CÓZAR
Erratum to "An attempt of classification of the Palaeozoic *incertae sedis* Algospongia". Revista Española de Micropaleontología 42 (2010) 129-241 381-383



MINISTERIO
DE CIENCIA
E INNOVACIÓN



Instituto Geológico
y Minero de España